Photosynthesis, Photorespiration and Productivity of Wheat and Soybean Genotypes

Jalal A. Aliyev[1,2]*

[1]*Department of Plant Physiology and Biotechnology, Research Institute of Crop Husbandry, Ministry of Agriculture of Azerbaijan Republic, Pirshagi Village, II Sovkhoz, Baku AZ 1098, Azerbaijan*
[2]*Department of Fundamental Problems of Biological Productivity, Institute of Botany, Azerbaijan National Academy of Sciences, 40 Badamdar Shosse, Baku AZ 1073, Azerbaijan*

The results of the numerous measurements obtained during the last 40 years on gas exchange rate using an infrared gas analyzer URAS-2T (Germany), photosynthetic carbon metabolism by exposition in $^{14}CO_2$ and activities of enzyme of primary carbon fixation, ribulose-1,5-bisphosphate carboxylase/oxygenase (RuBPC/O), in various wheat genotypes grown over a wide area in the field and contrasting in photosynthetic traits and productivity are presented in this paper. It was established that high productive wheat genotypes with the optimal architectonics (7-9 t ha^{-1}) possess higher rate of CO_2 assimilation during leaf ontogenesis. Along with the high rate of photosynthesis, high values of photorespiration are characteristic for high productive genotypes. There is a parallel increase in the rates of true photosynthesis and photorespiration in ontogenesis. Genotypes with moderate (4-5 t ha^{-1}) and low (3 t ha^{-1}) grain yield are characterized by relatively low rates of both CO_2 assimilation and photorespiration. The ratio of true photosynthesis to photorespiration in genotypes with different productivity is equal on average to 3:1. A value of photorespiration constitutes 28-35% of photosynthetic rate in contrasting wheat genotypes. The activities of RuBP carboxylase and RuBP oxygenase were changing in a similar way in the course of the flag leaf and ear elements development. RuBP oxygenase activity was higher in high productive wheat genotypes than in low productive ones. The rates of sucrose (the main transport metabolite in plants) biosynthesis and products of glycolate metabolism also correlate with the CO_2 assimilation rate and the activity of RuBP oxygenase. High productive genotypes are also characterized by a higher rate of biosynthesis and total value of glycine-serine and a higher photosynthetic rate. Pattern of changes in biosynthesis rate and total value of glycine-serine as well as ratio of RuBP carboxylase to oxygenase activities and CO_2 assimilation rate predisposes to parallel change in the rates of photosynthesis and photorespiration during leaf ontogenesis. High rates of photosynthesis and photorespiration in conjunction with favourable photosynthetic traits, an optimum leaf area index and the best architectonics define high productivity of wheat genotypes. Therefore, contrary to conception arisen during many years on wastefulness of photorespiration, taking into account the versatile investigations on different aspects of photorespiration it was proved that photorespiration is one of the evolutionary developed vital metabolic processes in plants and the attempts to reduce this process with the purpose of increasing the crop productivity are inconsistent. Phosphoglycolate phosphatase, a key enzyme of photorespiration was first homogeneously purified from eukaryotic green algae *Chlamydomonas reinhardtii* with subsequent determination of complete nucleotide and deduced amino acid sequences (NCBI Nucleotide 1:AB052169). Since metabolic processes of photorespiration in the leaf occur in the light simultaneously with photosynthesis, it is evident that released energy is used in certain reactions of photosynthesis.

Keywords: *photosynthesis, photorespiration, productivity, architectonics, gas exchange, carbon metabolism, RuBPC/O, Triticum L. genotypes, soybean genotypes*

INTRODUCTION

Among the processes ensuring a high plant productivity leading role belongs to photosynthesis (Aliyev, 1974). Photosynthesis is unique process, in course of which light energy is utilized for carbon dioxide conversion into sugars. About 92% of all vascular plants that use only Calvin-Benson cycle belong to C_3-plants because their first product of CO_2 fixation is three-carbon compound termed

---

*E-mail: aliyev-j@botany-az.org

3-phosphoglycerate (PGA). In plants with C_3-metabolism photosynthesis takes place simultaneously with the opposite process, which relates both to the oxygen and carbon dioxide gas exchange. This process occurs only in the light and is associated with photosynthetic metabolism, and therefore was named photorespiration. Photorespiration was discovered in 1955 by I. Decker (1955). Photosynthesis and photorespiration are closely linked processes catalysed by the key photosynthetic enzyme, ribulose-1,5-bisphosphate carboxylase/oxygenase (Rubisco, EC 4.1.1.39) with the dual catalytic activity. The process of photorespiration is associated with oxygenase activity of RuBP, the function of which is to fix carbon dioxide (Lorimer and Andrews, 1973). The adhesion of CO_2 to this enzyme substrate results in formation of two molecules of 3-phosphoglycerate. Rubisco has affinity not only for CO_2, but also for molecular oxygen, that results in formation of one molecule of 3-phosphoglycerate (integrated into the Calvin cycle) and one molecule of 2-phosphoglycolate (starting molecule of photorespiratory glycolate cycle) instead of two molecules of 3-phosphoglycerate (Ogren and Bowes, 1971). During photorespiratory metabolism oxygen is fixed and carbon dioxide is released. Photorespiratory carbon metabolism requires the integration of biochemical pathways in three separate leaf cell organelles: chloroplasts, peroxisomes and mitochondria (Figure 1). In mesophyll cells peroxisomes, chloroplasts and mitochondria are often located nearby, supporting an intensive metabolism between these organelles. Currently biochemical mechanism of photorespiratory pathway is sufficiently enough studied. The initial stage of photorespiration takes place in chloroplast stroma. According to the most researchers, the initial substrate for the photorespiration is glycolate. Reactions associated with photooxidative transformation of RuBP and formation of phosphoglycolate are considered to be key processes of photorespiration (Somerville and Ogren, 1979; Andersson, 2008). Under the influence of a key photorespiratory enzyme, phosphoglycolate phosphatase (PGPase, EC 3.1.3.18), phosphoglycolate is converted into glycolate which then leaves the chloroplast and enters the peroxisome. Carbon metabolism in photorespiration describes the sequence of reaction series of so-called "glycolate pathway", most of which take place in peroxisomes and mitochondria.

Photosynthesis and photorespiration are high-flux pathways that involve redox exchange between intracellular compartments. In particular, the photorespiratory pathway interacts directly with the redox signaling cascades that control plant growth and defence responses as well.

Photorespiration has been studied for more than 50 years. For a long period of time the rate of photorespiration was considered as a negative factor in determining the dependence of plant productivity on photosynthesis. While evaluating photorespiration magnitude many researchers supposed that carbon losses in photorespiration occur through the use of newly formed products, and therefore this process was considered to be wasteful. Hence, it was proposed to search the ways for elimination or decreasing photorespiration by biochemical or genetic means with the purpose of increasing the crop productivity (Zelitch, 1966, 1971, 1973, 1975; Zelitch and Day, 1973; Hough, 1974; Chollet and Ogren, 1975; Kelly and Latzko, 1976; Ogren, 1976; Servaites and Ogren, 1977; Holaday and Chollet, 1984; Somerville, 2001; Ogren, 2003; Igarashi et al., 2006; Long et al., 2006; Kebeish et al., 2007; Khan, 2007; Mueller-Cajar and Whitney, 2008; Maurino and Peterhansel, 2010; Peterhansel et al., 2010; Peterhansel and Maurino, 2010). However, screening for species with low level of photorespiration and high productivity was not successful. Any intervention in the plant functions led to decrease in plant growth and productivity. But few researchers believed that photorespiration is essential for normal plant functioning (Barber, 1998; Evans, 1998; Eckardt, 2005). Taking into account very high rates of photorespiration comparable only to the rates of photosynthesis, it remained unclear why such a wasteful process of energy dissipation has not disappeared during the evolution. On the contrary, there is a complex enzyme apparatus for recycling of phosphoglycolate, inevitable product of RuBP oxygenase reactions (Tolbert, 1997).

The fact that photorespiration has not been completely eliminated even in evolutionary more advanced C_4-plants (Dever et al., 1995; Zelitch et al., 2008) along with the discovery that C_4-plants have photorespiratory enzymes (Popov et al., 2003; Majeran et al., 2005) may reflect the functional relevance of the pathway.

The study of photorespiration also occupies a central position in the history of modern plant biology (Eckardt, 2005; Maurino and Peterhansel, 2010; Peterhansel et al., 2010; Peterhansel and Maurino, 2010). A lot of plant scientists attempt to resolve this dilemma. The pathways of biochemical reactions, the genes of key photorespiratory enzymes, energetics, redox signaling, and transporters of photorespiratory intermediates were discovered (Leegood et al., 1995; Booker et al., 1997; Wingler et al., 1999; Mamedov et al., 2001, 2002; Mamedov and Suzuki, 2002; Eisenhut et al., 2006; Schwarte and Bauwe, 2007; Foyer et al., 2009; Peterhansel et al., 2010).

But, there is still no unanimous opinion about the role of this process in photosynthesis and plant
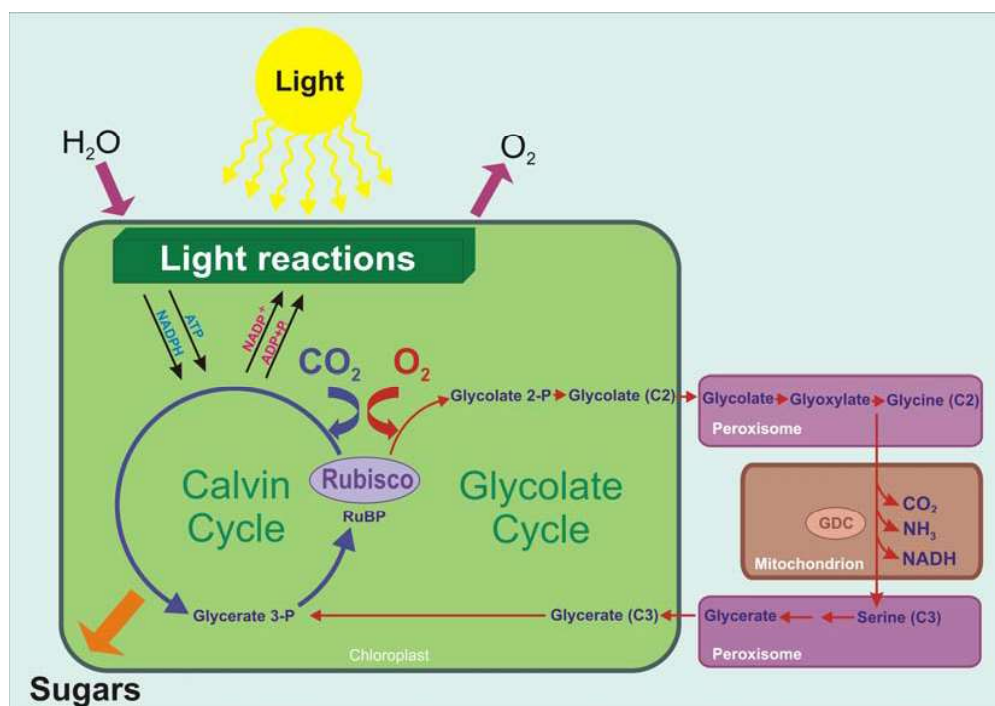
Figure 1. Schematic overview of photosynthesis and photorespiration.

productivity. It is particularly important to note that most of the previous studies on photorespiration were performed mainly in controlled environment experiments. The results of such studies cannot fully reveal real environmental conditions.

In the present paper the results of long-term experiments on the relationship between the rates of photosynthesis, photorespiration and productivity of wheat genotypes grown in the field are presented.

MATERIALS AND METHODS

The rich genefund, comprising several thousand wheat genotypes, selected from both the ancient, aboriginal varieties of national selection and introduced from the world genefund, particularly, from *CIMMYT, ICARDA* and other International Centres, with contrasting photosynthetic traits, productivity and tolerance to water stress was created (Figure 2). All these genotypes were grown in field conditions in a wide area at the Absheron Experimental Station of the Research Institute of Crop Husbandry at the optimal regime of mineral nutrition and water supply (Figure 3).

Genotypes were also grown with normal water supply and at severe water deficit under the guidelines established by the Department of Plant Physiology and Biotechnology of the Research Institute of Crop

Husbandry on the base of long-term studies of morpho-physiological traits of the varieties. The experimental plot area was 54 m^2; all experiments were replicated at least four times. Numerous winter wheat genotypes were the main targets of the researches, and most typical of them are presented in this paper. The main parameters for selection of these genotypes were grain yield, plant phenotypic features (stem height, area and architectonics of the leaf surface, etc.), duration of the vegetation and other morpho-physiological traits, as well as drought resistance (Figure 4, 5, 6, 7, 8, 9, 10) (Aliyev and Kazibekova, 1977; Aliyev et al., 1982 b; Aliyev, 1983, 2002). Due to leaves oriented under different inclination angles, plants create canopies with drooping (the angle is 30-40º from the vertical), semi-vertical (20-27º) and erect (10-18º) leaves. Varieties of intensive type are short-stemmed, leaves of vertical orientation, high productive, and varieties of extensive type are long-stemmed with drooping leaves of horizontal orientation, low productive. Bread wheat (*Triticum aestivum* L.) varieties contrast in architectonics, Gyrmyzy gul and Azamatli-95, are short-stemmed (with the stem height of 85-90 and 60-75 cm, respectively), intensive type, with vertically oriented small leaves, high productive (7-9 t ha^{-1}); Giymatli-2/17 is short-stemmed (85-95 cm), intensive type, with broad drooping leaves, high productive (7 t ha^{-1}), and Kansas-63323 is medium-stemmed (90 cm), with a small ear and small leaves, and grain yield of 3 t ha^{-1}. Durum wheat (*Triticum durum* L.) varieties,

9

Shiraslan-23 and Garagylchyg-2, are short-stemmed (78 and 82-85 cm, respectively), intensive type, with the vertical orientated leaves and potential grain yield of 6-8 t ha^{-1}; Shark and Caucasus are medium-stemmed (110-120 cm), semi-intensive, with semi-vertical leaf arrangement and medium grain yield (4-5 t ha^{-1}); Oviachik-65 (*CIMMYT*) is short-stemmed (60-70 cm), with erect leaves and average grain yield of 6 t ha^{-1}; Gyrmyzy bugda and Sary bugda are long-stemmed (150-180 and 125-150 cm), extensive type, with drooping horizontal leaves and grain yield of 3 t ha^{-1} were used. Except Kansas-63323, Oviachik-65 (*CIMMYT*) and Caucasus (*Krasnodar Agricultural Research Institute*) all other varieties are of local selection (Figure 11) (Catalogue, 2000; Aliyev, 2006).

At the same time, various soybean (*Glycine max* (L.) Merr.) genotypes differing in height (40-110 cm), duration of vegetation, grain yield (2-4 t ha^{-1}) and other morpho-physiological traits were also research targets (Figure 12). All genotypes were grown in field conditions over a large area following guidelines of the experimental procedure (Figure 13). The experiments were performed in irrigated area at the Absheron Experimental Station of the Research Institute of Crop Husbandry.

The basic parameters of photosynthetic activity: leaf, stem and ear area, the rates of photosynthesis and photorespiration were determined during the ontogenesis.

In order to measure the rate of gas exchange in leaves of various layers and other assimilating organs, an infrared gas analyzer URAS-2T ("Hartman and Braun", Germany) with a short exposure of the whole plant in sowings in $^{14}CO_2$ atmosphere (Figure 14) was used. The limits of measurements were 0.005-0.05% CO_2, error was ± 0.5% of the upper limit of the scale (Voznesensky, 1977; Aliev et al., 1996 b). CO_2 concentration in the analyzed air was recorded using automatic recorder. The measurements were performed in an open air flow system connected in the differential mode (Karpushkin, 1971). The initial air flow was divided into two parts. One part passed through the air dehumidifier, filled with calcium chloride, through the filter, and then through the control cuvette of the gas analyzer. The other part passed through the leaf chamber, dehumidifier, filter, and then through the measuring cuvette. The air flow velocity through the entire system was adjusted using needle valves and rotometer. The gas analyzer recorded the difference in CO_2 concentration at the inlet and outlet of the leaf chamber. The rate of gas exchange in leaves placed in the leaf chamber was determined by the difference in CO_2 concentration and air velocity passing through the leaf chamber. For the measurements a hermetically sealed clip chamber with the area of 0.1 dm^2, which has two inlets and outlets

for air flow, separately surrounding the upper and lower leaf surface, was used.

During the measurements chamber was attached to leaves of different layers close to the stem maintaining their natural location and orientation, and exposed to sunlight until the gas exchange reached the steady-state level. The CO_2 concentration in air was determined close to the leaf chamber before each gas exchange measurement. Night respiration was determined using the above mentioned equipment without use of thermostat, in a steady night temperature. In the heat of the day a light filter SZS-24 (Voznesensky, 1977; Aliev et al., 1996 b) was used to prevent overheating of leaves in the chamber. Photorespiration was determined using two methods, in atmosphere without CO_2 and in atmosphere with reduced oxygen content (2%) (Šesták et al., 1971; Akhmedov, 1986). In the first case, after photosynthesis had reached the steady-state level the CO_2-lacking air was passed through the leaf chamber. The increase in CO_2 concentration at the chamber outlet is an indicator for the estimation of photorespiration. In the second case, after photosynthesis had reached the steady-state level the air with a reduced content of oxygen was blown into the chamber, and the obtained values of photosynthesis were measured. The value of photorespiration was determined as the difference between the photosynthetic values in low and normal oxygen content of the air.

The gas analyzer which was placed in a mobile laboratory allowed multiple measurements in the sowings of different genotypes to be performed in a short time while keeping the high sensitivity of the facility in the field and maintaining the natural course of physiological processes in entire plants (Figure 14).

Photosynthetic carbon metabolism and utilization of main photosynthetic products were studied radiometrically under ambient CO_2 (0.03%) and O_2 (21%) (Aliev et al., 1996 b, c). In the experiments an open gas system was used for the $^{14}CO_2$ incorporation into various organs of plants. The required air reserve with radiolabelled carbon dioxide was prepared and kept under high pressure in 10-liter steel cylinder with a needle valve. The 50 cm^3 thermostated leaf chamber made of organic glass was used.

Transparent plastic bags were used for the $^{14}CO_2$ incorporation into the entire plants. The experiments were carried out under direct sunlight illumination. Initially, photosynthesis reached the steady-state level in an atmospheric air flow, then the radiolabelled air from the cylinder was blown through the leaf chamber with velocity of 1 l/min and CO_2 specific radioactivity of 1.000MBq/l. After 10 minutes of exposure, plants were removed from

Figure 2. Wheat genefund at the Research Institute of Crop Husbandry.

Figure 3. Experimental crop fields of the Department of Plant Physiology and Biotechnology of the Research Institute of Crop Husbandry.

Figure 4. Wheat genotypes with contrast architectonics.

Figure 5. *Triticum aestivum* L. wheat variety Gyrmyzy gul with ideal architectonics.

Figure 6. *Triticum aestivum* L. wheat variety Giymatli-2/17.

Figure 7. *Triticum durum* L. wheat variety Barakatli-95.

Figure 8. Drought resistant *Triticum* L. wheat variety developed at the Department of Plant Physiology and Biotechnology of the Research Institute of Crop Husbandry.

Figure 9. Professor Jalal Aliyev at his experimental wheat field of the Research Institute of Crop Husbandry.

Figure 10. Winter wheat genotype.

Figure 11. *Triticum durum* L. and *Triticum aestivum* L. wheat varieties developed at the Department of Plant Physiology and Biotechnology of the Research Institute of Crop Husbandry.

Figure 12. Different soybean genotypes (*Glycine max* (L.) Merr.): low productive (Volna) and high productive (Komsomolka and Visokoroslaya-3) (left to right).
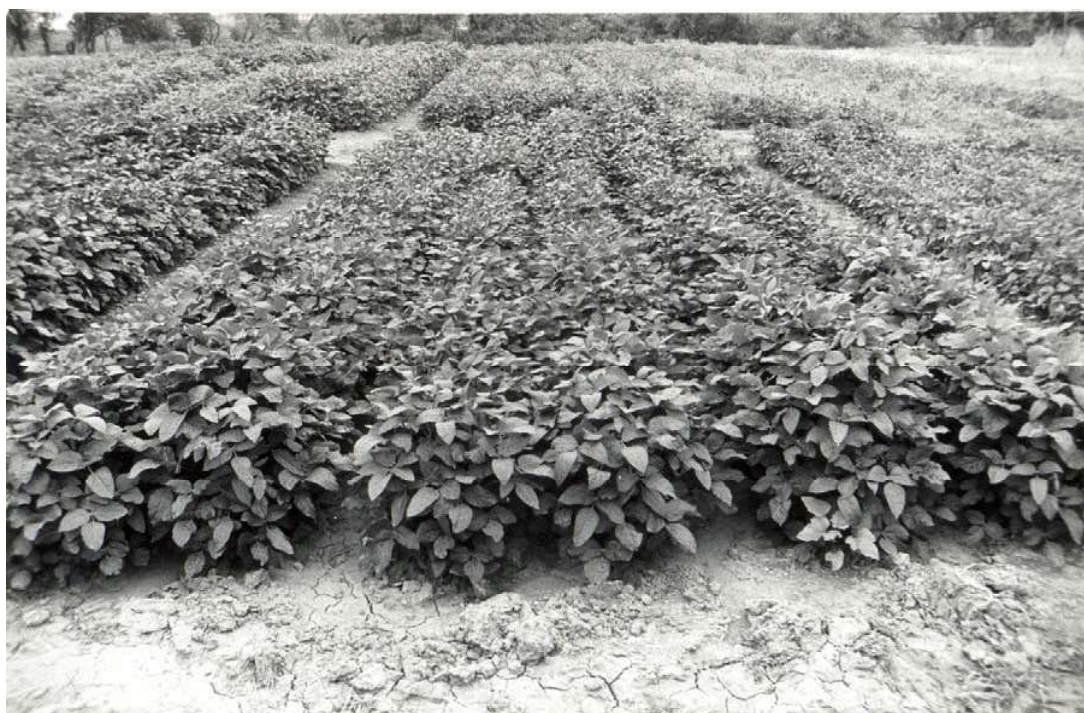

Figure 13. Sowings of different soybean genotypes at the period of intensive growth.

the leaf chamber and quickly fixed with boiling ethyl alcohol. Experiments were repeated 4-5 times. Radiochemical analysis of fixed plant material was carried out using the standard technique (Voznesensky et al., 1965; Keerberg et al., 1970). Water- and alcohol-soluble products were separated by two-dimensional paper chromatography. Measure-

ment of the radioactivity of fractions and separate compounds was carried out using a scintillation counter SL-30 in dioxane-based standard scintillator. Radioactivity of fractions and separate compounds was calculated taking into account the self-absorption coefficient.

Figure 14. Various devices used to carry out studies on photosynthesis and photorespiration in the field.

To investigate the transport and distribution of photosynthetic products under field conditions, $^{14}CO_2$ of ambient concentration and specific activity of 200 MBq/l was incorporated during photosynthesis into leaves of certain layers for 15-20 min, and then samples preparation to determine their radioactivity were made. After a 20 min exposure, the chamber was removed from the plant; then after 24 h or at the end of plant growth the plants were withdrawn from the soil, fixed with dry heat,

dissected into individual organs and dried. The plant organs were weighed and then grounded for sample preparation (Aliev et al., 1996 a), and the radioactivity calculated per units of weight and per organ was measured. The radioactivity of the samples was measured using the end-window counter of SBT-13 in a layer of complete absorption.

The rate of true photosynthesis was determined in the short exposures (15-30 sec) in $^{14}CO_2$. The rates of the net photosynthesis and dark respiration

in the light were measured using infrared gas analyzer INFRALYT-4. The magnitude of photorespiration was estimated on the basis of the values of true and net photosynthesis and dark respiration as well (Jahangirov, 1987).

In order to determine the enzymes activities, the leaves were washed, after both ends were cut off they were homogenized by mechanical MPW-302 type disintegrator for 3 min in 0.05 M Tris-HCl buffer, pH 8.5, containing 1 mM dithiothreitol (DTT), 5 mM $MgCl_2$, 1 mM EDTA and 1% polyvinylpyrrolidone K-25 ("FERAK"). Homogenization of wheat ear elements was performed in a mortar after the ear had been divided into separate elements, i.e. awns, glume and grains. Homogenate was squeezed through the 4-layered gauze and centrifuged first for 10 min at 1000×g, then for 30 min at 5000×g at 4°C. The precipitate was removed, and the supernatant was decanted and immediately used for enzymes assays.

The activity of Rubisco was determined spectrophotometrically ("ULTRASPEC", LKB, Sweden) at the 340 nm of optical density and 30°C based on the quantitative determination of 3-phosphoglycerate (3-PGA) in the presence of phosphoglycerate kinase and glyceraldehyde phosphate dehydrogenase (Aliev et al., 1988, 1996 b, c). The reaction mixture contained 0.05 M Tris-HCl buffer, pH 7.8, 0.05 M $NaHCO_3$, 0.01 M $MgCl_2$, 0.005 M DTT, 0.01 M ATP, 0.25 mM NADH, 0.3 mM RuBP, 10 U of glyceraldehyde phosphate dehydrogenase, 10 U of phosphoglycerate kinase and 0.2-0.4 mg of the studied preparation. Control contained all components excepting NADH.

The activity of RuBPO was assayed by amperometric method (Romanova, 1980; Aliev et al., 1988, 1996 b, c). The reaction mix contained 50 mM Tris-HCl buffer, pH 8.6, 5 M $MgCl_2$, 0.5 mM RuBP, 1-3 mg of protein of preliminarily activated enzyme preparation. The enzyme was activated by incubation at room temperature for 5-10 min in the presence of 10 mM $NaHCO_3$ and 5 mM $MgCl_2$ at pH 8.6.

The rate of light-saturated electron transport was measured spectrophotometrically.

Leaf assimilating area was measured using an automatic area meter "AAC-400" ("Kayashi" Delkon Co LTD, Japan). The specific leaf density was calculated as the ratio of its dry weight to the area.

Parameters of water regime were determined according to the procedure (Methodological guidelines, 1987; Boyer, 1995). Determination of relative water content and water deficit was repeated ten times.

Protein concentration was determined according to the Lowry et al. (1951).

The arithmetic mean and standard errors pre-

sented in the figures and tables were calculated based on the data from at least 4 biological replicates. The obtained data was statistically processed by standard analysis methods (Kaplan, 1970; Dospekhov, 1985).

RESULTS AND DISCUSSION

During 50 years of comprehensive investigations of photosynthesis and productivity of various wheat genotypes in natural conditions of cultivation, characteristics and parameters of photosynthetic activity of these genotypes in crop fields most closely correlating with plant productivity, have been established. The main emphasis was put on: 1) architectonics; 2) CO_2 assimilation; 3) leaf activity within the day and vegetation, and others. One of the aspects of the study was photorespiration.

According to our previous concept (Aliyev, 1974; Aliev and Kazibekova, 1979; Aliyev and Kazibekova, 1988), the optimum plant height and favourable leaf orientation in compact sowings contribute to the effective absorption of solar radiation and development of vegetative and economically valuable organs, i.e. activate those key links of productivity, which ultimately determine the high productivity of wheat variety of "ideal" type (Aliyev, 1983).

Analysis of various wheat genotypes with different values of photosynthetic traits and productivity in conjunction with a range of environmental factors, including mineral nutrition, water, light, etc. showed the wide range of CO_2 assimilation variability in ontogenesis, depending on the morpho-physiological peculiarities of genotypes and their sink-source relations (Aliev and Kazibekova, 1995).

The photosynthetic rate has increased steadily during flag leaf development and reached its maximum value in the earing stage (Figure 15). Two peaks of CO_2 exchange in the most active leaves were observed during ontogenesis: the first peak at the beginning of stalk emergence and the second one at the beginning of flowering. It is important to search genotypes with no or less evident decrease of the photosynthetic rate in this period. High productive genotypes posses a higher rate of CO_2 assimilation throughout the whole lifespan of their flag leaves up to the end of the grain filling stage. This pattern of carbon dioxide exchange at the end of growth period in different genotypes may be due to early death of the lower leaves of extensive varieties. However, in the intensive genotypes, in comparison with extensive ones, the decrease in CO_2 assimilation in the flag leaf was counterbalanced by the ac-

tive CO_2 assimilation in the lower leaves. High productive varieties significantly exceeded (up to 1.5 times) low productive ones by the mean of the photosynthetic rate of upper leaves (flag leaf and the second leaf from the top).

In intensive varieties with the best architectonics, the rate of photosynthesis is higher in the morning, and especially in the evening hours, and afternoon depression of photosynthesis occurs later and is much weaker than that of semi-intensive and extensive varieties. The total photosynthesis during the daytime is higher in high productive varieties than in low productive ones.

The study of the dynamics of photosynthetic rate in ontogenesis showed the availability of multiple peaks specific for genotypes depending on the crop architectonics at the period, when rate of photosynthesis was determined.

It was found out that the rate of photorespiration is higher in intensive varieties than in extensive types. The rate of photorespiration reaches its maximum in the earing stage, and then decreases (Figure 16). In high productive varieties photorespiration remains at a high level during the periods from stalk emergence up to the grain formation and filling than in the low productive ones. Along with increase of photosynthetic rate, the rate of photorespiration increases too. Photorespiration follows the course of photosynthesis, the more intense is photosynthesis, and the more intense is photorespiration. Daily course of photorespiration, in general, coincides with the daily course of leaf photosynthesis at various stages of plant development. However, photorespiration begins at the later hours than photosynthesis, and ends earlier; the curve of its course is unimodal.

The rate of CO_2 assimilation in leaves and other photosynthesizing organs is determined by the size and structure of these organs, plant architectonics both at the individual cultivation and in crop fields, by the sink-source relations genetically stipulated in each genotype, taking into account all affecting factors (Aliyev, 2001 a). The average results from multiple measurements are presented in the Table 1.

Wheat genotypes are characterized by following parameters: leaf length, width, surface area, specific leaf density, leaf inclination angle and orientation, that create an optimal architectonics more favourable for turbulence and high rate of CO_2 assimilation, and possibly for long-term photosynthetic activity of all leaves, ear and other non-leaf organs during grain formation.

The genotypes with two or three times less leaf areas than that with broad leaves produce similar or even greater grain yield. Genotype Gyrmyzy bugda with flag leaf area of 28 cm^2 yields up to 3 t ha^{-1}, and those of 18-19 cm^2 – 7-9 t ha^{-1}. In highly productive genotypes with grain yield ~ 7-9 t ha^{-1}, the flag leaf areas differ almost three times. The studied varieties of winter wheat exhibited significant differences in the rate of flag leaf CO_2 assimilation. The highest values were detected in high productive genotypes Gyrmyzy gul and Azamatli-95, whereas the lowest CO_2 assimilation was characteristic for genotype Gyrmyzy bugda. Vertically oriented small leaves creating an optimal architectonics, probably, promote a relatively high CO_2 assimilation of photosynthesizing leaves of all layers during grain filling.

A comparative study of photosynthetic rate of wheat genotypes with contrast architectonics during the day showed that the diurnal changes in the photosynthetic rate of leaves of all layers and genotypes are characterized by a double-peaked pattern indicating a drastic increase in the photosynthetic

Table 1. Rates of CO_2 assimilation and photorespiration, flag leaf area and grain yield of wheat genotypes

	Genotype	Potential grain yield, t ha^{-1}	Mean flag leaf area, cm^2	Rate [mg CO_2 dm^{-2} h^{-1}]	
				Photosynthesis	Photorespiration
Triticum aestivum L.	Azamatli-95	9	19	34.0±1.7	12.4±0.5
	Giymatli-2/17	7	47	25.2±1.4	8.1±0.4
	Gyrmyzy gul	7	18	36.5±2.1	10.9±0.6
Triticum durum L.	Gyrmyzy bugda	3	28	21.3±1.1	6.2±0.3

*Measurements were carried out at the earing stage, when the rate of photosynthesis reached its maximum, and at the end of leaf growth.
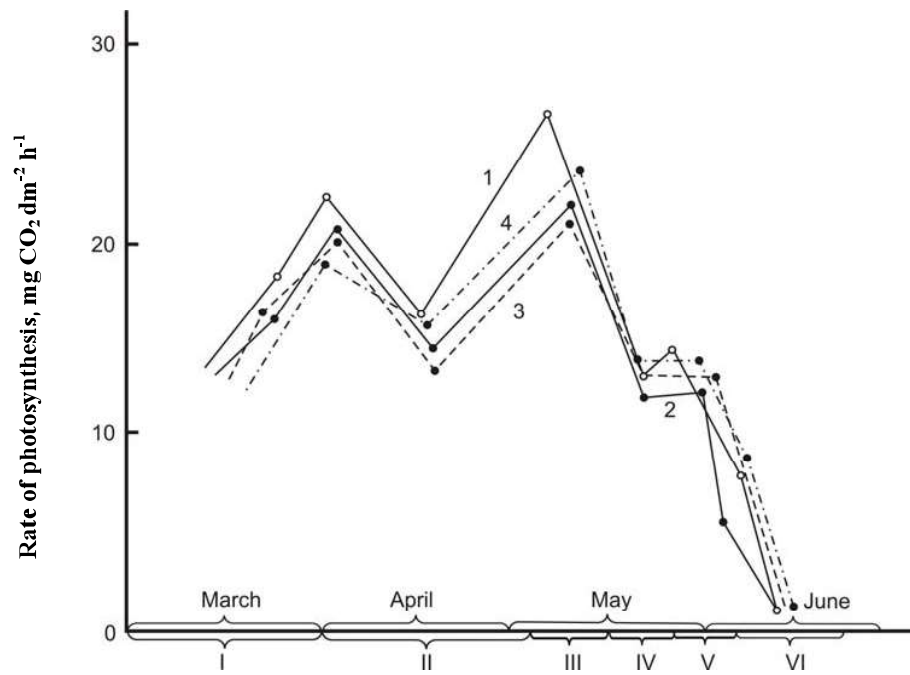
Figure 15. Ontogenetic changes in the rate of CO_2 assimilation in different wheat genotypes:
1 – Oviachik-65, 2 – Shark, 3 – Gyrmyzy bugda, 4 – Caucasus
I – stalk emergence, II – earing, III – flowering, IV – grain formation and filling.
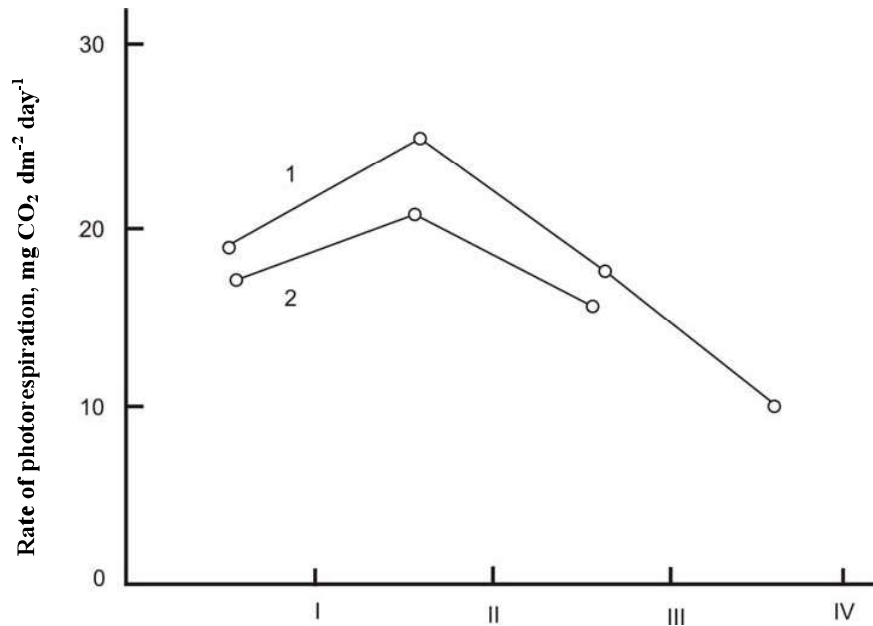

Figure 16. Ontogenetic course of total photorespiration in high productive (Oviachik-65 –
(1)) and low productive (Gyrmyzy bugda – (2)) genotypes:
I – stalk emergence, II – earing, III – flowering, IV – grain formation and filling.

rate in the morning and decrease in the evening (Figure 17). Photosynthesis in the flag leaves began early in the morning (at 6 a.m.), increased during sunrise, reaching its maximum level at 11 a.m. Then photosynthetic rate declined to its lowest at midday. After midday depression of photosynthesis, the second peak was observed at 5 p.m. that correlates with increased photosynthesis.

Not all genotypes with small leaves are high productive and not all genotypes with broad leaves are high or low productive. Genotypes with broad leaves and high yield require sufficient water supply.

In order to better understand the correlation between rates of CO_2 assimilation, photorespiration and productivity, the consideration of basic parameters of plant architectonics is also essential (Figure 18). Obtained data indicates that genotypes with vertically oriented short and narrow leaves (20-30 cm^2), high specific leaf density (SLD) – 600 $mg/100$ cm^2, with stable and long-term intensive CO_2 assimilation (30-40 mg dm^{-2} h^{-1}) and a high tolerance to water stress yield up to 10 t ha^{-1}.
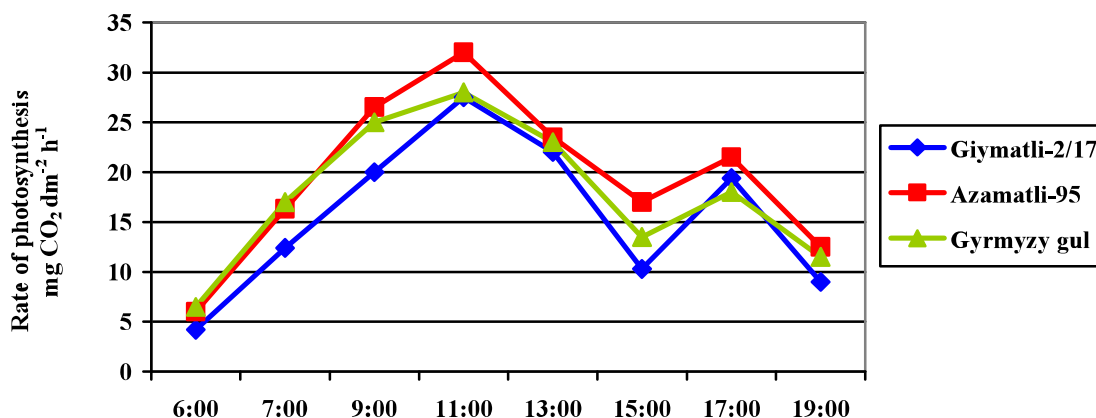

Figure 17. Diurnal course of CO_2 gas exchange of flag leaves of wheat genotypes with different architectonics at the milk ripeness stage.

The high rate of CO_2 assimilation is not accompanied by low rate of photorespiration. For high productive genotypes, the high values of photorespiration are common. Genotypes with grain yield of 7-9 t ha^{-1} possess high rates both of CO_2 assimilation and photorespiration at corresponding architectonics. Genotypes with moderate (4-5 t ha^{-1}) and low (3 t ha^{-1}) grain yield have relatively low rates of CO_2 assimilation and photorespiration.

Gas exchange data closely agree with the measured enzymes activities directly involved in CO_2 fixation.

Throughout the entire period of flag leaf development high productive intensive genotypes in comparison with extensive ones were distinguished by higher activities of RuBP carboxylase and carbonic anhydrase (Aliev et al., 1988, 1996 b). RuBP carboxylase activity as well as CO_2 assimilation rate, increased monotonously since the beginning of the flag leaf formation, reaching its maximum at the earing stage, and then decreased up to the end of the leaf growth (Figure 19). On the contrary, activity of this enzyme in high-stemmed wheat varieties of extensive type decreases rapidly after it has achieved its maximum.

The fact that activities of RuBP carboxylase and carbonic anhydrase changed in parallel during the flag leaf development is evident, indicating that there is a coordinated operation of these enzymes in wheat genotypes (Aliev et al., 1988, 1996 b, c; Aliev and Kazibekova, 1995). Such correlation was found between the rate of CO_2 assimilation and the activity of these enzymes in high productive varieties. Thus, our data show that high activities of RuBP carboxylase and carbonic anhydrase play an important role in maintaining a high CO_2 assimilation rate in the high productive wheat varieties (Aliev et al., 1988, 1996 b).

The activities of the RuBP carboxylase and RuBP oxygenase were higher in the high productive wheat genotypes than in the lower ones (Figure 19, 20). The variation of RuBPO activity in the course of the flag leaf development was similar to that of RuBP carboxylase. As known, RuBPC/O catalyzes a unique reaction of carboxylation and oxidation of RuBP with the subsequent formation of 3-PGA, the primary product of photosynthesis, and phosphoglycolic acid, which is a substrate for photorespiration (Zelitch, 1975). On the other hand, photorespiration is a process, in which part
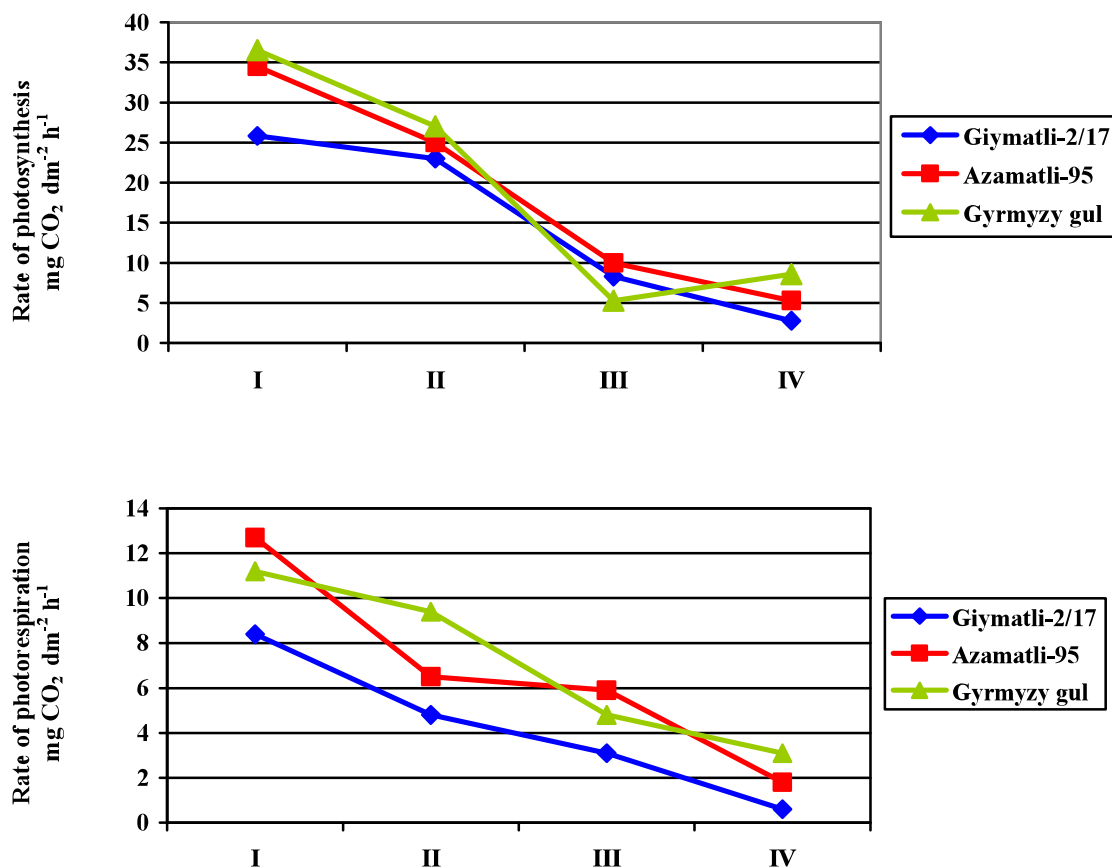
Figure 18. Ontogenetic changes of the rates of photosynthesis and photorespiration in wheat genotypes with different architectonics:
I – earing-flowering, II – milk ripeness, III – end of the milk ripeness, IV – wax ripeness.

of assimilated CO_2 is lost. However, we also observed that short-stemmed wheat varieties with high RuBP oxygenase activity had high grain yield.

During flag leaf ontogenesis of the studied genotypes the ratio of RuBPC/RuBPO activities was maintained approximately at the same level, tending to have a high ratio in intensive types (Garagylchyg-2 – 19.0 ± 1.4; Shiraslan-23 – 18.7 ± 0.9; Gyrmyzy bugda – 16.0 ± 2.0; Sary bugda – 16.2 ± 1.1) (Figure 21) (Aliev et al., 1988, 1996 b; Aliev and Kazibekova, 1995; Aliyev and Kazibekova, 2002). Nevertheless, the variation in the ratio of RuBPC/RuBPO activities during the flag leaf formation is associated with a certain genotypic difference. Hence, studied genotypes differed in the rates of photosynthesis and photorespiration.

Large changes in the RuBPC activity of different ear elements depend on its development and peculiarities of the plant genotype (Figure 22). In comparison with other ear elements, the glume of both intensive and extensive genotypes is character-

ized by higher RuBP carboxylase activity. At the beginning of the grain formation, the RuBPC activity in the ear glume of the intensive genotype was also higher than in the extensive one. However, later this activity, calculated per mg of protein, decreased in the intensive genotypes, but remained the same in the extensive ones. Later, during grain filling, a significant increase of RuBPC activity in the glume occurred both in the intensive and extensive genotypes.

During all periods of measurements, the ear awns of the intensive genotype had a higher activity of RuBP carboxylase than those of the extensive genotype at the earing and grain filling stages.

The RuBPC activity in grain of the low productive genotype was higher than that of the high productive one only at the beginning of grain filling. A gradual decrease in the enzyme activity during grain formation was observed in both genotypes.

The measurement of RuBP oxygenase activity in the different ear elements indicated that
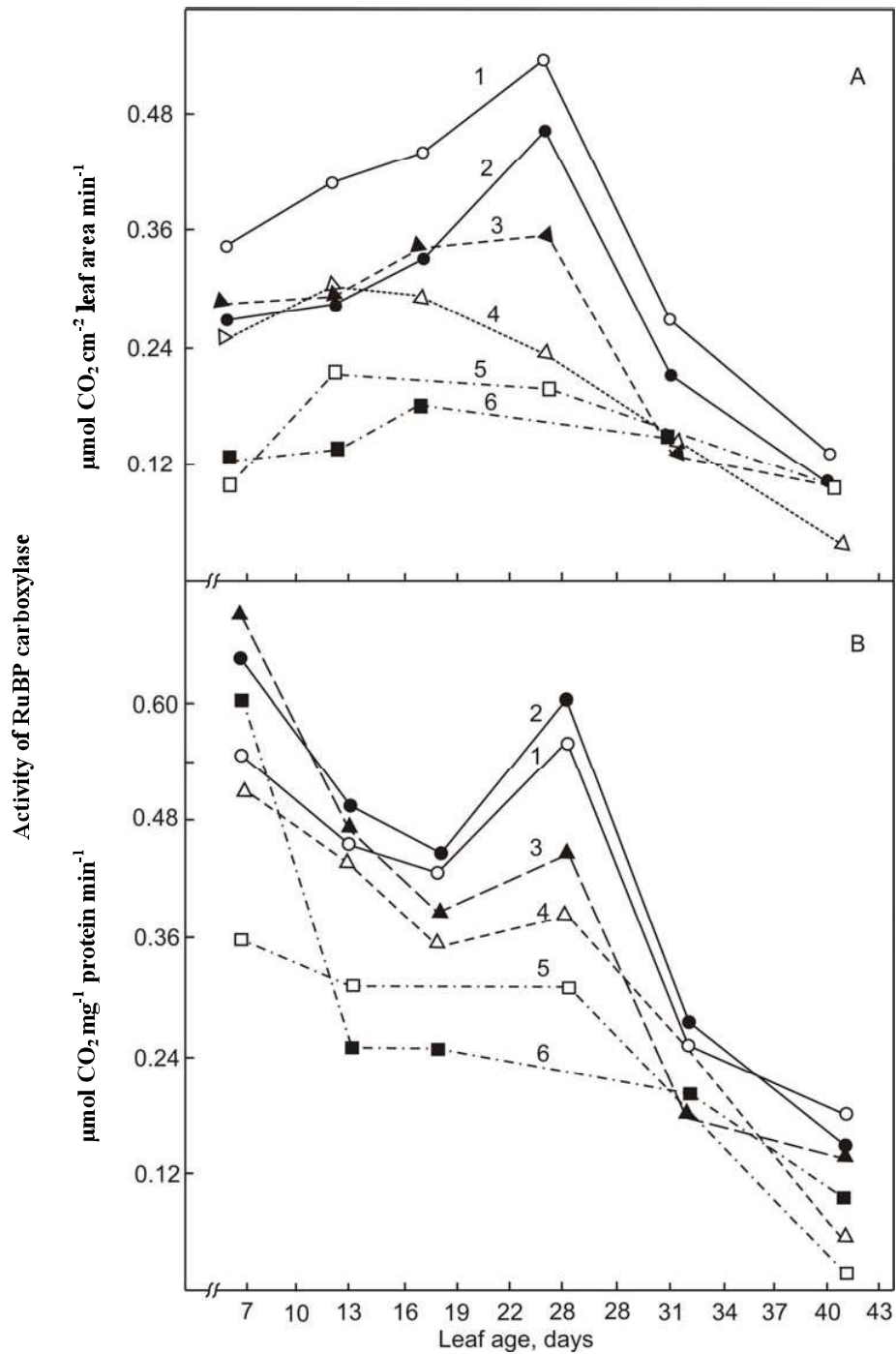
Figure 19. Ontogenetic changes in RuBP carboxylase activity (A - μmol cm^{-2} (leaf area) min^{-1}; B - μmol mg^{-1} (protein) min^{-1}) in flag leaves of wheat genotypes:
1, 2 – short-stemmed, high productive; 3, 4 – small leaves, medium productive; 5, 6 – long-stemmed, low productive wheat varieties.

Figure 20. Ontogenetic changes in RuBP oxygenase activity (A - μmol cm^{-2} (leaf area) min^{-1}; B - μmol mg^{-1} (protein) min^{-1}) in flag leaves of wheat genotypes:
1, 2 – short-stemmed, high productive; 3, 4 – small leaves, medium productive; 5, 6 – long-stemmed, low productive wheat varieties.
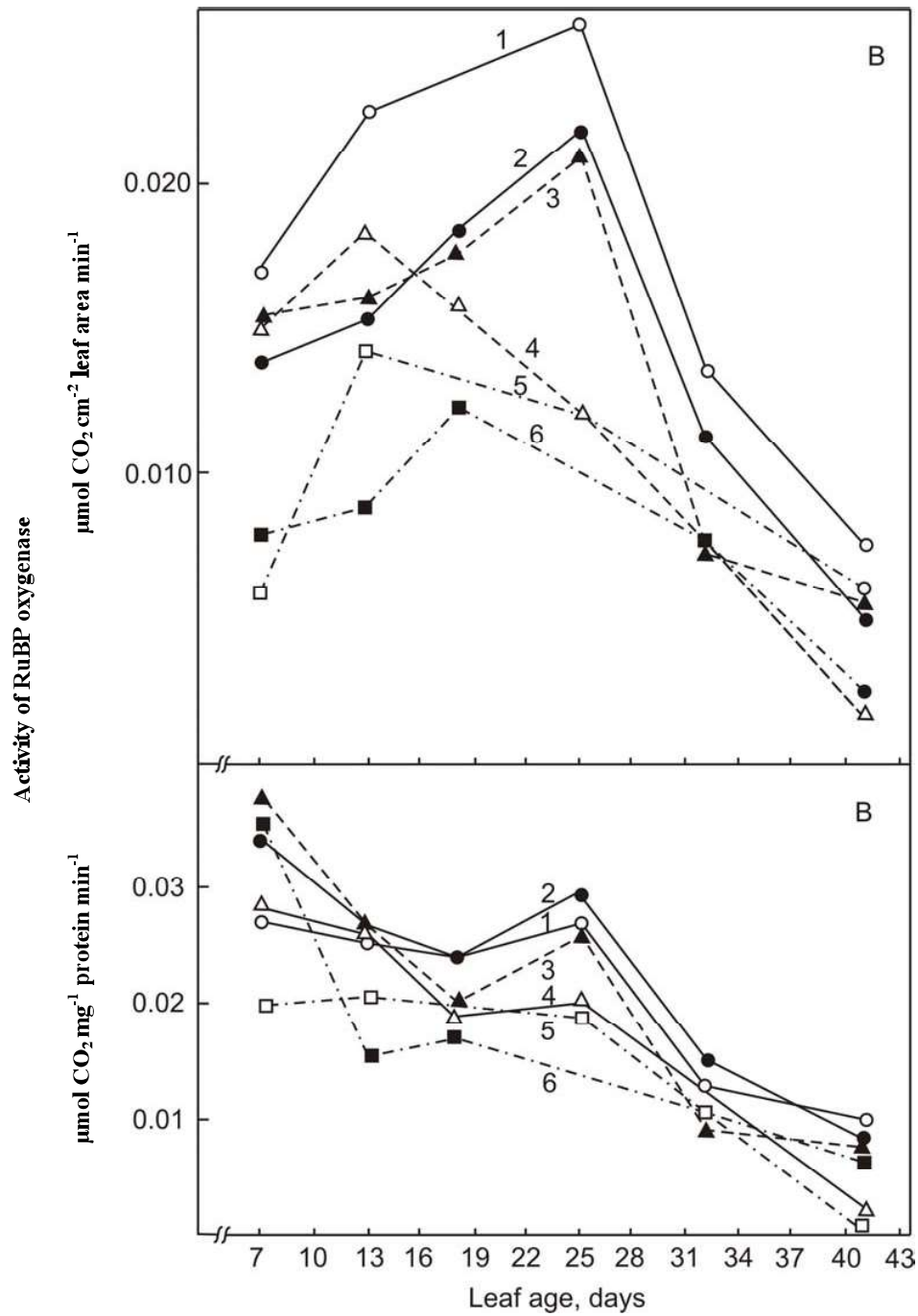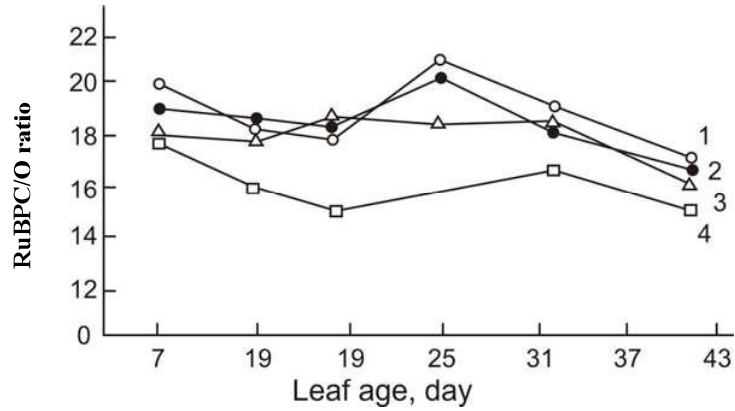
Figure 21. Changes in the ratio of RuBP carboxylase to oxygenase activities in flag leaf ontogenesis of different wheat genotypes:
1 – Garagylchyg-2, 2 – Shiraslan-23, 3 – Gyrmyzy bugda, 4 – Sary bugda.

Figure 22. Variations in activities of RuBP carboxylase (A) and RuBP oxygenase (B) in ear elements of wheat genotypes during grain filling:
1 – awn, 3 – glume, 5 – grain of short-stemmed high productive genotype Shiraslan-23;
2 – awn, 4 – glume, 6 – grain of long-stemmed low productive genotype Gyrmyzy bugda.

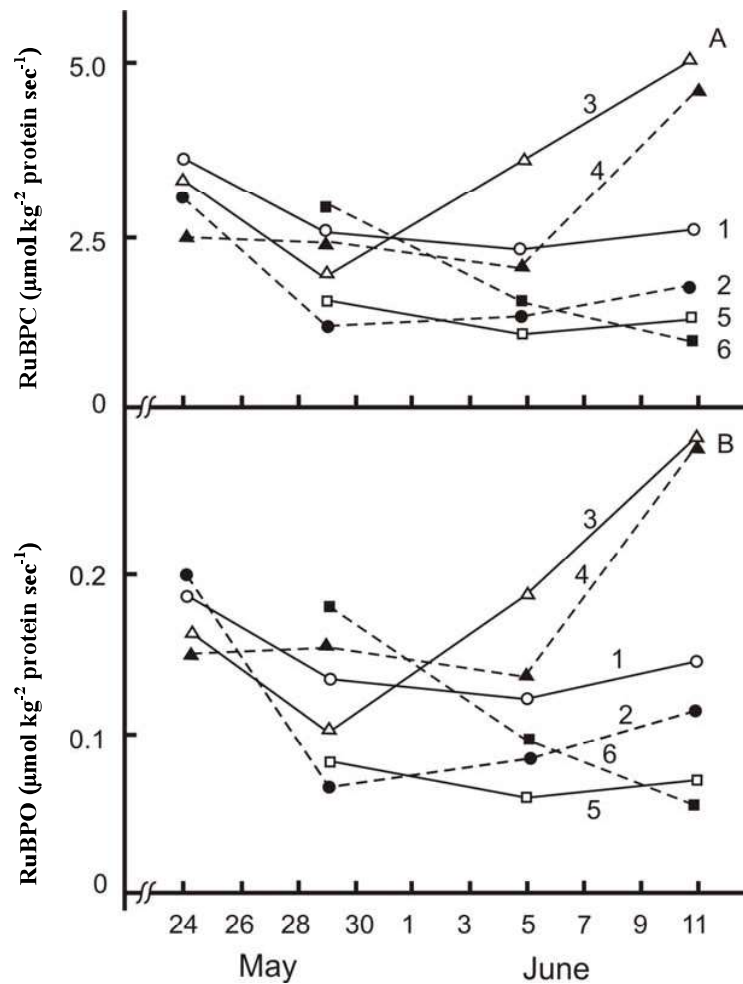during grain formation the activities of RuBPC and RuBPO changed in parallel similarly as it is observed for the flag leaf (Figure 20).

Activities of RuBP carboxylase and RuBP oxygenase in high and low productive genotypes increased in awns, and especially in the glume, during grain filling. Notably, the sharp increase in the activity of both enzymes in the glume coincides temporally with a decrease in their activity in flag leaf. Therefore, during the period of grain filling, the ear elements and the glume actively participated in the process of CO_2 assimilation (Aliyev, 2002).

Thus, the results obtained using various methods on different plant genotypes showed that RuBP carboxylase and oxygenase activities change in parallel in the course of plant breeding process. Each wheat genotype was characterized by a definite value of RuBPC/O ratio and its variation under different influences (in particular, under artificial violation of the sink-source relations) was temporary.

Photorespiration requires the integration of biochemical pathways in three separate leaf cell organelles: chloroplasts, peroxisomes and mitochondria (Figure 23). Peroxisomes as glyoxysomes refer to microbodies. In mesophyll cells peroxisomes, chloroplasts and mitochondria are often located nearby, supporting an intensive metabolism between these organelles. Currently the biochemical mechanism of photorespiratory pathway is sufficiently well studied. The initial stage of photorespiration takes place in chloroplast stroma. According to most researchers, the initial substrate for the photorespiration is glycolate. Reactions associated with photooxidative transformation of RuBP and formation of phosphoglycolate are considered to be key processes of photorespiration. As a result of oxygenase activity, one molecule of 3-phosphoglycerate (integrated into the Calvin cycle) and one molecule of 2-phosphoglycolate (first molecule of photorespiratory glycolate cycle) instead of two molecules of 3-phosphoglycerate are formed. Under the influence of a key photorespiratory enzyme, phosphoglycolate phosphatase (PGPase), the phosphoglycolate is converted into glycolate, which then leaves the chloroplast and enters the peroxisome.

$$RuBP + O_2 \rightarrow phosphoglycolate + PGA$$
$$Phosphoglycolate \rightarrow glycolate + P_i$$
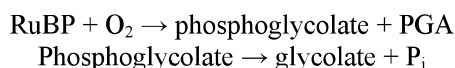
Phosphoglycolate phosphatase catalyzes the hydrolysis of phosphoglycolate, which is produced under the ribulose-1,5-bisphosphate oxygenase activity of ribulose-1,5-bisphosphate carboxylase/oxygenase. PGPase-deficient mutants cannot grow in the ambient air (0.04% CO_2 and 21% O_2)

and require elevated levels of CO_2 (Randall, 1976; Husic and Tolbert, 1984; Hall et al., 1987; Suzuki et al., 1990; Norman and Colman, 1991). This is most likely because phosphoglycolate accumulated during photosynthesis in the ambient air strongly inhibits an enzyme triose phosphate isomerase (Wolfendon, 1970; Anderson, 1971; Suzuki et al., 1999).

Richardson and Tolbert (1961) were the first to find a phosphatase activity specific for phosphoglycolate in tobacco leaves. Later it was shown that all plants and algae possess such activity (Randall and Tolbert, 1971; Randall et al., 1971). The occurrence of phosphoglycolate in mammalian cells was first shown by Rose and Salon (1979) and has been confirmed by Spear and Vora (1986). Data obtained with pyruvate kinase-deficient red blood cells suggest that phosphoglycolate is synthesized by pyruvate kinase *in vivo* (Rose, 1976). The remarkable similarity in the kinetic characteristics of animal PGPases to plant PGPases has been described previously (Seal and Rose, 1987). Although PGPase requires a divalent cation such as Mg^{2+} and a monovalent anion such as Cl^- for its activity in presence of phosphoglycolate as a substrate.

PGPase has also been partially purified from human red blood cells and other tissues (Turner and Hopkinson, 1981). The one autosomal gene locus for PGPase has been assigned to human chromosome 16 (Povey et al., 1980), and enzyme exhibits genetic polymorphism in some ethnic groups.

It is known that phosphoglycolate as a specific substrate for the PGPase initiates a 2,3-bisphosphoglycerate phosphatase activity of the bifunctional enzyme 1,3-phosphoglycerate mutase (BPGM, EC 5.4.2.1). In the presence of phosphoglycolate phosphatase BPGM activity is stimulated more than 100 times (Rose, 1976). Phosphoglycolate inhibits rabbit (Wolfendon, 1970) muscle triose phosphate isomerase (EC 5.3.1.1) and it activates the breakdown of 2,3-bisphosphoglycerate (Rose and Liebowitz, 1970), which is a regulator of the oxygen affinity of hemoglobin (Rose et al., 1986). PGPase also seems to have an important role in animals by affecting the phosphoglycolate level.

Thus, the PGPase is essential for all autotrophic organisms and is also important for the function of human red blood cells (Rose et al., 1986; Mamedov et al., 2001). Another reaction catalyzed by bisphosphoglycerate mutase, which transforms 1,3-bisphosphoglycerate into 2,3-bisphosphoglycerate (2,3-BPG), which may be then converted into 3-phosphoglycerate, a glycolysis metabolite by 2,3-bisphosphoglycerate phosphatase activity (EC 3.1.3.28), can occur in glycolytic pathway. In the erythrocytes 2,3-BPG is produced in significant quantities and serves as the allosteric regulator of hemoglobin. 2,3-BPG binding to hemoglobin de-

creases its affinity for oxygen, promotes the dissociation of oxygen and its transition into tissues. Hemoglobin, oligomeric protein, is able to bind 4 different ligands: O_2, H^+, CO_2 and BPG to its specific sites. All these ligands are bound to spatially separated sites, but the conformational changes of the protein in the one ligand binding site are transmitted to the whole oligomeric protein and alter the affinity of the other ligands to this protein (Severin, 2006, 2009). So, the O_2 amount that enters the tissue depends not only on the partial pressure of O_2, but also on the concentration of allosteric ligands that increases possibilities of hemoglobin functions regulation.

Further conversion of glycolate takes place in the peroxisomes. Carbon metabolism in photorespiration describes the sequence of reactions series of so-called "glycolate pathway", most of which are localized in peroxisomes and mitochondria (Beevers, 1969; Zelitch, 1972; Tolbert, 1973, 1981, 1997). Surrounded by single membranes peroxisomes are small, ubiquitous eukaryotic organelles mediating a wide range of oxidative metabolic activities that vary by the species, cell type, and environmental conditions, in which organism lives (Beevers, 1979; Van den Bosch et al., 1992). Plant peroxisomes are essential to physiological processes such as lipid metabolism, photorespiration, and plant hormone biosynthesis and metabolism (Olsen and Harada, 1995; Reumann and Weber, 2006; Reumann et al., 2009). Peroxisomes are characterized by high activity of catalase and flavin oxidases and contain most of the enzymes of the glycolate pathway.

In peroxisomes glycolate is oxidized to glyoxylate by glycolate oxidase (EC 1.1.3.1.), a flavin-containing enzyme. The second product of the reaction, hydrogen peroxide, is decomposed to H_2O and O_2 by catalase (EC 1.11.1.6) due to high content of latter in peroxisomes (Grodzinski, 1978; Walton and Butt, 1981; Wingler et al., 1999). The next reaction step in the photorespiratory pathway is the transamination of glyoxylate to glycine (Igarashi et al., 2006) by glutamate:glyoxylate aminotransferase (GGAT, EC 2.6.1.4.), which transfer the amino group from glutamate to glyoxylate with production of 2-oxyglutamic acid.

Further photorespiratory reactions occur in mitochondria. Glycine produced in peroxisomes moves to mitochondria, where conversion to L-serine occurs via condensation reaction of two molecules of glycine with release of one molecule of ammonia (NH_3) and carbon dioxide (CO_2) (Walker and Oliver, 1986; Oliver, 1994; Bauwe and Kolukisaoglu, 2003; Voll et al., 2006). NADH is generated during glycine decarboxylation, which oxidation in the mitochondria requires additional O_2 fixation. NH_4^+ synthesized in the reaction of decarboxylation is effectively refixed to produce glutamate. The oxidation of glycine to serine is accompanied by the synthesis of three ATP molecules. This amount of ATP is more than enough to reassimilation of ammonia and its utilization in glutamine synthesis, so the plant does not lose its nitrogen. Nitrogen assimilation in the process of photosynthetic carbon assimilation consumes ~ 13% of recovery force. Proteins synthesis from amino acids and synthesis of carbohydrates such as sucrose and starch require additional energy consumption. In another way the recovered energy from glycine oxidation can be transferred to peroxisomes and used in recovery of hydroxypiruvate to glyceric acid.

The synthesized serine returns to peroxisomes. Serine is converted to hydroxypiruvate by serine:glyoxylate aminotransferase (EC 2.6.1.45), which is then reduced by hydroxypiruvate reductase (EC 1.1.1.29) to form the glycerol. Further metabolism of serine may also be related to its inclusion into proteins. Glycerate returns from peroxisomes to the chloroplasts. Glycerol kinase (EC 2.7.1.31) localized in chloroplasts (Boldt et al., 2005) catalyzes glycerol conversion to 3-phosphoglycerate, which then enters the Calvin cycle.

Translocators in the inner membrane of chloroplasts and mitochondria perform the exchange of metabolites between compartments involved in photorespiration. Metabolism occurs through porin-like channels localized in the membrane of leaf peroxisomes, which are integral pore membrane proteins performing direct non-selective transport of low-molecular-mass compounds (Yu et al., 1983; Weber and Flügge, 2002; Reumann and Weber, 2006; Kaur et al., 2009).

Hence, the reactions associated with the conversion of glycolate to phosphoglycerate and accompanied by oxygen fixation (in the chloroplasts and peroxisomes) and CO_2 release occur during photorespiration. Accordingly, the total balance of gas exchange in leaves in the light consists of two processes - photosynthesis and photorespiration.

The rate of integral photosynthetic process and also its enzymatic and metabolic activity changes during the leaf life cycle. Obtained results showed that studied genotypes also differed significantly in the level of photosynthetic carbon metabolism (Jahangirov, 1987, Aliev et al., 1996 b).

During flag leaf formation the rate of CO_2 assimilation increases, but reaches the maximum at the earing stage (Figure 24, A). Flag leaf grows to its largest area in this stage (Figure 24, B). At flowering stage rate of CO_2 assimilation decreases and then remains almost constant until milk ripeness. As far as leaf grows and active photosynthetic ap-
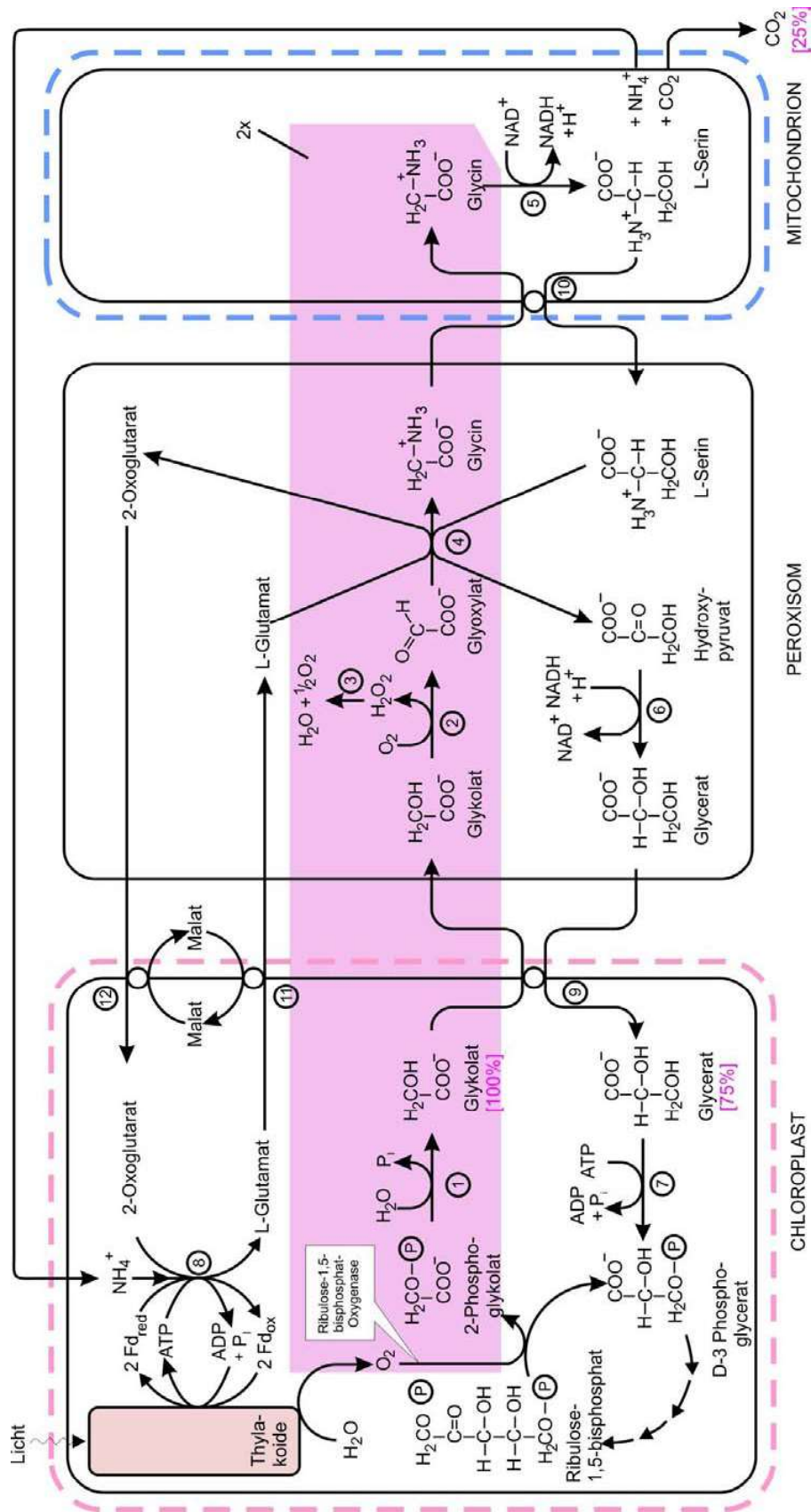
Figure 23. Reaction pathways and compartmentation of photorespiration (Grafic: E. Weiler) (Bresinsky et al., 2008).

paratus develops, it completely changes from acceptor of assimilates into it source. In the flag leaf ontogenesis, the biosynthesis of non-sugar compounds such as alanine, malate and aspartate decreased in absolute and relative units (Figure 24, C, D), and the biosynthesis of sucrose, the main transport form, increased (Figure 25, A). The rate of sucrose biosynthesis was about 80% of the total rate of CO_2 assimilation (Jahangirov, 1987). The pattern of sucrose biosynthesis changes in the same way as the total CO_2 assimilation during ontogenesis. Unlike the abovementioned compounds, the starch biosynthesis was more constant (Figure 25, A, B). Value of sucrose/starch ratio was maintained at a very high level (Figure 25, B).

Studies showed that the biosynthesis rate and the total value of glycine-serine increased during transition from the stalk emergence to earing, then decreased at the flowering stage, and then its level remained virtually constant (Figure 25, C, D).

These characteristics directly depend on the rate of CO_2 assimilation. It is known that under the ambient CO_2 and O_2, the biosinthesis of glycine and serine is linked to photorespiratory carbon pathway during photosynthesis. **Therefore, correlation between biosynthesis rate as well as the total value of glycine-serine and photosynthesis is due to the fact that photosynthesis and photorespiration change proportionally to one another during the wheat leaf ontogenesis.**

Kinetic characteristics of photosynthetic carbon assimilation calculated from the kinetics of $^{14}CO_2$ incorporation into photosynthetic products are listed in the Table 2. The data show that radiocarbon was allotted to sugars (mainly, sucrose), glycolate metabolites (glycine-serine) and, to a small extent, amino and organic acids such as malate, aspartate and alanine. Flag leaves were fully expanded at the time of labeling and served as active assimilate sources and, perhaps, the rates of amino and organic acid labeling were similar in both groups of wheat varieties, measured as 3-6% of the total rate of $^{14}CO_2$ assimilation (Aliev et al., 1996 b, c).

The studied varieties hardly differed in ^{14}C incorporation into starch. Unlike sugars, starch incorporated not more than 5-8% of the label.

Comparative studies of the photosynthetic carbon metabolism showed that at the milk ripeness stage the rates of sucrose and glycine-serine synthesis averaged 5.7 and 1.1 μmol CO_2 $dm^{-2}min^{-1}$, respectively, and these rates were similar both in extensive and intensive varieties. It should be noted that value of the sucrose biosynthesis and the rate of the total value and biosynthesis of glycine-serine at the stage of earing was higher in the short-stemmed intensive genotypes compared with the extensive ones. The rate of sucrose synthesis for high productive genotypes averaged 10.8 and 8.0 μmol CO_2 dm^{-2} min^{-1} for low productive ones; and rates of glycine-serine synthesis for high and low productive genotypes were approximately 2.7 and 1.64 CO_2 $dm^{-2}min^{-1}$, respectively. At earing stage, these genotypes had higher rate of CO_2 assimilation. Photorespiration rate could be evaluated by the rate of synthesis and total value of glycine-serine. Experimental data suggest that photorespiration rate at this stage was also higher in high productive genotypes.

Thus, the rates of $^{14}CO_2$ incorporation into starch and also alanine, malate and aspartate in high and low productive genotypes were similar. However, the rate of ^{14}C incorporation into glycolate metabolites and sucrose, as well as CO_2 assimilation rates, were higher in high productive genotypes.

Wheat along with other C_3-plants is characterized by relatively high value of CO_2 release in the light, which consists of photorespiration and dark respiration in the light. A similar conclusion can be drawn on the basis of measurements of the components of carbon dioxide exchange in different wheat varieties. Accordingly, the rates of net and true photosynthesis were highest in Garagylchyg-2. The rate of CO_2 release in the light was 11.4 and 8.7 mg CO_2 dm^{-2} h^{-1} in Garagylchyg-2 and Gyrmyzy bugda, respectively (Figure 26).

The rate of CO_2 release in the light due to dark respiration was similar in all studied genotypes. However, the rate of CO_2 release due to photorespiration was higher in genotype Garagylchyg-2 and reached 8.7 and 6.2 mg CO_2 dm^{-2} h^{-1} in Garagylchyg-2 and Gyrmyzy bugda, respectively. The ratio of CO_2 release rate in the light due to photorespiration to the net CO_2 assimilation rate was similar in both varieties and averaged about 22.0 and 21.2%, respectively, that indicates a positive correlation between the rates of photosynthesis and photorespiration (Jahangirov, 1987; Aliev et al., 1996 b). These results demonstrate that, despite increased photorespiration in high productive genotypes, they showed high rates of net photosynthesis due to increased true photosynthesis. This statement is also confirmed by higher rates of true photosynthesis and the amount of CO_2 released in the light by photorespiration. Thus, there is a parallel increase in the rates of true photosynthesis and photorespiration in leaf ontogenesis. The ratio of true photosynthesis to photorespiration in genotypes with different productivity is equal on average to 3:1 and a slight increase in intensive genotypes. A value of photorespiration constitutes 28-35% of photosynthetic rate in contrasting wheat genotypes.

Based on these results we can conclude that attempts to find or create high productive genotypes
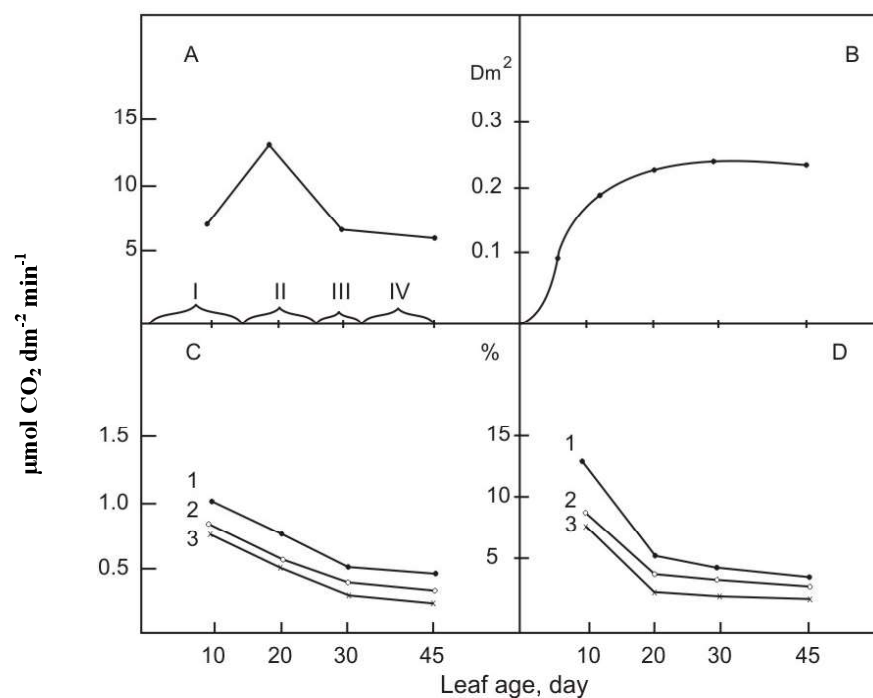
Figure 24. Biosynthesis of malate, aspartate and alanine in flag leaf ontogenesis of wheat variety Garagylchyg-2:

I – stalk emergence, II – earing, III – flowering, IV – grain filling
A – rate of CO_2 fixation; B – leaf area; C – malate (1), aspartate (2), alanine (3); D – the same as C (% of the total CO_2 fixation rate).
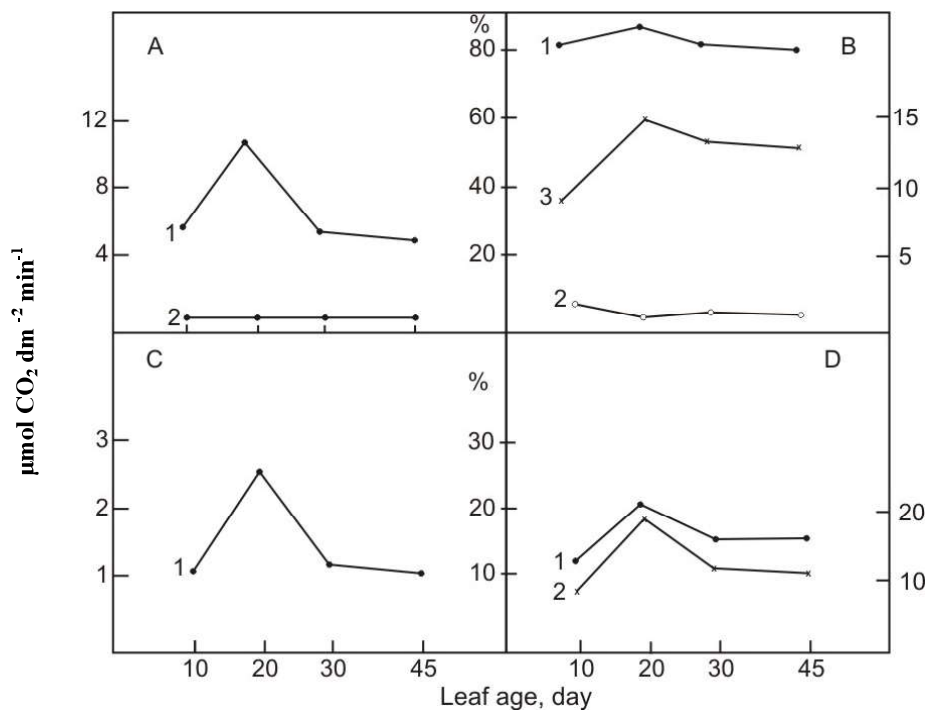

Figure 25. Biosynthesis of sucrose, starch and total glycine-serine in flag leaf ontogenesis of wheat variety Garagylchyg-2:
A – sucrose (1), starch (2); B - the same as A (% of the total CO_2 fixation rate) (1, 2), rate of sucrose to starch (3); C – glycine-serine; D – the same as C (% of the total CO_2 fixation rate) (1), total value of glycine-serine (2).

Table 2. Kinetic characteristics of photosynthetic carbon metabolism in different varieties of winter wheat at the earing and milk ripeness stages

Metabolite		Garagylchyg-2		Azamatli-95		Gyrmyzy bugda		Sary bugda	
		earing	milk ripeness	earing	milk ripeness	earing	milk ripeness	earing	milk ripeness
Total assimilation, [μmol CO_2 dm^{-2} min^{-1}]		12.3	7.0	13.0	7.3	9.6	7.1	9.8	6.8
Alanine	1	0.41	0.21	0.40	0.25	0.36	0.23	0.32	0.20
	2	3.30	3.00	3.20	2.40	3.90	3.20	3.30	2.90
Malate	1	0.70	0.29	0.68	0.30	0.59	0.32	0.56	0.31
	2	5.70	4.10	5.20	4.20	6.10	4.50	5.70	4.60
Aspartate	1	0.49	0.23	0.51	0.24	0.47	0.20	0.50	0.22
	2	4.00	3.30	3.90	3.30	4.90	2.80	5.10	3.20
Glycine-serine	1	2.50	1.10	2.80	1.20	1.57	1.0	1.70	1.10
	2	20.7	15.7	21.5	16.0	16.4	14.7	17.0	15.7
Sucrose	1	10.6	5.50	10.9	5.80	7.80	5.50	8.20	5.80
	2	86.0	78.0	84.0	79.0	81.0	77.0	82.0	81.0
Starch	1	0.70	0.45	0.72	0.48	0.70	0.50	0.65	0.53
	2	5.70	6.40	5.50	6.60	7.30	7.00	6.60	7.80

Note: 1 – rate of synthesis [μmol CO_2 dm^{-2} min^{-1}]; 2 – rate of synthesis (% of the total CO_2 fixation rate). The kinetic characteristics were calculated from the pattern of $^{14}CO_2$ incorporation into photosynthetic products.
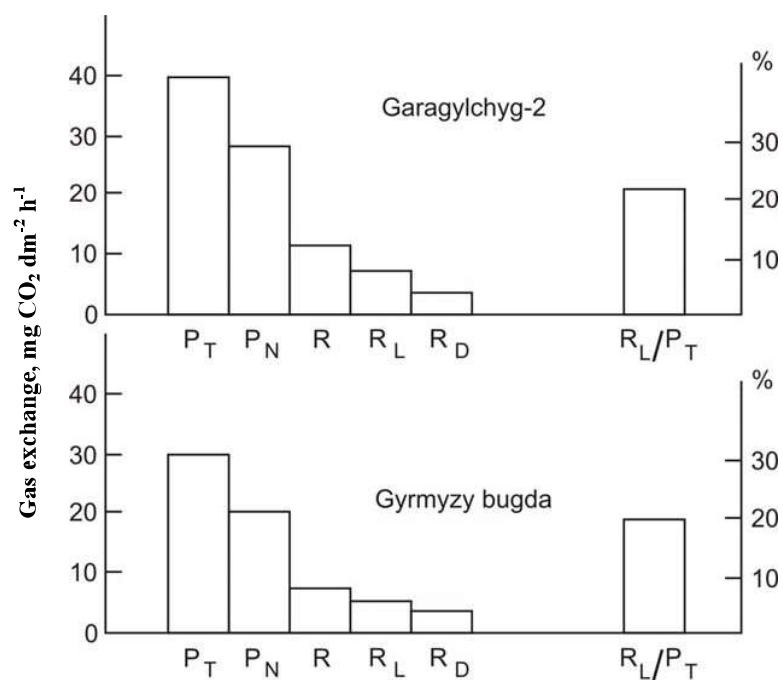
Figure 26. Components of CO_2 exchange in the wheat varieties Garagylchyg-2 and Gyrmyzy bugda (mg CO_2 dm^{-2} h^{-1}):

P_T – true photosynthesis; P_N – net photosynthesis; R – CO_2 release in the light; R_D – CO_2 release in the light due to dark respiration; R_L – CO_2 release in the light due to photorespiration; R_L/R_T – rate of photorespiratory CO_2 release to true photosynthesis (%).

with high photosynthesis and low photorespiration (or low RuBP oxygenase activity) have no future and it is advisable for plant breeders to focus on genotypes that have higher activities of carbonic anhydrase and RuBP carboxylase and high photo-respiration.

As mentioned above, high productive wheat genotypes are characterized by higher value of RuBP oxygenase activity and rate of CO_2 release during photorespiration. Obtained data shows that short-stemmed varieties developed by plant breeders with optimal architectonics for the effective use of solar energy, despite high rate of photorespiration have a high rate of net photosynthesis due to enhanced true photosynthesis provided by high activities of RuBP carboxylase and carbonic anhydrase, and the latter contributes to the efficient functioning of the former at carboxylation sites of chloroplasts. On the other hand, it should be noted that the products of glycolate metabolism can also be used in sucrose synthesis or may be transported from the leaves. Therefore, under certain conditions the products of glycolate metabolism can contribute to the active transport of assimilates, thereby creating conditions for the maintenance of photosynthesis at a high level.

Investigation of the transport and distribution of assimilates showed that the higher a leaf layer, the greater an amount of assimilates exported to the ears (Aliev et al., 1996 a). At the same time because of a shorter distance between the leaf and the ear and high attractive force of the ear in high productive genotypes, more assimilates exported from the leaves than in other genotypes. Particularly, the lower leaves of high productive genotypes in all growth stages more actively involved in grain filling than lower leaves of low productive ones, and they gain assimilates from the flag leaf. In the short-stemmed genotype synthesized assimilates are more effectively used in grain formation and less are spent on vegetative mass growth.

Intensive varieties distinguish by higher rate of photosynthetic rate of ear (Figure 27) (Aliyev et al., 1987). Under similar conditions the rate of flag leaf photosynthesis is higher than that of the ear, and ear exports more assimilates into the grain than the flag leaf. Apparently, assimilating ear mass is higher than that of the flag leaf and ear assimilates directly exported to the grain.

Contribution of ear in formation of grain yield is higher in high productive genotypes than in low productive ones (Table 3). After leaf death, the role of the ear gain a particular importance, since at this time ear become, in fact, the only source of assimilates required for the completion of grain filling.
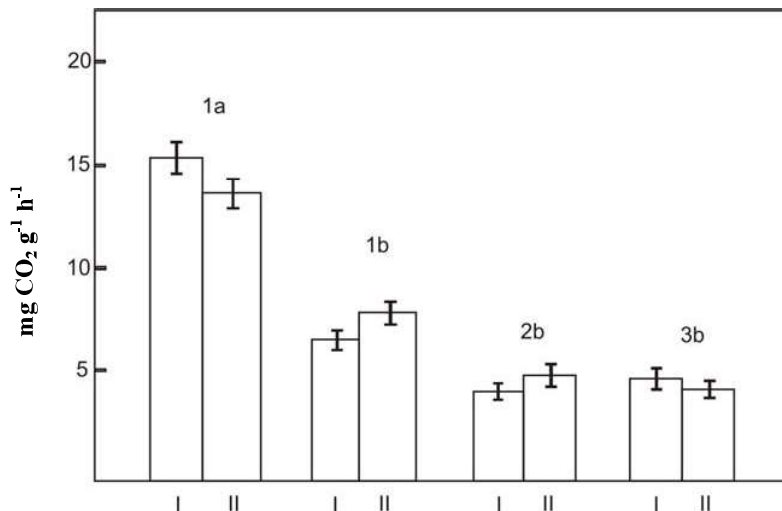

Figure 27. The rate of ear photosynthesis in different wheat genotypes:
I – flowering, II – milk ripeness; a – flag leaf, b – ear;
1 – Garagylchyg-2, 2 – Gyrmyzy bugda, 3 – Kansas-63323.

Table 3. The radioactivity of ear under $^{14}CO_2$ incorporation into ear and flag leaf ($\times 10^3$ impulse per min)

Genotype		Garagylchyg-2		Gyrmyzy bugda		Kansas-63323	
Phase of $^{14}CO_2$ incorporation		flowering	milk ripeness	flowering	milk ripeness	flowering	milk ripeness
Donor of ^{14}C	Ear	75.0±3.8	118.3±5,8	63.1±2.5	86.6±3.5	32.3±1.2	30.4±1.9
	Flag leaf	54.0±2.7	53.1±1.9	41.1±1.8	59.0±2.0	20.6±2.0	21.1±2.6

36

Changed sink-source relationships with the removal of leaves ^{14}C incorporation into carbohydrates increased and into glycolate metabolites decreased in low productive genotypes due to increase in source capacity of flag leaf. In high productive genotypes it is less expressed. The removal of a part of the ear resulted in a reduction of its acceptor force; and the rate of ^{14}C incorporation into the glycine-serine decreased and into sucrose slightly increased in extensive genotypes. At the same time the activity of all studied enzymes, including RuBP oxygenase, decreased. In intensive genotype removal of the ear part is accompanied by a slight increase in the rate of ^{14}C incorporation into the glycine-serine, and labeling into sucrose decreased notably. In high productive genotype removal of the ear part resulted in reduced RuBP carboxylase activity in the flag leaf. However, the activities of the RuBP oxygenase and carbonic anhydrase slightly increased (Khudiyev, 1998).

Similar results were obtained in the study of photosynthesis, photorespiration and key indexes of photosynthetic activity of the other wide spread C_3-plant, the representative of leguminous family, the soybean (Glycine max (L.) Merr.). The soybean is one of the oldest cultivated plants. The seeds of soybean are widespread food known in China as early as the third millennium BC. In 62 countries the total area under the soybean grown as a universal food, forage and industrial legume, is more than 60 million ha and the gross grain production exceeds 100 million tons. Soybean is distinguished by not typical for plants right balance of proteins, fats and carbohydrates and other valuable substances: vitamins (A, B, C, D, E), easily digestible mineral salts (Ca, K, M, P), enzymes and phosphatides. The soybean seeds contain up to 50% of proteins, 27% of fats, and about 30% of carbohydrates. About 400 kinds of different products are made from soybean (Aliyev and Akperov, 1995, 1998).

As a result of long-term researches on photosynthetic activity of highly contrasting soybean genotypes under different growth conditions the optimal morpho-physiological traits, parameters which determine the formation of the optimal structure of crop were revealed, and a model that meets the time, place and environmental requirements was created (Aliyev et al., 1981, 1982 a; Aliyev and Akperov, 1985, 1986, 1995, 1998). "Ideal" soybean genotypes under the optimal growth conditions should maximize the use of environmental factors (light, water, mineral and organic elements sources, etc.), should be characterized by a high level of homeostasis, high photosynthetic productivity, increased synthesis of high-quality proteins, compact shape of bunch, medium-sized leaves with minor inclination angles between petioles from stem and branches, multibean tassels, and well filled pods and medium-sized seeds.

Analysis of morpho-physiological traits of the soybean genotypes showed that the main yield factors are the conditions of all photosynthetic systems functioning at the crop level determined by the cultivation conditions, especially, mineral nutrition and irrigation. It was shown that high agricultural background provides not only the increase in productivity, but also a significant improvement in grain quality (Aliyev and Akperov, 1986). Intensive genotypes with the optimal architectonics have high photosynthetic activity and provide high yield (3.5-4 t ha^{-1}) and high grain quality (40% of proteins).

The dynamics of diurnal variations in CO_2 gas exchange is similar in various soybean genotypes in many respects and possess some common trends (Figure 28). It was established that regardless of growth conditions the observed photosynthetic activity is characterized by double-picked curves, sharply increasing photosynthetic value in the morning and the midday depression. At sunset the photosynthetic gas exchange turns into the respiratory one. The high productive genotypes are distinguished by a higher rate of photosynthesis. Application of mineral fertilizers significantly improves the photosynthetic activity of plants in field and influence on the course of diurnal variations in gas exchange. This, generally, manifests as maximum values of photosynthesis and respiration over the day (Mirzoyev, 1990; Aliyev et al., 1992).

The rate of photosynthesis in leaves of various soybean genotypes gradually increases from branching stage, and reaches a maximum value in high productive genotypes (on average 24 mg CO_2 dm^{-2} h^{-1}) during the periods from pod formation till grain filling. In the low productive genotypes, the greatest value of photosynthetic rate (21 mg CO_2 dm^{-2} h^{-1}) was observed at the initial stage of grain filling, and it lasted for a short period of time (Figure 29). Consequently, the duration of the periods from pod formation till grain filling has a great importance for the grain yield (Mirzoyev, 1988 a, b; Akperov and Mirzoyev, 1990; Aliyev et al., 1992). Improvement of the growth conditions significantly contributes to increasing of photosynthetic activity of plants in field. And rate of photosynthesis increases by 30-50% (Aliyev et al., 1992).

The change in carbon dioxide gas exchange components, excepting dark respiration, in all studied genotypes occurs proportionally during ontogenesis (Figure 30). The maximum value of these components in the low productive genotypes is observed at 60 days of age, in the high and medium productive ones - at 80-90 days of age. The ratio of true photosynthesis to photorespiration in leaves is quite constant and averages 29% in the low productive varieties and 35%
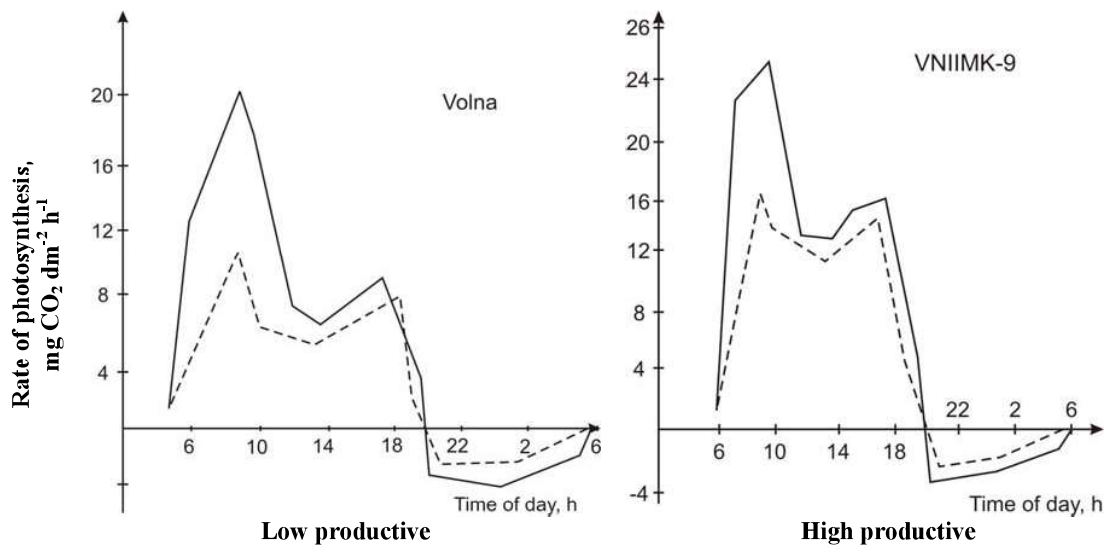
Figure 28. The diurnal pattern of the gas exchange rate in leaves of various soybean genotypes at the grain filling stage. Solid lines – the gas exchange rate in the leaves of plants grown using mineral fertilizers, dotted lines – the gas exchange rate in leaves of plants grown without mineral fertilizers (control).
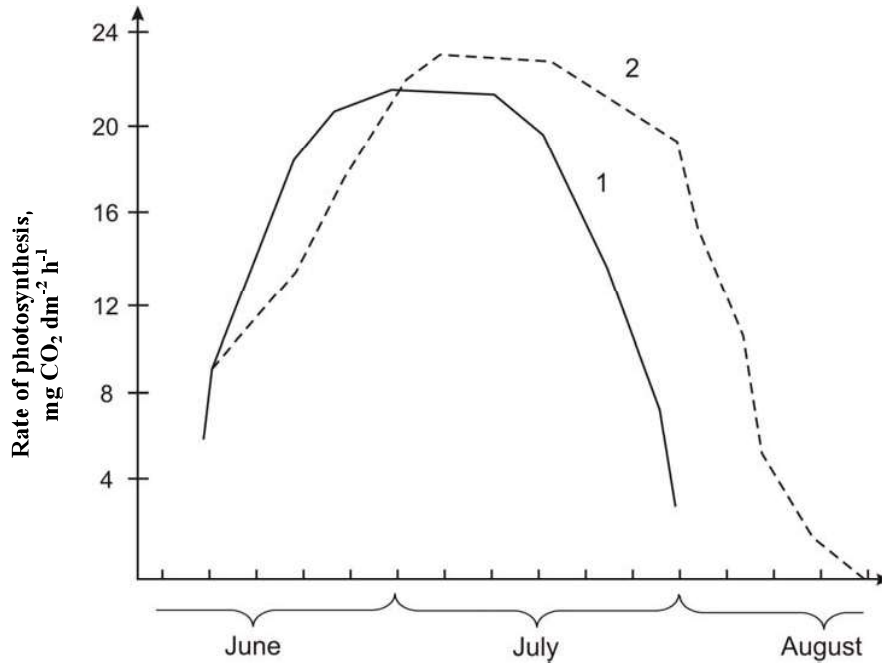

Figure 29. Ontogenetic changes in the rate of photosynthesis in low (1) and high productive (2) soybean genotypes.
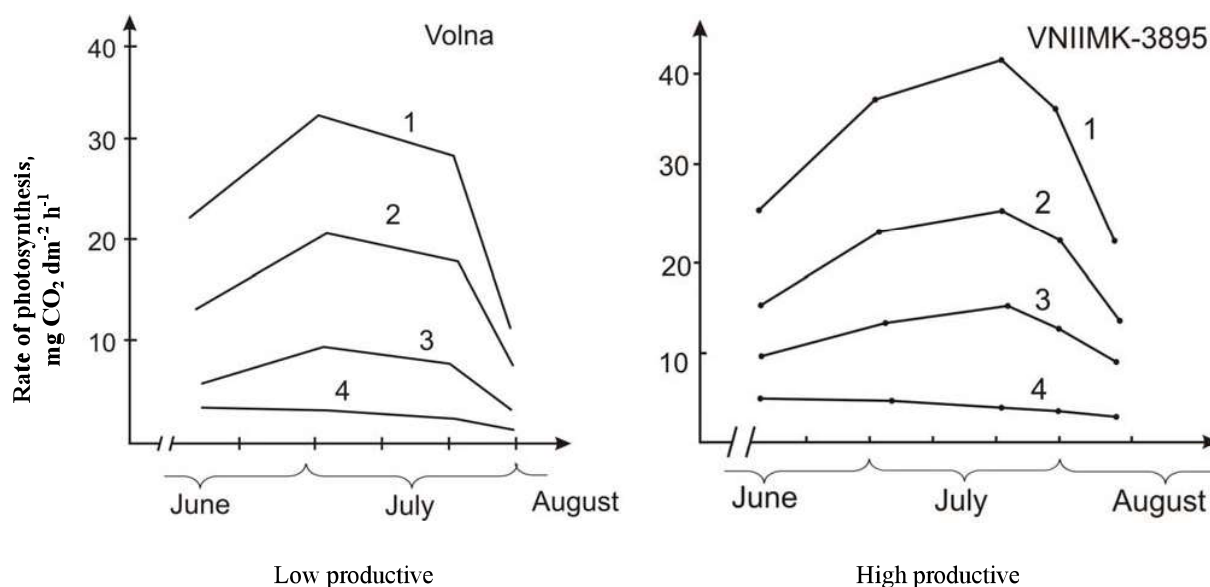
Figure 30. Components of carbon dioxide gas exchange in soybean leaves:
1 - true photosynthesis; 2 - net photosynthesis; 3 - photorespiration; 4 - dark respiration.

in the high productive ones (Mirzoyev, 1988 a, b, 1990; Aliyev et al., 1992).

The similarity in the pattern of change in the rates of true photosynthesis and photorespiration during ontogenesis exhibits a positive relationship between them. The absolute value of dark respiration in the studied soybean genotypes differ slightly. Our research findings showed that the value of photorespiration in the high productive soybean genotypes compared to the same of the low productive ones is higher. Hence, during the execution of purposeful breeding program with the aim of developing high productive soybean varieties, genotypes with higher photorespiration value should be used as a starting material.

Under the water stress active photosynthetic function of different assimilating organs, mainly of an ear, plays a crucial role in yield formation. Drought as a negative environmental factor adversely affects the photosynthetic gas exchange in wheat, reducing its rate by 30-40% in the short-stemmed varieties and by 35-45% in long-stemmed ones. Lower leaves are more affected by drought than the upper leaves. The greatest decrease in the photosynthetic rate during ontogenesis in short-stemmed varieties occurs at the flowering and grain formation, and in the long-stemmed varieties - at the flowering and milk ripeness (Figure 31). Hence, in intensive genotypes the critical period of water deficit is the end of flowering and grain formation, in extensive ones it starts from beginning of flowering and covers the whole following period of ontogenesis (Maharramov, 1995).

Leaf area begins to decrease starting from the

earing and flowering stages, and at the end of ontogenesis its area shortens by more than half. The ear surface area at the end of ontogenesis decreases in short-stemmed varieties by 32% and in long-stemmed ones by 23%.

Alterations in the correlation between assimilating and consuming organs in different wheat genotypes under drought led to a change in photosynthetic rate. Variation of the source potential with the removal of 7-layered leaves increased the rate of the 8-layered leaves in the short-stemmed varieties under normal irrigation and water deficit on average by 19 and 21%, in long-stemmed ones by 36 and 28%. After removal of 8-layered leaves, these parameters changed to 22 and 28% in short-stemmed and 37 and 23% in long-stemmed genotypes. The decrease of the ear acceptor force leads to a decrease of the rate of photosynthesis of leaves in the control and stressed variants on average to 15 and 9.5% in intensive types, and 18 and 12.5% in extensive ones, respectively (Ahmadova, 1996).

In drought tolerant intensive wheat variety in sowing more than 60% of grain yield and protein synthesis occurs due to ear photosynthesis. Such benefits of intensive and tolerant to water stress genotypes as great assimilating ability of the ear in current photosynthesis and the best acceptor activity in the utilization and reutilization of reserve products of photosynthesis are crucial in developing of both high productive and drought tolerant genotypes. When leaves lose their photosynthetic functions under drought an ear does the main contribution to the photosynthesis at the earing and grain filling (Aliyev, 1998). In compact sowings of

these genotypes with optimal assimilating surface and sufficient donor ability the value of photosynthetic rate is always high. Together with high photosynthetic activity and attractive force of the ear it constitutes the basis of high yield. For this reason in high productive genotypes with high photosynthetic function of the ear grain yield is considerable under extreme water supply.

The rate of photorespiration is to some extent in inverse correlation with the water supply. With increasing tolerance of genotypes to water stress or with strengthening of the drought, the photorespira-

tion rate decreases to a large degree in the ear elements.

The regular alterations of carboxylase, oxygenase and glycolate oxygenase contribute to direct correlation between the rates of photosynthesis and photorespiration. Study of plant gas exchange fully confirms the close relationship and direct correlation between these processes (Somerville and Ogren, 1980; Bidwell, 1983; Chanh et al., 1985). When the rate of photosynthesis is high, photorespiration is active too. The increase of temperature
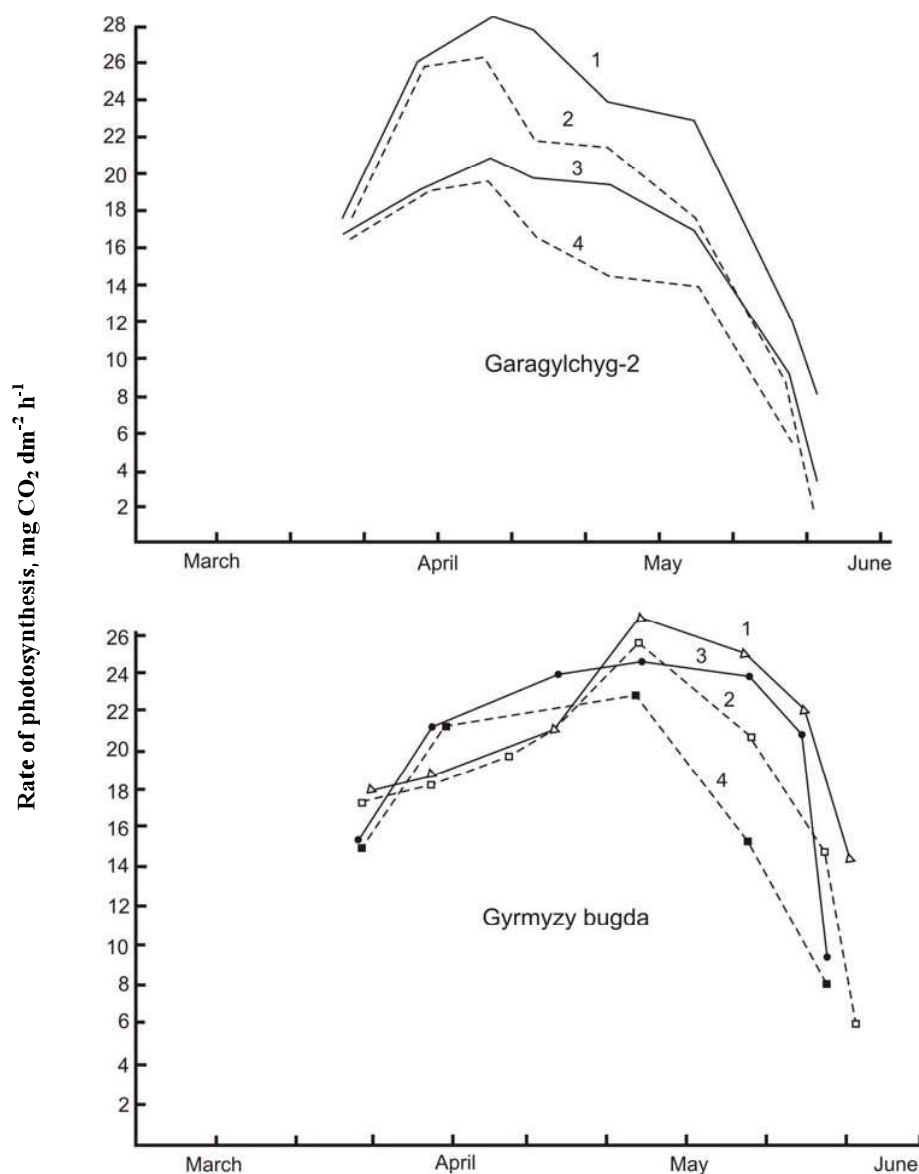

Figure 31. Ontogenetic changes of photosynthetic rate in wheat leaves under normal water supply and water deficit:
1, 2 – leaves of eighth layer, 3, 4 – leaves of seventh layer;
Control - solid curves, Stress - dashed curves.

enhances photorespiration relative to photosynthesis. Yield of glycolate metabolism may vary depending on the photosynthesis conditions. It increases when the outflow of assimilates from the leaves is inhibited and when nitrate levels in the environment is getting high (Lenz, 1979).

Decrease of photorespiration rate as a result of genetic abnormality of the individual reactions is accompanied with decreased rate of photosynthesis. In *Arabidopsis* mutants deficient in the serine glyoxylate aminotransferase, enzyme responsible for the completion of glycolate pathway, photosynthesis decreased by 79% over 30 min and quantity of ^{14}C in glycine and serine increased 2-2.5 times in ambient air (21% O_2) in comparison with the wild type. Reduced photorespiration could be the reason for abnormalities of nitrogen conversions associated with inhibition of growth processes and reducing overall productivity.

Investigations of primary processes of photosynthesis allowed to specify that chloroplasts from high productive genotypes were characterized by high rates of electron transport and photophosphorylation, and also to approve the availability of relationship between photosynthetic electron transport, CO_2 assimilation and productivity (Kazibekova et al., 1985).

High rates of photosynthesis and photorespiration in conjunction with favorable photosynthetic traits, an optimum leaf area index and the best architectonics define the high productivity of wheat genotypes. Therefore, contrary to conception on wastefulness of photorespiration, proposed in the many years by different authors (Zelitch, 1966, 1971, 1973, 1975; Zelitch and Day, 1973; Chollet and Ogren, 1975; Kelly and Latzko, 1976; Ogren, 1976; Servaites and Ogren, 1977; Ogren and Chollet, 1982; Holaday and Chollet, 1984; Leegood et al., 1995; Somerville, 2001; Ogren, 2003; Igarashi et al., 2006; Long et al., 2006; Kebeish et al., 2007; Khan, 2007; Mueller-Cajar and Whitney, 2008; Maurino and Peterhansel, 2010; Peterhansel et al., 2010; Peterhansel and Maurino, 2010), our comprehensive investigations on different aspects of photorespiration indicate that photorespiration is one of the evolutionary developed vital metabolic processes in plants. The attempts to reduce this process with the purpose of increasing the crop productivity are inconsistent (Aliev et al., 1988, 1996 b, c; Aliyev et al., 1992; Aliev and Kazibekova, 1995; Aliyev, 1995, 1998, 2001 a, b, 2002, 2004, 2007, 2010; Aliyev and Kazibekova, 2002). Phosphoglycolate phosphatase, a key enzyme of photorespiration was first homogeneously purified from eukaryotic green algae *Chlamydomonas reinhardtii* with subsequent determination of complete nucleotide and deduced amino acid sequences (Mamedov et al., 2001, 2002;

Mamedov and Suzuki, 2002) (NCBI Nucleotide 1:AB052169). Later the same gene was identified in *Arabidopsis* (Schwarte and Bauwe, 2007). Since metabolic processes of photorespiration in the leaf in the light take place simultaneously with photosynthesis, it is possible that released energy is used in certain reactions of photosynthesis.

Although long time generations of plant scientists have pondered the incongruous nature of the photorespiratory pathway's complexity and its apparent disadvantages, we are perhaps only now gaining sufficient knowledge to address the potential benefits of photorespiratory metabolism.

So, there are high productive genotypes among plants with C_3-photosynthesis and low productive among plants with C_4-photosynthesis. Despite the low value of photorespiration in C_4-plants (such as maize, sorghum, amaranth, etc.), many plants of C_3-type with high photorespiration, including major crops (wheat, rice, peas, etc.) compete successfully with C_4-plants and have high potential productivity and biological yield.

Along with establishing the key indicators of "ideal" wheat it is necessary to study the genetic basis of valuable qualities, i.e., the degree of inheritance of these valuable traits. In modern breeding one of the important steps is to identify genes responsible for the necessary morphological parameters, to transfer them into the genomes of developing variety and fixing there. Presence of the genetic potential in grain crops is expressed by physiological realization in the field. Therefore, selecting practical specimens for direct breeding and establishing an effective framework for decoding the molecular mechanisms of drought resistance in wheat it is necessary to use fully physiological potential of various genotypes under water limited conditions. Tolerance to water stress is not determined by one gene, i.e. it is a trait controlled by many genes. Many genotypes created by us, especially Barakatli-95, possess a number of core genes of the tolerance (Huseynova et al., 2006, 2007, 2009, 2010 a, b).

Photorespiration, in which part of organic compounds produced in photosynthesis is used, has gained a certain physiological value in the integrated system of plant organism. Goldsworthy (1969) opined that glycolate formation appeared in photosynthesizing plants during evolution as a result of reducing the carbon dioxide concentration in the atmosphere. Higher plants oxidize glycolate and metabolize it to more useful compounds. RuBPC/O is one of the most ancient enzymes. Appeared later in evolution PEP carboxylase does not have oxygenase function. Photorespiration prevents the accumulation of toxic intermediates (phosphoglycolate, glyoxylate) (Peterhansel et al., 2010). On the

other hand, photorespiration is a source of a number of significant metabolites (glutamate, γ-glutaric acid, glycine, serine) required for various biosyntheses (synthesis of proteins and phytohormones) (Novitskaya et al., 2002). Recently photorespiration gained a special importance as a producer of H_2O_2, the reactive oxygen species, which plays a role in cell signaling (Queval et al., 2007). Since hydrogen peroxide production significantly increases in peroxisomes under stress and is associated with activation of photorespiration, it is supposed that this process protects reaction cascade in the cell on purpose to provide adaptation of C_3-plants to unfavorable conditions (Noctor et al., 2002). Photorespiration utilizes excess energy that arises due to photochemical processes and is not used in photosynthesis and, thus, prevents photoinhibition of CO_2 fixation, which may be due to photooxidation and destruction of the photosynthetic apparatus (Heber et al., 1996; Kozaki and Takeba, 1996; Wingler et al., 2000). In addition, it was stated that under field conditions there is no doubt that photorespiration plays a significant protective role in preventing chronic photoinhibition (Osmond and Grace, 1995). It regulates the redox balance in the cell during decrease of CO_2 assimilation, when the power of the Calvin cycle is not enough to use the entire amount of NADPH and ATP produced in the light phase of photosynthesis. Energy dissipation during photorespiration prevents chloroplast over-reduction leading to photoinhibition of photosynthesis, thus supporting the functional activity of photosynthetic apparatus (Takahashi et al., 2007).

Photorespiration contributes to the maintenance of CO_2 level inside the leaf. It is known that at extreme conditions of water supply stomata are being closed and photorespiration increases sharply. ATP produced at intermediate stages of photorespiration is metabolized within mitochondria, where its concentration sharply drops due to limitations of triose phosphate outflow from the chloroplast and CO_2 entering to the tissue. Photorespiration is closely associated with general metabolism in the green cell; it often increases with decreasing of plant requirements in photosynthesis products and, in principle, aimed at maintenance of the enzyme system activity and chloroplasts and mitochondria functions. The role of photorespiration is sometimes associated with the nitrogenous compounds metabolism. The nitrogen conversion in glycolate pathway is closely linked to the carbon reactions (Oliver, 1994; Husic et al., 1987) and, thus, undoubtedly represents photorespiration, a substantial part of the photosynthetic oxidative cycle. Keys et al. (1978) suggested the inseparable link between photorespiration and nitrogen metabolism. It was established that the conversion of ni-

trogenous compounds during photorespiration is a cyclical process, called photorespiration nitrogen cycle (Keys et al., 1978; Walker et al., 1984; Schneidereit et al., 2006).

It is assumed that organic acids and their oxidation products, which are formed during photorespiration, via interaction with oxygen can act as antioxidants (Foyer and Noctor, 2005; Foyer et al., 2009), ensuring persistent operation of non-cyclic electron transport chain.

Phosphorylation in C_3-plants is balanced with chloroplast carbon metabolism and therefore, chloroplast is not able to export the ATP and provide energy to the entire cell. At the same time respiration (glycolysis - Krebs cycle) can not occur simultaneously with photosynthesis. Therefore, there is a change of respiratory substrate in the light, and acid oxidation in the Krebs cycle is replaced by glycine oxidation. Respiratory chain and phosphorylation remain active, that is, changes affect only the carbon metabolism. Thus, in the light respiratory chain accomplish the same reactions as that of dark respiration, then respiratory substrate is glycine produced in the photorespiratory pathway (Husic et al., 1987; Gardeström and Wigge, 1988; Oliver, 1994). Moreover, the photo-oxidative processes, in particular the glycolate oxidation, are energetically useful.

All these data indicate that photorespiration, which is, virtually, an integral part of the production process cannot be considered as wasteful, useless or even harmful process.

Recently new information about possible alternative pathways in phosphoglycolate metabolism was revealed, showing the metabolic flexibility of photorespiration (Maurino and Flügge, 2009; Peterhansel et al., 2010). The point is to change the course of photorespiration instead of its decrease.

However, photorespiration is not always linked to photosynthesis. For example, chlorophyll-deficient *Chlorella* mutants are able to synthesize only carotenoids. Photorespiration occurs in such mutants under strong illumination, and compose 50% of the dark respiration. When disabling photosynthesis by respiratory poison, O_2 absorption and CO_2 release also occurs in green photosynthetic cells.

In conclusion, we emphasize the close relationship between photosynthesis and photorespiration; the optimal correlation of these two essential processes is one of the most important conditions that secure the highest plant productivity. High rate of true photosynthesis and photorespiration, high activity of the primary photochemical processes in conjunction with favourable phenotypic traits, the optimum leaf area index and architectonics are crucial to the high productivity of wheat genotypes.

REFERENCE

Ahmadova F.A. (1996) Photosynthetic activity and productivity of perspective wheat varieties of various donor-acceptor ratio in the time of adaptation against water stress. PhD thesis, Baku: 28 p. (in Russian).

Akhmedov G.A. (1986) CO_2 exchange in wheat ontogenesis depending on phenotypic traits, growth conditions and photosynthetic productivity. PhD thesis, Baku: 183 p. (in Russian).

Akperov Z.I., Mirzoyev R.S. (1990) Photosynthetic traits of various soybean genotypes contrasting in grain yield. Vestnik selskokhozaystvennoy nauki AzSSR, Baku **2:** 6-9 (in Russian).

Aliev D.A., Kazibekova E.G. (1979) Peculiarities of photosynthetic rate in extensive and intensive wheat cultivars. Izv. Akad. Nauk Azerb. SSR (ser. biol. nauk) **3:** 3-10 (in Russian).

Aliev D.A., Kerimov S.Kh., Dzhangirov A.A., Akhmedov A.A. (1996 a) Transport and distribution of ^{14}C-assimilates in wheat genotypes with various photosynthetic characteristics and economic yields. Russian J. Plant Physiol. **43(1):** 57-61.

Aliev D.A., Kerimov S.Kh., Guliev N.M., Akhmedov A.A. (1996 b) Carbon metabolism in wheat genotypes with contrasting photosynthetic characteristics. Russian J. Plant Physiol. **43(1):** 42-48.

Aliev J.A., Guliev N.M., Kerimov S.Kh., Hidayatov R.B. (1988) Enzymes of the primary CO_2 fixation in flag leaf ontogenesis of wheat genotypes. Izv. Akad. Nauk Azerb. SSR (ser. biol. nauk) **4:** 12-20 (in Russian).

Aliev J.A., Guliev N.M., Kerimov S.Kh., Hidayatov R.B. (1996 c) Photosynthetic enzymes of wheat genotypes differing in productivity. Photosynthetica **32(1):** 77-85.

Aliev J.A., Kazibekova E.G. (1995) Peculiarities of highly productive wheat photosynthesis and usage of photosynthetic signs in selection. Proceedings of the Xth International Congress on Photosynthesis, Montpellier, France, 1995. In: Photosynthesis: from light to Biosphere (Mathis P., ed.), Kluwer Academic Publishers, Dordrecht, Boston, London **54:** 659-662.

Aliyev J.A. (1974) Photosynthetic activity, mineral nutrition and plant productivity. Elm, Baku: 335 p. (in Russian).

Aliyev J.A. (1983) Modern notion of the perfect wheat plant. Izv. Akad. Nauk Azerb. SSR (ser. biol. nauk) **3:** 3-14 (in Russian).

Aliyev J.A. (1995) Physiological bases of donor genotypes choosing and drought-resistant wheat varieties selection. Abstracts of International Congress of Integrated Studies on Drought Tolerance of Higher Plants "Inter Grought-95", Montpellier (France) **VIII:** 24.

Aliyev J.A. (1998) Importance of photosynthesis of various organs in protein synthesis in grain of wheat genotypes under water stress. Proceedings of the XIth International Congress on Photosynthesis, Budapest, Hungary, 1998. In: Photosynthesis: Mechanisms and Effects (Garab G., ed.), Kluwer Academic Publishers, Dordrecht, Boston, London **4:** 3171-3174.

Aliyev J.A. (2001 a) Diversity of photosynthetic activity of organs of wheat genotypes and breeding of high-yielding varieties tolerant to water stress. Proceedings of the 12th International Congress on Photosynthesis, Brisbane, Australia, 2001. www.publish.csiro.au/ps2001, S28-006.

Aliyev J.A. (2001 b) Physiological bases of wheat breeding tolerant to water stress. Proceedings of the 6th International Wheat Conference, Budapest, Hungary, 2000. In: Wheat in a Global Environment (Bedo Z., Lang L., eds.), Kluwer Academic Publishers, Dordrecht, Boston, London **9:** 693-698.

Aliyev J.A. (2002) The role of photosynthesis of various organs on protein synthesis in grain of wheat genotypes under water stress. Proceedings of Azerbaijan National Academy of Sciences (biological sciences) **1-6:** 5-19 (in Russian).

Aliyev J.A. (2004) CO_2 assimilation, architectonics and productivity of wheat genotypes in sowing. Proceedings of the 13th International Congress of Photosynthesis, Montreal, Canada, 2004. In: Photosynthesis: Fundamental Aspects to Global Perspectives (van der Est A., Bruce D., eds.), Alliance Communications Group, Kansas **2:** 1047-1048.

Aliyev J.A. (2006) Wheat breeding in Azerbaijan. Proceedings of Azerbaijan National Academy of Sciences (biological sciences) **3-4:** 3-32 (in Russian).

Aliyev J.A. (2007) The intensity of CO_2 assimilation, photorespiration and productivity of wheat genotypes *Triticum* L. Abstracts of the 14th International Congress on Photosynthesis, Glasgow, Scotland, 2007. In: Photosynthesis Research **91(2-3):** 278.

Aliyev J.A. (2010) Photosynthesis, photorespiration and productivity of wheat genotypes (*Triticum* L.). Abstracts of the 15th International Congress of Photosynthesis, Beijing, China, 2010. In: Photosynthesis Research for Food, Fuel and the Future: 305.

Aliyev J.A., Akhmedov A.A., Mirzoyev R.S. (1992) Dynamics of CO_2 gas exchange in leaves of soybean in field. Izv. Akad. Nauk Azerb. SSR (ser. biol. nauk) **1-6:** 76-82 (in Russian).

Aliyev J.A., Akperov Z.I. (1985) Dynamics of sowing structure and photosynthetical traits of soybean genotypes. Izv. Akad. Nauk Azerb. SSR (ser. biol. nauk) **3**: 3-10 (in Russian).

Aliyev J.A., Akperov Z.I. (1986) Conception of ideal soybean. Izv. Akad. Nauk Azerb. SSR (ser. biol. nauk) **2**: 3-11 (in Russian).

Aliyev J.A., Akperov Z.I. (1995) Photosynthesis and soybean grain yield. Rodnik, Moscow-Baku: 126 p. (in Russian).

Aliyev J.A., Akperov Z.I. (1998) Fotosinteza şi recolta de soia. Chişina: Ştininta: 127 p.

Aliyev J.A., Akperov Z.I., Nabiyev M.H. (1981) Soybean cultivation under irrigation conditions of Azerbaijan SSR (Guidelines). Baku: 8 p. (in Russian).

Aliyev J.A., Akperov Z.I., Nabiyev M.H. (1982 a) Soybean cultivation in irrigated lands of Azerbaijan SSR. Azerneshr, Baku: 54 p. (in Russian).

Aliyev J.A., Jahangirov A.A., Kerimov S.Kh., Akhmedov A.A. (1987) About contribution of the ear in grain filling of wheat genotypes differing in photosynthetic traits and yield. Izv. Akad. Nauk Azerb. SSR (ser. biol. nauk) **3**: 3-7 (in Russian).

Aliyev J.A., Kazibekova E.G. (1977) About architectonics and photosynthetic function of high-yielding wheat. Russian J. Plant Physiol. **24(5)**: 662-667.

Aliyev J.A., Kazibekova E.G. (1988) Importance of photosynthetic traits in grain yield and their use in breeding of ideal wheat. In: Photosynthesis and production process (Nichiporovich A.A., ed.). Nauka, Moscow, USSR: 237-243 (in Russian).

Aliyev J.A., Kazibekova E.G. (2002) Peculiarities of high productive wheat photosynthesis and usage of photosynthetic signs in selection. Proceedings of Azerbaijan National Academy of Sciences (biological sciences) **1-6**: 20-29 (in Russian).

Aliyev J.A., Kazibekova E.G., Safarov S.A. (1982 b) The main parameters of leaves of wheat phenotypes with various yield. Izv. Akad. Nauk Azerb. SSR (ser. biol. nauk) **5**: 3-8 (in Russian).

Anderson L.E. (1971) Chloroplast and cytoplasmic enzymes. II. Pea leaf triose phosphate isomerases. Biochem. Biophys. Acta **235**: 237-244.

Andersson I. (2008) Catalysis and regulation in Rubisco. J. Exp. Bot. **59**: 1555-1568.

Barber J. (1998) What limits the efficiency of photosynthesis and can there be beneficial improvements? In: Feeding a World Population of More Than Eight Billion People – a Challenge to Science (Waterlow J.C., Armstrong D.G., Fowdenand L., Riley R., eds.). Oxford University Press, Cary, NC, USA: 112-123.

Bauwe H., Kolukisaoglu U. (2003) Genetic manipulation of glycine decarboxylation. J. Exp. Bot. **54**: 1523-1535.

Beevers H. (1969) Glyoxysomes of castor bean endosperm and their relation to gluconeogenesis. Ann. N.Y. Acad. Sci. **168**: 313-324.

Beevers H. (1979) Microbodies in higher plants. Annu. Rev. Plant Physiol. **30**: 159-193.

Bidwell R.G.S. (1983) Carbon nutrition of plants: photosynthesis and respiration. In: Plants Physiology: A treatise (Steward E.C., Bidwell R.G.S., eds.) Academic Press, New York **VIII**: 287-457.

Boldt R., Edner C., Kolukisaoglu U., Hagemann M., Weckwerth W., Wienkoop S., Morgenthal K., Bauwe H. (2005) D-glycerate 3-kinase, the last unknown enzyme in the photorespiratory cycle in *Arabidopsis*, belongs to a novel kinase family. Plant Cell **17**: 2413-2420.

Booker F.L., Reid Ch.D., Brunschön-Harti S., Fiscus E.L., Miller J.E. (1997) Photosynthesis and photorespiration in soybean [Glycine max (L.) Merr.] chronically exposed to elevated carbon dioxide and ozone. J. Exp. Bot. **48**: 1843-1852.

Boyer J.S. (1995) Measuring the water status of plants and soils. Academic Press, San Diego.

Bresinsky A., Körner Ch., Kadereit J.W., Neuhaus G., Sonnewald U. (2008) Strasburger – Lehrbuch der Botanik. 36. Aufl. Spektrum Akademischer Verlag: 1176 p.

Catalogue of varieties, released at Agriculture Institute of Azerbaijan (2000).

Chanh T.A., Joy K.W., Ireland R.J. (1985) Role of asparagines in the photorespiratory nitrogen metabolism of pea leaves. Plant Physiol. **78(2)**: 334-337.

Chollet R., Ogren W.L. (1975) Regulation of photorespiration in C_3 and C_4 species. Bot. Rev. **41(2)**: 137-179.

Decker J.P. (1955) A rapid, postillumination deceleration of respiration in green leaves. Plant Physiol. **30**: 82-84.

Dever L.V., Blackwell R.D., Fullwood N.J., Lacuesta M., Leegood R.C. (1995) The isolation and characterization of mutants of the C_4 photosynthetic pathway. J. Exp. Bot. **46**: 1363-1376.

Dospekhov B.A. (1985) Methods of field experience. Agropromizdat, Moscow: 351 p. (in Russian).

Eckardt N.A. (2005) Photorespiration revisited. Plant Cell **17(8)**: 2139-2141.

Eisenhut M., Kahlon S., Hasse D., Ewald R., Lieman-Hurwitz J., Ogawa T., Ruth W., Bauwe H., Kaplan A., Hagemann M. (2006) The plant-like C2 glycolate cycle and the bacterial-like glycerate pathway cooperate in phosphoglycolate metabolism in cyanobacteria. Plant Physiol. **142**: 333-342.

Evans L.T. (1998) Greater crop production: whence and whither? In: Feeding a World Population of More Than Eight Billion People – a Challenge to Science (Waterlow J.C., Armstrong D.G., Fowdenand L., Riley R., eds.). Oxford University Press, Cary, NC, USA: 89-97.

Foyer C.H., Bloom A.J., Queval G., Noctor G. (2009) Photorespiratory metabolism: genes, mutants, energetic, and redox signaling. Annu. Rev. Plant Biol. **60:** 455-484.

Foyer C.H., Noctor G. (2005) Oxidant and anti-oxidant signaling in plants: a re-evaluation of the concept of oxidative stress in a physiological context. Plant, Cell and Environment **29:** 1056-1071.

Gardeström P., Wigge B. (1988) Influence of photorespiration on ATP:ADP ratios in the chloroplasts, mitochondria, and cytosol, studied by rapid fractionation of barley (*Hordeum vulgare*) protoplasts. Plant Physiol. **88:** 69-76.

Goldsworthy A. (1969) Riddle of photorespiration. Nature **224(5218):** 501-502.

Grodzinski B. (1978) Glyoxylate decarboxylation during photorespiration. Planta **144:** 31-37.

Hall N.P., Kendall A.C., Lea P.J., Turner J.C, Wallsgrove R.M. (1987) Characteristics of a photorespiration mutant of barley (*Hordeum vulgare* L.) deficient in phosphoglycolate phosphatase. Photosynth. Res. **11:** 89-96.

Heber U., Miyake C., Mano J., Ohno C., Asada K. (1996) Monodehydroascorbate radical detected by electron paramagnetic resonance spectrometry is a sensitive probe of oxidative stress in intact leaves. Plant Cell Physiol. **37:** 1066–1072.

Holaday A.S., Chollet R. (1984) Photosynthetic/photorespiratory characteristics of C_3-C_4 intermediate species. Photosynth. Res. **5:** 307-323.

Hough R.A. (1974) Photorespiration and productivity in submersed aquatic vascular plants. Limnol. Oceanogr. **19:** 912-927.

Huseynova I.M., Rustamova S.M., Mammadov A.Ch., Aliyev J.A. (2010 a) Dreb 1 genes that positively regulate drought-resistance in wheat genotypes. Reports of Azerbaijan National Academy of Sciences **LXVI(2):** 92-100.

Huseynova I.M., Rustamova S.M., Mammadov A.Ch., Aliyev J.A. (2010 b) RAPD markers associated with drought tolerance in wheat *Triticum* L. genotypes. Reports of Azerbaijan National Academy of Sciences **LXVI(1):** 104-110 (in Russian).

Huseynova I.M., Suleimanov S.Y., Aliyev J.A. (2006) Protein composition and native state of pigments of thylakoid membrane of wheat genotypes differently tolerances to water stress. Biochemistry (Moscow) **71:** 223-228.

Huseynova I.M., Suleymanov S.Y., Aliyev J.A. (2007) Structural-functional state of thylakoid membranes of wheat genotypes under water stress. Biochim. Biophys. Acta **1767(6):** 869-875.

Huseynova I.M., Suleymanov S.Y., Rustamova S.M., Aliyev J.A. (2009) Drought-induced changes in photosynthetic membranes of two wheat (*Triticum aestivum* L.) cultivars. Biochemistry (Moscow) **74(8):** 1109-1116.

Husic D.W., Husic H.D., Tolbert N.E. (1987) The oxidative photosynthetic carbon cycle or C_2 cycle. CRC critical reviews. Plant Sci. **5:** 45-100.

Husic H.D., Tolbert N.E. (1984) Anion and divalent cation activation of phosphoglycolate phosphatase from leaves. Arch. Biochem. Biophys. **229:** 64-72.

Igarashi D., Tsuchida H., Miyao M., Ohsumi Ch. (2006) Glutamate: Glyoxilate aminotransferase modulates amino acid content during photorespiration. Plant Physiol. **142:** 901-910.

Jahangirov A.A. (1987) Products of photosynthesis and peculiarities of their utilization with plants of different productivity. PhD thesis, Baku: 135 p. (in Russian).

Kaplan B.G. (1970) Express-calculation of the basic mathematical and statistical indicators. Maarif, Baku: 447 p. (in Russian).

Karpushkin L.T. (1971) The use of infrared gas analyser to study CO_2 gas exchange in plants. In: Biophysical methods in plant physiology (Molotkovskiy Yu.G., ed.). Nauka, Moscow: 44-71 (in Russian).

Kaur N., Reumann S., Hu J. (2009) Pero-xisome biogenesis and function. In: The Arabidopsis Book (Somerville C.R., Meyerowitz E.M., eds.), The American Society of Plant Biologists, Rockville, MD: 1-41.

Kazibekova E.G., Azizov I.V., Aliev D.A. (1985) Photosynthetic activity of chloroplasts in wheat cultivars of different productivity. Izv. Akad. Nauk Azerb. SSR (ser. biol. nauk) **5:** 3-10 (in Russian).

Kebeish R., Niessen M., Thiruveedhi K., Bari R., Hirsch H.-J., Rosenkranz R., Stäbler N., Schönfeld B., Kreuzaler F., Peterhänsel C. (2007) Chloroplastic photorespiratory bypass increases photosynthesis and biomass production in *Arabidopsis thaliana*. Nature Biotech. **25:** 593–599.

Keerberg O.F., Vark E.Y., Keerberg Kh.I., Parnik T.R. (1970) The study of kinetics of ^{14}C incorporation in photosynthetic products in legume leaves. DAN SSSR **195(1):** 238-241 (in Russian).

Kelly G.J., Latzko E. (1976) Inhibition of spinach-leaf phosphofructokinase by 2-phosphoglycollate. FEBS Lett. **68:** 55-58.

Keys A.J., Bird I.F., Cornelius M.J., Lea P.J.,

Wallsgrove R.M., Miflin B.J. (1978) Photorespiratory nitrogen cycle. Nature **275**: 741-743.

Khan M.S. (2007) Engineering photorespiration in chloroplasts: a novel strategy for increasing biomass production. Trends in Biotech. **25(10)**: 437-440.

Khudiev A.V. (1998) The peculiarities of metabolism and utilization of the main products of photosynthesis under different source-sink relations in wheat genotypes with different photosynthesis activity and grain yield. PhD thesis, Baku: 30 p. (in Russian).

Kozaki A., Takeba G. (1996) Photorespiration protects C_3 plants from photooxidation. Nature **384**: 557-560.

Leegood R.C., Lea P.J., Adcock M.D., Hausler R.E. (1995) The regulation and control of photorespiration. J. Exp. Bot. **46**: 1397-1414.

Lenz F. (1979) Fruit effects on photosynthesis, light and dark respiration. In: Photosynthesis and Plant Development (Marcelle R., Clijsters C., van Poucke M., W. Junke, eds.), The Hague: 271-81.

Long S.P., Zhu X.-G., Naidu S.L., Ort D.R. (2006) Can improvement in photosynthesis increase crop yields? Plant, Cell and Environ. **29**: 315-330.

Lorimer G.H., Andrews T.J. (1973) Plant photorespiration: An inevitable consequence of the existence of atmospheric oxygen. Nature **248**: 359-360.

Lowry O.H., Rosebrough N.J., Farr A.L., Randall R.J. (1951) Protein measurement with the folin phenol reagent. J. Biol. Chem. **193**: 265-275.

Maharramov M.Y. (1995) CO_2 gas exchange in various productive wheat genotypes according their drought resistance. PhD thesis, Baku: 24 p. (in Russian).

Majeran W., Cai Y., Sun Q., van Wijk K.J. (2005) Functional differentiation of bundle sheath and mesophyll maize chloroplasts determined by comparative proteomics. Plant Cell **17**: 3111-3140.

Mamedov T.G., Aliyev J.A., Suzuki K. (2002) Nucleotide and amino acid sequences of phosphoglycolate phosphatase from *Chlamidomonas reinhardtii*. Proceedings of Azerbaijan National Academy of Sciences (biological sciences) **1-6**: 50-56 (in Russian).

Mamedov T.G., Suzuki K. (2002) Phosphoglycolate phosphatase from *Chlamidomonas reinhardtii*. Proceedings of Azerbaijan National Academy of Sciences (biological sciences) **1-6**: 91-107 (in Russian).

Mamedov T.G., Suzuki K., Miura K., Kucho K.K., Fukuzawa H. (2001) Characteristics and sequence of phosphoglycolate phosphatase from an eukaryotic green alga *Chlamydomonas reinhardtii*. J. Biol. Chem. **276**: 45573-45579.

Maurino V.G., Flügge U.-I. (2009) Means for improving agrobiological traits in a plant by providing a plant cell comprising in its chloroplasts enzymatic activities for converting glycolate into malate. Patent application, EP08151759.1-1212.

Maurino V.G., Peterhansel C. (2010) Photorespiration: current status and approaches for metabolic engineering. Curr. Opin. Plant Biol. **13**: 249-256.

Methodological guidelines of Vavilov N.I. Institute of Plant Breeding (1987) Comprehensive physiological evaluation of drought- and heat-tolerant wheat in Uzbekistan (Kojushko N.N., ed). Leningrad: 23 p. (in Russian).

Mirzoyev R.S. (1988a) Seasonal variations of photosynthesis intensity of various soybean genotypes. Proceedings of IV Republic Conference, Baku: 78 p. (in Russian).

Mirzoyev R.S. (1988b) CO_2 gas exchange and photosynthetic traits of various soybean genotypes. Proceedings of Republic Conference of Young Scientists, Tbilisi: 38 p. (in Russian).

Mirzoyev R.S. (1990) CO_2 gas exchange of soybean genotypes different in photosynthetic traits and productivity. PhD thesis, Baku: 22 p. (in Russian).

Mueller-Cajar O., Whitney S. (2008) Directing the evolution of Rubisco and Rubisco activase: first impressions of a new tool for photosynthesis research. Photosynth. Res. **98**: 667-675.

Noctor G., Novitskaya L., Lea P., Foyer C. (2002) Co-ordination of leaf minor amino acid contents in crop species: significance and interpretation. J. Exp. Bot. **53**: 939-945.

Norman E.G., Colman B. (1991) Purification and characterization of phosphoglycolate phosphatase from the cyanobacterium *Coccochloris peniocystis*. Plant Physiol. **95**: 693-698.

Novitskaya L., Trevanion S.J., Driscoll S., Foyer C.H., Noctor G. (2002) How does photorespiration modulate leaf amino acid contents? A dual approach through modelling and metabolite analysis. Plant Cell Environ. **25**: 821-835.

Ogren W.L. (1975) Control of photorespiration in soybean and maize. In: Environmental and Biological Control of Photosynthesis. (Marcelle R., ed.) The Hague, W. Junk: 45-52.

Ogren W.L. (2003) Affixing the O to Rubisco: discovering the source of photorespiratory glycolate and its regulation. Photosynth. Res. **76**: 53-63.

Ogren W.L., Bowes G. (1971) Ribulose diphosphate carboxylase regulates soybean photorespiration. Nature New Biol. **230**: 159-160.

Ogren W.L., Chollet R. (1982) Photorespiration.

In: Photosynthesis: Development, Carbon Metabolism, and Plant Productivity **II:** 191-230.

Oliver D. J. (1994) The glycine decarboxylase complex from plant mitochondria. Ann. Rev. Plant Physiol. Plant Mol. Biol. **45:** 323-337.

Olsen L.J., Harada J. (1995) Peroxisomes and their assembly in higher plants. Ann. Rev. Plant Physiol. **46:** 123-146.

Osmond C.B., Grace S.C. (1995) Perspectives on photoinhibition and photorespiration in the field: quintessential inefficiencies of the light and dark reactions of photosynthesis? J. Exp. Bot. **46:** 1351-1362.

Peterhancel C., Maurino V.G. (2011) Photorespiration redesigned. Plant Physiol. **155:** 49-55.

Peterhansel C., Horst I., Niessen M., Blume Ch., Kebeish R., Kürkcüoglu S., Kreuzaler F. (2010) Photorespiration. The Arabidopsis Book. American Society of Plant Biologists, 10.1199/tab.0130, p. 1-24.

Popov V.N., Dmitrieva E.A., Eprintsev A.T., Igamberdiev A.U. (2003) Glycolate oxidase isoforms are distributed between the bundle sheath and mesophyll tissues of maize leaves. J. Plant Physiol. **160:** 851-857.

Povey S., Jeremiah S.J., Barker R.F., Hopkinson D.A., Robson E.B., Cook P.J.L., Solomon E., Bobrow M., Carrit B., Buckton K.E. (1980) Assignment of the human locus determining phosphoglycolate phosphotase (PGP) to chromosome 16. Ann. Hum. Genet. **43:** 241-248.

Queval G., Issakidis-Bourguet E., Hoeberichts F.A., Vandorpe M., Gakiere B., Vanacker H. et al. (2007) Conditional oxidative stress responses in the *Arabidopsis* photorespiratory mutant *cat2* demonstrate that redox state is a key modulator of daylength-dependent gene expression, and define photoperiod as a crucial factor in the regulation of H_2O_2-induced cell death. Plant J. **52:** 640-657.

Randall D.D. (1976) Phosphoglycolate phosphatase in marine algae. Isolation and characterization from *Hallimeda cylindracea*. Aust. J. Plant. Physiol. **3:** 105-111.

Randall D.D., Tolbert N.E. (1971) The phosphatases associated with photosynthesis and the glycolate pathway. In: Photosynthesis and Photorespiration (Hatch M.D., Osmond C.B., Slayter R.O., eds). John Wiley & Sons, New York: 259-266.

Randall D.D., Tolbert N.E., Gremel D. (1971) 3-phosphoglycerate phosphatase in leaves. II. Distribution, physiological considerations, and comparison with p-glycolate phosphatase. Plant Physiol. **48:** 480-487.

Reumann S., Quan S., Aung K., Yang P., Manandhar-Shrestha K., Holbrook D., Linka N., Switzenberg R., Wilkerson C.Y., Weber A.P.M., Olsen L.J., Hu J. (2009) In-depth proteome analysis of *Arabidopsis* leaf peroxisomes combined with *in vivo* subcellular targeting verification indicates novel metabolic and regulatory functions of peroxisomes. Plant Physiol. **150:** 125-143.

Reumann S., Weber A.P. (2006) Plant peroxisomes respire in the light: some gaps of the photorespiratory C_2 cycle have become filled – other remain. Biochem. Biophys. Acta **1763:** 1496-1510.

Richardson K.E., Tolbert N.E. (1961) Phosphoglycolic acid phosphatase. J. Biol. Chem. **236:** 1285-1290.

Romanova A.K. (1980) Biochemical methods of autotrophic study in microorganisms. Nauka, Moscow: 160 p. (in Russian).

Rose Z.B. (1976) A procedure for decreasing the level of 2,3-bisphosphoglycerate in red cells *in vitro*. Biochem. Biophys. Res. Commun. **73:** 1011-1017.

Rose Z.B., Grove D.S., Seal S.N. (1986) Mechanism of activation by anions of phosphoglycolate phosphatases from spinach and human red blood cells. J. Biol. Chem. **261(24):** 10996-11002.

Rose Z.B., Liebowitz J. (1970) Direct determination of 2,3-diphosphoglycerate. Anal. Biochem. **35(1):** 177-180.

Rose Z.B., Salon J. (1979) The identification of glycolate-2-P as a constituent of normal red blood cells. Biochem. Biophys. Res. Commun. **87:** 869-875.

Schneidereit J., Hausler R., Fiene G., Kaiser W.M., Weber A.P.M. (2006) Antisense repression reveals a crucial role for the plastidic 2-oxoglutarate/malate translocator DiT1 at the interface between carbon and nitrogen metabolism. Plant J. **45:** 206-224.

Schwarte S., Bauwe H. (2007) Identification of the photorespiratory 2-phosphoglycolate phosphatase, PGLP1, in *Arabidopsis*. Plant Physiol. **144:** 1580-1586.

Seal S.N., Rose Z.B. (1987) Characterization of a phosphoenzyme intermediate in the reaction of phosphoglycolate phosphatase. J. Biol. Chem. **262(28):** 13496-13500.

Servaites J.C., Ogren W.L. (1977) Chemical inhibition of the glycolate pathway in soybean leaf cells. Plant Physiol. **60:** 461-466.

Šesták Z., Jarvis P.G., Catsky J. (1971) Criteria for the selection of suitable methods. In: Plant photosynthetic production. Manual of methods (Šesták Z., Jarvis P.G., Catsky J., eds.). W. Junk Publishing Co., Hague: 1-48.

Severin E.S. (2006) Biochemistry (Severin E.S., ed.), 4th edition, GEOTAR-Media, Moscow: 784 p. (in Russian).

Severin E.S. (2009) Biochemistry (Severin E.S., ed.), 5th edition, GEOTAR-Media, Moscow: 768 p. (in Russian).

Somerville C.R. (2001) An early *Arabidopsis* demonstration. Resolving a few issues concerning photorespiration. Plant Physiol. **125(1):** 20-4.

Somerville C.R., Ogren W.L. (1979) A phosphoglycolate phosphatase-deficient mutant of *Arabidopsis*. Nature **280:** 833-836.

Somerville C.R., Ogren W.L. (1980) Inhibition of photosynthesis in *Arabidopis* mutants lacking leaf glutamate synthase activity. Nature **286:** 257-259.

Spear D., Vora S. (1986) Demonstration and quantification of phosphoglycolate in human red cells: a potential regulator of 2,3-DPG metabolism. Fed. Proc. **45:** 1840.

Suzuki K., Mamedov T.G., Ikawa T. (1999) A mutant of *Chlamydomonas reinhardtii* with reduced rate of photorespiration. Plant Cell Physiol. **40:** 792-799.

Suzuki K., Marek L.F., Spalding M.H. (1990) A photorespiratory mutant of *Chlamydomonas reinhardtii*. Plant Physiol. **93:** 231-237.

Takahashi S., Bauwe H., Badger M. (2007) Impairment of the photorespiratory pathway accelerates photoinhibition of photosystem II by suppression of repair but not acceleration of damage processes in *Arabidopsis*. Plant Physiol. **144:** 487-494.

Tolbert N.E. (1973) Activation of polyphenol oxidase of chloroplasts. Plant Physiol. **51:** 234-244.

Tolbert N.E. (1981) Metabolic pathways in peroxisomes and glyoxysomes. Annu. Rev. Biochem. **50:** 133-157.

Tolbert N.E. (1997) The C2 oxidative photosynthetic carbon cycle. Annu. Rev. Plant Physiol. Plant Mol. Biol. **48:** 1-15.

Turner V.S., Hopkinson D.A. (1981) Biochemical characterization of the genetic variants of human phosphoglycolate phosphatase (PGP). Ann. Hum. Genet. **45(2):** 121–127.

Van den Bosch H., Schutgens R.B., Wanders R.J., Tager J.M. (1992) Biochemistry of peroxisomes. Annu. Rev. Biochem. **61:** 157-197.

Voll L.M., Jamai A., Renne P., Voll H., McClung C.R., Weber A.P.M. (2006) The photorespiratory *Arabidopsis* shm1 mutant is deficient in SHM1. Plant Physiol. **140:** 59-66.

Voznesensky V.L. (1977) Photosynthesis of desert plants. Nauka, Leningrad, USSR: 256 p. (in Russian).

Voznesensky V.L., Zalenskiy O.V., Semikhatova O.A. (1965) Methods of plant photosynthesis and respiration researches. Nauka, Leningrad: 305 p. (in Russian).

Walker J.L., Oliver D.J. (1986) Glycine decarboxylase multienzyme complex. Purification and partial characterization from pea leaf mitochondria. J. Biol. Chem. **261:** 2214-2221.

Walker K., Givan C., Keys A.G. (1984) Glutamic acid metabolism and the photorespiratory nitrogen cycle in wheat leaves. Plant Physiol. **75(1):** 60-66.

Walton N.J., Butt V.S. (1981) Metabolism and decarboxylation of glycollate and serine in leaf peroxisomes. Planta **155:** 218-224.

Weber A., Flügge U.-I. (2002) Interaction of cytosolic and plastidic nitrogen metabolism in plants. J. Exp. Bot. **53:** 865-874.

Wingler A., Lea P.J., Quick W.P., Leegood R.C. (2000) Photorespiration: metabolic pathways and their role in stress protection. Philos. Trans R. Soc. Lond. B. Bio. Sci. **355:** 1517-1529.

Wingler A., Quick W.P., Bungard R.A., Bailey K.J., Lea P.J., Leegood R.C. (1999) The role of photorespiration during drought stress: an analysis utilizing barley mutants with reduced activities of photorespiratory enzymes. Plant Cell Environ. **22:** 361-373.

Wolfendon R. (1970) Binding of substrate and transition state analogs to triosephosphate isomerase. Biochem. **9:** 3404-3407.

Yu C., Claybrook D.L., Huang A.H.C. (1983) Transport of glycine, serine, and proline into spinach leaf mitochondria. Arch. Biochem. Biophys. **227:** 180-187.

Zelitch I. (1966) Increased rate of net photosynthetic carbon dioxide uptake caused by the inhibition of glycolate oxidase. Plant Physiol. **41:** 1623-1631.

Zelitch I. (1971) Photosynthesis, photorespiration, and plant productivity. Acad. Press, New York/London: 247 p.

Zelitch I. (1972) The photooxidation of glyoxylate by envelope-free spinach chloroplasts and its relation to photorespiration. Arch. Biochem. Biophys. **150:** 698-707.

Zelitch I. (1973) Plant productivity and the control of photorespiration. Proc. Nat. Acad. Sci. USA **70(2):** 579-584.

Zelitch I. (1975) Improving the efficiency of photosynthesis. Science **188:** 626-633.

Zelitch I., Day P.R. (1973) The effect on net photosynthesis of pedigree selection for low and high rates of photorespiration in tobacco. Plant Physiol. **52:** 33-37.

Zelitch I., Schultes N.P., Peterson R.B., Brown P., Brutnell T.P. (2008) High glycolate oxidase activity is required for survival of maize in normal air. Plant Physiol. **149:** 195-204.

Response of Photosynthetic Apparatus and Antioxidant Defense Systems in *Triticum aestivum* L. Genotypes Subjected to Drought Stress

Irada M. Huseynova*, Saftar Y. Suleymanov, Samira M. Rustamova
Institute of Botany, Azerbaijan National Academy of Sciences, 40 Badamdar Shosse, Baku AZ 1073, Azerbaijan

Two wheat *(Triticum aestivum* L.) genotypes contrasting in architectonics and differing in drought-resistance, Azamatli-95 (short-stemmed, with vertically oriented small leaves, drought-tolerant) and Giymatli-2/17 (short-stemmed, with broad and drooping leaves, drought-sensitive) were grown in field conditions in a wide area under normal water supply and severe water deficit. It was found out that the content of CPI (M_r 115 kDa), apoprotein of P_{700} with M_r 63 kDa and LHCII polypeptides insignificantly increases in the drought-resistant Azamatli-95 under extreme water supply condition while their content decreases in drought-sensitive Giymatli-2/17. The intensity of synthesis of α- and β-subunits of CF_1 (55 and 53.5 kDa) and 33-30.5 kDa proteins also decreases in sensitive genotype. The intensity of short wavelength peaks at 687 and 695 nm sharply increases in the fluorescence spectra (77K) of chloroplasts from Giymatli-2/17 under water deficiency and there is a stimulation of the ratio of fluorescence band intensity F687/F740. After exposure to drought Giymatli-2/17 shows a larger reduction in the actual PSII photochemical efficiency of chloroplasts than Azamatli-95. The activitites of antioxidant enzymes such as catalase, peroxidase, glutathione reductase and superoxide dismutase differently change in wheat genotypes during ontogenesis.

Keywords: drought, reactive oxygen species, relative water content, photosystem, chlorophyll, sodium dodesyl sulphate, fluorescence, activity, antioxidant enzymes, wheat genotypes

INTRODUCTION

Plants are subjected to a range of abiotic and biotic stresses that affect their growth and development. In particular, it is predicted that water deficit will continue to be a major abiotic stress factor affecting global crop yields (Sharma and Lavanya, 2002). One third of the world's population resides in water-deficient regions, and with elevated CO_2 levels in the atmosphere and climatic changes predicted in the future, drought could become more frequent and severe.

Wheat is one of the widely cultivated crops in Azerbaijan, where drought is the main abiotic stress limiting its grain yield (Aliev, 2001; Aliyev, 2002).

In response to stress, plants activate a number of defense mechanisms that function to increase tolerance to adverse conditions. The response to drought stress which involves a number of biochemical-molecular mechanisms is complex. The application of this emerging understanding to the genetic engineering of food crops has already led to examples of improved drought tolerance and increased yield under drought (Hu et al., 2008).

Production of reactive oxygen species (ROS) and other radicals increases dramatically during water deficiency, and enhanced levels of reactive oxygen species are generated in various intracellular compartments in plants and may cause oxidative damage or act as signals (Gechev et al., 2006). The enhanced production of ROS in chloroplasts and peroxisomes has been correlated with drastic changes in nuclear gene expression that reveals the transfer of $^1O_2$-derived signals from the plastid to the nucleus. Many of the $^1O_2$-responsive genes are different from those activated by superoxide ($O_2{}^{\cdot-}$) or H_2O_2, suggesting that $O_2{}^{\cdot-}/H_2O_2$- and $^1O_2$-dependent signaling occurs via distinct pathways. These pathways could act independently or may interact with each other (Baruah et al., 2009). Plants protect cellular and subcellular system from the cytotoxic effects of active oxygen radicals with antioxidative enzymes such as superoxide dismutase (SOD), peroxidase (POD), catalase (CAT), and glutathion reductase (GR) as well as metabolites like glutathione, ascorbic acid, α-tocopherol and carotenoids.

In response to drought the adaptation shown by many plants could partly be due to changes in membrane composition and phase behavior, which optimizes the fluidity. Indeed, models for thylakoid membrane function require mobility of protein components and redox carriers. Membrane proteins are particularly important for the functionality of the photosynthetic apparatus (Friso et al., 2004).

**E-mail: huseynova-i@botany-az.org

The aim of this study was to investigate structural and functional characteristics of thylakoid membrane and antioxidant enzymes that ensure resistance of plant organisms to water deficit. For these purposes two bread wheat genotypes with contrast architectonics and different genetically stipulated sensitivities to drought were used. Such approach allows to identify not only precise bounds of variation of plant reaction to stress, but also to reveal specific features typical for high resistant genotypes that may be taken into consideration in crop breeding practice for developing drought tolerant varieties.

MATERIALS AND METHODS

In the experiments we used two bread wheat genotypes (*Triticum aestivum* L.), contrasting in architectonics and differing in drought resistance, Giymatli-2/17 – short-stemmed, with broad and drooping leaves and grain yield of 7-8 t ha^{-1}, drought-sensitive; Azamatli-95 – short-stemmed, with vertically oriented small leaves and grain yield of 8-9 t ha^{-1}, drought-tolerant. All genotypes were grown in field conditions in the wide area under normal water supply and dryland conditions. The plants were provided by Experimental Station of the Research Institute of Crop Husbandry (Baku, Azerbaijan). Different sensitivities of these genotypes to drought were determined during some years in different regions of Azerbaijan based on grain yield (Aliev, 1998, 2001). A group of plants from both genotypes was cultivated under optimum irrigation condition (control), and another set of plants was subjected to water deficit. Dehydration was imposed by withholding water supply. Samples were collected from control and stressed plants at grain filling period up 9^{30} to 10^{30}. Roots and shoots were separated, fresh weight was recorded and samples were taken for dry weight measurements. Three different samples for each treatment were taken and analyzed twice.

Leaf relative water content (RWC) was estimated gravimetrically according to Tambussi et al. (2005).

Leaves were homogenized with a Waring blender at full speed four times for 20 sec each in an ice-cold grinding chloroplast isolation medium (1:6 w/v) containing 0.4 M sucrose, 20 mM Tris, 10 mM NaCl, 1 mM EDTA (sodium salt), 5 mM sodium ascorbate, and 0.1% polyethylene glycol, pH 7.8 following the procedure of Aliev et al. (1992).

The chlorophyll (Chl) concentration was determined in 80% acetone extract (Mc-Kinney, 1941). Samples were frozen in liquid nitrogen and stored at -80°C until required.

For polypeptide analysis samples of thylakoid membranes were separated under denaturing conditions at 2° to 3°C in the presence of 0.1% (w/v) SDS (sodium dodecyl sulphate) using a 10 to 25% (w/v) linear gradient polyacrylamide gel (acrylamide:methylenebisacrylamide ratio = 30/0.8) in combination with the Laemmli buffer system (Laemmli, 1970) as described previously (Guseynova et al., 2001). To each slot 20 to 45 μl of samples (an equal Chl content) were applied. The gels were stained for 30 min with 0.04% (w/v) Coomassie brilliant blue G-250 (France) prepared in 3.5% perchloric acid (HClO$_4$). Immediately after electrophoresis the gels were scanned using an Ultroscan 2202 densitometer (LKB, Sweden) with a 633 nm laser as the light source. A set of standard proteins (Sigma, USA) was used for the determination of the molecular masses of polypeptides.

The measurements of fluorescence (F) at 77 K were performed using a Hitachi-850 (Japan) fluorescence spectrophotometer as reported previously (Asadov et al., 1986). Fluorescence emission spectra were corrected for the spectral sensitivity of the spectrophotometer using rhodamine B. Chlorophyll fluorescence was excited by dark blue light with wavelength of 440 nm. The samples on quartz glass fiber were quickly frozen at 77 K by dipping the glass fiber into liquid nitrogen.

Electron transport activities of chloroplasts isolated from control and drought-stressed plants were followed polarographically as O$_2$ evolution or uptake at 20°C using a water-jacketed Clark type oxygen electrode chamber under illumination with saturating white actinic light (850 μE m^{-2}s^{-1}), according to Guseynova et al. (2006). Chloroplasts concentrations equivalent to 100 μg Chl were used for all measurements.

Measurements of photoinduced changes of fluorescence yield from F$_o$ level to F$_{max}$ were carried out at room temperature using laboratory-built set-up as described earlier (Klimov et al., 1982). Potential quantum yield of photosystem (PS) II was estimated according to the formula:

$$\Phi_p = F_v/F_m = (F_m-F_o)/F_m$$

Enzyme extract was prepared by homogenizing leaf material (1 g fr wt) with a pestle in an ice-cold mortar with Na$_2$HPO$_4$/NaH$_2$PO$_4$ buffer. The homogenates were filtered through four layers of cheesecloth and then centrifuged at 4°C. The supernatant were collected and used for the assays of enzymatic activities.

The activity of catalase was determined as a decrease in absorbance at 240 nm for 1 min following the decomposition of H$_2$O$_2$ as described by Kumar and Knowles (1993). The reaction mixture contained 50 mM phosphate buffer (pH 7.0) and

15 mM H_2O_2, and reaction was initiated by adding enzyme extract.

The activity of ascorbat peroxidase (APO) was assayed according to Nakano and Asada (1981). The assay mixture consisted of 0.05 mM ASA, 0.1 mM H_2O_2, 0.1 mM EDTA, 50 mM sodium phosphate buffer (pH 7.6), and 0.3 mL enzyme extract. The activity was measured as a decrease in absorbance at 290 nm for 30 sec.

Glutathione reductase activity was determined at 340 nm for 10 min in reaction mixture containing 100 mM potassium phosphate buffer (pH 7.8), 1 mM EDTA, 0.2 mM NADPH and 0.5 mM GSSG (Yannarelli et al., 2007).

Superoxide dismutase activity was estimated by using SOD Assay Kit-WST (Sigma-Aldrich, USA). The absorbance was recorded at 450 nm and one enzyme unit of SOD activity was defined as the amount of enzyme recuired to cause 50% inhibition of the rate of NBT reduction.

Protein concentration was determined according to Sedmak and Grossberg (1977) by using bovine serum albumin as a standard.

RESULTS AND DISCUSSION

Investigated genotypes respond to water deficit through various changes in physiological and biochemical processes.

Significant differences in relative water content (RWC) were observed between normally irrigated plants and those subjected to water stress. Giymatli-2/17 genotype grown in normal water supply condition showed the higher RWC in the leaves. Drought stress conditions induced a slightly larger decrease in RWC in the more sensitive Giymatli-2/17 than in the more tolerant Azamatli-95; dehydration decreased the RWC by 14% in comparison with fully irrigated plants. The rate of water loss during drought was low in Azamatli-95. The RWC lowered from 83.9% to 72.1% following stress. Exposure to drought caused a reduction in dry weight accumulation in Giymatli-2/17 plants, whereas it had smaller insignificant effects in Azamatli-95, even though both genotypes showed a certain drop in RWC.

A reduction in the total chlorophyll content and Chl *a/b* ratio occurred during drought stress. This pattern of change was not evident in tolerant genotype Azamatli-95, in which these parameters did not change statistically, whereas the difference was significant in sensitive Giymatli-2/17. A drought-induced decrease in pigment contents was previously reported in several plant species, including pea (Moran et al., 1994), durum wheat (Loggini et al., 1999) and *Boea hydroscopica* (Navari-Izzo et al., 2000). The more drought-sensitive

Giymatli-2/17 showed a slight increase in the pool size of xantophyll-cycle components, but such effect was not shown in the tolerant Azamatli-95, that may be explained by its higher rate of electron transport compared with Giymatli-2/17 (Guseynova et al., 2006).

Total protein synthesis was slightly reduced by water deficit in these experiments. The decrease of thylakoid proteins observed during dehydration may be associated with degradation of lipoprotein thylakoid membrane structure. In addition, the photosynthetic apparatus may show acclimation responses such as changes in the relative proportion of stacked and unstacked membrane domains (Anderson and Aro, 1994). At the ultrastructural level the thylakoid system of hydrated chloroplasts was organized in several well-defined and regularly distributed grana connected by parallel stroma lamellae. The increased thylakoid stacking in dried chloroplasts could be a consequence of membrane and/or environmental changes leading to a weakening of the repulsive force between the membrane surfaces. Another influential factor might be the rise due to water loss in the stroma ionic charge screening the repulsive force between thylakoids (Barber, 1982).

The protein profiles of thylakoid membranes in non-stressed and water-stressed plants were analysed. Figure 1 shows density patterns from Coomassie blue staining SDS-PAGE analysis of membrane proteins of two wheat genotypes with different tolerance to drought and contrast architectonics. As shown in Figure 1, thylakoid membranes isolated from the wheat genotypes grown under normal water supply appeared to have about 26 polypeptides with M_r from 115 to 11 kDa. It was found out that Giymatli-2/17 genotype with broad and lodging leaves and drought-sensitive is characterized by low content of chlorophyll *a*-protein of PSI core (CPI) and β-subunit of CF_1 ATP-synthase complex, the high content of proteins in the 33-30.5 kDa region and the relative high amount of polypeptides of light-harvesting complex (LHC) under normal irrigation in comparison with drought-tolerant genotype Azamatli-2/17, having vertically oriented small leaves. Drought stress caused significant changes in the content and composition of thylakoid membranes proteins. The content of CPI (115 kDa) and apoprotein of P_{700} (63 kDa) were maintained at relatively high levels in tolerant genotype Azamatli-95, but were slightly little affected by drought in more sensitive genotype Giymatli-2/17. It is interesting to note that the intensity of 60 kDa polypeptide strongly increases (about 2-fold higher) in the drought-resistant genotype Azamatli-95. However, a detection of this polypeptide was not available in the experiments with

seedlings of wheat grown in growth chamber under controlled environmental conditions (Guseynova et al., 2006). On the basis of obtained results and literature data it is possible to suggest that this protein is related to dehydrins (PCA 60). Seasonal expression of dehydrins has been noted in several species (Wisnewski et al., 1999). The dehydrin family of proteins is induced by environmental stresses that result in cellular dehydration (Close, 1997). All these protein groups are characterized with high hygrophilous protein molecules. During dehydration of cells they prevent water loss on account of high hydrophilic capacity and stabilize cell proteins. PCA 60 was freely distributed in the cytosol, plastid, and nucleus. Although the functional role of dehydrins remains speculative, the data support the hypothesis that it plays a role in preventing denaturation of proteins exposed to dehydrative stresses in a manner similar to chaperones.

The synthesis of α- and β-subunits of CF_1 ATP-synthase complex (55 and 53.5 kDa, respectively) tended to increase slightly in stressed plants of Azamatli-95 and to decrease in Giymatli-2/17. The low content of β-subunits of CF_1 ATP synthase complex has been also shown in pea plants subjected to water deficit at high light exposure (Giardi et al., 1995; Guseynova et al., 2006). Steady-state levels of the core antenna of PSII (CP 47 and CP 43) serve as the connecting antenna between the main light harvesting complex LHCII

and reaction center of PSII remained more or less unchanged in both genotypes. These results agree with data that were obtained earlier (Giardi et al., 1995; Guseynova et al., 2006).

The most striking change was a reveal of protein with molecular mass of 40.5 kDa in tolerant genotype Azamatli-95. It is absent in leaves from non-stressed plants, but at a lower level was detected only in tolerant genotypes subjected to water deficit. According to the current literature, C 40.4 protein share high sequence homology with 34 kDa thylakoid protein CDSP (chloroplastic drought-induced stress protein), previously described in tomato in response to drought. Substantial increases in CDSP 34 transcript and protein abundance were also observed in potato plants, subjected to high illumination (Gillet et al., 1998). The accumulation of two chloroplastic nuclear-encoded proteins in water-stressed *Solanum tuberosum* plants were reported (Pruvot et al., 1996). A stromal protein of 32 kDa related to thioredoxins was suggested to maintain the redox state of chloroplastic proteins upon drought stress (Rey et al., 1998). CDSP 34 protein is proposed to participate in structural stabilization of thylakoids upon environmental constraints and prevent damage resulting from osmotic or oxidative stress. It is supposed that C 40.4 protein is closely bounded with LHCII and has functional role by modeling photosynthetic effectiveness and light dissipation of excess absorbed light energy inside antenna complex (Monte et al., 1999).
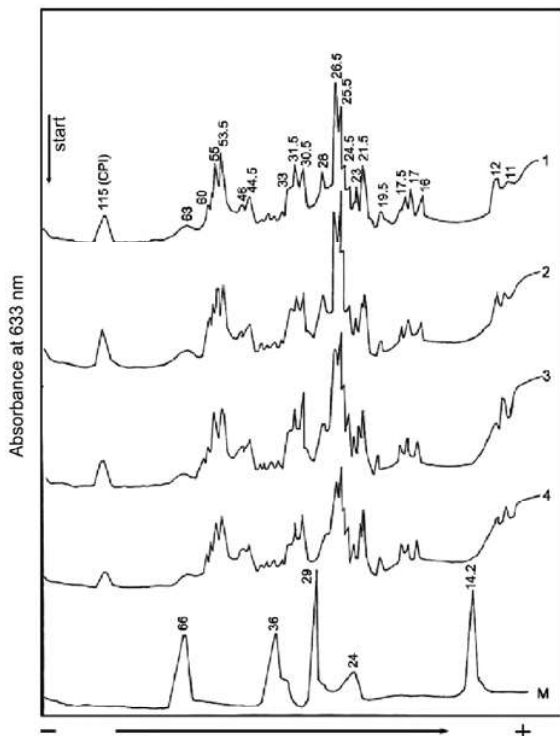

Figure 1. Density patterns from Coomassie blue staining SDS-PAGE (10-25% gel) analysis of thylakoid membrane proteins from wheat plants grown in field conditions under normal water supply (Azamatli-95) (1) and Giymatli-2/17 (3) and drought stress (Azamatli-95) (2) and Giymatli-2/17 (4). M, standard proteins (kDa): bovine serum albumin (66), glyceraldehydes-3-phosthate dehydrogenase (36), carbonic anhydrase (29), trypsinogen (24), and α-lactalbumin (14.2).

At the same time in the more sensitive genotype Giymatli-2/17 there was a considerable decrease of amounts of proteins in 33-30.5 kDa region. The decrease in the content of 31.5 kDa protein in thylakoid membrane from water-stressed plants (especially in Giymatli-2/17) seems to be in part due to its enhanced degradation rate (Sippola et al., 1998; Guseynova et al., 2006). High rate of D1-protein turnover provides stability of thylakoid membranes and their electron transport chain to damaging action of free radicals forms under stress conditions. On the other hand, thylakoid membranes from stressed plants showed an increased level of LHC polypeptides (28-24.5 kDa) in tolerant Azamatli-95 compared to Giymatli-2/17, at which the level of these units decreases.

A slight increase in 21.5 kDa polypeptide (according to literature data it relates to WSCP-water-soluble chlorophyll proteins) was also observed in both genotypes under drought. Such effect was found by us in previous researches with durum wheat seedlings under water stress (Guseynova et al., 2006). It is supposed that this protein might be involved in decrease of protease activity in leaf senescence.

Drought also caused a decrease in the synthesis of low molecular weight polypeptides of 17.5-12 kDa in both genotypes under extreme condition of water supply. The intensity of 11 kDa polypeptide slightly increased in Azamatli-95, but significantly decreased in Giymatli-2/17.

Correlation between tolerance and overexpression of some proteins including 60, 40.5 and 28-24.5 kDa assumes that changes in expression of these polypeptides genes can be functionally involved in the ability of plants to survive and grow under water deficiency.

According to the current literature, there is a cycle of PSII reparation during which the most damaged 32 kDa protein (D1) of reaction center of PSII is replaced (Melis, 1998). Selective proteolysis is involved, inactive form of D1-protein is removed, and newly synthesized D1-polypeptide is integrated into the PSII holocomplex (Chaloub et al., 2003). High rate of D1-protein turnover provides stability

of thylakoid membranes and their electron-transport chain to damaging action of free radicals formed under stress conditions (Guseynova et al., 2006). Thus, the literature and our results suggest that biochemical response at the level of D1-turnover and intensive synthesis of polypeptides 60, 40.5 and 28-24.5 kDa could act as a general adaptation signal for the plant in response to water stress. Table 1 represents the data of membrane proteins in which quantitative changes are significant under drought stress.

In parallel we also measured the fluorescence emission spectra (77 K) of chloroplasts from normally irrigated and drought-stressed plants. As shown in Figure 2, chloroplasts from drought-sensitive genotype Giymatli-2/17 have more intensive fluorescence at 740 nm from PSI under normal water supply. The F687/F740 ratio of control (non-drought stressed) chloroplasts of genotype Azamatli-95 was close to 0.38 and for genotype Giymatli-2/17 − 0.35. The shift of the main peak from 742 to 740 (in Azamatli-95) and from 740 to 738 nm (in Giymatli-2/17) is observed in both genotypes grown under water deficit. According to the data on pigments content in leaves with normal irrigation and in the plants subjected to water deficit a short wavelength shift of the main maximum in the fluorescence spectra is coupled with a decrease in the amount of chlorophyll in PSI antenna (Figure 2). The fluorescence intensity at 740 also slightly increased. The short wavelength peaks at 687 and 695 nm (fluorescence from the PSII core complex CP 47 and CP 43) remained and their fluorescence intensities started to increase sharply under water deficit. It is especially observed in drought-sensitive genotype Giymatli-2/17. At the same time, in chloroplasts from stressed plants, the F687/F740 ratio rises compared with control plants; the lowest value was that of the Azamatli-95 (F687/F740=0.45) and the highest - of Giymatli-2/17 (F687/F740=0.77), suggesting again that the most detrimental influence of drought stress occurs in Giymatli-2/17. The results suggest that

Table 1. Photosynthetic membrane proteins from wheat chloroplasts subjected to changes under drought stress

Samples	Molecular mass of proteins, kDa *					
Azamatli-95 (control)	CPI, 115 (PS I core)	60	55 and 53.5 α– and β–sub. CF₁	33-30.5	28-24.5 (proteins of LHC)	21.5
Azamatli-95 (drought)	0	+	+	0	+	+
Giymatli-2/17 (control)	CPI, 115 (PSI core)	60	55 and 53.5 α- and β-sub. CF₁	33-30.5	28-24.5 (proteins of LHC)	21.5
Giymatli-2/17 (drought)	-	0	-	-	-	+
* Comment: (+) – protein content is increasing, (-) – content is decreasing, 0 – no changes						

antenna system of the photosynthetic apparatus in the drought-tolerant genotype Azamatli-95 is rapidly reorganized and plants began to adapt to environmental stress.

More frequently changes in F687/740 ratio may be explained by redistribution of excitation light energy between PSII and PSI.

Significant differences were found in functional activity of photosynthetic apparatus at the level of photochemical reactions of chloroplasts in comparative studies of genotypes distinguishing by architectonics and drought resistance. In our experiments the highest PSII activity (oxygen evolution rate) of irrigated plants was found in drought-sensitive genotype Giymatli-2/17 with broad and drooping leaves (Table 2). Drought stress causes a significant change in the photochemical activity of chloroplasts in both genotypes. The electron transport activities of all stressed plants were lower than in the control plants. However, the activity of PSII was significantly affected by dehydration in Giymatli-2/17, only 41% of control values remained. In drought-stressed Azamatli-95 leaves the photochemical activity of PSII was about 78% of the control value. The case of PSII inactivation in both genotypes may be suppression of synthesis of 32 kDa protein (D1-protein of reaction centre (RC) of PSII), which is carrier of photochemical active forms of Chl a P_{680}, or breach of electron transfer from pheophytin, intermediate electron carrier on quinone acceptor (Q_A) in non-cyclic transport of electrons. All else possible, desiccation inhibited the energy transfer from the Chl molecules anchor to PSII core complexes.

PSI activity (O_2 uptake rate), however, was affected much less under drought stress (Table 2). It can be caused by a higher ability of PSI to adapt to dehydration.

Concerning the side of drought stress action several authors reported that PSII photochemistry is predisposed by drought stress to photoinhibitory damage (Peltier et al., 1995). In contradiction, Genty et al. (1987) concluded that PSI-mediated electron transport was inhibited by drought, whereas PSII electron transport remained the same. During rehydration PSII activities recover slowly, but PSI complexes recovered their functional forms very quickly (within 1 min) (Hirai et al., 2004).
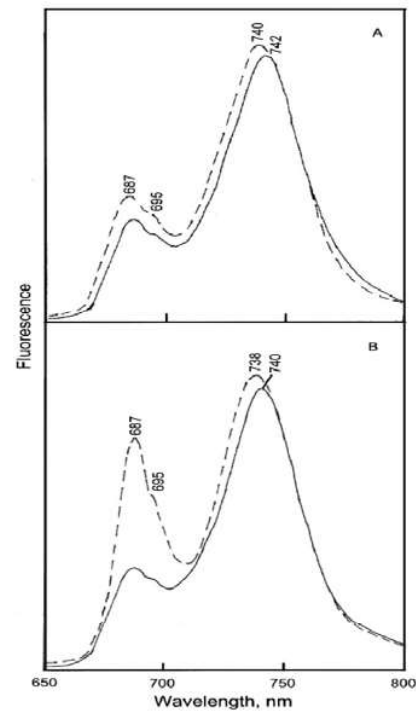

Figure 2. Fluorescence emission spectra at 77 K of chloroplasts from drought-tolerant Azamatli-95 (A) and drought-sensitive Giymatli-2/17 (B) genotypes grown under normal water supply (solid curves) or drought conditions (dashed curves).

It is known that fluorescence yield is minimal (F_o), when primary electron acceptor of PSII, plastoquinone (Q_A), is oxidized. Reduction of Q_A results in rise of chlorophyll fluorescence approximately 3-5 times up to F_m level. Rise of chlorophyll fluorescence yield from initial (F_o) to maximal (F_m) level, i.e. appearance of variable fluorescence (F_v, where $F_v=F_m-F_o$), reflects process of accumulation of reaction centers of PSII in "closed" state with reduced primary quinone acceptor (Q_A).

Values of fluorescent parameters that characterize the functional state of photosynthetic apparatus of winter wheat plants grown under different conditions of water regime are shown in Table 3. Potential quantum yield of photochemical reactions of PSII (F_v/F_m ratio) in chloroplasts from control (non-drought stressed) plants was 0.74 for

Table 2. The Photosystem II and Photosystem I activity in chloroplasts from wheat genotypes subjected to drought stress (μmol O_2 mg^{-1} chlorophyll h^{-1})

Genotypes	Photosystem II $H_2O \rightarrow K_3Fe(CN)_6$	in %	Photosystem I $DCIP\cdot H \rightarrow MV$	in %
Azamatli-95 (control)	45±4	100	250±12	100
Azamatli-95 (drought)	35±3	78	225±9	90
Giymatli-2/17 (control)	85±7	100	190±8	100
Giymatli-2/17 (drought)	35±4	41	150±4	79

Azamatli-95 and 0.81 for Giymatli-2/17, that is typical for normally grown plants. As it seems from Table 3 state of PSII in dehydration process was being significantly changed. Potential yield of photochemical reactions of PSII undergoes appreciable changes in comparison with control plants; the highest value of F_v/F_m was in Azamatli-95 ($F_v/F_m=0.71$) and the lowest one in Giymatli-2/17 ($F_v/F_m=0.69$). It is interesting to note, that chloroplasts from non-drought-tolerant genotype Giymatli-2/17 have higher value of photochemical efficiency of PSII under regular irrigation conditions of growing. However, low ratio of F_v/F_m again confirms that strong effect of drought is appeared in genotype Giymatli-2/17 (genotype Giymatli-2/17 is strongly affected by drought). Decreasing of a photochemical efficiency (F_v/F_m) under severe drought can be considered as a fact of damage of photosynthetic reaction centers.

Table 3. Change of parameters of chlorophyll *a* fluorescence in chloroplasts isolated from wheat leaves after drought. Fluorescence components: F_o - constant fluorescence; F_v - variable fluorescence; F_m - maximal fluorescence*

Variant	Control	Drought	% from control
Azamatli-95			
F_o	29.0 ± 1.2	30.0 ± 2.8	103
F_v	85.0 ± 6.1	74.5 ± 5.4	87
F_v/F_m	0.74	0.71	96
Giymatli-2/17			
F_o	27.0 ± 1.1	28.5 ± 2.9	106
F_v	118.0 ± 6.5	63.0 ± 4.3	54
F_v/F_m	0.81	0,69	85

*Comment: average arithmetic and standard mistakes from three independent experiments, each of which was carried out in double biological frequency, are shown in the table.

Both Q_B-reducing and Q_B-non-reducing complexes of PSII make a contribution in variable fluorescence (F_v). Charge separation is realized in Q_B-non-reducing complexes of PSII, but electrons are not transported to plastoquinone pool. Q_B-reducing complexes of PSII in active state are able to realize electron transport between Q_A and Q_B. They lose this ability when D1-protein is damaged and turn to Q_B-non-reducing complexes (Pshibytko et al., 2003). In optimal conditions due to reactions of reparation cycle the constant ratio between these types of complexes of PSII is supported. Probably, dehydration induces disruption of reactions at the acceptor side of PSII, expressed in increasing of a number of Q_B-non-reducing centers.

Under water deficit linear electron transport is

suppressed by accumulation of plastoquinones caused from difficulty of lateral diffusion of plastoquinones because of increased viscosity of lipid bilayer (Hirai et al., 2004), that could be caused by increasing of reduction level of plastoquinone pool, damage of Q_B-binding site with D1-protein and deterioration of conditions of damaged D1-protein reparation (Melis, 1998).

Activity of antioxidative enzymes differed in investigated wheat genotypes under normal water supply condition at all stages of ontogenesis. Catalase (CAT) activity increased in both genotypes under water deficiency. Maximum level of catalase activity was revealed at the end of flowering in response to drought stress (Figure 3). As it is shown from the Figure 3, catalase activity was higher in Azamatli-95 than the corresponding control at all the stages of study. Nevertheless, activity of this enzyme was lower in two stages – end of earing and flowering in drought-sensitive genotype Giymatli-2/17 than the control. The increase of CAT activity in plants under water stress has been reported in other study (Quartacci and Navari-Izzo, 1992).

It is known that catalase reacts with H_2O_2 directly to form water and oxygen. The decrease in CAT activity in the end of ontogenesis could indicate its inactivation by the accumulated hydrogen peroxide by water shortage and could be explained partly by photoinactivation of the enzyme. When plants are not exposed to water stress, resynthesis of CAT compensates for the loss of total activity caused by irradiance. Inhibition of protein synthesis induced by water stress conceivably could impair resynthesis and partly account for the marked decrease in CAT activity in plants subjected to water stress in the light.

Ascorbate peroxidase (APO) activity in Giymatli-2/17 was higher under water deficiency than the corresponding control at all stages of development. In Azamatli-95 higher level of APO activity was revealed at the end of earing and at flowering stage, and in a stage of milky ripeness (Figure 4). Detailed study of APO activity dynamics in wheat plants grown under drought conditions allows to conclude that the function of APO increases during water deficiency. An increase of peroxidase (POD) activity was also observed by different authors during a drought and salt stress (Siegel, 1993). It indicates the formation of large amounts of H_2O_2 during water stress. Increases of activity can explain with some assumptions: elevated H_2O_2 concentrations could release POD from membrane structures, with which it is normally associated. POD could be synthesized *de novo* at least in some cases. Water stress could increase the accumulation of POD substrates, such as glutathione, ascorbate, and phenolic compounds, which, in turn, are scavengers of activated oxygen species.
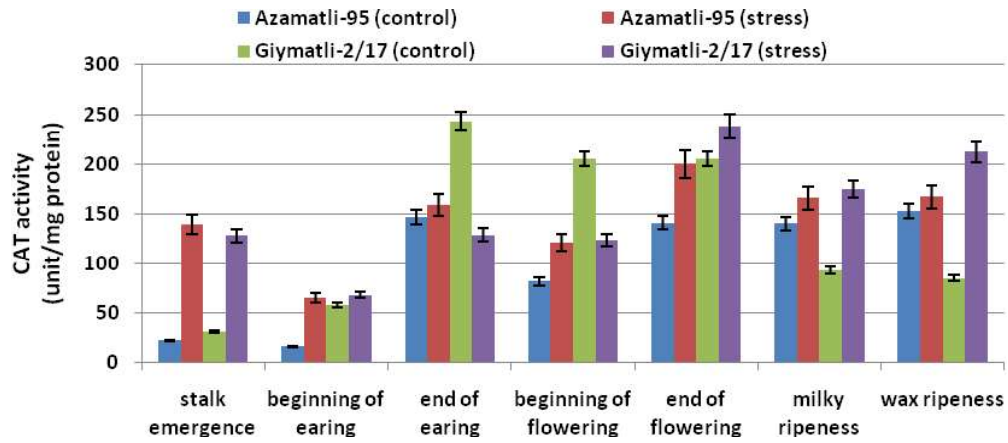
Figure 3. Effect of water stress on catalase activity in leaves from wheat genotypes at different stages of ontogenesis.
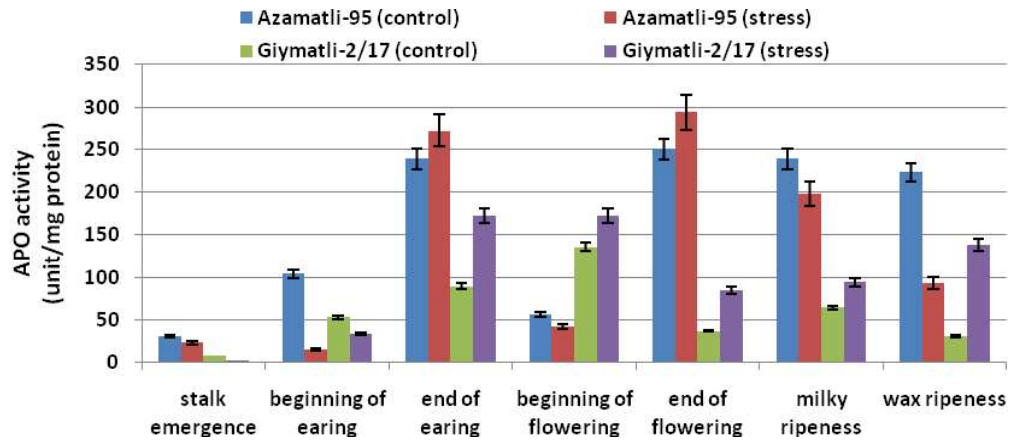

Figure 4. Effect of water stress on ascorbate peroxidase activity in leaves from wheat genotypes at different stages of ontogenesis.
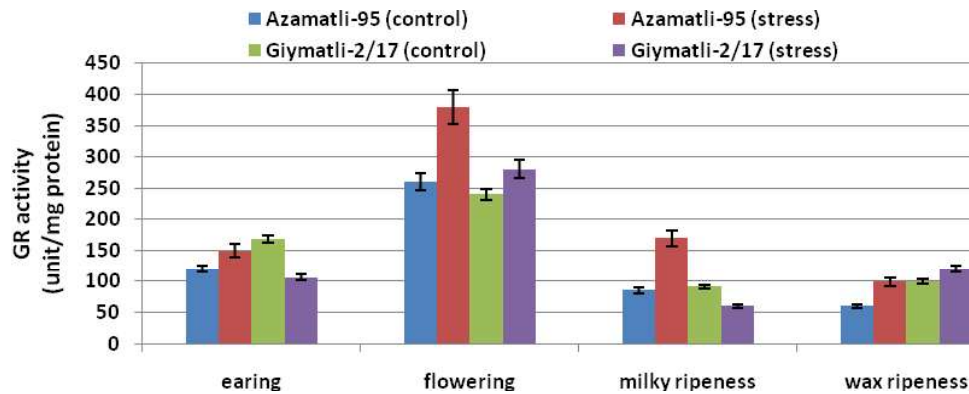

Figure 5. Effect of water stress on glutathione reductase activity in leaves from wheat genotypes at different stages of ontogenesis.
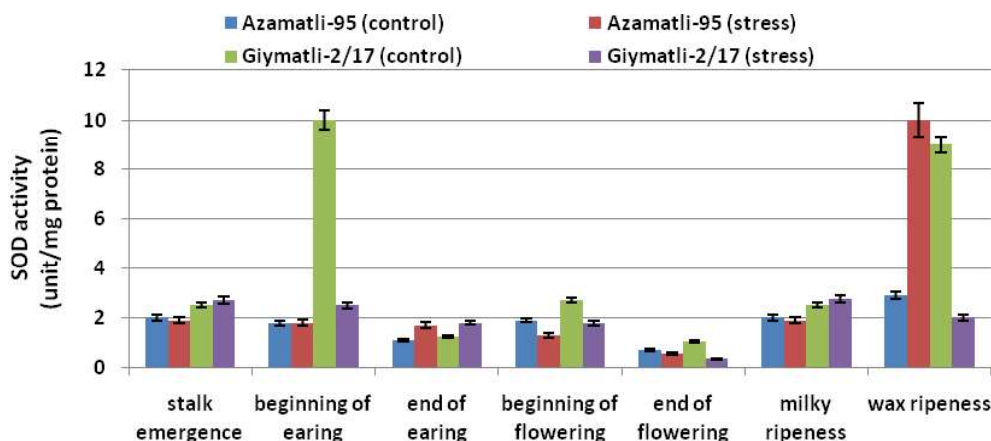
Figure 6. Effect of water stress on superoxide dismutase activity in leaves from wheat genotypes at different stages of ontogenesis.

Also it is known that H_2O_2 participates in signal transduction during development of oxidizing stress, inducing genes of cytosolic POD.

The maximum activity of glutathione reductase (GR) both as in the control, as well as in drought-subjected plants was observed at the flowering stage (Figure 5). In tolerant genotype Azamatli-95 in all the stages of ontogenesis GR activity was higher in the stress conditions compared with the control. In sensitive genotype Giymatli-2/17 the increase of activity was observed only in the stages of flowering and wax ripeness.

Dynamics of superoxide dismutase (SOD) functioning differed from other enzymes. SOD activity was lower in both genotypes as compared with control variants (Figure 6). Only in the end of ontogenesis, at wax ripeness stage, when drought effect is greatest, SOD activity increased in tolerant genotype Azamatli-95. Many authors specify key role SOD in antioxidative protection (Alscher et al., 2002). However, results obtained by us on SOD activity differed partly from the literary data. Nevertheless, it is known that plant cells contain a little izoform of SOD which probably unequally react to water deficiency. The study of these SOD isoforms during water stress induction revealed differential regulation of their activities: MnSOD and FeSOD activities increased rapidly while Cu/ZnSOD activities decreased in cowpea plants (Brou et al., 2007).

Obtained results suggest that water stress alters the equilibrium between free radicals production and enzymatic defense reactions in wheat genotypes and Giymatli-2/17 has less efficient antioxidant systems than Azamatli-95.

The more drought-sensitive genotype Giymatli-2/17 responded to a period of stress by reducing photosynthetic efficiency and biomass accumula-

tion. In this genotype the defense mechanisms prevent plants from suffering irreversible damages during drought. Therefore, in Azamatli-95 the photosynthetic electron transport was probably sufficient to preclude the build-up of excess energy in PSII (Loggini et al., 1999). On the other hand, drought tolerant genotype Azamatli-95 seems able to avoid drought stress by maintaining a high photosynthetic activity, and does not suffer an oxidative stress high enough to trigger the defense mechanisms active in the genotype Giymatli-2/17. Dynamics of changes of antioxidative enzymes activity in wheat genotypes under normal water supply and deficiency of water in all stages of ontogenesis reveal that drought differently changes a balance between production of free radicals and enzyme reactions of protection.

The obtained results may provide an entry point and a reference to future analysis of gene expression during drought. In addition, these results can suggest possible targets for the enhancement of stress tolerance in crops by genetic engineering. The data presented by us here might be used for monitoring environmental stresses in field grown plants and help in selecting stress-resistant varieties for growth under unfavorable conditions.

REFERENCES

Aliev J.A. (1998) Importance of photosynthesis of various organs in protein synthesis in grain of wheat genotypes under water stress. Proceedings of the XIth International Congress on Photosynthesis, Budapest (Hungary), 1998. In: Photosynthesis: Mechanisms and Effects (Garab G., ed.), Kluwer Academic Publishers, Dordrecht, Boston, London **5:** 3829-3832.

Aliev J.A. (2001) Physiological bases of wheat breeding tolerant to water stress. Proceedings of the 6th International Wheat Conference, Budapest, Hungary, 2000. In: Wheat in a Global Environment (Bedo Z., Lang L., eds.), Kluwer Academic Publishers, Dordrecht, Boston, London **9**: 693-698.

Aliyev J.A. (2002) Peculiarities of high productive wheat photosynthesis and usage of photosynthetic signs in selection. Proceedings of Azerbaijan National Academy of Sciences (biological sciences) **1-6**: 5-29 (in Russian).

Aliev J.A., Suleymanov S.Y., Guseinova I.M., Asadov A.A., Ismailov M.A. (1992) Effect of specific translation inhibitors on polypeptide composition and spectral characteristics of wheat thylakoid membrane. Biochemistry (Moscow) **57**: 679-686.

Alscher R.G., Erturk N., Heath L.S. (2002) Role of superoxide dismutases (SODs) in controlling oxidative stress in plants. Exp. Bot. **53**: 1331-1341.

Anderson J.M., Aro E.M. (1994) Grana stacking and protection of photosystem II in thylakoid membranes of higher plant leaves under high irradiance: a hypothesis. Photosynth. Res. **41**: 315-326.

Asadov A.A., Zulfugarov I.S., Suleymanov S.Y, Aliev D.A. (1986) Pigment organization in light-harvesting complex and pigment-protein complex of photosystem I of spinach chloroplasts. DAN SSSR **287**: 444-447.

Barber J. (1982) Influence of surface charges on thylakoid structure and function. Annu Rev. Plant Physiol. **33**: 261-295.

Baruah A., Simkova K., Apel K., Laloi C. (2009) *Arabidopsis* mutants reveal multiple singlet oxygen signaling pathways involved in stress response and development. Plant Mol. Biol. **70**: 547-563.

Brou Y.C., Zeze A., Diouf O., Eyletters M. (2007) Water stress induces overexpression of superoxide dismutases that contribute to the protection of cowpea plants against oxidative stress. Afr. J. Biotech. **6 (17)**: 1982-1986.

Chaloub R.M., Silva L.M., Roodriges M.A., Santos C.P.D. (2003) Phase transition of thylakoid membranes photoinhibition in the cyanobacterium *Anabaena siamensis*. Photosynth. Res. **78**: 143-152.

Close T.J. (1997) Dehydrins: A commonality in the response of plants to dehydration and low temperature. Physiol. Plant. **100**: 291-296.

Friso G., Giacomeli L., Ytterberg A.J., Peltier J.-B., Rudella A., Sun Q. (2004) In-depth analysis of the thylakoid membrane proteome of *Arabidopsis thaliana* chloroplasts; new proteins, new functions, and a plastid proteome database. Plant Cell **16**: 478-499.

Gechev T.S., Breusegem F.V., Stone J.M., Denev I., Laloi C. (2006) Reactive oxygen species as signals that modulate plant stress responses and programmed cell death. Bio. Essays **28**: 1091-1101.

Genty B., Briantais J.-M., Viera Da Silva J.B. (1987) Effects of drought on primary photosynthetic processes of cotton leaves. Plant Physiol. **83**: 360-364.

Giardi M.T., Cona A., Kucera T., Masojidek J., Mattoo A.K. (1995) D1 turnover as an adaptation signal for plants to recover from drought. In: Proc. Int. Cong. Integrated Studies on Drought Tolerance of Higher Plants "Inter Drought 95": 1-5.

Gillet B., Beyly A., Peltier G., Rey P. (1998) Molecular characterization of CDSP34, a chloroplastic protein induced by water deficit in *Solanum tuberosum* L. plants, and regulation of CDSP 34 expression by ABA and ligh illumination. Plant J. **16**: 257-262.

Guseynova I.M., Suleymanov S.Y., Aliyev J.A. (2001) Regulation of chlorophyll-protein complex formation and assembly in wheat thylakoid membrane. J. Biochem. Mol. Biol. **34**: 496-501.

Guseynova I.M., Suleymanov S.Y., Aliyev J.A. (2006) Protein composition and native state of pigments of thylakoid membrane of wheat genotypes differently tolerant to water stress. Biochemistry (Moscow) **71**: 173-177.

Hirai M., Yamakawa R., Nishio J., Yamaji T., Kashino Y., Koike H., Satoh K. (2004) Deactivation of photosynthetic activities as triggered by loss of a small amount of water in a desiccation-tolerant cyanobacterium, Nostoc commune. Plant Cell Physiol. **45**: 872-878.

Hu H., You J., Fang Y., Zhu X., Qi Z., Xiong L. (2008) Characterization of transcription factor gene SNAC2 conferring cold and salt tolerance in rice. Plant Mol. Biol. **67**: 169-181.

Klimov V.V., Allakhverdiev S.I., Shuvalov V.A., Krasnovsky A.A. (1982) Effect of extraction and re-addition of manganese on light reactions of Photosystem II preparations. FEBS Lett. **148**: 307-312.

Kumar C.N., Knowles N. (1993) Changes in lipid peroxidation and lipolytic and free-radical scavenging enzyme during aging and sprouting of potato (*Solanum tuberosum* L.) seed-tubers. Plant Physiol. **102**: 115-124.

Laemmli U.K. (1970) Cleavage of structural proteins during the assembly of the head of Bacteriophage. Nature **227**: 680-685.

Loggini B., Scartazza A., Brugnoli E., Navari-Izzo F. (1999) Antioxidative defense system, pigment composition, and photosynthetic efficiency in two wheat cultivars subjected to drought. Plant Physiol. **119**: 1091-1098.

Mc-Kinney G. (1941) Absorption of light by chlorophyll solutions. J. Biol. Chem. **140**: 315-322.

Melis A. (1998) Dynamics of photosynthetic membrane composition and function. Biochim. Bio-

phys. Acta **1052**: 87-106.

Monte E., Ludevid D., Prat S. (1999) Leaf C 40.4: a carotenoid-associated protein involved in the modulation of photosynthetic efficiency. Plant J. **19**: 399-410.

Moran J.F., Becana M., Iturbe-Ormaetyl I., Frechilla S., Klucas R.V, Aparicio-Tejo P. (1994) Drought induced oxidative stress in pea plants. Planta **194**: 346-352.

Nakano Y., Asada K. (1981) Hydrogen peroxide is scavenged by ascorbate-specific peroxidase in spinach chloroplasts. Plant Cell Physiol. **22**: 867-880.

Navari-Izzo F., Quartacci M.F., Pinzino C., Rascio N., Vazzana C., Sgherri C.L.M. (2000) Protein dynamics in thylakoids of the desiccation-tolerant plant *Boea hydrosconica* during dehydration and rehydration. Plant Physiol. **124**: 1427-1436.

Peltier G., Tourneux C., Cournac L., Dimon B., Rumeau D. (1995) Effects of water deficit on the photosynthetic activity of C_3-plants measured using ^{18}O and mass spectrometry. In: Proc. Int. Congr. Integrated Studies on Drought Tolerance of Higher Plants "Inter Drought 95": VIII B.

Pruvot G., Cuine S., Peltier G., Rey P. (1996) Characterization of a novel drought-induced 34 kDa protein located in the thylakoids of *Solanum tuberosum* L. plants. Planta **198**: 471-479.

Pshibytko N.L., Kalitukho L.N., Kabashnikova L.F. (2003) Effect of water deficit and high temperature on photosystem II in *Hordeum vulgare* leaves of various ages. Russian J. Plant Physiol. **50**: 51-58.

Quartacci M.F., Navari-Izzo F. (1992) Water stress and free radical mediated changes in sunflower seedlings. J. Plant Physiol. **139**: 621-625.

Rey P., Pruvot G., Becuwe N., Eymery F., Rumeau D., Peltier G. (1998) A novel thioredoxin-like protein located in the chloroplast is induced by water deficit in *Solanum tuberosum* L. plants. Plant J. **13**: 97-107.

Sedmak J.J., Grossberg S.E. (1977) A rapid, sensitive, and versatile assay for protein using Coomassie brilliant blue G 250. Anal. Biochem. **79**: 544-552.

Sharma K.K., Lavanya M. (2002) Recent developments in transgenics for abiotic stress in legumes of the semi-arid tropics. In: Genetic Engineering of Crop Plants for Abiotic Stress (Ivanaga M., ed.). JIRCAS Working Report, JIRCAS: Tsukuba, Japan **23**: 61-73.

Siegel B.Z. (1993) Plant peroxidases: an organism perspective. Plant Growth Regul. **12**: 303-312.

Sippola K., Kanervo E., Murata N., Aro E.-M. (1998) A genetically engineered increase in fatty acid unsaturation in *Synechoccoccus sp.* PCC 7942 allows exchange of D1 proteins forms and sustenance of photosystem II activity at low temperature. Eur. J. Biochem. **251**: 641-648.

Tambussi E.A., Nogues S, Araus J.L. (2005) Ear of durum wheat under water stress: water relations and photosynthetic metabolism. Planta **221**: 446-458.

Wisnewski M., Webb R., Balsamo R., Close T.J., Yu X.-M., Griffith M. (1999) Purification, immunolocalization, cryoprotective, and antifreeze activity of PCA60: A dehydrin from peach (*Prunus persica*). Physiol. Plant. **105**: 600-608.

Yannarelli G.G., Fernandez-Alvarez A.J. (2007) Glutatione reductase activity and isoforms in leaves and roots of wheat plants subjected to cadmium stress. Phytochemistry **68**: 505-512.

Photosynthesis and Productivity of Soybean [*Glycine max* (L.) Merr.]

Jalal A. Aliyev[1,2]*****, **Rufat S. Mirzoyev**[1]

[1]*Research Institute of Crop Husbandry, Ministry of Agriculture of Azerbaijan Republic, Pirshagi Village, II Sovkhoz, Baku AZ 1098, Azerbaijan*
[2]*Institute of Botany, Azerbaijan National Academy of Sciences, 40 Badamdar Shosse, Baku AZ 1073, Azerbaijan*

The peculiarities of leaf carbon dioxide gas exchange in soybean genotypes grown in field over a large area and contrasting in duration of vegetation, photosynthetic traits and productivity were studied. Varietal differences in the daily and ontogenetic changes in photosynthesis and photorespiration were identified. It was established that the period of the high activity of photosynthetic apparatus in high productive soybean genotypes lasts for a longer time. The photosynthetic rate and the rate of CO_2 release in light due to photorespiration are higher in high productive genotypes. The magnitude of photorespiration in contrast soybean genotypes constitutes about 28-35% of photosynthetic rate. The ratio between true photosynthesis and photorespiration in genotypes with different productivity is constant enough during ontogenesis, indicating a direct positive correlation between true photosynthesis and photorespiration.

Keywords: photosynthesis, photorespiration, productivity, soybean genotypes

INTRODUCTION

Soybean belongs to the legume family (*Fabaceae*) originally from East Asia and one of the oldest cultivated plants. The cultivation of the soybean is referred to the Chinese literature as early as the third millennium BC. It was recognized only in the XIX century, and since then it has been widely spread worldwide. Cultural soybean is widely grown in Asia, Southern Europe, North and South America, Central and Southern Africa, Australia, the islands in the Pacific and Indian oceans at latitudes from the equator to 55-60°.

The soybean is often called "the miracle plant", such interest is determined by a high quality of its grain, which contains 35-55% of easily digestible proteins, 17-27% of fats, 30% of carbohydrates, vitamins, etc., depending on variety and growing conditions. Among all worldwide cultivated agricultural crops the soybean is one of the most high-protein ones. Due to rich and varied chemical composition it is widely used as a food, forage and industrial crop, having a great agrotechnological importance as well (Aliyev and Akperov, 1995, 1998; Osoki and Kennelly, 2003; Pimentel and Patzek, 2008; Sakai and Kogiso, 2008). The soybean has also the ability to assimilate air nitrogen (Burris and Roberts, 1993) and, therefore, requires minimal costs for nitrogen fertilizers, which is often considered the single major energy contribution to agriculture.

World soybean production was about 210.9 million metric tons in 2009 (Soystats, 2010). The consumption of soy-based products increases worldwide due to the described beneficial effects, which include reduction of cholesterol level, prevention of cancer, diabetes and obesity, protection against intestinal and kidney diseases (Friedman and Brandon, 2001).

The soybean is an annual plant with a pivotal root system. All species of the soybean has trifoliate leaves with drooping leaflets and pinnate venation, occasionally leaves with 5-, 7- and 9-leaflets are found.

The process of photosynthesis is the main part of total plant productivity. The soybean, like most agricultural crops, belongs to the so-called C_3-plants. A part of carbon dioxide assimilated during respiration in light is released from leaves simultaneously with photosynthesis (Sharkey, 1988). This results in much less real value of CO_2 assimilation in C_3-plants than the realized photosynthesis.

Since 1970's a concept on wastefulness of photorespiration has been formulated by many researches, and attempts to decrease or suppress it with the purpose to increase the crop productivity are still made (Zelitch, 1971, 1975; Ogren, 1975, 1976; Chollet and Ogren, 1975; Holaday and Chollet, 1984; Peterhansel and Maurino, 2010). The conception on possibility of significant increase in

*E-mail: aliyev-j@botany-az.org

productivity of C_3-plants through the selection of samples with low rate of photorespiration was developed. It was suggested to search the ways to eliminate or reduce photorespiration by genetic or chemical means (Zelitch, 1971, 1975, 1992; Ogren, 1975, 1976; Servaites and Ogren, 1977; Kebeish et al., 2007; Maurino and Peterhansel, 2010). However, chemicals which inhibit glycolate metabolism did not reduce photorespiration and increase photosynthetic efficiency (Servaites and Ogren, 1977). In addition, on the basis of the theory about the relationship between photosynthesis and photorespiration based on the competition between CO_2 and O_2 for ribulose-1,5-bisphosphate carboxylase, which appears at the level of carboxylase-oxygenase function of this enzyme, the existence of a positive relationship between the processes of photosynthesis and photorespiration at a constant intracellular CO_2 concentration has been demonstrated (Aliev et al., 1988, 1996b).

The results of comprehensive study of components of leaf carbon dioxide gas exchange in soybean genotypes contrasting in productivity and photosynthetic traits under a natural growth conditions are presented in the paper.

MATERIALS AND METHODS

Experiments were performed on irrigated area at the Absheron Experimental Station of the Research Institute of Crop Husbandry. Research targets include different soybean genotypes (*Glycine max* (L.) Merr.), contrasing in height, architectonics, duration of vegetation, productivity and other morpho-physiological traits, Rannaya-10, Bystritsa, Volna, VNIIMK-3895, Komsomolka, Provar, VNIIMK-9, Plamya, Biyson and Visokoroslaya-3 were used (Figure 1-4). The genotypes Bystritsa and Volna are short-stemmed (40-55 cm), early maturing (growing season takes 80-90 days), with small leaves, compact bushes, low productive (2-2.3 t ha^{-1}). Komsomolka and VNIIMK-3895 are medium-stemmed (60-70 cm), medium maturing (growing season lasts from 115 to 126 days), with medium-sized grain, distinguish by semi-compact bushes, medium branching, high fixation of inferior beans, high productive (3.5-4.0 t ha^{-1}). The genotype Rannaya-10 is a short-stemmed, the growing season lasts from 110 to 115 days, with small grains, semi-compact bushes, high productive (3.3 t ha^{-1}). Provar, Biyson, VNIIMK-9, Visokoroslaya-3 and Plamya varieties belong to the high-stemmed group (80-115 cm), medium maturing (growing season takes 120-138 days), with large grains, and are characterized by wide bushes and medium pro-

ductivity (2.5-3.0 t ha^{-1}). The varieties Provar and Biyson are introduced from the USA, the other varieties were bred at the All-union Research Institute of Oil and Essential Oil Crops (VNIIMK).

All genotypes were grown under identical field conditions over a large area in compliance with all requirements of cultivation agrotechnology and experimental work (Guidelines on soybean cultivation, 1978; Aliyev et al., 1981, 1982; Aliyev and Akperov, 1985; Mirzoyev, 1990). The record plot area was 54 m^2, field experiments were repeated 4-times, and the optimal inter-row space was 60 cm. High agricultural background (optimal conditions for mineral nutrition) was used to determine the potential photosynthetic capacity of the studied soybean varieties (Aliyev and Akperov, 1985, 1986).

Sowing was carried out at the end of April, under soil temperature no lower than 12-13°C. Soil moisture was maintained at 70-75% of TAW (total available water capacity). During the growing season phenological observation of plant growth and development was carried out.

The rate of carbon dioxide gas exchange was measured using an infrared gas analyzer URAS-2T ("Hartman and Braun", Germany) in an open air system (Aliyev et al., 1996a). The special brass made thermostatic leaf chamber with optical glass windows of 10 cm^2 area was made.

The rate of photorespiration was determined by difference between the values of CO_2 release rate in light without CO_2 and dark respiration.

Leaf assimilation surface was measured using the "AAC-400" automatic area meter ("Kayashi" Delkon Co LTD, Japan). The specific leaf density (SLD) was calculated by the ratio of its dry weight to the area. Photosynthetically active radiation (PAR) was calculated according to Tooming and Gulyaev (1967). Data were processed at the 5% level of statistical significance (Dospekhov, 1985).

RESULTS AND DISCUSSION

The analysis of morpho-physiological traits of the soybean harvest showed that main factors of the yield are conditions for the functioning of all photosynthetic systems at the crop level determined by cultivation conditions, particularly mineral nutrition and irrigation. It was shown that high agricultural background provides the increase in yield and significant improvement of grain quality (Aliyev and Akperov, 1986). Intensive genotypes with optimum architectonics possess higher photosynthetic activity and provide high yield (3-4 t ha^{-1}) and high grain quality (40% protein).

Figure 1. Soybean genotype *Glycine max* (L.) Merr.

Figure 2. Sowings of different soybean genotypes.

The contribution of leaves to the total CO_2 assimilation largely depends on their layer location and spatial orientation (Aliyev and Akperov, 1985; Mirzoyev, 1990). Physiologically active leaves of middle layers (9, 10, 11) with higher specific leaf density (0.44-0.51 g dm^{-2}) assimilate CO_2 more intense than leaves of the other layers. Leaves of upper layers also have a maximal value of SLD and photosynthetic rate in comparison with that of the lower ones. Obviously, the increase in SLD of the leaves of upper and middle layers under a favorable luminosity keeps the lower layers under the luminosity insufficient for active photosynthesis.

Comparative study of the rate of photosynthe-

sis during the day showed that, regardless of genotypes, diurnal variations in leaf photosynthetic rate are characterized by double-peak curves with sharp increase in photosynthetic rate in the morning (9-11 a.m.) and the evening (4-6 p.m.) and midday depression (Figure 5-7). Leaf photosynthesis in the low productive genotype Bystritsa starts at approximately 7 a.m., increases rapidly at sunrise and reaches its maximum value at 11 a.m. Then the rate of photosynthesis sharply drops at 2-3 p.m., and the lowest value during the day is being observed. After 3 p.m. the second peak is observed. It should be noted that solar radiation at 2 p.m. was the highest and amounted to 0.44 cal cm^{-2} min^{-1}.

Figure 3. Measurement of the rates of photosynthesis and photorespiration in soybean genotypes in the field.

Figure 4. Harvest of soybean genotypes.

Change in ambient temperature and PAR during the day shows that their maximum value is achieved at 12 a.m. – 4 p.m. (Figure 5A). Diurnal depression of photosynthesis occurs at this time. In the midday CO_2 assimilation drop is caused by increase in temperature of leaves, resulting in increased respiration, water regime disturbance, weakening of assimilates outflow and changes in other physiological processes.

In the evening the rate of photosynthesis decreases and carbon dioxide compensation point is being observed. At nightfall the photosynthetic gas exchange turns into the respiratory and carbon dioxide is released as a result of respiration. At night the

rate of dark respiration reaches its maximum value and then begins to decrease. After 5-6 p.m. the CO_2 release rate in the dark respiration decreases sharply, and after 7 a.m., at the sunrise the respiratory gas exchange turns into the photosynthetic, which increases dramatically within a short time.

High productive genotypes have a higher photosynthetic rate than low productive ones. A similar pattern is observed in the dynamics of the respiratory gas exchange. During the night period, high productive genotypes have relatively higher respiration rate.

The leaves of lower and middle layers of high productive genotypes during the branching stage assimilate rather more CO_2 than leaves in similar layers of medium productive genotypes. Leaves of the middle layer assimilate more CO_2 during this stage in all studied genotypes (Figure 8).
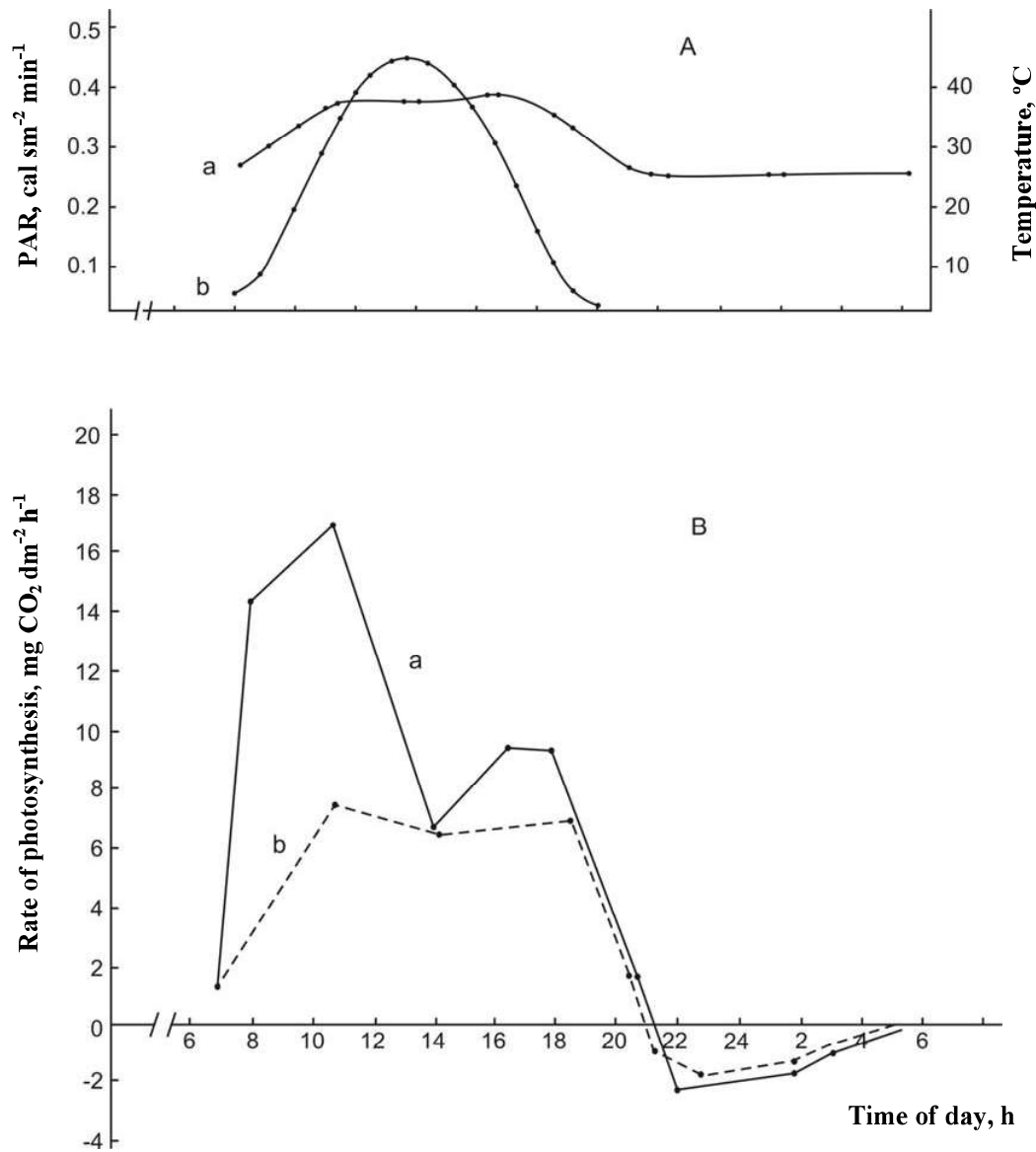

Figure 5. The diurnal patterns of the leaf gas exchange rate in the low productive genotype Bystritsa at the grain filling stage.
Aa – ambient temperature, Ab - PAR; Ba - the rate of leaf gas exchange in plants grown using mineral fertilizers; Bb - the rate of leaf gas exchange in plants grown without mineral fertilizers (control).

Figure 6. The diurnal pattern of the leaf gas exchange rate in the high productive genotype Komsomolka at the grain filling stage.
Aa – ambient temperature, Ab - PAR; Ba - the rate of leaf gas exchange in plants grown using mineral fertilizers; Bb - the rate of leaf gas exchange in plants grown without mineral fertilizers (control).
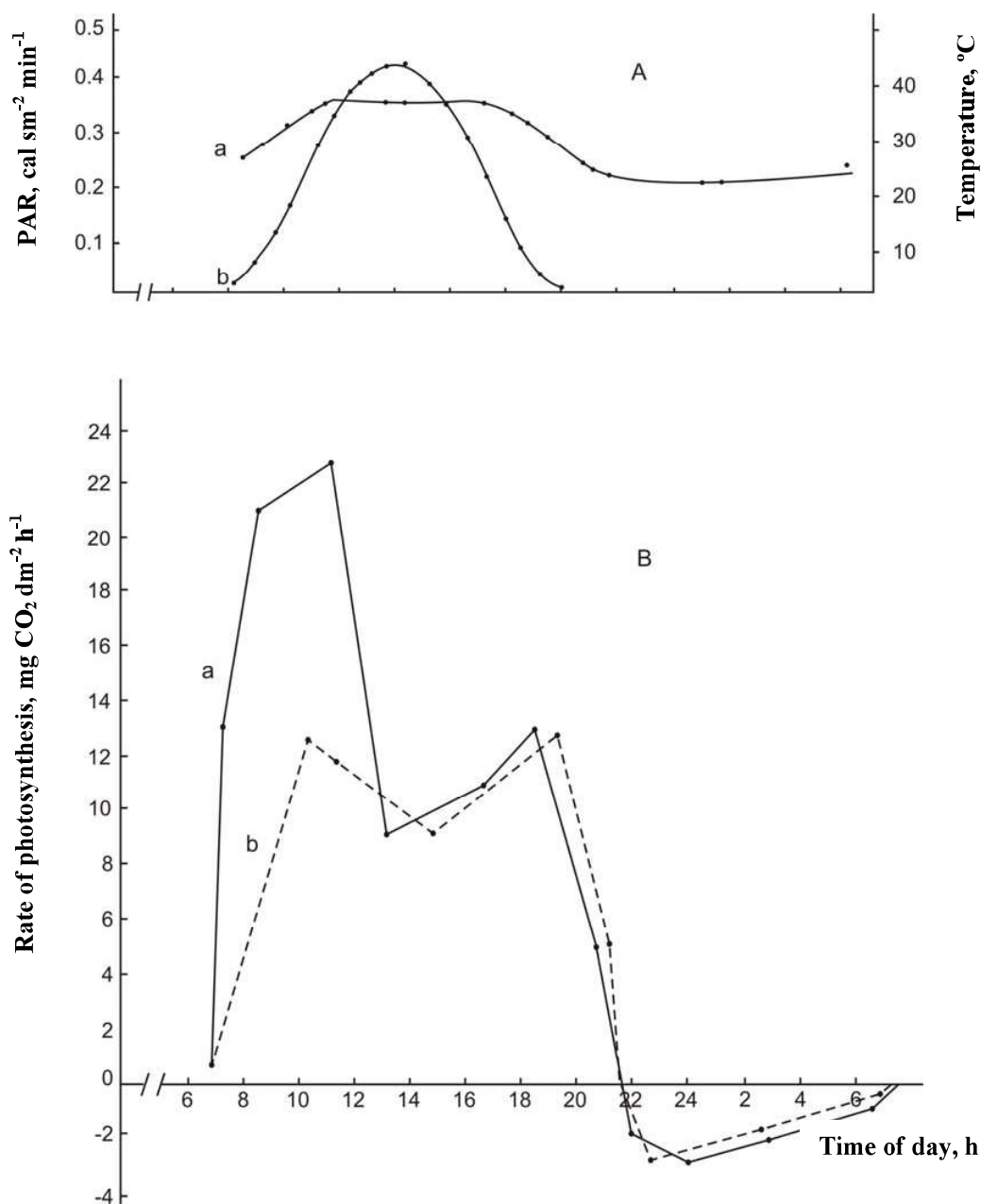
During the flowering stage the rate of CO_2 assimilation increases sharply in leaves of all layers in all genotypes, but the maximum value of CO_2 assimilation is observed in leaves of the middle layer. In the period of pod formation the intensity of lower layered leaves drops sharply. Throughout the growing season the leaves of the middle layer were distinguishing by the highest rate of photosynthesis. By the end of the growing season the activity of leaves of the upper layer remained high as well.

Soybean genotypes contrasting in genetic and phenotypic peculiarities differ by maximum value of photosynthetic rate and duration of their highly active period as well during ontogenesis (Figure 9). Photosynthetic rate in leaves of different soybean genotypes gradually increases since the branching stage and reaches the maximum at the flowering - pod formation stages, and then decreases at the end of pod formation.
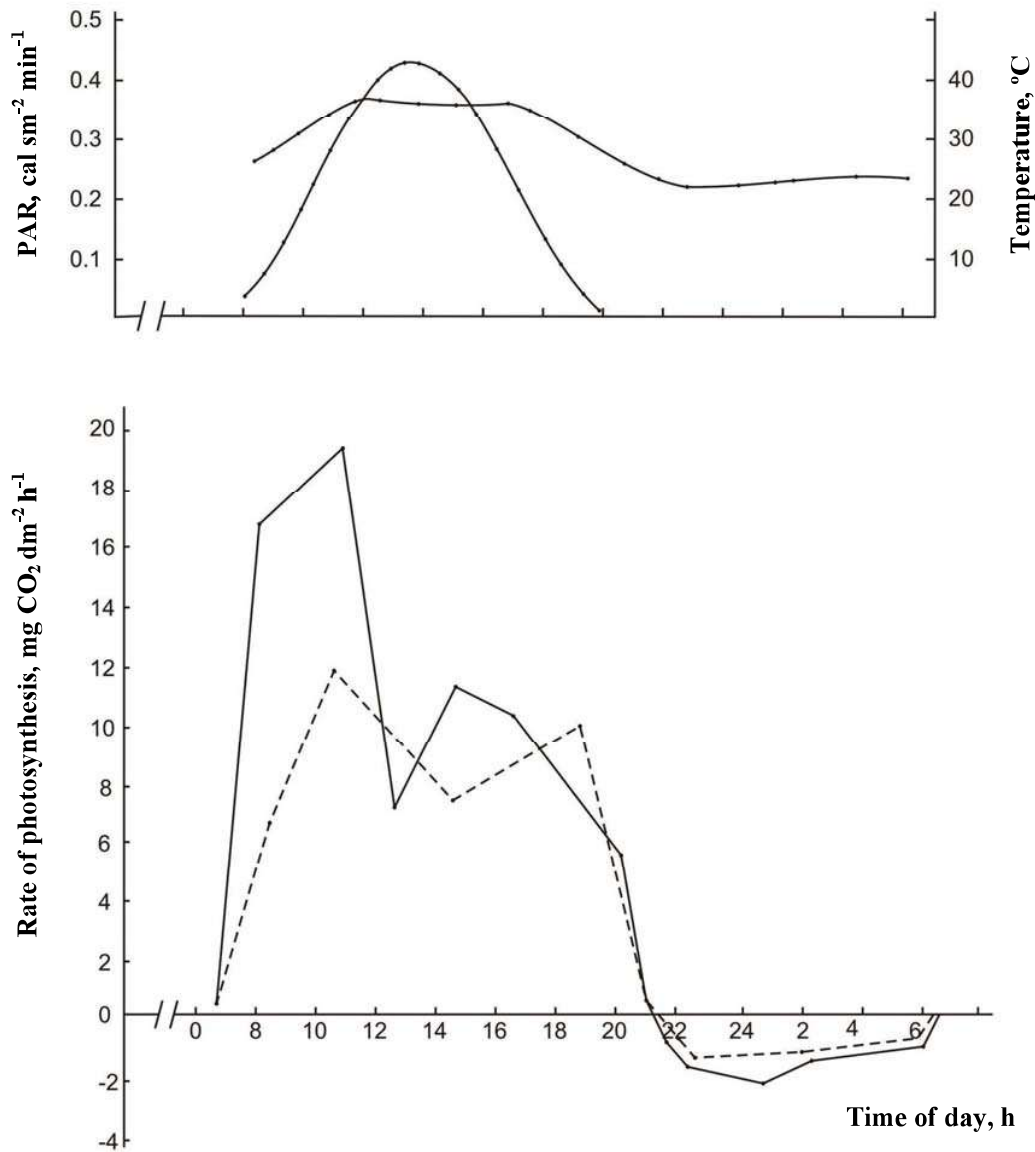
Figure 7. The diurnal pattern of the leaf gas exchange rate in the medium productive genotype Provar at the grain filling stage.
Aa – ambient temperature, Ab - PAR; Ba - the rate of leaf gas exchange in plants grown using mineral fertilizers; Bb - the rate of leaf gas exchange in plants grown without mineral fertilizers (control).

At the same time, leaves of the high productive genotypes (VNIIMK-3895 and Komsomolka) at all developmental stages, especially during flowering and pod formation, assimilate CO_2 more intensively and maintain high rate of photosynthesis for longer time. Pod formation stage in VNIIMK-3895 variety starts 5-8 days earlier and the rate of photosynthesis is maintained at a high level within 10-15 days. The longest flowering - pod formation period was observed in this variety (an average of 53 days over four years). Hence, the total longevity of the growing season does not play a major role in the grain yield but the duration of the period of pod forma-

tion and grain filling does (Mirzoyev, 1988 a, b; Akperov and Mirzoyev, 1990; Aliyev et al., 1992).

In contrast to medium- and long-stemmed genotypes, the short-stemmed early maturing genotypes (Bystritsa and Volna) are characterized by a short period of high values of the photosynthesis rate. It suggests that early maturity and short stature are not always accompanied by a high value of the photosynthetic rate. The medium productive genotype Plamya with relatively low CO_2 assimilation (23.3 mg CO_2 dm^{-2} h^{-1}) is characterized by longer period of photosynthetic activity, and is inferior to medium-stemmed genotypes in its yield (Figure 9).
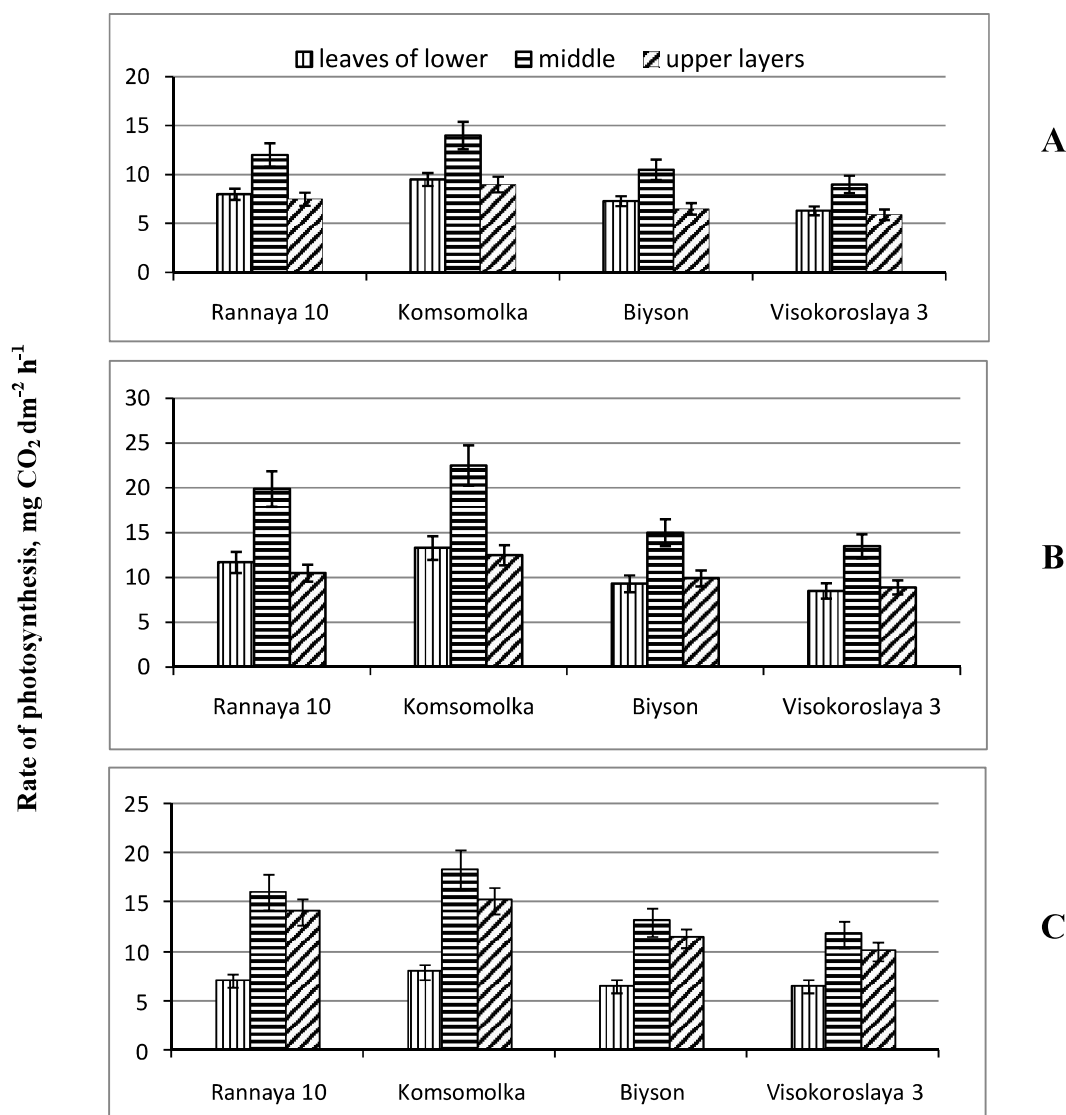
Figure 8. Seasonal dynamics of photosynthesis rate in leaves of different layers of the short-stemmed, high productive (Rannaya), medium-stemmed, high productive (Komsomolka) and long-stemmed, medium productive (Biyson, Visokoroslaya) soybean genotypes: A - branching, B - flowering, C - beginning of pod formation.

Improving the growing conditions significantly contributes to enhance the photosynthetic activity of plants in the cultivated area. Herewith, the rate of photosynthesis increases by 30-50%.

Like most major agricultural crops related to C_3-plants, soybean has active photorespiration that consumes the part of photosynthetic products.

Change in carbon dioxide gas exchange components, except dark respiration, occurs proportionally in all studied genotypes during ontogenesis (Figure 10-11). The maximum value of these components is observed in low productive varieties (Bistritsa, Volna) at 60th day of age, in high productive

(VNIIMK-3895 and Komsomolka) and medium productive ones (Provar and VNIIMK-9) at 80th day of age, while in the Plamya - at 90th day of age.

The ratio of true photosynthesis and photorespiration in the leaf ontogenesis is considerably constant and constitutes on average 29% for low productive varieties, 35% for high and 28% for medium productive ones (Mirzoyev, 1988 a, b, 1990; Aliyev et al., 1992). This suggests that about a third of the carbon assimilated in photosynthesis is being consumed during photorespiration.

The identical pattern of change in rates of true photosynthesis and photorespiration during the
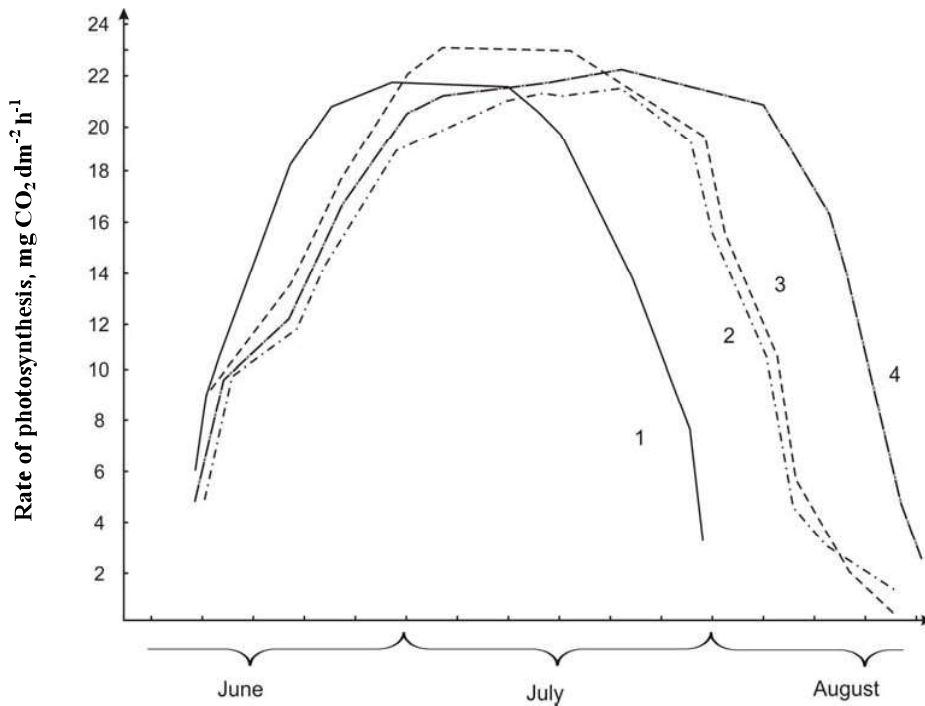
Figure 9. Ontogenetic changes in the photosynthesis rate in different soybean genotypes:
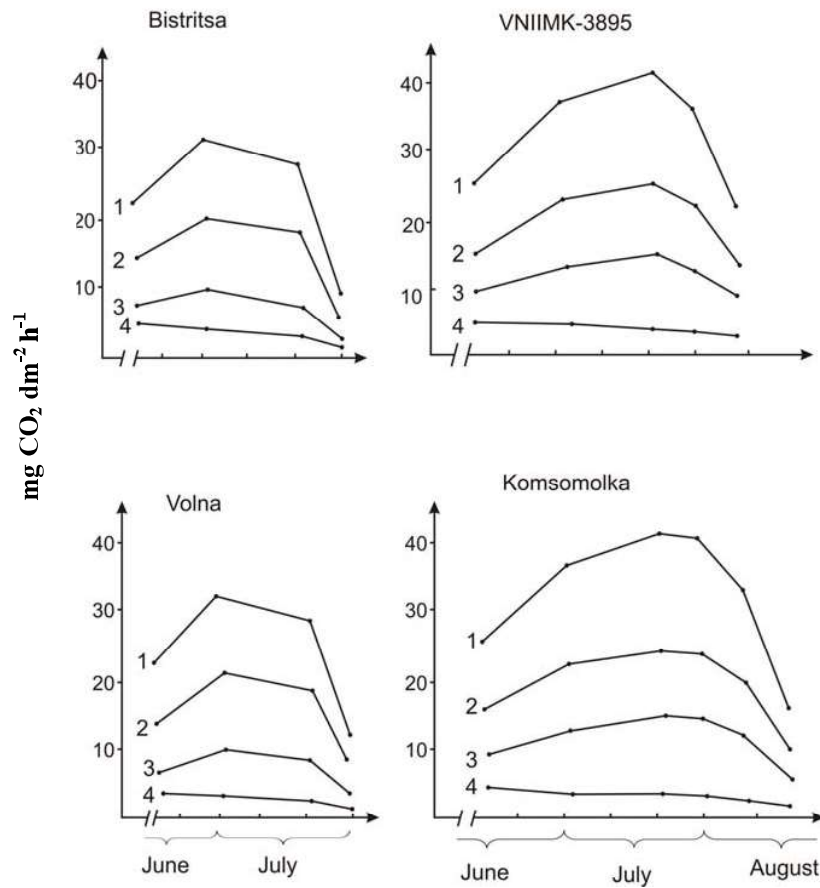1 – Volna; 2 – VNIIMK-9; 3 – VNIIMK-3895; 4 – Plamya.

Figure 10. Components of carbon dioxide gas exchange in leaves of the low productive (Bystritsa, Volna) and high productive (VNIIMK-3895, Komsomolka) soybean genotypes: 1 - true photosynthesis; 2 - net photosynthesis; 3 - photorespiration; 4 - dark respiration.
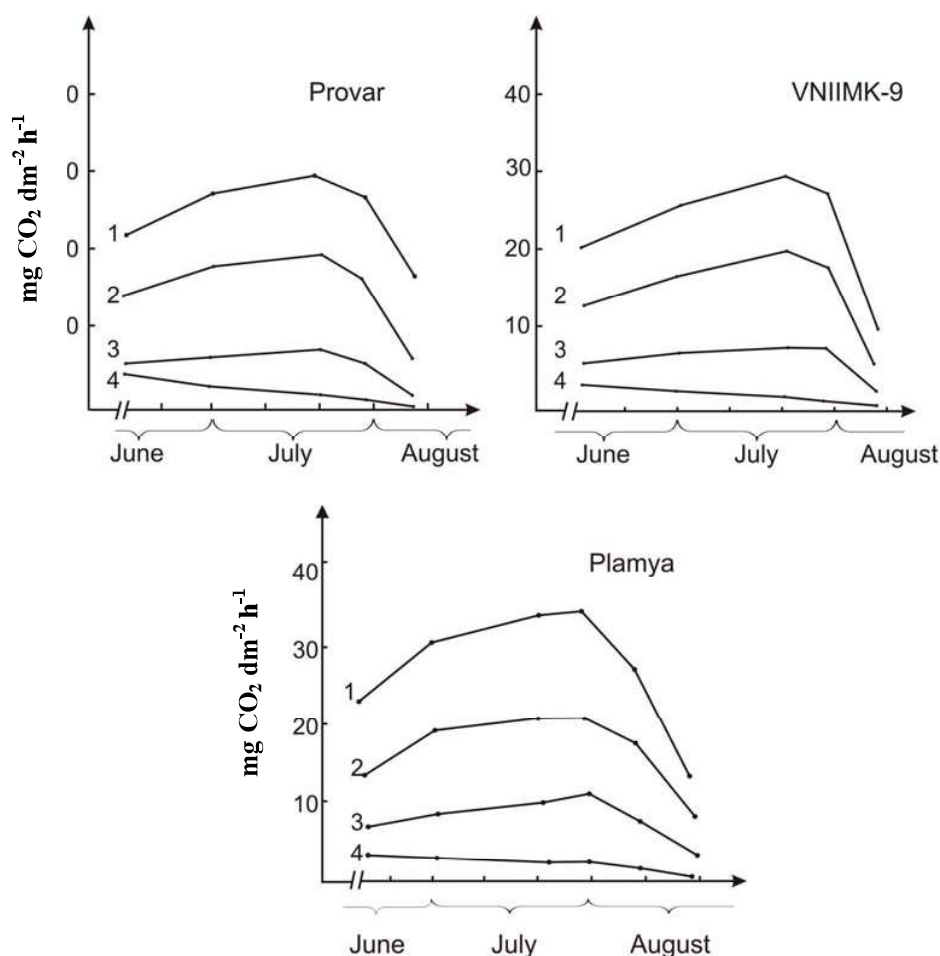
Figure 11. Components of carbon dioxide gas exchange in leaves of the medium productive (Provar, VNIIMK-9 and Plamya) soybean genotypes: 1 - true photosynthesis; 2 - net photosynthesis; 3 - photorespiration; 4 - dark respiration.

growing season suggests the existence of a positive relationship between them.

Quantitative characteristics of carbon dioxide gas exchange components demonstrates that if we consider the true value of photosynthesis as 100%, then the average value of the net photosynthesis in low productive wheat plants will be 65%, photorespiration - 29%, dark respiration - 6%, in high productive - 60%, 35%, 5%, and in medium productive ones - 66%, 28% and 6%, respectively. The data showed that the main role in the process of CO_2 release in light belongs to photorespiration that is greater in high productive soybean genotypes in comparison with low productive ones.

Based on these results, we can conclude that the attempts to find or create high productive genotypes that would have high photosynthesis and low photorespiration rates are unpromising and it is appropriate in breeding programs to focus on genotypes that have high rates of both photosynthesis and photorespiration.

Thus, the following parameters are suggested for the purposeful selection of high productive soybean genotypes: compact leaf shape, medium-sized leaves, which are located mainly in the middle layer, high rates of photosynthesis and photorespiration, high specific leaf density and longer period of pod formation-grain filling.

REFERENCES

Akperov Z.I., Mirzoyev R.S. (1990) Photosynthetic traits of various soybean genotypes contrast in grain yield. Vestnik selskokhozaystvennoy nauki AzSSR, Baku **2:** 6-9 (in Russian).

Aliev D.A., Kerimov S.Kh., Guliev N.M., Akhmedov A.A. (1996a) Carbon metabolism in wheat genotypes with contrasting photosynthetic characteristics. Russian J. Plant Physiol. **43(1):** 42-48.

Aliev J.A., Guliev N.M., Kerimov S.Kh., Hidaya-

tov R.B. (1988) Enzymes of the primary CO_2 fixation in flag leaf ontogenesis of wheat genotypes. Izv. Akad. Nauk Azerb. SSR (ser. biol. nauk) **4:** 12-20 (in Russian).

Aliev J.A., Guliev N.M., Kerimov S.Kh., Hidayatov R.B. (1996b) Photosynthetic enzymes of wheat genotypes differing in productivity. Photosynthetica **32(1):** 77-85.

Aliyev J.A., Akhmedov A.A., Mirzoyev R.S. (1992) Dinamics of CO_2 gas exchange in leaves of soybean in field. Izv. Akad. Nauk Azerb. SSR (ser. biol. nauk) **1-6:** 76-82 (in Russian).

Aliyev J.A., Akperov Z.I. (1985) Dinamics of sowing structure and photosynthetical traits of soybean genotypes. Izv. Akad. Nauk Azerb. SSR (ser. biol. nauk) **3:** 3-10 (in Russian).

Aliyev J.A., Akperov Z.I. (1986) Conception on ideal soybean. Izv. Akad. Nauk Azerb. SSR (ser. biol. nauk) **2:** 3-11 (in Russian).

Aliyev J.A., Akperov Z.I. (1995) Photosynthesis and soybean grain yield. Rodnik, Moscow-Baku: 126 p. (in Russian).

Aliyev J.A., Akperov Z.I. (1998) Fotosinteza şi recolta de soia. Ştininta, Chişina: 127 p.

Aliyev J.A., Akperov Z.I., Nabiyev M.H. (1981) Soybean cultivation under irrigation conditions of Azerbaijan SSR (Guidelines). Baku: 8 p. (in Russian).

Aliyev J.A., Akperov Z.I., Nabiyev M.H. (1982) Soybean cultivation in irrigated lands of Azerbaijan SSR. Azerneshr, Baku: 54 p. (in Russian).

Burris R.H., Roberts G.P. (1993) Biological nitrogen fixation. Annu. Rev. Nutr. **13:** 317-335.

Chollet R., Ogren W.L. (1975) Regulation of photorespiration in C_3 and C_4 species. Bot. Rev. **41(2):** 137-179.

Dospekhov B.A. (1985) Methods of field experience. Agropromizdat, Moscow: 351 p. (in Russian).

Friedman M., Brandon D.L. (2001) Nutritional and health benefits of soy proteins. J. Agric. Food Chem. **49:** 1069-1086.

Holaday A.S., Chollet R. (1984) Photosynthetic/photorespiratory characteristics of C_3-C_4 intermediate species. Photosynth. Res. **5:** 307-323.

Kebeish R., Niessen M., Thiruveedhi K., Bari R., Hirsch H.-J., Rosenkranz R., Stäbler N., Schönfeld B., Kreuzaler F., Peterhansel C. (2007) Chloroplastic photorespiratory bypass increases photosynthesis and biomass production in *Arabidopsis thaliana*. Nature Biotech. **25:** 593-599.

Maurino V.G., Peterhansel C. (2010) Photorespiration: current status and approaches for metabol-ic engineering. Curr. Opin. Plant Biol. **13:** 249-256.

Mirzoyev R.S. (1988a) Seasonal variations of photosynthesis intensity of various soybean genotypes. Proceedings of IV Republic Conference, Baku: 78 p. (in Russian).

Mirzoyev R.S. (1988b) CO_2 gas exchange and photosynthetic traits of various soybean genotypes. Proceedings of Republic Conference of Young Scientists, Tbilisi: 38 p. (in Russian).

Mirzoyev R.S. (1990) CO_2 gas exchange of soybean genotypes different in photosynthetic traits and productivity. PhD thesis, Baku: 22 p. (in Russian).

Ogren W.L. (1975) Control of photorespiration in soybean and maize. In: Environmental and Biological Control of Photosynthesis (Marchelle R., ed.), The Hague, W.Junk: 45-52.

Ogren W.L. (1976) Search for higher plants with modifications of the reductive pentose phosphate pathway of CO_2 assimilation. In: CO_2 Metabolism and Plant Productivity (Burris R.H., Black C.C., eds.), University Park Press, Baltimore: 19-29.

Ososki A.L., Kennelly E.J. (2003) Phytoestrogens: a review of the present state of research. Phytother. Res. **17:** 84-869.

Peterhansel C., Maurino V.G. (2011) Photorespiration redesigned. Plant Physiol. **155:** 49-55.

Pimentel D., Patzek T. (2008) Ethanol production using corn, switchgrass and wood; biodiesel production using soybean. In: Biofuels, Solar and Wind as Renewable Energy Systems (Pimentel D., ed.), Springer, New York: 373-394.

Guidelines on soybean cultivation on irrigated lands in the Northern Caucasus. (1978) Krasnodar: 19 p. (in Russian).

Sakai T., Kogiso M. (2008) Soy is of flavones an immunity. J. Med. Invest. **55:** 176-173.

Servaites J.C., Ogren W.L. (1977) Chemical inhibition of the glycolate pathway in soybean leaf cells. Plant Physiol. **60:** 461-466.

Sharkey T.D. (1988) Estimating the rate of photorespiration in leaves. Physiol. Plant. **73:** 147-152.

Tooming H.G., Gulyayev B.I. (1967) Methods of measurement of photosynthetically active radiation. Nauka, Moscow: 143 p. (in Russian).

Zelitch I. (1971) Photosynthesis, photorespiration, and plant productivity. Acad. Press, New York-London: 247 p.

Zelitch I. (1975) Improving the efficiency of photosynthesis. Science **188:** 626-633.

Zelitch I. (1992) Control of plant productivity by regulation of photorespiration. BioScience **42:** 510-516.

Oxygenic Photosynthesis: An Introduction[#]

Yashar M. Feyziyev*

Institute of Botany, Azerbaijan National Academy of Sciences, 40 Badamdar Shosse, Baku AZ 1073, Azerbaijan

The article briefly describes the current status of understanding of the molecular mechanisms involved in the oxygenic photosynthesis: energy and electron transfer in photosynthetic species, energy transduction, etc. The reference list includes a large number of review articles, book and book chapters intended to learning of the subject more deeply and independently.

Keywords: photosynthesis, photosystem II, photosystem I, Cyt $b_6 f$ complex, ATP-synthase

The primary source of energy for life in our planet is the Sun. The energy in sunlight is introduced into the biosphere by a process known as photosynthesis, the physico-chemical process by which plants, algae and certain bacteria convert light energy into chemical energy of organic compounds, with concomitant use of these components in the bioenergetic processes. Photosynthesis developed very early in the history of life. It is generally believed that the earth was formed about 4.6 billion years ago. Life on earth began about 3.5 billion years ago with the first photosynthetic organisms to appear being the photosynthetic bacteria and primitive algae. There are fossil records showing evidence for photosynthetic activity as far back as 3.5 billion years ago (Broda, 1975; van Gorkom, 1987; Wilmotte, 1994; Wolfe and Hoober, 1995; Whitmarsh and Govindjee, 1999; Ke, 2001). By combining light energy and available sources of chemicals, these organisms evolved into the first photosynthetic species. Fossil fuel such as coal and crude oil was created by decaying organic matter of photosynthetic organisms and accumulates millions of years.

In plants, algae and cyanobacteria, the photosynthetic processes results in the fixation of carbon dioxide (CO_2) from the atmosphere that is used to synthesize carbohydrates and release of molecular oxygen to the atmosphere. This process is known as oxygenic photosynthesis. Some photosynthetic bacteria can use light energy to extract electrons from molecules other than water. The ultimate source of electrons in this type of photosynthesis is sulphur compounds or simple organic molecules. Photosynthesis preformed by these organisms is known as

anoxygenic photosynthesis. These organisms are of ancient origin, presumed to have evolved at least 3.5 billion years ago, before oxygenic photosynthetic organisms (van Gorkom, 1987; Whitmarsh and Govindjee, 1999; Ke, 2001). Examples of organisms belonging to anoxygenic photosynthesis are the filamentous green bacteria, the green sulphur bacteria, the purple bacteria and the heliobacteria.

In spite of such differences some fundamental principles concerning to structure and energy conversion are, however, shared between different photosynthetic groups. These are represented schematically in the Figure 1.

The first step in photosynthesis is the absorption of photon by a pigment molecule of photosynthetic antenna resulting in conversion of the photon energy to an excited electronic state of pigment molecule. The antenna consists of hundreds of pigment molecules (chlorophylls, bacteriochlorophylls, carotenoids, etc.) that are bounded to proteins within the photosynthetic membrane. The excited electronic state is transferred over the antenna molecules as an exciton. Some excitons are converted back into photons and emitted as fluorescence, some converted to heat. For most of the excited pigment molecules the most useful decay pathway is "energy transfer" to a photochemical reaction centers, and it is of vital importance to photosynthesis. Excitons trapped by a reaction center provide the energy for the primary photochemical reaction of photosynthesis – the photoinduced transfer of an electron. Subsequent electron transfer reactions occur in the dark which results in accumulation of chemical bound energy. Electron transfer reactions in photosynthesis involve electron carriers or electron-transfer
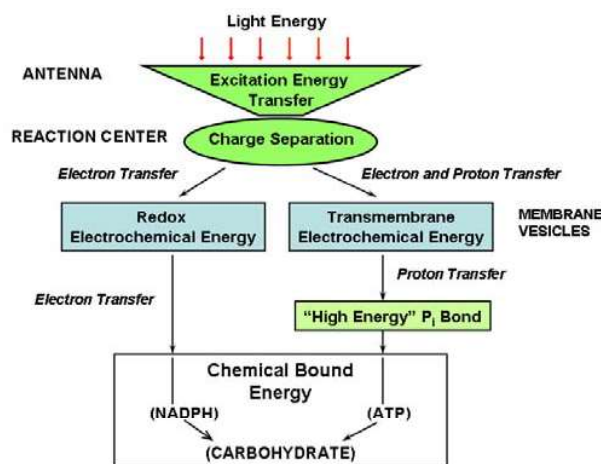

Figure 1. Energy transformation in photosynthesis: photosynthesis is shown as a series of reactions that transform energy from one to another (Whitmarsh and Govindjee, 1999).

proteins, among others, (bacterio)chlorophylls, quinones, cytochromes, and iron-sulfur proteins.

Research on the photosynthesis has been performed since the seventeenth century leading to a considerable basis of knowledge. The earliest studies of photosynthesis involve the nature of the components used and produced by plants. One well known result in the earliest study of photosynthesis was finding that plants could restore air that had been "injured" by a burning candle. It happened in 1771, when Joseph Priestley performed experiments, which demonstrated that plants releases molecular oxygen (today it is clear that a main source of oxygen in the earth atmosphere is photosystem II, one of major components of photosynthetic membrane of cyanobacteria, algae and higher plants). Although the importance of this process was immediately realized, it took another 150 years before some insight into the molecular mechanisms of photosynthesis began to evolve.

The late 1940's and early 1950's, which showed a rapid development of biochemical and physical techniques, also witnessed an unprecedented expansion of photosynthesis research, based on the application of these techniques. Due to work of Calvin and Benson in the forties and fifties it became clear that carbon dioxide fixation occurs by a sequence of enzymatic processes that can in principle function in the dark. Duysens's studies established the role of pigments in harvesting and transferring the energy of light, and gradually it became clear that the primary energy conversion steps consist of electron transfer reactions that take place in an entity called the reaction center. Around 1960 the basic difference between oxygenic and bacterial photosynthesis became known: bacteria have only one type of reaction center, whereas oxygenic species have two, one which produces a strong oxidant able to split water to molecular oxygen and protons.

During the last 50 years many important developments have taken place in photosynthesis science. The efforts of scientists have now provided a picture of the mechanisms of the photosynthetic reactions and the structure of different functional units of the photosynthetic apparatus. The application of advanced physical instrumentation combined with biochemical and molecular biology techniques, has provided a wealth of information concerning the primary reactions of photosynthesis and structure of the energy converting units of photosynthesis.

Photosynthetic reaction centers

Key steps in photosynthesis are the absorption of solar energy by antenna pigments and efficient transfer of excitation energy to photochemical reaction centers, where the energy is trapped in the form of stable charge separation. Photosynthetic reaction center is defined as the smallest unit which is able to convert light to electrochemical energy of separated charges by photo-induced electron transfer. It is membrane bound protein complexes which contain electronic cofactors – electron donor and acceptor, and accessory pigments. Charge separation in reaction centers resulted in series of electron transfer reactions and in the end accumulation of chemical bound energy.

All reaction centers which are found in contemporary photosynthetic organisms can be classified into two groups. One is iron-sulphur or type I reaction center that has iron-sulfur clusters as electron acceptors and is found in *Chlorobiaceae* (green sulfur bacteria), *Heliobacteriaceae* and in photosystem I of oxygenic photosynthesis. The other is (bacterio)pheophytin-quinone or type II reaction centre that contains a (bacterio)pheophytin and pair of quinones as electron acceptor. The reaction centers of purple bacteria, *Chloroflexaceae* (filamentous green bacteria) and photosystem II of oxygenic photosynthesis belong to the latter group (Wolfe and Hoober, 1995; Ke, 2001). Recent structural data obtained from X-ray analysis of type I and II reaction centers supports the hypothesis of the evolution of all photosynthetic reaction centers from one common ancestor (Ke, 2001; Zouni et al., 2001; Kamiya and Shen, 2003; Ferreira et al., 2004; Loll et al., 2005; Nelson and Yocum, 2006; Amunts et al., 2007).

Utilization of solar energy by oxygenic species

Higher plants, algae and cyanobacteria use photosynthesis to convert light energy into chemical energy and reducing equivalents, adenosine triposphate (ATP) and nicotinamide adenine dinucleotide phosphate (NADPH), which are used in the CO_2 fixa-

tion to produce carbohydrates $(CH_2O)_n$ (Ke, 2001). The key to utilization of reducing power is ferredoxin. The ATP formed by the energy coupling reactions is also consumed in a variety of reactions unrelated to carbon metabolism. From the chemical point of view, the overall reactions of oxygenic photosynthesis may be described by the basic equation:

$$6CO_2+12H_2O+\text{Light Energy} \rightarrow C_6H_{12}O_6+6O_2$$
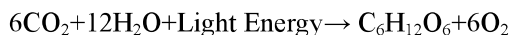
Oxygenic photosynthesis is driven by visible light (wavelengths from 400 to 700 nm) that is absorbed by different pigment molecules, chlorophyll *a* and *b*, carotenoids and phycobilins. The pigment molecules are bound to polypeptides forming pigment-protein complexes. Two types of antenna complexes, the inner (core) antenna consisting of pigment-proteins that are an integral part of the reaction center complex, and outer (peripheral) antenna complexes are distinguished in oxygenic species. In plants and green algae the light absorbing pigment molecules are chlorophyll *a*, chlorophyll *b* and carotenoids. The cyanobacteria and red algae have a different outer antenna system. In cyanobacteria and red algae, the phycobiliproteins are assembled into supromolecular aggregates called phycobilisomes, which are attached to the photosynthetic membrane surface and transfer electronic excitation energy (via chlorophyll) to the reaction centers to initiate photochemical reactions. Carotenoids and phycobiliproteins serve as accessory pigments, to absorb light energy not absorbed in the spectral region of chlorophyll absorption and transfer this energy to chlorophylls. The efficiency of singlet-singlet energy transfer from certain carotenoids to chlorophyll may be very high ranging from 70% to nearly 100%. Phycobilisomes can funnel the absorbed energy to the reaction center with more than 95% efficiency (Ke, 2001).

Oxygenic photosynthesis serves as a vital link between the light energy of the sun and all living creatures. Carbon dioxide and water, which both are energy poor compounds, are converted to the energy rich compounds, carbohydrates and molecular oxygen. In the cells of photosynthesizing organisms the compounds formed are utilized as building blocks for synthesis of other important molecules like proteins, lipids and nucleic acids. Other organisms, human and animals use the energy rich substances made by photosynthesizing organisms for food and respiration.

Oxygenic photosynthesis is a main source of oxygen in the earth atmosphere. Molecular oxygen liberated as a result of water splitting reactions. The water splitting reactions by photosynthetic organisms was an important event for life cycle on the earth. Water is never ending source of electrons and

protons utilized by photosynthesis for carbon fixation. This is of extreme importance, since when electrons are extracted from water, molecular oxygen is formed as a by-product. More than 2.5 billion years ago, photosynthetic cyanobacteria developed the capacity to split water into the molecular oxygen and protons (van Gorkom, 1987; Wilmotte, 1994; Wolfe and Hoober, 1995; Ke, 2001), which had the major advantage that substrate was abudant, essentially unlimited, and photosynthetic species that developed mechanisms to master this chemistry became dominant. Appearance of the oxygenic photosynthesis leads to a gradual change in the atmosphere from being reducing to being oxidizing. This was a catastrophic environmental change for the dominating life on earth at that time. Before this event, all organisms on earth were adapted to an anaerobic environment. However, as oxygen started to accumulate in the atmosphere, the existing organisms either died or adapted to the new environment. Life had to adapt to the new oxygen rich environment and try to make the best use of it. However, more efficient energy metabolism systems could evolve, where molecular oxygen was used as the terminal oxidant in respiration. This provided the foundations for the thermodynamically more efficient aerobic respiration and for the development of higher organisms. Today oxygenic photosynthesis occurs in almost all the eukaryotic photosynthetic species, plants and algae, and in cyanobacteria.

One more important effect, which followed with the development of oxygenic photosynthesis and the accumulation of oxygen in the atmosphere, was the formation of the ozone layer that protects living organisms from destructive ultraviolet (UV) radiation from the sun. Protected from harmful UV radiation, life could finally climb out of the water, beginning with the plants about 400 million years ago (Ke, 2001).

Chloroplasts and thylakoid membranes

In higher organisms, plants and algae, all the molecular complexes involved in photosynthetic energy conversion are concentrated in special cell organelles, chloroplasts (Figure 2) (Taiz and Zeiger, 2002). The chloroplasts are self-replicating and contain own genetic material. The chloroplasts genome encodes a large portion of the proteins necessary for photosynthetic function and for replication (Erickson, 1995; Roell and Cruissem, 1995). However, many proteins involved in the photosynthesis are nuclear encoded and post-translationally imported into the chloroplasts (Gray, 1995). The chloroplast is separated from rest of the plant cell by a double membrane. Internal space of the organelle, stroma, is filled with a system of lamellae and flat-

tened thylakoids. The stroma contains soluble enzymes, plastid encoded DNA and protein synthesis apparatus.

The thylakoid membranes are located in the aqueous stroma phase of chloroplasts in plants and algae and in cytosol of the cyanobacterium. Thylakoids form a physically continuous three-dimensional network enclosing an aqueous space called the lumen and are differentiated into two distinct physical domains: flattened disk-like stacked structures, called grana and interconnecting single membrane regions, stroma lamellae. Each chloroplast contains about 10 to 100 such grana. Stroma lamellae connect between grana, so that a continuous closed membrane system is formed. Since all grana are interconnected by the unstacked stroma lamellae, the lumen of each thylakoid region is also connected with the lumen of all other thylakoid region. Thus the inner space of the thylakoid membrane, lumen, is completely separated from the stroma, which is vitally important for the proper functioning of the energy conversion system of photosynthesis (Gantt, 1994; Staehelin and van der Stay, 1995; Ke, 2001; Dekker and Boekema, 2005).

The cyanobacteria are prokaryotes and thus do not have organelles like chloroplasts. However, the whole cyanobacterial cell in it self closely resembles the chloroplast (Douglas, 1994; Gantt, 1994). The photosynthetic apparatus in the cyanobacteria is also located to a highly folded internal membrane system, the thylakoid. This has the same function as the thylakoid membranes of the chloroplasts, but they are not differentiated in grana stacks and stroma lamellae. The cyanobacterial cell is divided in two compartements by the thylakoid membrane, the cytoplasm and the thylakoid lumen. Cyanobacteria have a simpler genetic system than plants and algae that enable them to be easily modified genetically. Because of this cyanobacteria have been used as a model to understand photosynthesis in plants. By genetically altering photosynthetic proteins, researchers can investigate the relationship between molecular structure and mechanism in photosynthesis (Barry et al., 1994).

Molecular complexes of thylakoid membranes

The photosynthetic energy conversion of oxygenic organisms is divided in two distinct phases, the light reactions and the dark reactions. Light reactions are almost exclusively confined to the membranes. During the light reactions, light energy is used for generation of reducing power and energy rich compounds in the form of NADPH and ATP. Fixation of CO_2 and biosynthesis of carbohydrates from carbon dioxide occurs in the chloroplasts stroma via the Calvin cycle. This process carries the name of dark reaction since it does not require light, although reducing equivalents (NADPH) and chemical energy (ATP)

generated by "light reactions" are necessary for CO_2 fixation. Most, if not all, enzymes involved in dark reactions are soluble, but there is evidence that some of them can function as membrane bound complexes (Andersson and Anderson, 1980; Süss et al., 1993; 1995).
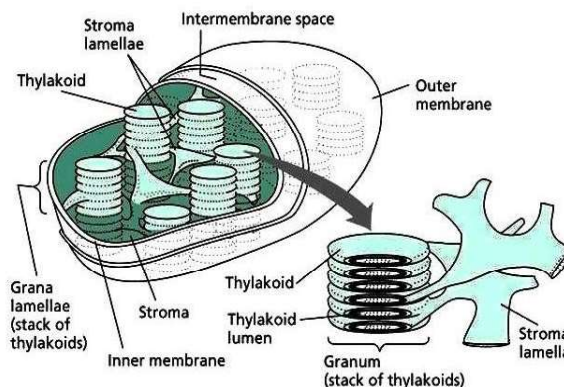

Figure 2. Topological representation of plant chloroplast: The chloroplast is about 6Å long. Inside of chloroplast is a complicated membrane system, known as photosynthetic membrane or thylakoid membrane that contains most of proteins required for the light reactions. The proteins required for fixation of CO_2 are located outside the photosynthetic membrane in the surrounding aqueous phase. The photosynthetic membrane is composed mainly of glycerol lipids and protein (Taiz and Zeiger, 2002).

The energy converting apparatus of the photosynthesing oxygenic species organized in several different multisubunit protein complexes associated with thylakoid membranes. These protein assemblies, the photosystem II and I, each with antenna, the cytochrome b_6f (Cyt b_6f) complex, the ATP-synthase, and the $NADP^+$, bind and organize pigments and other cofactors, which together with mobile electron carriers in the stroma (ferredoxin, ferredoxin-$NADP^+$ reductase), lumen (plastocyanin) and the plastoquinol cooperate in the convertion of radiant energy (Ke, 2001). The protein complexes that catalyze electron transfer and energy transduction are unevenly distributed in thylakoid. Photosystem II (PSII) is largely found in the grana stacks while photosystem I (PSI) and ATP-synthase are located in the stroma exposed regions and the cytochtome b_6f complex is evently distributed in grana and grana margins (Andersson and Anderson, 1980; Melis, 1991; Staehelin and van der Stay, 1995; Ke, 2001; Danielsson, 2005). A schematic view of the protein complexes and the redox centers involved in the electron transfer and proton translocation in the thylakoid membrane is shown in Figure 3.

In plants (algae and cyanobacteria) two photosystems, photosystem II and photosystem I operate
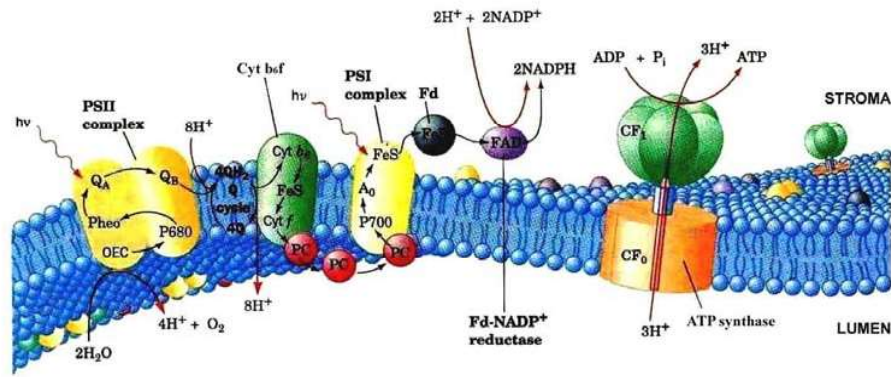
Figure 3. A schematic representation of the protein complexes of the thylakoid membrane involved in the photosynthetic light reactions of oxygenic photosynthesis: photosystem II (PSII), the cytochrome b_6f (Cyt b_6f) complex, photosystem I (PSI) and ATP-synthase. The first three enzymes are connected through the reduction and oxidation of the plastoquinole pool and through the electron carrier plastocyanin (PC). Upon light absorption, the primary donor chlorophylls (P_{680} in PSII and P_{700} in PSI) are excited and oxidized, which initiates a series of redox reactions in each photosystem. The photosystems work in series so that they together with three other electron carriers, plastoquinole pool, Cyt b_6f complex, and water soluble plastocyanin molecule can perform electron translocation from the water-splitting site on the lumenal side of PSII to the ferredoxin-NADP$^+$ reductase on the stromal side of PSI: plastoquinole moves electrons from PSII to heme containing Cyt b_6f, while the plastocyanin transfer electrons from Cyt b_6f to PSI. During the electron transfer processes, protons are released into the lumen by the water splitting reaction and with reactions inside Cyt b_6f. These reactions create an electrochemical gradient over the thylakoid membrane. The free energy of this proton gradient is utilized by the ATP-synthase for ATP production as the protons are translocated back to stroma. ATP is released into the stroma where the Calvin cycle proceeds (Voet and Voet, 2004).

in series. This enables these organisms to use water as a source of electrons. The combined action of these photosystems results in transfer of an electron across the thylakoid membrane from H_2O ($E_{m, pH 7.0}$ = +0.82 V) to NADP$^+$ ($E_{m, pH 7.0}$ = −0.32 V), using two photons, one in each photosystem, per electron transferred. The energetics of the electron transfer is usually represented in a redox potential scale as Z-scheme of photosynthesis (Hill and Bendall, 1960; Hil, 1965; Ke, 2001). In this scheme the two photoreactions are connected via an electron transport chain containing plastoquinol pool, Cyt b_6f and plastocyanin (Figure 4).

On the acceptor side of PSI, the light driven 2-electron reduction of NADP$^+$ occurs whereas on the donor side of photosystem II the 4-electron oxidation of H_2O to molecular oxygen takes place. Thus two photochemical reactions of oxygenic photosynthesis couples the 1-electron charge separation in reaction centers to multielectron redox chemistry of subsequent electron transfer reactions.

Photosystem II

Photosystem II is the first in the series of three complexes that couple photochemical excitation of electrons to electron transfer from H_2O to NADP$^+$ in higher plants, algae and cyanobacteria. According to the function carrying-out in photosynthesis, PSII is

often referred as a "light driven water-plastoquinole oxidoreductase". Photosystem II has an outer antenna dominated by light harvesting complex II (LHCII), which binds chlorophylls *a* and *b* and carotenoids, and inner antenna of chlorophyll *a* binding proteins CP47 and CP43. The D_1 and D_2 polypeptides form the heterodimer of core of PSII reaction center that carries most of cofactors involved in electron transfer. Most proteins in the PSII complex are membrane spanning, but the three extrinsic proteins involved in oxygen evolution are located on the lumenal side of the thylakoid membrane. In higher plants and green algae these proteins are nuclear encoding subunits of PsbO (33 kDa), PsbP (23 kDa) and PsbQ (16 kDa), which together form the lumenally exposed water splitting center and closely associated with the Ca-(Mn)$_4$ cluster. Cyanobacterial PSII contains PsbO, but a PsbV (Cytochrome c_{550}) and PsbU (12 kDa) replace the PsbP and Q subunits in eukaryotes. The primary electron donor in photosystem II, P_{680} is a chlorophyll multimer. Upon excitation, it is oxidized and electrons through the intermediary electron carriers, pheophytin and plastoquinones Q_A and Q_B are transferred to the plastoquinol. PQH$_2$-pool serves as a reservoir for the electrons coming from photosystem II. While Q_A is a one electron acceptor, Q_B is reduced first to a semiquinone (Q_B^-) and thereafter, by accepting two protons from

stroma and another electron from photochemical reaction, to a hydroquinol (Q_BH_2). Moreover, Q_BH_2 has a low affinity for its binding site and is readily displaced by another plastoquinone, Q_B from the diffusible PQH_2-pool.
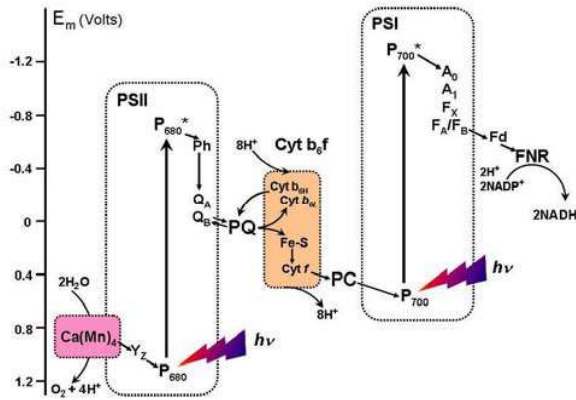

Figure 4. Z-scheme diagram of oxygenic photosynthesis demonstrates the relative redox potentials of the co-factors in the linear electron transfer from water to NADP. The relative redox potentials show that P_{680} and P_{700} are highly oxidising. Their excited forms (P_{680}^* and P_{700}^*) of the reaction centre pigments are highly reducing and located in the upper part of the diagram. To reduce $P_{680}^{\bullet+}$ electrons are transferred from water, through Y_Z. $P_{700}^{\bullet+}$ is reduced by electrons from PSII, transferred via plastoquinole, through Cyt b_6f complex and plastocyanin (PC).

The primary electron donor of PSII, $P_{680}^{\bullet+}$ is a very powerful oxidant that is finally reduced at the expense of water, which is oxidized in the water splitting center, attached to PSII at the lumen of thylakoid membrane (Knaff, 1977; Klimov and Krasnovsky, 1981; Govindjee et al., 1986; Mathis and Rutherford, 1987; Debus, 1992; Renger, 1992; Seibert, 1993; Barry et al., 1994; Diner and Babcock, 1995; Ke, 2001; Nelson and Yokum, 2006). This occurs by extracting of an electron from the cluster of Ca-$(Mn)_4$ via the tyrosine residue denoted as Y_Z (tyrosine-161 on the D_1-protein). Release of oxygen is a result of concerted four-electron oxidation of two molecules of water. This process is coupled to the reduction of $P_{680}^{\bullet+}$ via the formation of neutral $Y_Z^\bullet$ radical. In turn, $Y_Z^\bullet$ is reduced by cluster of Ca-$(Mn)_4$, that is the catalytic center for water oxidation. The coupling of the four electron water oxidation reactions to the one electron charge separation events of the reaction center is achieved with the accumulation of oxidizing equivalents within the Ca-$(Mn)_4$-cluster. This four step process followed by oxidation of water is called S-state cycle of PSII which is include five successive intermediate states denoted as S_0, S_1,...,S_4. The S_0

state is the most reduced state. Removal of electron from S_0 leads to the S_1 state which is dark-stable. The further sequential removal of three more electrons results in formation of S_2, S_3 and S_4 states. The S_4 state is an unstable, transient state that spontaneously converts to the S_0 with concomitant release of molecular oxygen.

Photosystem I

Photosystem I operate at the final stage of light-induced electron transfer. It reduces $NADP^+$ via a series of intermediary acceptors that are reduced upon excitation of the primary donor P_{700} and oxidize plastocyanin. Thus PSI is often referred as a "light driven plastocyanin-NADP oxidoreductase". The PSI antenna is organized similar to PSII antenna with outher light harvesting complex I (LHCI) antenna and inner chlorophyll a binding antenna. The pigment composition of PSI is very different from PSII, mainly containing chlorophyll b. The reaction center of PSI is formed by a special pair of chlorophylls, P_{700}, near the lumenal side of membrane. A second chlorophyll molecule (A_0), phylloquinone (A_1) and three iron sulfur clusters (F_X, F_A and F_B) function as electron acceptors. Upon excitation P_{700} reduces a chlorophyll species referred to as A_0. From this very low-potential chlorophyll anion ($E_m < -1.0$ V) an electron transferred to the next acceptor, A_1 and then subsequent electron acceptors, iron-sulfur centers denoted as F_X, F_B and F_A. The electrons are finally transferred from the RC to ferredoxin (Fd), a small (10 kDa) protein with a 2Fe-2S cluster as active centre (Golbeck, 1987; Mathis and Rutherford, 1987; Golbeck, 1994; Malkin, 1995; Brettel, 1997; Brettel and Leibl, 2001; Fromme et al., 2001; Gobets and van Grondelle, 2001; Ke, 2001; Scheller et al., 2001; Setif, 2001; Vassiliev et al., 2001; Webber and Lubitz, 2001; Xu et al., 2001; Nelson and Yokum, 2006). Although most proteins in the PSI complex are also membrane-spanning, a few, the iron-sulfur proteins that contain F_A, F_B, and the Fd-docking proteins are located toward the stromal side of the thylakoid membrane. Ferredoxin interacts with the thylakoid membrane at two distinct sites. It accepts electrons from the reducing side of PSI, then is reoxidized by the thylakoid-bound FAD-flavoprotein, ferredoxin-NADP reductase (FNR) which forms a one-to-one complex with Fd. The reduced FNR, then oxidized by NADP.

Why two photochemical reactions?

The overall reaction driven by the light reactions of PSII and PSI during the linear electron flow is the reduction of $NADP^+$ with electrons derived from water. The midpoint potential (E_m) of the $NADP^+/NADP$ redox couple is 0.38 V at pH 8.0 (E_m

$_{(pH\ 7.0)}$ − 59 mV/pH unit), which is prevailing pH in the stroma. The potential of the H_2O/O_2 couple is +0.93 V at a lumenal pH of 5.0. The difference ΔE_m of -1.31 V (126.4 kJ/mol) represents a chemical potential generates per electron transferred through the linear electron flow of oxygenic photosynthesis and stored in the molecular oxygen and NADP.

The efficiency of PSII in converting solar energy to redox energy is approximately 45%. This estimation is based on the comparison between the energies of absorbed photons with the redox energies stored in the final products. Photosystem II can be driven by 680 nm photons equal to 1,82 eV per photon, which is converted into the H_2O/O_2 and Q_B^-/Q_BH_2 redox couples with a difference in midpoint potential equivalents to 0.82 eV per electron. That is, 45% of the incident photon energy is converted to chemical potential in the final, stable products of the photochemistry. For similar reason the overall efficiency of PSI is also in order 45%. With this 45% efficiency, the transfer of one electron through Z-scheme requires photon energy of 2.91 eV which corresponds to wavelengths of 426 nm or shorter. Consequently, in theory, it is energetically possible to drive the reduction of $NADP^+$ by H_2O by using only one light reaction which is driven by light in the visible region of solar spectrum.

However, oxygenic species engages two photosystems operating in series, rather than one, which suggests the existence of benefits with such an arrangement. A clear advantage with two photosystems, as compared to one photon oxidation of water and production of NADPH becomes evident upon inspection of the solar spectrum. PSII and PSI use photons of 680 and 700 nm to produce charge separation, respectively. The antennae pigments of the photosystems harvest light at shorter wavelengths. The light energy is transferred and accompanied by small energy losses, towards the low-energy traps of the reaction centers. By using photons of longer wavelengths for the final photochemistry, PSII and PSI can harvest light from the major part of the solar spectrum. If only one photosystem driven by 426 nm photons, were to be involved, the useful part of the solar spectrum would be narrowed. Thus, the strategy to split one high-energy reaction into two reactions involving lower energies, results in a substantial extension of the photosynthetically useful part of the solar spectrum.

Cytochrome b_6f complex

In thylakoid membranes electron transfer between PSII and PSI occurs via the plastoquinol pool, cytochrome b_6f complex and water soluble protein plastocyanin. The Cyt b_6f complex contains four large subunits (18 to 32 kDa), including Cyt f, Cyt b_6, the Rieske iron-sulfur (2F-2S) protein, and subunit IV, as well as four small hydrophobic subunits, PetG, PetL, PetM, and PetN. The two b-hemes of Cyt b_6 (Cyt b_{6L} and Cyt b_{6H}) and the subunit IV span the thylakoid membrane, while the Rieske 2Fe-2S protein and Cyt f are located near the lumen side. The function of the Cyt b_6f complex in thylakoid membrane is to oxidize plastoquinole formed by PSII and transfer these electrons to plastocyanin (Hore, 1993; Kallas, 1994; Hauska et al., 1995; Hore, 2000; Ke, 2001; Kurisu et al., 2003). Accordingly, the Cyt b_6f complex has therefore also been called the "plastoquinole-plastocyanin oxidoreductase". The PQH_2 is first oxidized by the Rieske center. Within the Cyt b_6f complex, one electron subsequently is transferred from plastoquinol to a Rieske 2Fe-2S protein and then Cyt f in a series, which can release electron to the plastocyanin. The plastocyanin, which is small (10.5 kDa) copper containing protein, is located to the lumenal surface of the thylakoid membrane and drives one electron from Cyt f to the PSI complex where reduces $P_{700}^{·+}$ (Gross, 1995; Sigfridsson, 1998; Hore, 2000; Ke, 2001). After loss of one electron by PQH_2, the resulting semiquinone loses an electron on to the two b-hemes in series. The b-hemes operate in the so-called "Q-cycle", similar to that in the mitochondrial or bacterial cytochrome bc_1 complex, and provide a translocation of additional protons across the membrane into the lumenal space. When the plastoquinole becomes fully oxidized, it loses two electrons and also releases two protons to the lumen phase. Thus with splitting two water molecules by PSII to form one oxygen molecule, eight protons are translocated across the membrane (Ke, 2001).

ATP-syntase

From the Z-scheme it is seen that PSII generates a strong oxidant in $P_{680}^{·+}$, which is able extract electrons from water, while PSI generates a strong reductant in P_{700}^*, which can reduce $NADP^+$. The overall electron flow from the water-splitting center on the lumen toward $NADP^+$ on the stroma is linear and vectorial. The consequence of this vectorial electron flow, or displacement of electric charges, is creation of an electric potential across the membrane, with positive charges on the inside and negative on the outside. First, protons formed by the oxidation of water are released to the inside, resulting in an acidification of the thylakoid lumen space. In addition, protons are extracted from the outside, leading to the formation of PQH_2, and are ultimately released on the lumenal side during the reoxidation of this PQH_2. The proton release in the water splitting reaction by PSII, and proton pumping from stroma to lumen by PQH_2/Cyt b_6f create a proton gradient and electrochemical potential across the thylakoid membrane.

The generated potential energy is utilized by

ATP-synthase for synthesis of ATP. This complex has two essential parts, CF_1, the chloroplast ATP coupling factor, and CF_0, the membrane spanning portion of the holoenzyme. Each CF_1 and CF_0 contains several polypeptides and has remarkably similar structures. These enzyme systems are ubiquitously distributed in membrane systems where electron transfer reactions are coupled to ATP synthesis. The critical subunits of CF_1 are designated α, β, γ, δ, and ϵ. The enzyme is comprised of three copies of α and β, and single copies of δ and ϵ. The CF_0 portion of the ATP-synthase is an oligomer comprised of four different intrinsic protein subunits that self-assemble in the membrane bilayer to form H^+ conducting "pore" as well as the site to which CF_1 binds.

ATP-synthase pumps the proton in the opposite direction to electron transport, from lumen to stroma, and in the stroma, ADP is phosphorylated to ATP (Avron, 1987; Frash, 1994; McCarty, 1995; Ke, 2001). The light driven reactions catalyzed by PSII and PSI result in formation of the energy-rich mobile molecules NADPH and ATP. The stored energy in the NADPH and ATP is subsequently used by the photosynthetic organisms to drive the synthesis in the Calvin cycle.

Energetic efficiency of photosynthesis

Oxygenic photosynthesis is globally the most fundamental biochemical process that provides energy, organic matter, and oxygen for nearly all biotic processes, which is essential for life. It captures and converts the energy we need to live and grow, bringing it into our ecosystem for us to use in the form of food, and in the form of fuel, fossil and otherwise.

The quantum requirement for oxygenic photosynthesis, according to Z-scheme, is 8 quanta for each molecule of oxygen released (four quanta required by PSII and four by PSI), and requiring 8 moles of photons or 381 kcal energy for each mole of CO_2 reduced. The reduction of one mole of CO_2 molecule to glucose requires 112 kcal of energy. The quantum yield measurements show that the quantum yields of PSII and PSI reaction centers are near 100%. If 8 red quanta are absorbed (381 kcal/mol) for each CO_2 molecule reduced (112 kcal/mol), the calculated maximum energy efficiency (free energy stored / light energy absorbed) for carbon reduction is ~30% (Ke, 2001).

However under normal growing conditions the actual performance of the plants is far below these theoretical values. The annual flux of sunlight energy toward the earth's surface is estimated to be 1.2×10^{21} kcal. A large fraction of this energy is either reflected by the atmosphere ($\sim 4 \times 10^{20}$ kcal) or absorbed by it ($\sim 2 \times 10^{20}$ kcal). About 1.8×10^{20} kcal of sunlight energy falls on land. Of the total, the energy stored by green plants and algae has been estimated to be 6×10^{17} kcal. From this amount the energy from substances suitable for use as fuel amounts to 8×10^{15} kcal, food stuff amounts to 4×10^{15} kcal, and agricultural waste amounts to 2×10^{16} kcal. Based on the total energy (1.8×10^{20} kcal) from sun, falling on the earth's surface, only 6×10^{17} kcal, less than 0.4% appears to be efficiently utilized by photosynthesis (Ke, 2001). The factors that conspire to lower the quantum yield of photosynthesis include limitations imposed by biochemical reactions in the plant and environmental conditions that limit photosynthetic performance.

Why study photosynthesis?

Knowledge of the molecular mechanisms of oxygenic photosynthesis is essential for understanding the relationship between living organisms and the balance of atmosphere and life on earth. In spite of only small part of energy that reaches the earth is captured photosynthesis is still premier solar energy conversion process on earth. It provides paradigms for sustainable global energy production and efficient energy transformation.

Approximately 80% of the world energy consumption is based on three sources of fossil fuel, coal, oil and natural gas. These fuels are mostly used to generate electricity for industry and home, run vehicles with combustion engines, gives heat at home. Over the course of the last 100 years, the world consumption of energy based on fossil fuels has increased immeasurable due to constantly growing requirements of world industry. At the moment, the total fossil fuel reserve, a remnant of ancient photosynthetic products is driving the modern industrial civilization and estimated to be $\sim 10^{19}$ kcal. Current world annual consumption of fuel is $\sim 5 \times 10^{16}$ kcal. Consequently the current fuel reserve at the present rate of consumption will be last about 150-200 years. It is still unclear where most of energy will come from in the longer-term future. A fundamental problem of the energy industry is that traditional fossil fuel is only renewable on a very long time scale, that the rate of formation fossil fuels in the nature is many orders of magnitude slower than the rate of their consumption. Therefore, the reserves that can be recovered in an energetically feasible manner are shrinking rapidly, in parallel with an increasing worldwide energy demand. Therefore, in times of deforestation, acidification, and other negative effects due to lack of respect for and understanding of the earth and larger ecosystems, combined with rapidly growing population with increasing demands on living standards, study of photosynthesis is highly relevant.

The eventual solution for the fuel-energy is

developments of new energy technologies using energy of sun. The promising can be man made devices on the basis of photosynthesis, more precisely creating artificial photosynthesis. Scientists around the world study the photosynthetic structure and functions relation and try to understand photosynthesis in order to use the knowledge for energy conversion in the bio-mimetic systems. It is important to establish an artificial model of photosynthesis not only for understanding and simulating the photosynthesis, but also to construct artificial photosynthesis, which is attracting a great deal of interest to convert solar energy into fuels. The idea is to create artificial systems that exploit the basic chemistry of photosynthesis in order to produce fuels for engines and electricity. If one ever wants to mimic the natural processes of photosynthesis, the key physical chemical and biological elements of the process should be fully understood. Duplication of that catalytic activity in industrial setting would have considerable economic benefit but will require a solid understanding of the mechanism of the biological catalysis. Understanding its unique chemistry is not only important in its own right, but could have implications for the agricultural industry since photosynthetic processes are a main site of damage during environmental stress.

Methodology

The main focus in the studies of photosynthesis is to identifying pigment and subunit composition, electronic cofactors (their functions and arrangements on the proteins), amino acid sequences of main proteins and identifying amino acid residues surrounding redox cofactors. This has lead to the development of different biochemical and physical methods, a large variety of preparation, each with particular properties of purity, activity and stability as well as techniques during the last decades. Certain knowledge obtained from the protein amino acid sequencing and computer modeling of the protein folding geometry. Together with traditional, the advanced physical methods of XAS (X-ray Absorption Spectroscopy), FT-IR (Fourier Transform Infra Red), ultra-fast optic spectroscopy and large varieties of EPR (Electron Paramagnetic Resonance) spectroscopy have also widely applied to this field allowing one to identify the redox active components in photosynthetic species and providing the information about electronic structure, local environment and distance between them. The knowledge obtained from the spectroscopy, and research on biochemistry, biophysics and molecular biology together with highly purified preparations build up the basis for the determination at high resolution X-ray structures most of the proteins involved in the complexes PSII, PSI and Cyt b_6f and

geometry most of cofactors. Recently an essential progress is achieved in determination of those photosynthetic structures by X-ray crystallography (Zouni et al., 2001; Kamiya and Shen, 2003; Kurisu et al., 2003; Ferreira et al., 2004; Loll et al., 2005; Nelson and Yocum, 2006; Amunts et al., 2007).

Photosynthesis Community (Govindjee, 2007; Orr and Govindjee, 2007)

The photosynthetic science is coordinated by the international society of photosynthesis research (ISPR), the International Congresses of Photosynthesis, specialized conferences dedicated to different topics of research of photosynthesis and the results of photosynthesis research are subject of the proceedings of Congress and conferences, and international journals such as Photosynthesis Research, Biochemistry, Journal of Biological Chemistry, Biochimica et Biophysica Acta (Bioenergetics), Biophysical journal, Plant Physiology, Photosynthetica, etc.

The ISPR was founded August 22, 1995 at the 10th International congress of photosynthesis at Montpellier, France. The purposes of ISPR are to:
(1) encourage the growth and to promote the development of photosynthesis as a pure and applied science;
(2) to facilitate publication of research in photosynthesis;
(3) to sponsor the organization of a triennial international conferences;
(4) to promote international cooperation in photosynthesis research and education.

ISPR membership spans six continents and its members work across academia, education and training, as well as in government, industrial and commercial research environments. The Society plays a key role in uniting the photosynthesis research community internationally. Membership of ISPR is open to those concerned with all aspects (molecular, genetic, cellular and organismal) of the biochemistry, biophysics and physiology of photosynthesis in plants in agriculture and forestry, natural ecosystems and the marine and global environment. An official journal of ISPR is the journal of Photosynthesis Research and official meeting of ISPR is an International Congress of Photosynthesis (ICP). In spite of the ISPR was formed late, at 1995, the ICP was organized every three years since 1968. International Congress of Photosynthesis covers the achievements in photosynthesis research of every last three years. In the other hand every congress is accompanied by several specialized satellite discussion meetings related to the important problems of photosynthesis organized by leading scientists in the field. Organization of the Congresses and conferences aims to provide a dy-

namic exchange of information and new research finding in all areas, a celebration of the achievements of the photosynthesis community, providing a forum for the discussion of recent developments, advances in current concepts and understanding, as well as relevant applications.

REFERENCES

Amunts A., Drory O., Nelson N. (2007) The structure of plant photosystem I supercomplex at 3.4 Å resolution. Nature **447:** 58-63.

Andersson B., Anderson J.M. (1980) Lateral heterogeneity in the distrubituon of chlorophyll-protein complexes of the thylakoid membranes of spinach chloroplasts. Biochim. Biophys. Acta **593:** 427-440.

Avron M. (1987) Photophosphorylation in chloroplasts. In: Photosynthesis (Amesz J., ed.), Elsevier, Amsterdam: 159-173.

Barry B.A., Boerner R.J., De Paula J.C. (1994) The use of cyanobacteria in the study of the structure and function of photosystem II. In: The molecular biology of cyanobacteria. (Bryant D.A., ed.), Kluwer Academic Publishers, Dordrecht: 217-257.

Brettel K. (1997) Electron transfer and arrangement of the redox cofactors in photosystem I. Biochim. Biophys. Acta **1318:** 322-373.

Brettel K., Leibl W. (2001) Electron transfer in photosystem I. Biochim. Biophys. Acta **1507:** 100-114.

Broda E. (1975) The evolution of the bioenergetic processes. Pergamon Press, Oxford: 211 p.

Danielsson R. (2005) On the lateral organization of the thylakoid membrane. PhD thesis. Lund university.

Debus R.J. (1992) The manganese and calcium ions of photosynthetic oxygen evolution. Biochim. Biophys. Acta **1102:** 269-352.

Dekker J.P., Boekema E.J. (2005) Supramolecular organization of thylakoid membrane proteins in green plants. Biochim. Biophys. Acta **1706:** 12-39.

Diner B.A., Babcock G.T. (1995) Structure, dynamics, and energy conversion efficiency in photosystem II. In: Oxygenic photosynthesis: The light reactions (Ort D.R., Yocum C.F., eds.), Kluwer Academic Publishers, Dordrecht: 213-247.

Douglas S.E. (1994) Chloroplast origins and evolution. In: The molecular biology of cyanobacteria. (Bryant D.A., ed.), Kluwer Academic Publishers, Dordrecht: 91-118.

Erickson J.M. (1995) Chloroplast transformation: Current results and future prospects. In: Oxygenic

photosynthesis: The light reactions. (Ort D.R., Yocum C.F., eds.), Kluwer Academic Publishers, Dordrecht: 589-619.

Ferreira K.N., Iverson T.M., Maghlaou K., Barber J., Iwata S. (2004) Architecture of the photosynthetic oxygen-evolving center. Science **303:** 1831-1838.

Frash W.D. (1994) The F-type ATPase in cyanobacteria: Pivotal point in the evolution of a universal enzyme. In: The molecular biology of cyanobacteria. (Bryant D.A., ed.), Kluwer Academic Publishers, Dordrecht: 361-380.

Fromme P., Jordan P., Krauӭ N.(2001) Structure of photosystem I. Biochim. Biophys. Acta **1507:** 5-31.

Gantt E. (1994) Supramolecular membrane organization. In: The molecular biology of cyanobacteria. (Bryant D.A., ed.), Kluwer Academic Publishers, Dordrecht: 119-138.

Gobets B., van Grondelle R. (2001) Energy transfer and trapping in photosystem I. Biochim. Biophys. Acta **1507:** 80-99.

Golbeck J.H. (1994) Photosystem I in cyanobacteria. In: The molecular biology of cyanobacteria. (Bryant D.A., ed.), Kluwer Academic Publishers, Dordrecht: 319-360.

Golbeck J.H. (1987) Structure, function and organization of the photosystem I reaction center complex. Biochim. Biophys. Acta **895:** 167-204.

Govindjee H.H. (2007) The Internatiuonal Society of Photosynthesis Research (ISPR) and its associated International Congress on Photosynthesis (ICP): a pictorial report. Photosynth. Res. **91:** 95-106.

Govindjee, Kambara T., Coleman W. (1986) The electron donor side of photosystem II: The oxygen evolving complex. Photochem. Photobiol. **42:** 187-210.

Gray J.C. (1995) Regulation of expression of nuclear genes encoding polypeptides required for the light reactions of photosynthesis. In: Oxygenic photosynthesis: The light reactions. (Ort D.R., Yocum C.F., eds.), Kluwer Academic Publishers, Dordrecht: 621-641.

Gross E.L. (1995) Plastocyanin: Structure, location, diffusion and electron transfer mechanisms. In: Oxygenic photosynthesis: The light reactions. (Ort D.R., Yocum C.F., eds.), Kluwer Academic Publishers, Dordrecht: 413-429.

Hauska G., Schӑtz M., Bӑttner M. (1995) The cytochrome b₆f complex – Composition, structure and function. In: Oxygenic photosynthesis: The light reactions. (Ort D.R., Yocum C.F., eds.), Kluwer Academic Publishers, Dordrecht: 377-398.

Hill R. (1965) The biochemist's green mansions: the photosynthetic electron-transport chain in

plants. In: Essays in Biochemistry. (Campbell P.N., Greville G.D., eds.), Academic Press, London **1**: 121-151.

Hill R., Bendall F. (1960) Function of two cytochrome components in chloroplasts: A working hypotesis. Nature **1186**: 136-137.

Hore A.B. (1993) The chloroplast cytochrome b_6f complex: a critical focus on function. Biochim. Biophys. Acta **1143**: 1-22.

Hore A.B. (2000) Electron transfers amongst cytochrome *f*, plastocyanin and photosystem I: Kinetics and mechanisms. Biochim. Biophys. Acta **1456**: 5-26.

Kallas T. (1994) The cytochrome b_6f complex. In: The molecular biology of cyanobacteria. (Bryant D.A., ed.), Kluwer Academic Publishers, Dordrecht: 259-317.

Kamiya N., Shen J.-R. (2003) Crystal structure of oxygen-evolving photosystem II from *Thermosynechococcus vulcanus* at 3.7-Å resolution. Proc. Natl. Acad. Sci. USA **100**: 98-103.

Ke B. (2001) Photosynthesis: Photobiochemistry and photobiophysics. Kluwer Academic Publishers, Dordrecht: 763 p.

Klimov V.V., Krasnovsky A.A. (1981) Pheophytin as the primary electron acceptor in photosystem II reaction centres. Photosynthetica **15**: 592-609.

Knaff D.V. (1977) The primary reaction of plant photosystem II. Photochem. Photobiol. **26**: 327-340.

Kurisu G., Zhang H., Smith J.L., Cramer W.A. (2003) Structure of the cytochrome b_6f complex of oxygenic photosynthesis: Tuning the cavity. Science **302**: 1009-1014.

Loll B., Kern J., Saenger W., Zouni A., Biesiadka J. (2005) Towards complete cofactor arrangement in the 3.0 Å resolution structure of photosystem II. Nature **438**: 1040-1044.

Malkin R. (1995) Photosystem I electron transfer reactions – Components and kinetics. In: Oxygenic photosynthesis: The light reactions. (Ort D.R., Yocum C.F., eds.), Kluwer Academic Publishers, Dordrecht: 313-332.

Mathis P., Rutherford A.W. (1987) The primary reactions of photosystem I and II of algae and higher plants. In: Photosynthesis. (Amesz J., ed.), Elsevier, Amsterdam: 63-96.

McCarty R.E. (1995) An overview of the function, composition and structure of the chloroplast ATP synthase. In: Oxygenic photosynthesis: The light reactions. (Ort D.R., Yocum C.F., eds.), Kluwer Academic Publishers, Dordrecht: 439-451.

Melis A. (1991) Dynamics of photosynthetic membrane composition and function. Biochim. Biophys. Acta **1058**: 87-106.

Nelson N., Yocum C.F. (2006) Structure and function of photosystems I and II. Annu. Rev. Plant Biol. **57**: 521-565.

Orr L., Govindjee (2007) Photosynthesis and the Web: (2008) Photosynthesis Res. **91**: 106-131.

Renger G. (1992) Energy transfer and trapping in photosystem II. In: The photosystems: Structure, function and molecular biology. (Barber J., ed.) Elsevier, Amsterdam: 45-100.

Roell M.K., Cruissem W. (1995) Chloroplast gene expression: Regulation and multiple levels. In: Oxygenic photosynthesis: The light reactions. (Ort D.R., Yocum C.F., eds.), Kluwer Academic Publishers, Dordrecht: 565-587.

Scheller H.V., Jensen P.E., Haldrup A., Lunde C., Knoetzel J. (2001) Role of subunits in eucariotic photosystem I. Biochim. Biophys. Acta **1507**: 41-60.

Seibert M. (1993) Biochemical, biophysical and structural characterization of the isolated photosystem II reaction center complex. In: The photosynthetic reaction center. (Deisenhofer J., Norris J., eds.) Academic Press Inc., San Diego: 289-318.

Setif P. (2001) Ferredoxin and flavodoxin reduction by photosystem I. Biochim. Biophys. Acta **1507**: 161-179.

Sigfridsson K. (1998) Plastocyanin, an electron-transfer protein. Photosynth. Res. **57**: 1-128.

Staehelin L.A., van der Stay G.W.M. (1995) Structure, composition, functional organization and dynamic properties of thylakoid membranes. In: Oxygenic photosynthesis: The light reactions. (Ort D.R., Yocum C.F., eds.), Kluwer Academic Publishers, Dordrecht: 11-30.

Süss K.H., Arkona C., Manteuffel R., Adler K. (1993) Calvin cycle multienzyme complexes are bound to chloroplast thylakoid membranes of higher plants *in situ*. Proc.Natl. Acad. Sci. USA **90**: 5514-5518.

Süss K.-H., Prokherenko I., Adler K. (1995) *In situ* association of Calvin cycle enzymes, ribulose-1.5-bisphosphate carboxylase/oxy-genase activase, ferredoxyn-$NADP^+$ reductase, and nitrite reductase with thylakoid membranes of *Chlamydomonas reinhardtii* chloroplasts as revealed by immunoelectron microscopy. Plant Physiol. **107**: 1387-1397.

Taiz L., Zeiger E. (2002) Plant physiology. 3rd ed. Sinauer Associates, Redwood City: 690 p.

Van Gorkom H.J. (1987) Evolution of photosynthesis. In: Photosynthesis. (Amesz J., ed.), Elsevier Science Publishers B.V., Amsterdam: 343-350.

Vassiliev I.R., Antonkine M.L., Golbeck J.H. (2001) Iron-sulphur clusters in type I reaction centers. Biochim. Biophys. Acta **1507**: 139-160.

Voet D., Voet J.G. (2004) Biochemistry. 3rd ed.

John Wiley and Sons Inc., New York: 1591 p.

Webber A.N., Lubitz W. (2001) P_{700}: The primary electron donor of photosystem I. Biochim. Biophys. Acta **1507**: 61-79.

Whitmarsh J., Govindjee (1999) The photosynthetic process. In: Concepts of in photobiology: Photosynthesis and photomorphogenesis. (Singhal G.S., Renger G., Sopory S.K., Irrgang K.-D., Govindjee, eds.), Narosa Publishers, New Delhi and Cluwer Academic Publishers, Dordrecht: 11-51.

Wilmotte A. (1994) Molecular evolution and taxonomy of the cyanobacteria. In: The molecular biology of cyanobacteria. (Bryant D.A., ed.),

Kluwer Academic Publishers, Dordrecht: 1-25.

Wolfe G.R., Hoober J.K. (1995) Evolution of thylakoid structure. In: Oxygenic photosynthesis: The light reactions. (Ort D.R., Yocum C.F., eds.), Kluwer Academic Publishers, Dordrecht: 31-40.

Xu W., Tang Y., Chitnis P.P. (2001) Proteins of the cyanobacterial photosystem I. Biochim. Biophys. Acta **1507**: 32-40.

Zouni A., Witt H.-T., Rthy J., Fromme P., Krauϴ N., Saenger W. Orth P. (2001) Crystal structure of photosystem II from *Synechococcus elongates* at 3.8 Å resolution. Nature **409**: 739-743.

Derivatives of Hydroxyperfluoroisopropyldinitrobenzole Inhibit Electron Transfer in Photosystem II

Sergey K. Zharmukhamedov, Suleyman I. Allakhverdiev*, Vyacheslav V. Klimov

Institute of Basic Biological Problems, Russian Academy of Sciences, Pushchino, Moscow Region 142290, Russia

We have revealed new highly efficient inhibitors of electron transfer in photosystem II (PSII) of plants – hydroxyperfluoroisopropyldinitrobenzole derivatives, designated as K15-type inhibitors. Their inhibitory effect is based on the redox interactions with PSII reaction centre (RC) components accompanied by formation of a short cyclic electron transfer chain which leads to rapid recombination of separated charge in PSII. This conclusion is supported by the following effects obtained upon treatment of isolated chloroplasts of higher plants or PSII preparations with K15: (1) inhibition of the photoinduced changes in chlorophyll fluorescence yield (ΔF) related to photoreduction of the primary electron acceptor Q_A and photoinduced absorption changes (ΔA) related to photoaccumulation of the primary electron donor P_{680} in its oxidized form P_{680}^+; (2) acceleration of dark relaxation and the decrease of the amplitude of ΔA and ΔF related to photoreduction of the intermediary electron acceptor pheophytin and the decrease in the fluorescence yield when Q_A was prereduced; (3) disappearance of all these effects upon addition of dithionite (which reduces K15 in the dark) accompanied by an accelerated electron donation to RC; (4) coincidence of the concentration dependences of the inhibition by these compounds of both oxygen evolution and the above mentioned reactions related to electron transfer in PSII RC (the value of the inhibition constant K_i was found to be equal to 45 nM for K15).

Keywords: hydroxyperfluoroisopropyldinitrobenzole, K15 inhibitors, PSII, cyclic electron transfer

INTRODUCTION

As was shown earlier (Allakhverdiev et al., 1989; Klimov et al., 1989), dinoseb (2,6-dinitro-sec-butyl phenol), a herbicide of the phenolic group, along with blocking the electron transfer between quinones Q_A and Q_B (Trebst and Draber, 1979) is also capable of redox interaction with the reaction centre (RC) components in photosystem II (PSII). This leads to the enhanced oxidation of the reduced pheophytin (Pheo⁻) and reduction of the oxidized chlorophyll P_{680}^+ (Pheo and P_{680}, intermediary acceptor and primary donor of electron in PSII, respectively) and, as a result, to a more rapid recombination of $[P_{680}^+ Pheo^-]$ pair. The dinoseb induced cyclic electron transfer which competes with the functional reactions of Pheo⁻ oxidation and P_{680}^+ reduction and contributes to the total effect of PSII inhibition only at relatively high concentrations of this inhibitor (Allahverdiev et al., 1989; Klimov et al., 1989).

In this article, we summarize recent progress in studies of the inhibitory effect exerted on electron transport in PSII by hydroxyperfluoroisopropyldinitrobenzole (HPFIPDNB) derivatives exhibiting a growth-regulatory and herbicidal activity (Konstantinova et al., 1980). The structural formulas of these inhibitors are illustrated in Figure 1.

RESULTS

Figure 2A shows that compound K15 taken at concentrations of 0.9 μM, 2 μM and 7 μM inhibits the photoinduced evolution of oxygen in pea chloroplasts measured in the presence of ferredoxin and NADP⁺ by 30%, ~ 60% and ~ 90%, respectively.

Similar dependence was observed for the photoinduced ΔF associated with the photoreduction of Q_A, the primary electron acceptor of PSII (Figure 2B). Compound K15 does not inhibit the NADP⁺ photoreduction in the presence of the reduced 2,6-dichlorophenolindophenol, i.e., under the conditions of involvement of PSI alone in this reaction (see Table 1).

Of all known inhibitors of PSII dinoseb is regarded to be the closest to these compounds by its chemical structure. But, as shown in Figure 3, the efficiency of the inhibitory action of compound K15 is much higher (~80-100 times) than that of dinoseb. Furthermore, in contrast to dinoseb, compound K15 suppresses the electron transport and
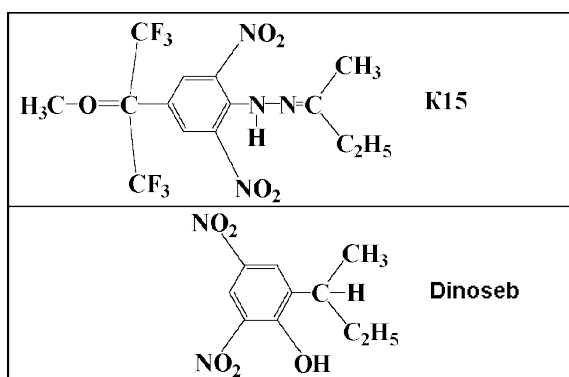
Figure 1. Structural formulas of inhibitor K15 and dinoseb.

photoinduced ΔF in chloroplasts within the same concentration range. Consequently, in contrast to dinoseb (Allakhverdiev et al., 1989; Klimov et al., 1989), in the case of compound K15 the inhibition of electron transport and repression of photoinduced ΔF in PSII appears to be based on the same action mechanism.

Figure 4 shows the results derived from comparison of the effect of compound K15 on F and photoinduced ΔF of PSII subchloroplast particles (DT-20) with that of diuron and dinoseb during measurements with the use of light of saturating intensity. Already at a concentration of 18 nM (curve 3) K15 causes a decrease of the maximum level of fluorescence ($F_M = F_0 + \Delta F$) due to a 15%, decrease of ΔF compared to the control. At concentrations of 80 nM and 360 nM, K15 was found to inhibit the photoinduced ΔF by 57% and 86%, respectively (curves 4 and 5).

It is noteworthy that in contrast to diuron, compound K15 does not virtually affect the magnitude of F_0 and the rate of dark relaxation of ΔF (reflecting reoxidation Q_A^-). The inhibitory effect of K15 on ΔF is totally preserved during prolonged (>5 min) illumination with the actinic light even at a 0.05-0.1 μM concentration of inhibitor (in contrast to the well-known electron acceptor 2,5-dibromo-3-methyl-6-isopropylbenzoquinone (DBMIB) whose addition to DT-20 preserved the fluorescence quenching only during the first 5-10 s of illumination, which then disappeared due to photoreduction of DBMIB). Multiple wash-off of PSII preparations treated with inhibitor K15 (by centrifugation) did not eliminate the inhibitor from PSII, which is evidenced by the preservation of the inhibitory effect.

It is known that the decrease of F_M due to repression of ΔF can occur as a result of inactivation of the PSII electron donor site, e.g., after complete removal of manganese (curve 8). In this case addition of exogenous PSII electron donors restores the magnitude of ΔF to its initial value (curve 8), which was

also observed in some earlier studies (Klimov et al., 1982). Figure 3 shows that the efficiency of the inhibition of photoinduced ΔF by K15 does not virtually change upon addition of artificial PSII electron donor - Mn^{2+} (0.1-20 μM, curve 5), sodium ascorbate (2 mM), diphenylcarbazide (1 mM), NH_2OH (1 mM) (data not shown) - irrespective of the sequence of the reagent addition.

Table 1. Decrease of the rate of $NADP^+$ photoreduction by pea chloroplasts upon addition of compounds K15.

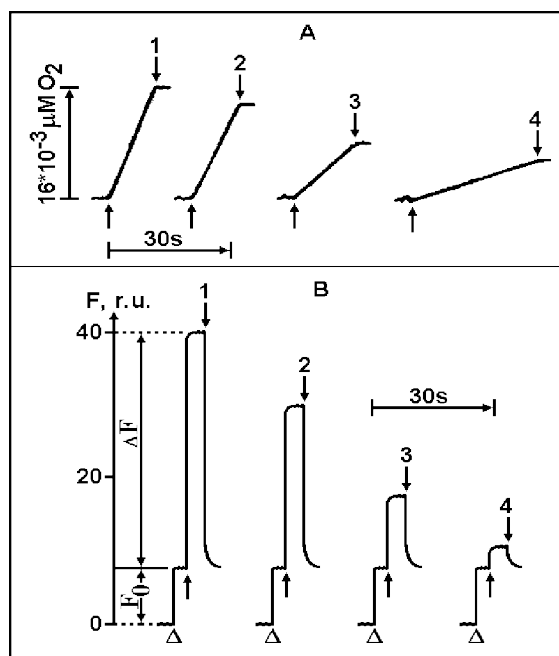| Additions	Reduction rate	
	nmole/(mg chlorophyll h)	%
-	117.0	100
K15		
0.6 μM	80.7	69
2 μM	45.6	39
7 μM	11.7	10
+ $DCPIPH_2$ (0.1 mM)	124.0	106

Figure 2. Effect of compound K15 at concentrations of 0.6 μM (2), 2 μM (3) and 7 μM (4) on the photoinduced electron transfer in pea chloroplasts measured by: A, the rate of oxygen evolution in the presence of 20 μM ferredoxin, 20 μM ferredoxin-$NADP^+$ reductase and $NADP^+$ (5 mg·ml^{-1}); B, photoinduced changes of chlorophyll fluorescence yield in PSII due to photoreduction of Q_A. 1, control (measurement in the absence of K15). Here and below the triangles indicate the moments of switching on the measuring light ($\lambda = 490$ nm; 0.15 J m^{-2} s^{-1}) which induces the chlorophyll fluorescence ($\lambda > 650$ nm); the upward and downward arrows indicate switching the actinic light ($\lambda > 600$ nm; 100 J m^{-2} s^{-1}) on and off, respectively. Chlorophyll concentration, 100 μg ml^{-1}; 20°C.
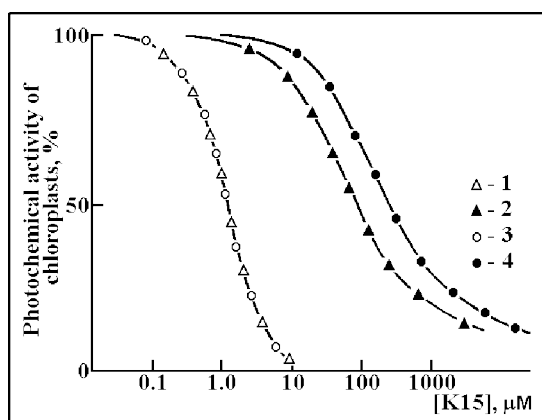
Figure 3. Dependence of photochemical activity of pea chloroplasts estimated from the rate of oxygen evolution in the presence of exogenous electron acceptors (ferredoxin, ferredoxin-$NADP^+$ reductase and $NADP^+$) (3, 2) and from photoinduced ΔF of PSII chlorophyll related to photoreduction of Q_A (3, 4) on concentration of K15 (1, 3) and dinoseb (2, 4). Chlorophyll concentration, 100 μg ml^{-1}; 20°C. For the conditions of measurements see the legend to Figure 1.

Addition of dithionite ($\cong 0.8$ mg ml^{-1}) totally eliminates the inhibitory effect of K15 on ΔF of PSII. Fluorescence rises to its maximal level, whereas the application of the actinic light causes a decrease of fluorescence (curve 9) related, as shown earlier in (Allakhverdiev et al., 1989; Klimov et al., 1989), to the photoreduction of Pheo. Dithionite induces the dark reduction of K15, which is evidenced by the disappearance of characteristic absorption bands in the range of 200-500 nm with the maximum at 410 nm (not shown).

It is known that the decrease of F_M due to repression of ΔF can occur as a result of inactivation of the PSII electron donor site, e.g., after complete removal of manganese (curve 8). In this case addition of exogenous PSII electron donors restores the magnitude of ΔF to its initial value (curve 8), which was also observed in some earlier studies (Klimov et al., 1982). Figure 3 shows that the efficiency of the inhibition of photoinduced ΔF by K15 does not virtually change upon addition of artificial PSII electron donor - Mn^{2+} (0.1-20 μM, curve 5), sodium ascorbate (2 mM), diphenylcarbazide (1 mM), NH_2OH (1 mM) (data not shown) - irrespective of the sequence of the reagent addition.

Addition of dithionite ($\cong 0.8$ mg·ml^{-1}) totally eliminates the inhibitory effect of K15 on ΔF of PSII. Fluorescence rises to its maximal level, whereas the application of the actinic light causes a decrease of fluorescence (curve 9) related, as shown earlier in (Allakhverdiev et al., 1989; Klimov et al., 1989), to the photoreduction of Pheo.
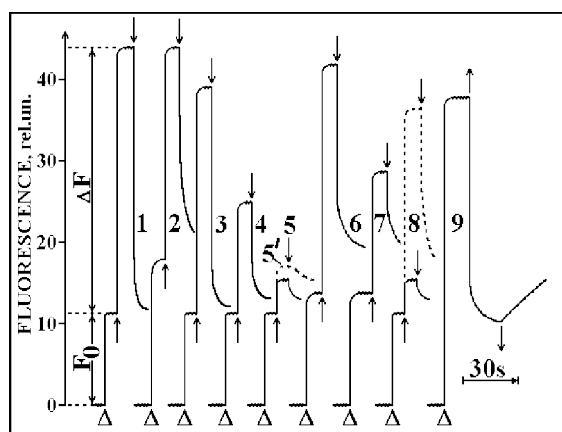

Figure 4. The level of dark fluorescence (F) and the kinetics of photoinduced changes F (ΔF), related to photoreduction of Q_A in PSII, under anaerobic conditions in subchloroplast DT-20 particles (1-7, 9; solid lines) before (1) and after addition (2) of 0.5 μM diuron; compound K15 added at concentrations of 20 nM (3), 80 nM (4) and 360 nM (5) in the absence of other additives and after addition of 0.8 mg ml^{-1} of dithionite to (5) (9); dinoseb at concentration of 1 μM (6) and 5 μM (7) and in DT-20 particles after a complete removal of Mn (8). Curves 5' and 8' (dashed line) are the same as curves 5 and 8 but after addition of 20 mM $MnCl_2$. For designations and measurement conditions see the legend to Figure 1. Chlorophyll concentration, 10 μg ml^{-1}; 20°C.

Dithionite induces the dark reduction of K15, which is evidenced by the disappearance of characteristic absorption bands in the range of 200-500 nm with the maximum at 410 nm (not shown).

Figure 5 shows the variation of I_{50} (the inhibitor concentration inducing a 50% inhibition) for compound K15 as a function of the concentration of DT-20 particles expressed as the level of chlorophyll they contain. The magnitude of I_{50} approximated to the zero chlorophyll concentration, as it was done earlier for other inhibitors (Tischer and Strotmann, 1977; van Rensen et al., 1978; Fedtke, 1985), has values of 45 nM for K15, whereas the values of pI_{50} defined as -$logI_{50}$ (Fedtke, 1985) are 7.4 for K15. The data presented in Figure 5 also indicate that one inhibitor molecule is bound to one RC of PSII.

It is known (Klimov et al., 1985, 1986) that photoreduction of Pheo to $Pheo^-$ in PSII may also occur in the absence of dithionite - when anaerobic conditions are created. In this case the value of fluorescence also reaches the level F_M as a result of Q_A photoreduction to Q_A^- by a weak measuring light, whereas during the illumination with the acting light one can observes a decrease of fluorescence (-ΔF) and changes in absorption (ΔA) related to reversible photoreduction of Pheo (Figure 6).
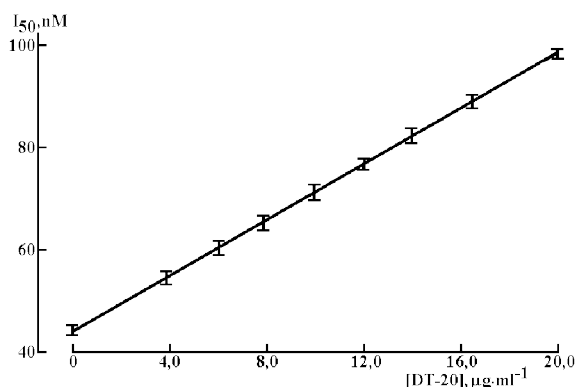
Figure 5. Dependence of the K15-induced 50% - inhibition of photoinduced ΔF (I_{50}) in DT-20 particles on their concentration expressed as concentration of chlorophyll they contain (μg ml⁻¹).

Addition of K15 at a concentration of 38 nM leads to a dramatic (15-20-fold) increase of the rate of dark relaxation ΔA and -ΔF which is indicative of the increased rate of dark oxidation of reduced Pheo (Figure 6A, B). The increase of K15 concentration from 65 nM to 360 nM (Figure 6) results in a considerable decrease of -ΔF and ΔA as well as in a lower level of F_M. It should be noted that in this case the illumination with the actinic light does not lead to the appearance of photoinduced rise of F associated with the photoreduction of Q_A. On the other hand, when K15 is replaced by a PSII electron acceptor inducing the dark oxidation of Q_A^-, for example DCPIP, such a decrease in F_M under anaerobic conditions is accompanied by the appearance of photoinduced increase of F (Figure 6A, curve 6). Application of 50-100 μM diuron did affect neither the time course, nor the magnitudes of ΔA and -ΔF related to the photoreduction of Pheo or F_M under anaerobic conditions.

Other experiments showed that compound K15 at concentrations up to 100 μM did not inhibit the fluorescence of chlorophyll in the light-harvesting pigment-protein complexes isolated from pea chloroplasts, as described in (Klimov et al., 1982, 1989; Allahverdiev et al., 1989) as well as the fluorescence of chlorophyll solution in 1% Triton X-100.

It was shown earlier that the photoinduced -ΔF associated with the reversible photoreduction of Pheo may be observed in the presence of a strong reductant, dithionite (Klimov et al., 1979, 1989). Investigation of this photoreaction in DT-20 preparations freed of Mn (Klimov et al., 1982) showed that addition of 0.5 μM K15 (as well as addition of Mn^{2+} (Klimov et al., 1982)) leads to a 1.5-2-fold increase of the Pheo photoreduction rate (Figure 7), whereas the rate of dark
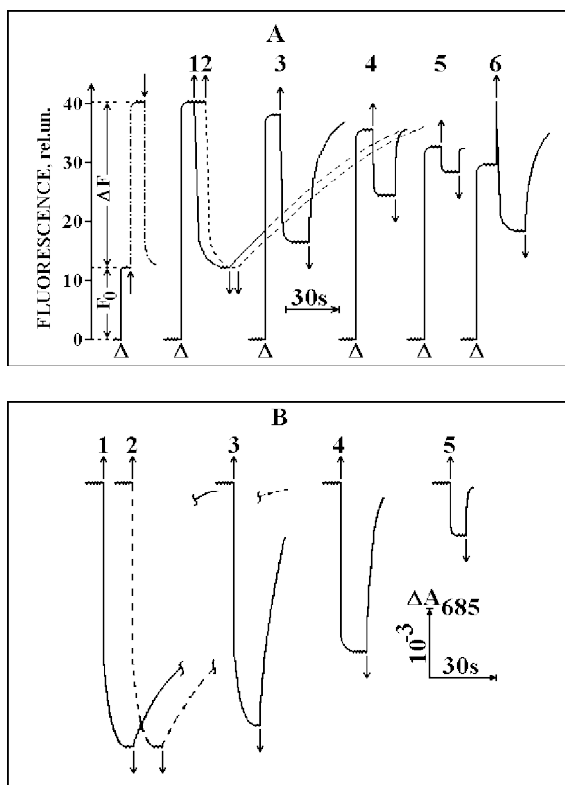
Figure 6. The level of F and the kinetics of photoinduced -ΔF (A) and absorbance changes at 685 nm (B), related to pheophytin photoreduction in PSII, in DT-20 particles under anaerobic conditions (upon addition of 10 mM glucose, ~50 U ml⁻¹ glucose oxidase, ~1000 U ml⁻¹ catalase, 5 mM sodium ascorbate and 1 μM CCCP) without other additives (1) and after addition of compound K15 at concentrations of 38 nM (3), 65 nM (4) and 360 nM (5); 10 μM DCPIP (6) or 50 nM diuron (2). A, the dash-dot line shows the time course of ΔF related to photoreduction of Q_A in an identical sample placed under aerobic conditions. Chlorophyll concentration, 10 μg ml⁻¹; 20°C.

Figure 7. The kinetics of photoinduced fluorescence (F) decrease related to photoreduction of pheophytin in RC of PSII in Mn-depleted DT-20 particles upon addition of dithionite (0.8 mg ml⁻¹) in the absence of other additives (1) and after addition of 0.5 μM K15 (2) or 0.1 mM $MnCl_2$ (3); pH 8.5. For measurement conditions see the legend to Figure 1.

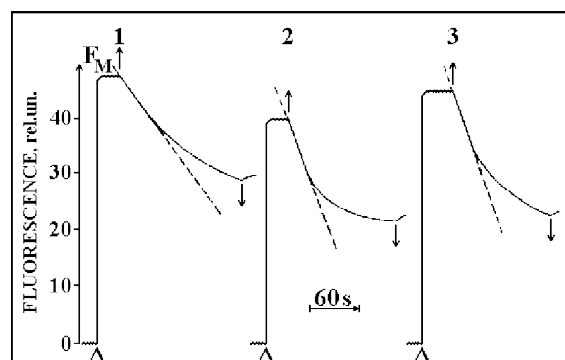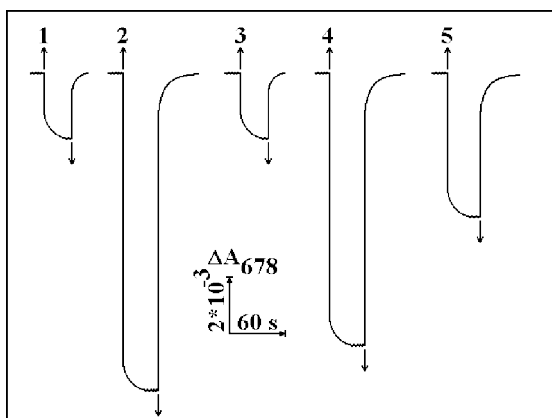**Figure 8.** The kinetics of photoinduced absorbance changes at 678 nm related to photooxidation of P_{680} in DT-20 preparations in the presence of 1 mM ferricyanide and 0.1 mM silicomolybdate prior to (2) and after (2-5) complete removal of Mn; the measurement in the absence of other additives (2) and upon addition of 3 μM $MnCl_2$ (3) or compound K15 at concentrations of 22 nM (4) and 80 nM (5).
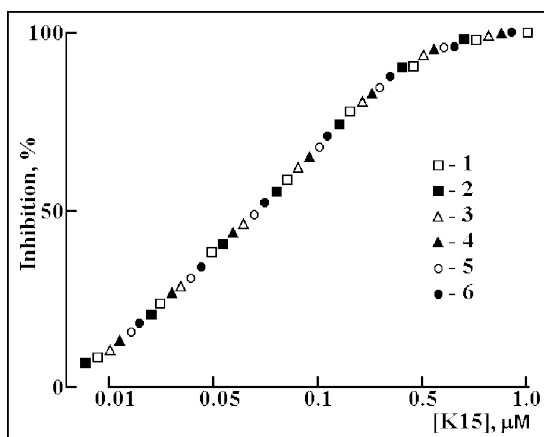

Figure 9. The [K15] dependence of the inhibition (in %) of photoinduced ΔF related to photoreduction of the primary electron acceptor in PSII, plastoquinone Q_A (1), magnitude of F_M under aerobic conditions (2), magnitude F_M under anaerobic conditions (3), photoinduced -ΔF and ΔA_{685} related to photoreduction of the intermediary electron acceptor, pheophytin, under anaerobic conditions (4 and 5, respectively), photoinduced ΔA_{678} related to photooxidation of the primary electron donor in PSII, chlorophyll P_{680} (6). Chlorophyll concentration, 10 μg ml^{-1}.

oxidation of Pheo remains unchanged.

Furthermore, the use of such preparations to study another characteristic photoreaction in PSII - photooxidation of the primary electron donor P_{680} (registered as photoinduced ΔA at 678 nm in the presence of potassium ferricyanide and silicium molyb-date) - showed that addition of 22 nM and 80 nM K15 results in the decrease of ΔA_{678} values by 17% and

57%, respectively (Figure 8, curves 4 and 5). It was shown earlier (Allakhverdiev et al., 1985) that a similar decrease of ΔA is observed upon addition of Mn^{2+} (0.1-3 μM) to such preparations, which is conducive to the reactivation of electron donation in RC of PSII.

Figure 9 features comparison of the curves showing the dependences of the inhibition of various photoreactions occurring in PSII on the concentration of K15: (1) photoinduced ΔF associated with the photoreduction of Q_A; (2) magnitudes of F_M under aerobic and anaerobic conditions; (3) photoinduced -ΔF and ΔA_{685} associated with the photoreduction of Pheo and (4) photoinduced ΔA_{678} associated with the photooxidation of chlorophyll P_{680}. It should be noted that all these dependences are similar.

DISCUSSION

The inhibition of oxygen evolution and photoreduction of $NADP^+$ in chloroplasts upon addition of K15 is indicative of the ability of these compounds to perturb the electron transport from water to $NADP^+$. On the other hand, the preservation of $NADP^+$ photoreduction by photosystem I from reduced DCPIP in the presence of K15 (see Table 1) shows that this compound acts at the level of PSII.

This suggestion is also supported by the K15-stimulated inhibition of photoinduced ΔF of PSII in chloroplasts (Figure 2) and in subchloroplast preparations of PSII (Figure 4).

Furthermore, both the inhibition of electron transport measured from the oxygen evolution and the repression of ΔF in PSII are apparently based on the common inhibition process which is supported by the similar dependence of these effects on concentration of K15 (Figure 3, curves 1, 2).

On the other hand, in the case of dinoseb the inhibition of electron transport (estimated from the measurements of O_2-evolution) occurs earlier than the repression of ΔF (curves 3, 4). Therefore, the authors of an earlier study (Klimov et al., 1989) concluded that the inhibition of photochemical activity of PSII manifested in the repression of ΔF makes a substantial contribution to the total inhibitory effect only at relatively high levels of dinoseb.

It should be noted that the efficiency of the inhibitory effect of K15 on the activity of PSII is ~80-100 times higher than of dinoseb (Figure 3). The total inhibition occurs upon binding of approximately one inhibitor molecule (K15) per one RC of PSII. Of high interest are the results of comparison of the inhibitory effects exerted on ΔF of PSII by compounds K15, diuron and dinoseb (Figure 4). In contrast to diuron and low levels of dinoseb (Klimov et al., 1989), compound K15 does not increase

the level of F (curves 3-5) which indicates to the absence of blockade of the electron transfer on the acceptor side of PSII. This assumption is also confirmed by the data indicating that, in contrast to diuron (curve 2), K15 does not slow down the dark decrease of ΔF which is known to reflect reoxidation of Q_A^-. This is also supported by the fact that compound K15 (in contrast to diuron and dinoseb) does not disturb, via the electron transport chain, the interaction between PSII and PSI estimated from the characteristic decrease of PSII fluorescence as a result of Q_A oxidation during additional excitation of PSI in chloroplasts (data not shown).

The effect of K15 does not appear to be related to the blockade of the electron transfer on the donor side of PSII, which is supported by the inhibition (and not the increase or at least preservation expected for such a case) of ΔA related to photooxidation of P_{680}. Moreover, after the inhibition of ΔF of PSII by K15 it is not reactivated upon subsequent addition of Mn^{2+} or other electron donors.

On the other hand, the inhibition of ΔF and the decrease of the total F level (as it is the case during the increase of electron transfer from PSII as a result of addition of DCPIP or ferricyanide oxidizing Q_A^- (Izava, 1980)) do not appear to be explainable by the acception of electrons from Q_A^-. This is confirmed by: (1) the absence of the effects of increased rate of dark relaxation ΔF related to photoreduction of Q_A; (2) the absence of positive ΔF, reflecting photoreduction of Q_A, upon addition of K15 under anaerobic conditions, which leads to a decreased F level.

A dramatic increase of the rate of dark relaxation of spectral effects associated with the photoreduction of Pheo as a result of reaction $[P_{680}Pheo]Q_A^- \rightarrow [P_{680}Pheo^-]Q_A^-$ and as a consequence of that - the decrease of these effects (Figure 6) - indicates that in the presence of K15 the life-time of the Pheo⁻ decreases due to its reoxidation.

Then the decreased values of ΔF under aerobic conditions and lower levels of F under anaerobic conditions may be interpreted as a result of a more rapid decay of $[P_{680}^+Pheo^-]$ pair induced by compounds K15 due to Pheo⁻ oxidation (which is also confirmed by the K15-induced quenching of the long-lived components of PSII chlorophyll fluorescence (Allakhverdiev et al., 1989)).

It may be suggested that the effect of K15 on the redox state of Pheo is not determined by its direct involvement into oxidation of Pheo⁻ but this is, e.g., the result of increased O_2 access to Pheo⁻. However, the preservation of characteristic efficiency of the inhibitory effect of K15 under anaerobic conditions (Figure 6) is an argument against such an assumption.

At the same time the inhibitory effect of K15 cannot be explained solely by the oxidation of Pheo⁻ with this compound. Then one should observe a decrease of the inhibitory effect of K15 upon prolonged illumination due to accumulation of reduced molecules of the inhibitor which is not the case.

On the other hand, the increase in the rate of Pheo photoreduction upon addition of K15 in Mn-depleted preparations in the presence of dithionite (Figure 7) is a direct indication of the ability of the reduced (by dithionite) K15 form to donate electron(s) to PSII reaction center. The ability of K15 to donate electrons to PSII is supported by the inhibition of ΔA related to photooxidation of P_{680} upon addition of this inhibitor (Figure 8). Furthermore, compound K15 represses both the photoinduced and dark EPR signals II associated with the photooxidation of secondary electron donor Z (data not shown).

The similar concentration dependences of the inhibitory effect of these compounds for all photoreactions considered above are indicative of a common nature of the inhibition (Figure 9).

Thus, electron transfer from Pheo⁻ to K15 seems to take place with subsequent donation of the electron to Z^+ (or P_{680}^+) which leads to the repression of the basal electron flow through PSII. In other words, compound K15 closes the chain of electron transfer in PSII by accepting an electron from Pheo⁻ and donating it to Z^+ (or directly to P_{680}^+).

We showed earlier (Allakhverdiev et al., 1989; Klimov et al., 1989) that dinoseb is also capable of redox interaction with PSII reaction center components leading to a more rapid oxidation of Pheo⁻ and reduction of P_{680}^+ and, as a result, to a faster decay of $[P_{680}^+Pheo^-]$ pair. However, the cyclic electron transfer from Pheo⁻ to P_{680}^+ with the involvement of dinoseb may compete with the functional reactions of Pheo⁻ oxidation and P_{680}^+ reduction and make a substantial contribution to the total effect of inhibition of electron transfer in PSII by dinoseb only at relatively high concentrations of this inhibitor. Moreover, in the case of the hydroxyperfluoroisopropyldinitrobenzole derivatives studied the redox interaction with PSII RC components, leading to the cyclic electron transfer seems to underlie their inhibitory action.

It is not ruled out that a K15 molecule reaching into RC of PSII performs the role similar to that of Q_A or even it replaces Q_A. This suggestion is supported by the following data: (1) the ability of these compounds to interact with the primary electron acceptor Pheo⁻; (2) high affinity of these compounds to RC of PSII - one inhibitor molecule per RC is sufficient for producing the effect; (3) high constant of inhibitor binding to PSII (which is expressed in its retention by RC even despite the multiple attempts to wash the inhibitor out); (4) the ab-

sence of a decrease of the inhibitory effect upon a prolonged illumination (despite the redox nature of its interaction with RC components); (5) the ability of these compounds to inhibit the electron transport in isolated RC of PSII (D1/D2/Cytb559 complexes) free of Q_A (Nanba and Satoh, 1979). Apparently, the redox potential of K15 is around -450 mV which is supported by the data indicating that dithionite (but not sodium ascorbate) eliminates its inhibitory effect on PSII. Consequently, after oxidation of Pheo⁻, K15 (in contrast to Q_A having a potential of about -130 mV) is unable to keep electron for a sufficiently long time, and the electron goes back to P_{680}^+ or Z^+ which leads to a disturbance of the basal electron transfer in PSII.

Thus, we revealed new highly efficient inhibitors of electron transfer in plant photosystem II - derivatives of hydroxyperfluoroisopropyldinitrobenzole - K15 whose action appears to be based on their redox interaction with the RC components of PSII and activation of a cyclic electron transfer. The inhibition constant for K15 is 45 nM.

ACKNOWLEDGEMENT

REFERENCES

Allakhverdiev S.I., Shafiev M.A., Klimov V.V. (1985) Effect of extraction and the subsequent addition of manganese ions on photooxidation of chlorophyll P_{680} in photosystem II preparations. Biofizika **31:** 223-226 (in Russian).

Allakhverdiev S.I., Zharmukhamedov S.K., Klimov V.V., Vasiliev S.S., Korvatovsky B.N., Pashchenko V.Z. (1989) The effect of dinoseb and other phenolic-type compaunds on the decay kinetics of chlorophyll fluorescence in photosystem II of higher plants. Biologicheskie Membrany **6:** 1147-1153 (in Russian).

Fedtke K. (1985) Biochemistry and physiology of herbicide action. (Baskakov Yu.A., ed.), Agropromizdat, Moscow: 14-15 (in Russian).

Izawa S. (1980) Acceptors and donors and chloroplast electron transport. Meth. Enzymol. **69:** 413-434.

Klimov V.V., Allakhverdiev S.I., Demeter S., Krasnovsky A.A. (1979) Photoreduction of pheophytin in the photosystem II of chloroplasts depending on the oxidation-reduction potential of the medium. Dokl. AN SSSR **249:** 227-230 (in Russian).

Klimov V.V., Allakhverdiev S.I., Ladygin V.G. (1986) Photoreduction of pheophytin in photosystem II of the whole cells of green algae and cyanobacteria. Photosynth. Res. **10:** 355-361.

Klimov V.V., Allakhverdiev S.I., Shuvalov V.A., Krasnovsky A.A. (1982) Effect of re-extraction of manganese on light reactions of photosystem II preparations. Dokl. AN SSSR **263:** 1001-1005 (in Russian).

Klimov V.V., Allakhverdiev S.I., Zharmukhamedov S.K. (1989) The oxidation-reduction interaction of phenolic herbicide, dinoseb, with pair [$P^{+\bullet}680$ Ff$^\bullet$] in reaction center of photosystem II in plants. Fiziologiya Rasteniy **36:** 770-777 (in Russian).

Klimov V.V., Shuvalov V.A., Heber U. (1985) Photoreduction of pheophytin as a result of electron donation from the water-splitting system to photosystem II reaction centers. Biochim. Biophys. Acta **809:** 345-350.

Konstantinova N.V., Kolobanova L.P., Trofimova G.I., Lifshits B.R., Baskakov Yu.A. (1980) Chemical means for plant protection. (Promenkov V.K., ed.), VNIIKhSZR i NIITEKhIM, Moscow: 4-9 (in Russian).

Nanba O., Satoh R. (1979) Isolation of a photosystem II reaction center consisting of D-1 and D-2 polypeptides and cytochrome b-559. Proc. Natl. Acad. Sci. USA **84:** 109-112.

Tischer W., Strotmann H. (1977) Relationship between inhibitor binding by chloroplasts and inhibition of photosynthetic electron transport. Biochim. Biophys. Acta **460:** 113-125.

Trebst A., Draber W. (1979) In: Advances in Pesticide Science. (Geissbihler H., ed.), part 2, Pergamon Press, Oxford: 223-234.

van Rensen J.J.S., Wong D., Govindjee (1978) Characterization of the inhibition of photosynthetic electron transport in pea chloroplasts by the herbicide 4,6-dinitro-o-cresol by comparative studies with 3-(3-4-dichlorophenyl)-1,1-dimethylurea. Z. für Naturforschg. **33:** 413-420.

Quantitative Analysis of Cyclic Electron Flow in Rice Plants (*Oryza sativa* L.) Lacking PsbS Protein of Photosystem II

Ismail S. Zulfugarov[1,2]*, Sujata R. Mishra[1], Choon-Hwan Lee[1]

[1]*Department of Molecular Biology, Pusan National University, Jangjeondong, Keumjungku, Busan 609-735, Republic of Korea*
[2]*Institute of Botany, Azerbaijan National Academy of Sciences, 40 Badamdar Shosse, Baku AZ 1073, Azerbaijan*

In the natural environment, when plants receive excess light energy than that can be utilized in driving photosynthesis, devise different short and long-term mechanisms for photoprotection from harmful effects of high light stress. Non-photochemical quenching (NPQ) of the chlorophyll fluorescence is one of the short-term responses to high light stress that operates in the plants to protect them *in vivo*. But, under the conditions in which plants are deficient of NPQ, what is the alternative mechanism that takes the role as photoprotective means is a study of interest. Besides NPQ, other alternative pathways of photoprotection are there and one among them is the cyclic electron transport around PSI. In the present study, we evaluate the role of cyclic electron transport by quantifying its contribution to the overall process of electron transport and photoprotection using rice plants which lack energy-dependent part of NPQ (qE). It was found that efficiency of the cyclic electron flow around PSI was higher in rice T-DNA inserted plants (OsPsbS-KO), while there was no difference in the linear electron flow. In the absence of qE, cyclic electron flow around PSI can be as alternative pathway for protection from excess energy absorbed by C_3-plants. The relationship between cyclic electron flow around PSI and NPQ is discussed. Since there is the availability of mutant plants lacking of NPQ or cyclic electron transport which are sensitive to photoinhibitory illumination, these plants provide a tool for investigating into the role of different pathways.

Keywords: photosystem I, cyclic electron flow, non-photochemical quenching, PsbS protein, photosynthesis

INTRODUCTION

Sunlight is the main energy source on Earth which is energy used by photosynthesis to convert light energy to chemical energy. In nature, sometimes light intensity exceeds the capacity of the linear electron transport of the chloroplasts of higher plants. Therefore, plants have developed adaptive mechanisms to control the efficiency of utilization of the energy and photosynthetic electron transport (Chow, 1994; Osmond, 1994). These photoprotective mechanisms are classified as either long-term or short-term responses. The long-term responses include avoidance mechanisms that involve changes in the orientation of leaves (Björkman and Demmig-Adams, 1994) or chloroplasts (Park et al., 1996) and modulation of the composition of the photosynthetic apparatus by light acclimation (Anderson and Osmond, 1987). The most prominent short-term response is non-photochemical quenching (NPQ), which plays an important role in the photoprotection of photosystem (PS) II *in vivo*. NPQ is subdivided into three components according to their relaxation kinetics in darkness

following a period of illumination, as well as their responses to various inhibitors. The slowest component of NPQ is qI, which is related to photoinhibition or the slowly reversible damage to PSII reaction centers (Osmond et al., 1997). The second component of NPQ is qT, which reflects the phosphorylation-mediated migration of light-harvesting complex (LHC) II between PSII and PSI (state transition) (Harrison and Allen, 1993). The fastest and the most important component of NPQ is qE, the energy-dependent quenching. This component depends on three major parameters: the development of transthylakoid proton gradient (ΔpH), the amount of pigments involved in xanthophyll cycle, and the existence of a PsbS subunit in PSII (Müller et al., 2001). qE is characterized by: (1) its sensitivity to uncouplers of the proton gradient (Oxborough and Horton, 1988) and, inhibition by N,N'-dicyclohexylcarbodiimide, an inhibitor of protonation of protein residues (Walters et al., 1994), (2) the light-induced absorbance changes at 535 nm (Ruban et al., 1993), (3) the shortening of the lifetime of a specific chlorophyll (Chl) fluorescence component from ~2.0 to ~0.4 ns (Gilmore et al., 1995)

and (4) carotenoid cation radical formation (Holt et al., 2005).

Since the NPQ may reduce the efficiency of photosynthesis under low-light conditions regulated by monitoring of the transthylakoid proton gradient (ΔpH). In such kind of circumstances, alternative electron transport pathways, such as the cyclic electron transport within PSII, the cyclic electron flow around PSI and the water-water cycle, may regulate the generation of NPQ. The cyclic electron flow around PSI and water-water cycle regulates the NPQ by modifying the rate of ΔpH generation through ATP balance (Heber and Walker, 1992; Asada, 1999). The ATP pool is one of the main parameters that control the NPQ and the rate of electron flow through the Benson-Calvin cycle. Although cyclic electron flow around PSI was discovered several decades ago (Arnon et al., 1954), its role, especially in C_3-plants was controversial. After the discovery set of the *Arabidopsis thaliana* mutants, *pgr* and *crr* (Munekage and Shikanai, 2005), the role of cyclic electron flow around PSI, as well as the different routes for cyclic electron flow with participation of the cyt b_6f complex, plastoquinone, plastocyanin, and NDH complex, have been highlightened. The plants lacking either energy-dependent quenching of chlorophyll fluorescence (*npq4-1* (Li et al., 2000); *npq1-2* (Niyogi et al., 1998) of *Arabidopsis*; PsbS-KO rice plants (Koo et al., 2004)) or defective in cyclic electron flow around PSI (*pgr1* (Munekage et al., 2001); *pgr5* (Munekage et al., 2002) and *crr2-4* (Munekage et al., 2004)) are sensitive to high light stress.

Therefore, in the present study, we investigated the efficiency of the cyclic electron flow around PSI in both wild-type (WT) and qE-less (OsPsbS-KO) mutant rice plants. We found that efficiency of the cyclic electron flow around PSI is higher in OsPsbS-KO plants, while there is no difference in the linear electron flow.

MATERIALS AND METHODS

One-month-old seedlings of WT and OsPsbS-knockout mutant rice (*Oryza sativa* L.) plants (Munekage et al., 2004) were grown in soil in a greenhouse under sunlight at a temperature of 28±2°C. The oxidation and re-reduction of P_{700} in rice leaves were determined with a dual wavelength (820/870 nm) unit (ED-p700DW) attached to a phase amplitude modulation fluorometer, PAM101/102 (Walz, Effeltrich, Germany). To obtain the steady-state signal was reached by applying far-red light (12 μmol photons $m^{-2}s^{-1}$, peak wavelength 715 nm). The maximum signal amplitude at end of actinic light excitation (white or green light) was taken as the total amount of photo-oxidizable P_{700}.

To measure the re-reduction kinetics and to calculate half-lifetime of the oxidized P_{700} data obtained after switch of the actinic light. Data transformed by Data Acquisition System NI-DAQ Model USB-6009 (National Instruments, Australia) by rate 100 Hz.

Infiltration of the chemicals into rice leaf segments was done as described (Kim et al., 2002).

RESULTS AND DISCUSSION

It has been evidenced that cyclic electron flow has an important role on the protection against photoinhibitory illumination (Munekage et al., 2004). In *pgr5* mutant of *Arabidopsis thaliana* plants defective in cyclic electron flow around PSI non-photochemical quenching (NPQ) of chlorophyll fluorescence also decreased (Munekage et al., 2002). Because the both processes participate in photoprotection mechanism, hence to know the relation between NPQ and cyclic electron flow around PSI we measured cyclic electron flow in WT and PsbS-KO rice plants.

We used detached rice leaves infiltrated with different chemicals to switch between cyclic and linear electron transport pathways. Control detached dark-adapted WT and PsbS-KO rice leaves were infiltrated with 150 mM sorbitol to prevent chloroplasts from osmotic shock (Joliot and Joliot, 2005). Far-red illumination during 10 s which leads to P_{700} oxidation was much slower (Figure 1) in the leaves of both WT and PsbS-KO rice plants showing that cyclic electron flow around PSI operate very slowly. In other experiment we infiltrated detached dark-adapted WT and PsbS-KO rice leaves with 150 mM sorbitol plus 1 mM methyl vilologen (MV) to switch linear electron transport pathway only, because MV accept electrons from all PSI. Far-red illumination leads to P_{700} oxidation occurs less than 4 s due to direct electron transfer from P_{700}^+ to MV. In regards to the linear electron transport pathway we did not observed any differences between WT and PsbS-KO rice plants confirming our previous observation on whole chain electron transport rate (Zulfugarov et al., 2007). The remarkable difference were observed when the electron transport pathway switched to cyclic mode by infiltration with 150 mM sorbitol plus 40 μM 3-(3,4-dichlorophenyl)-1,1-dimethylurea (DCMU) plus 2 mM hydroxylamine of dark-adapted WT and PsbS-KO rice leaf segments.

Although kinetics of P_{700} oxidation were slower with compared MV infiltrated leaf segments in both WT and PsbS-KO plants (Figure 1), in PsbS-KO plants it was much more slower and even did not completed after 20 s (data not shown). Accord-

ing to Joliot and Joliot (2005) the slow oxidation of P_{700}, in such kind of conditions where no artificial electron donor, is due to an efficient recycling of electrons to P_{700} via the cyclic electron flow around PSI. It has also been proposed that leakage of electrons is from cyclic electron flow to oxygen (Mehler reaction) or to the Benson-Calvin cycle (Joliot and Joliot, 2002, 2006).

Illumination of dark-adapted leaves of WT and PsbS-KO plants with 30 s far-red light leads to oxidation of P_{700} (Figure 1), while termination of illu-

mination resulted in re-reduction of oxidized P_{700}. Re-reduction rate of oxidized P_{700} allow us to estimate cyclic electron flow around PSI in C_3 plants, too (Fan et al., 2007). Figure 2 shows the results of the re-reduction of oxidized P_{700} in WT and PsbS-KO plants under same conditions as in Figure 1. In control leaves infiltrated with 150 mM sorbitol after turn off far-red illumination oxidized P_{700} rapidly reduced. Re-reduction rate of oxidized P_{700} in MV and DCMU infiltrated leaves of WT and PsbS-KO rice plants was relatively slow (Figure 2).
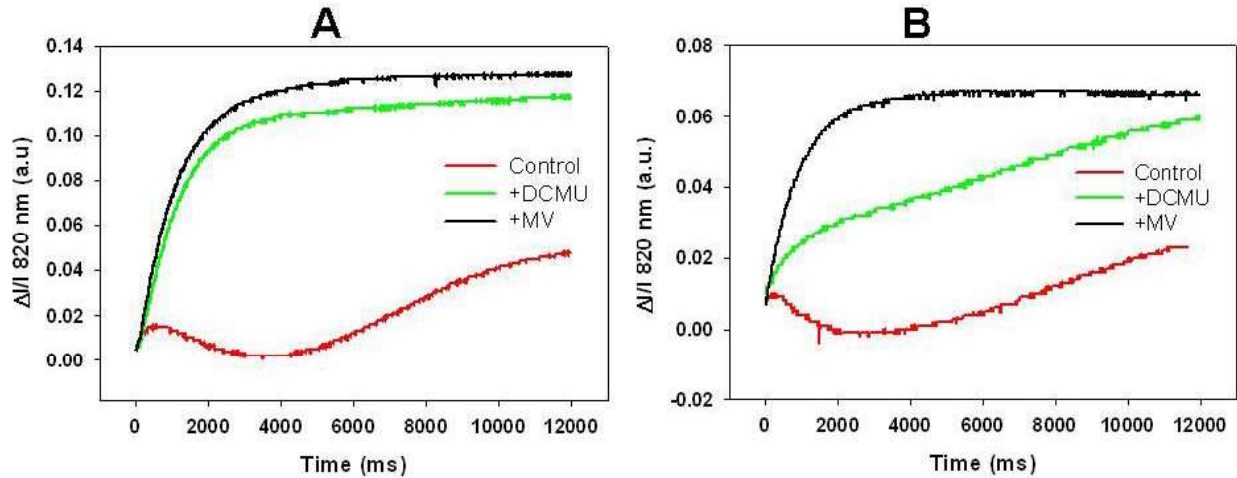
Figure 1. Absorption changes due to oxidation of P_{700} measured at 820 nm induced by far-red illumination of dark-adapted leaves of rice WT (A) and PsbS-KO (B) plants. Red – control leaves were infiltrated with 150 mM sorbitol only; Green – Leaves were infiltrated with 150 mM sorbitol plus 40 μm DCMU plus 2 mM hydroxylamine; Black – Leaves were infiltrated with 150 mM sorbitol plus 1 mm MV. The experiments were repeated at least for three times and the representative curves shown.
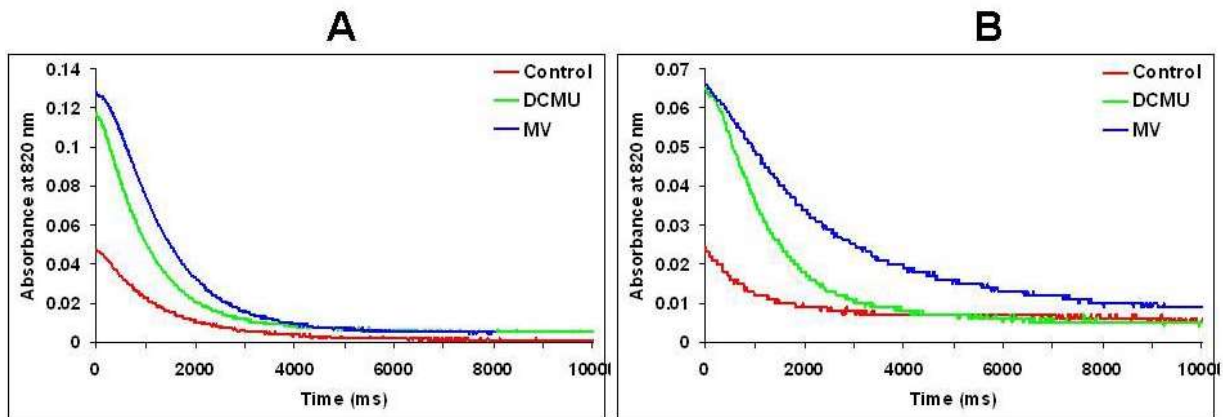
Figure 2. The re-reduction kinetics of oxidized P_{700} measured as absorption changes at 820 nm after termination of far-red illumination of dark-adapted leaves of rice WT (A) and PsbS-KO (B) plants. Red – control leaves were infiltrated with 150 mM sorbitol only; Green – Leaves were infiltrated with 150 mM sorbitol plus 40 μm DCMU plus 2 mM hydroxylamine; Black – Leaves were infiltrated with 150 mM sorbitol plus 1 mm MV. The experiments were repeated at least for three times and the representative curves are shown.

We determined the contribution of cyclic electron flow around PSI in WT and PsbS-KO plants in dark-adapted condition where Benson-Calvin cycle

is fully deactivated and by applying the green light to activate Benson-Calvin cycle. The kinetics of P_{700} oxidation determined by switching off the

green light for a 10 s and applying a far-red light excitation at indicated time (Figure 3). The curve in black shows the kinetics of P_{700} oxidation after 20 min green light illumination to fully activate the Benson-Calvin cycle which dark-adapted for 2 min before measuring the P_{700} oxidation kinetics. It can be seen that with activation of Benson-Calvin cycle (green light illumination) the amount of the oxidized P_{700} increases in both WT and PsbS-KO rice plants. But there are differences between WT and PsbS-KO rice plants. So, we have calculated the efficiency of the cyclic electron flow around PSI in WT and PsbS-KO rice plants during activation of Benson-Calvin cycle. To calculate the efficiency of the cyclic electron flow around PSI the re-reduction kinetics of oxidized P_{700} after turn off the 10 s far-red light for each time point were analyzed. The half-life time of reduction of the oxidized P_{700} were plotted against the illumination time. Figure 4 displays the relative amount of the cyclic electron flow in WT and PsbS-KO rice plants.

It is interesting that during the firsts minutes of illumination when occurs a partial oxidation of P_{700} (Harbinson and Hedley, 1993; Joliot and Joliot, 2006) there was no difference between WT and

PsbS-KO rice plants in the efficiency of the cyclic electron flow around PSI. Although, later when Benson-Calvin cycle activated more and the oxidized P_{700} decreased the efficiency of the cyclic electron flow around PSI differed remarkably. Thus, our data in agreement with findings (Golding and Johnson, 2003) that the inactivation of Benson-Calvin cycle by dark-adaptation which plants lacks CO_2 is associated with an increase rather than a decrease in oxidized P_{700} concentration. As suggested in (Joliot and Joliot, 2005) the dark-adapted leaf of C_3-plants includes 30% of the cyclic electron flow around PSI and 70% of the linear electron flow. The data in Figure 4 fitted to these values for WT rice plants, but in the case of PsbS-KO rice plants shows different values; 40% of the cyclic electron flow around PSI and 60% of the linear electron flow.

Of course we can not rule out the other possibilities, because a part of the slow oxidation of P_{700} is associated with the oxidation of the ferredoxin or by oxygen via Mehler reaction (Johnson, 2005; Joliot and Joliot, 2006). It has been suggested that the concentration of ATP has a crucial role on the formation of the cyclic electron flow around PSI (Crowther et
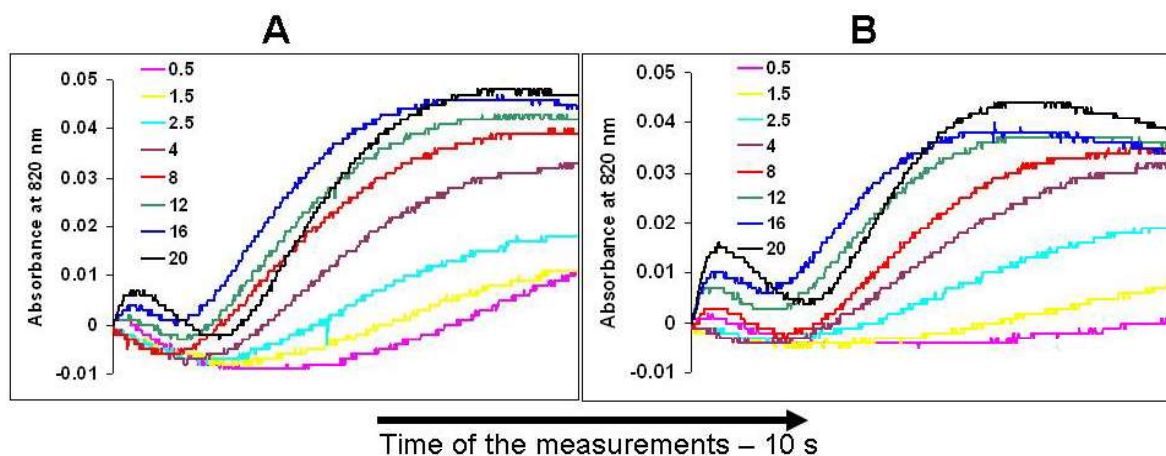
Figure 3. The oxidation of P_{700} measured as absorption changes at 820 nm induced by far-red illumination measured at different times of green-light illumination. Digits in the figure green light illumination time in minutes. The experiments were repeated at least for three times and the representative curves shown.
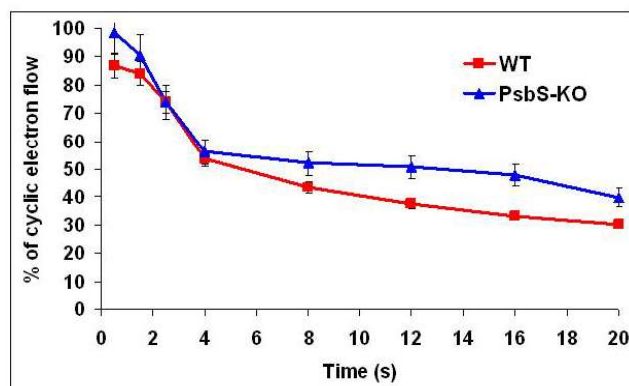
Figure 4. Efficiency of the cyclic flow around PSI determined as a function of the time of green light illumination. Same experimental condition as in Figure 3.

al., 1979). It has also been proved that proton motive force (Avenson et al., 2005) play a vital role on the generation of the energy-dependent (qE) quenching of chlorophyll fluorescence and ATP synthesis. Taken together these data indicate that these two processes, cyclic electron flow around PSI and energy-dependent quenching of chlorophyll fluorescence have very close relations. Role of the different routes of cyclic electron flow around PSI and quantitative analysis of cyclic electron flow around PSI under conditions were no limitation of the Benson-Calvin cycle under investigation. Thus, the increased efficiency of the cyclic electron flow around PSI may function as alternative protection mechanism against photoinhibitory illumination when the NPQ is much less. It has been shown that in *pgr5* mutant of *Arabidopsis thaliana* plants which defective in the cyclic electron flow around PSI NPQ level also become less and these plants do not grow well under high light (Munekage and Shikanai, 2005). Despite a large number of the observations reported so far, but there is no clear explanation for the role of the energy-dependent quenching in photoinhibition (Zulfugarov et al., 2005) and its relations with cyclic electron flow around PSI (Munekage and Shikanai, 2005). Also, the relationship between different routes of cyclic electron flow around PSI is unclear at present (Endo et al., 2008). Development of a method for quantification of each routes of cyclic electron flow around PSI separately and its relation to linear electron transport and NPQ is necessary for understanding the relationship between these processes. Although it is widely accepted that PSII is the primary site of photoinhibition (Aro et al., 1993), photoinhibition of PSI also occurs even under low light intensities when it combined with chilling (Sonoike, 1996; Kim et al., 2005). The exact process of photoinhibition of PSI in the absence of cyclic electron flow around PSI remains unclear. The energetic imbalance of overall photosynthesis due to lack of cyclic electron flow around PSI, most probably, causes over-reduction of the stroma, which directly triggers PSI photoinhibition. It might be the reason why in the plants lacking energy-dependent-quenching cyclic electron flow around PSI is activated.

ACKNOWLEDGMENTS

REFERENCES

Anderson J.M., Osmond C.B. (1987) Shade-sun responses: compromises between acclimation and photoinhibition. In: Photoinhibition. (Kyle D.M., Osmond C.B., Arntzen C.J., eds.), Elsevier, Amsterdam: 15-44.

Arnon D.I., Allen M.B., Whatley F.R. (1954) Photosynthesis by isolated chloroplasts. Nature **174:** 394-396.

Aro E.-M., Virgin I., Andersson B. (1993) Photoinhibition of Photosystem II. Inactivation, protein damage and turnover. Biochim. Biophys. Acta **1143:** 113-134.

Asada K. (1999) The water-water cycle in chloroplasts: Scavenging of active oxygens and dissipation of excess photons. Annu. Rev. Plant Physiol. Plant Mol. Biol. **50:** 601-639.

Avenson T.J., Cruz J.A., Kanazawa A., Kramer D.M. (2005) Regulating the proton budget of higher plant photosynthesis. Proc. Natl. Acad. Sci. USA **102:** 9709-9713.

Björkman O., Demmig-Adams B. (1994) Regulation of photosynthetic light capture, conversion, and dissipation in higher plants. In: Ecophysiology of Photosynthesis (Schulze E.-D., Caldwell M.M., eds.), Springer-Verlag, Berlin: 17-24.

Chow W.C. (1994) Photoprotection and photoinhibitory damage. Adv. Mol. Cell Biol. **10:** 151-196.

Crowther D., Mills J.D., Hind G. (1979) Proton-motive cyclic electron flow around photosystem I in intact chloroplasts. FEBS Lett. **98:** 386–390.

Endo T., Ishida S., Ishikawa N., Sato F. (2008) Chloroplastic NAD(P)H dehydrogenase complex and cyclic electron transport around photosystem I. Mol. Cells **25:** 158-162.

Fan D.-Y., Nie Q., Hope A.B., Hillier W., Pogson B.J., Chow W.S. (2007) Quantification of cyclic electron flow around photosystem I in spinach leaves during photosynthetic induction. Photosynth. Res. **94:** 347-357.

Gilmore A.M., Hazlett T.L., Govindjee (1995) Xanthophyll cycle-dependent quenching of photosystem II chlorophyll fluorescence: Formation of a quenching complex with a short fluorescence lifetime. Proc. Natl. Acad. Sci. USA **92:** 2273-2277.

Golding A.J., Johnson G.N. (2003) Down-regulation of linear and activation of cyclic electron transport during drought. Planta **218:** 107-114.

Harbinson J., Hedley C.L. (1993) Changes in P_{700} oxidation during the early stages of the induction of photosynthesis. Plant Physiol. **103:** 649-660.

Harrison M.A., Allen J.F. (1993) Differential phosphorylation of individual LHCII polypeptides during short-term and long-term acclimation to light regime in the green alga *Dunaliella salina*. Biochim. Biophys. Acta **1141:** 37-44.

Heber U., Walker D. (1992) Concerning a dual function of coupled cyclic electron transport in

leaves. Plant Physiol. **100:** 1621-1626.

Holt N.E., Zigmantas D., Valkunas L., Li X.-P., Niyogi K.K., Fleming G.R. (2005) Carotenoid cation formation and the regulation of photosynthetic light harvesting. Science **307:** 433-436.

Johnson G.N. (2005) Cyclic electron transport in C_3-plants: fact or artefact? J. Exp. Bot. **56:** 407–416.

Joliot P., Joliot A. (2006) Cyclic electron flow in C_3-plants. Biochim. Biophys. Acta **1757:** 362-368.

Joliot P., Joliot A. (2002) Cyclic electron transfer in plant leaf. Proc. Natl. Acad. Sci. USA **99:** 10209-10214.

Joliot P., Joliot A. (2005) Quantification of cyclic and linear flows in plants. Proc. Natl. Acad. Sci. USA **102:** 4913-4918.

Kim J.-H., Jung J.-E., Lee C.-H. (2002) *In vivo* monitoring of the incorporation of chemicals into cucumber and rice leaves by chlorophyll fluorescence imaging. J. Plant Biotech. **4:** 171-178.

Kim J.-H., Kim S.-J., Cho S.H., Chow W.S., Lee C.-H. (2005) Photosystem I acceptor side limitation is a prerequisite for the reversible decrease in the maximum extent of P_{700} oxidation after short-term chilling in the light in four plant species with different chilling sensitivities. Physiol. Plant. **123:** 100-107.

Koo H.Y., Zulfugarov I.S., Oh M.-H., Moon Y.-H., Jansson S., An G., Lee C.-H. (2004) The function of the PsbS protein in relation to non-photochemical energy dependent quenching in rice plants. In: Photosynthesis: Fundamental Aspects to Global Perspectives. (van der Est A., Bruce D., eds.), Montreal: 527-530.

Li X.-P., Bjürkman O., Shih C., Grossman A.R., Rosenquist M., Jansson S., Niyogi K.K. (2000) A pigment-binding protein essential for regulation of photosynthetic light harvesting. Nature **403:** 391-395.

Mğller P., Li X.-P., Niyogi K.K. (2001) Non-photochemical quenching. A response to excess light energy. Plant Physiol. **125:** 1558-1566.

Munekage Y., Hashimoto M., Miyake C., Tomizawa K., Endo T., Tasaka M., Shikanai T. (2004) Cyclic electron flow around photosystem I is essential for photosynthesis. Nature **429:** 579-582.

Munekage Y., Hojo M., Meurer J., Endo T., Tasaka M., Shikanai T. (2002) PGR5 is involved in cyclic electron flow around photosystem I and is essential for photoprotection in *Arabidopsis.* Cell **110:** 361-371.

Munekage Y., Shikanai T. (2005) Cyclic electron transport through photosystem I. Plant Biotech.

22: 361-369.

Munekage Y., Takeda S., Endo T., Jahns P., Hashimoto T., Shikanai T. (2001) Cytochrome b_6f mutation specifically affects thermal dissipation of absorbed light energy in *Arabidopsis.* Plant J. **28:** 351-359.

Niyogi K.K., Grossman A.R., Bjürkman O. (1998) *Arabidopsis* mutants define a central role for the xanthophyll cycle in the regulation of photosynthetic energy conversion. Plant Cell **10:** 1121–1134.

Osmond B., Badger M., Maxwell K., Bjürkman O., Leegood R. (1997) Too many photons: photorespiration, photoinhibition and photooxidation. Trends Plant Sci. **2:** 119-121.

Osmond C.B. (1994) What is photoinhibition? Some insights from comparisons of shade and sun plants. In: Photoinhibition of Photosynthesis: from Molecular Mechanisms to the Field. (Baker N.R., Rowyer J.R., eds.), Bios Scientific, Oxford: 1-24.

Oxborough K., Horton P. (1988) A study of the regulation and function of energy-dependent quenching in pea chloroplasts. Biochim. Biophys. Acta **934:** 135-143.

Park Y.-L., Chow W.S., Anderson J.M. (1996) Chloroplast movement in the shade plant *Tradescantia albiflora* helps protect photosystem II against light stress. Plant Physiol. **111:** 867-875.

Ruban A.V., Young A.J., Horton P. (1993) Induction of non-photochemical energy dissipation and absorbance changes in leaves. Evidence for changes in the state of the light harvesting system of Photosystem II *in vivo.* Plant Physiol. **102:** 741-750.

Sonoike K. (1996) Photoinhibition of photosystem I: Its physiological significance in the chilling sensitivity of plants. Plant Cell Physiol. **37:** 239-247.

Walters R.G., Ruban A.V., Horton P. (1994) Higher plant light-harvesting complexes LHCIIa and LHCIIc are bound by dicyclohexylcarbodiimide during inhibition of energy dissipation. Eur. J. Biochem. **226:** 1063-1069.

Zulfugarov I.S., Ham O.-K., Mishra S.R., Kim J.-Y., Krishna Nath K., Koo H.Y., Kim H.-S., Moon Y.-H., An G., Lee C.-H. (2007) Dependence of reaction center-type energy-dependent quenching on photosystem II antenna size. Biochim. Biophys. Acta **1767:** 773-780.

Zulfugarov I.S., Mishra S.R., Ham O.-K., Safarova R.B., Nath K., Lee C.-H. (2005) Current understanding of the mechanism of qE, a major component of non-photochemical quenching in green plants. J. Photosci. **12:** 175-183.

Pigment Content and Activity of Chloroplasts of Wheat Genotypes Grown Under Saline Environment

Ibrahim V. Azizov*, Mayakhanum A. Khanisheva
Institute of Botany, Azerbaijan National Academy of Sciences, 40 Badamdar Shosse, Baku AZ 1073, Azerbaijan

The purpose of this work was the study of salt tolerance of wheat from local selection. Twenty wheat genotypes were grown under a naturally salinized (1.5-2.0%) soil conditions and studied during the ontogenesis. The obtained results showed that the chlorophyll content and photochemical activity of chloroplasts were reduced in all the genotypes by salinity. Genotypes Giymatli-2/17, Nurlu-99, Qobustan, Azamatli-95, Saratovskaya-29 and Gyrmyzy bugda are more tolerant to salinity.

Keywords: wheat genotypes, chlorophyll, photochemical activity

INTRODUCTION

Soil salinity is one of the major constraints responsible for low agriculture production in many regions of Azerbaijan. Out of total hectares irrigated land, 1.3 million hectares are salt affected (Azizov and Guliyev, 1999). The major inhibitory effect of salinity on plant growth and yield has been attributed to: a) osmotic effect; b) ion toxicity; c) nutritional imbalance leading to reduction photosynthetic efficiency and other physiological disorders.

Adverse effects of salinity on seed germination and seedling growth as well as some physiological activities of cultivated plant species have been investigated previously (Khan et al., 1995; Ashraf and Khanum, 1997). Generally, the trend and magnitude of adverse changes varied with in species and genotypes according to the level of salinity.

So far little emphasis has been placed on aspects relevant to photosynthetic efficiency of plants at moderate and high salinity. It has been suggested that by increasing photosynthetic efficiency crop production could be increased (Aliyev et al., 1998).

The aim of the present paper is to study the effect of salinity on chlorophyll content and photochemical activity of chloroplasts in wheat genotypes.

MATERIALS AND METHODS

The study was conducted during the years 2006-2007 in naturally salinized privately owned farm of Akhsu district of Azerbaijan. The experimental material comprised of twenty genotypes of wheat, which was also grown in normal soil conditions, simultaneously. Chlorophyll *a* and *b* content of leaves were determined according to Arnon (Arnon, 1949). The isolation medium for chloroplasts contained 400 mM sucroze, 1 mM EDTA, 5 mM $MgCl_2$, 10 mM NaCl and 50 mM tris-HCl buffer, pH 7.8. Photochemical activity of chloroplasts were measured by monitoring oxygen evolving activity at 25°C using Clark-type oxygen electrode in presence of 0.5 mM potassium ferrycianide as acceptor of electrons from photosystem (PS) II (Aliyev et al., 1998; Azizov and Rasulova, 2000). Uncoupled PSI driven electron transport was assayed with 5mM ascorbate using 50 mM DCPIP as electron donor in the presence of 10 mM DCMU, 200 mM MV as electron acceptor, 1 mM NaN_3 and 5 mM NH_4Cl.

RESULTS AND DISCUSSION

Leaf dry weight, leaf area and yield per plant decreased significantly in response to salinity in all wheat genotypes. The biosynthesis of green pigments (chlorophyll *a*, *b*) and carotenoids also was affected with salinity stress (Table 1).

The genotypes Gyrmyzy gul, Pirshahin, Vugar-80, Shiraslan-23 and Dagdash showed maximum percent reduction over control for chlorophyll total concentration and were graded as sensitive to salinity stress. The genotypes Giymatli-2/17, Nurlu-99, Qobustan, Saratovskaya-29, Akinchi-84, Azamatli-95 and Gyrmyzy bugda demonstrated relatively less reduction in chlorophyll content and were graded as salt tolerant.

Photochemical activity of chloroplasts was

Table 1. Effect of salinity on chlorophyll and carotenoid content in different wheat genotypes grown under normal and salinity conditions (mg/g leaf)

Genotypes	Chlorophyll *a*		Chlorophyll *b*		Chlorophyll (total)		Carotenoids	
	control	salinity	control	salinity	control	salinity	control	salinity
Akinchi-84	5.4	4.4	1.8	1.5	7.2	5,9	1.8	1.9
Garagylchyg-2	6.2	4.5	2.1	1.5	8.3	6.0	1.9	2.1
Vugar-80	5.6	4.1	1.9	1.1	7.5	5.2	1.7	1.9
Shiraslan-23	5.8	3.9	2.0	1.0	7.8	4.9	1.6	1.8
Barakatli-95	6.1	4.2	2.1	1.4	8.2	5.6	2.0	2.2
Alindja-84	5.1	3.5	1.7	1.2	6.8	4.7	1.5	1.7
Tartar	6.2	3.8	2.2	1.3	8.4	5.1	1.8	2.0
Gobustan	6.3	5.6	2.1	1.8	8.4	7.4	2.1	2.2
Nurlu-99	5.9	5.5	1.9	1.8	7.8	7.3	1.9	2.1
Giymatli-2/17	6.8	6.2	2.3	2.1	9.1	8.3	2.3	2.5
Pirshahin	4.9	2.8	1.3	0.9	6.2	3.7	1.4	1.7
Gyrmyzy gul	4.8	2.6	1.4	0.8	6.2	3.4	1.5	1.8
Azamatli-95	5.4	5.0	1.7	1.5	7.1	6.5	1.8	2.0
Ruzi-84	6.1	3.5	2.0	1.1	8.1	4.6	1.7	1.9
Tale-38	6.0	3.3	2.0	1.2	8.0	4.5	1.5	1.7
Saratovskaya-29	5.1	4.9	1.7	1.6	6.8	6.5	1.4	1.5
Dagdash	5.4	2.7	1.8	0.9	7.2	3.6	1.7	2.0
Sharg	6.3	2.9	2.1	0.9	8.4	3.8	1.8	2.1
Gyrmyzy bugda	5.4	5.0	1.7	1.6	7.1	6.6	1.9	2.1
FEFWSN-4th No 1[6]	4.6	3.5	1.8	1.1	6.4	4.6	1.2	2.0

Table 2. Effect of salinity on PSII and PSI activities of chloroplasts isolated from wheat genotypes grown under normal and saline conditions (mkmol O_2/mg chl h)

Genotypes	PSII activity		PSI activity	
	control	salinity	control	salinity
Akinchi-84	85.0±2.1	79.0±1.2	125.0±5.4	119.0±3.2
Garagylchyg-2	92.0±4.3	80.0±3.1	136.0±6.2	115.0±2.6
Vugar-80	89.0±3.2	75.0±2.2	129.0±4.5	110.0±3.4
Shiraslan-23	95.0±5.4	76.0±1.4	141.0±7.2	112.0±4.6
Barakatli-95	98.0±4.5	79.0±1.1	152.0±6.6	125.0±4.5
Alindja-84	82.0±1.3	70.0±1.5	123.0±5.7	99.0±3.2
Tartar	77.0±2.1	50.0±1.0	115.0±6.1	90.0±2.6
Gobustan	91.0±3.3	85.0±2.1	130.0±5.8	125.0±5.4
Nurlu-99	94.0±4.4	83.0±1.9	129.0±4.6	120.0±4.3
Giymatli-2/17	99.0±5.6	85.0±1.7	133.0±3.5	126.0±6.2
Pirshahin	87.0±2.7	60.0±2.1	109.0±2.9	90.0±3.4
Gyrmyzy gul	81.0±1.2	59.0±1.8	95.0±3.4	70.0±5.6
Azamatli-95	105.0± 3.9	95.0±1.5	150.0±5.5	130.0±6.4
Ruzi-84	93.0±2.2	70.0±2.2	110.0±4.2	95.0±3.2
Tale-38	87.0±1.5	60.0±0.8	95.0±4.3	70.0±2.1
Saratovskaya-29	96.0±4.1	90.0±1.6	121.0±3.5	109.0± 6.1
Dagdash	87.0±2.4	60.0±1.9	98.0±2.8	71.0±2.3
Sharg	102.0± 4.1	85.0±2.2	135.0±5.4	95.0± 3.4
Gyrmyzy bugda	105.0± 6.2	90.0±3.1	131.0±5.1	120.0±5.6
FEFWSN[th]№16	98.0±4.3	70.0±2.5	116.0± 4.4	100.0±4.2

highly stable during salt stress. Photochemical activity of PSII and PSI was unaffected by salinity in some genotypes, while severely reduces in sensitive ones (Table 2).

A decrease in leaf area and yield per plant may be attributed to early senescence and death, reduced growth rate or delayed emergence (Everad et al.,

1994). The reduction in leaf area, yield and yield components under saline conditions were also due to reduced growth as a result of decreased water uptake, toxicity of sodium and chloride in the shoot cell as well as reduced photosynthesis.

Reduction in chlorophyll content is probably due to inhibitory effect of the accumulated ions of

various salts on the biosynthesis of the different chlorophyll fractions. Salt tolerance is not a function of single organ on plant attribute, but it is the product of all the plant attributes (Khan et al., 1995; Ali et al., 2004). Therefore, a genotype exhibiting relative salt tolerance for all the plant attributes may be ideal one. Fortunately, the genotypes Giymatli-2/17, Nurlu-99, Qobustan, Akinchi-84, Saratovskaya-29 and Gyrmyzy bugda showed comparatively minimal reduction induced by salinity for the plant attributes. Salinity could affect chlorophyll content of leaves through inhibition of chlorophyll synthesis or an acceleration of its degradation. Impairment of the carboxylation capacity, which in turn inhibits electron transport, is also indicated by the measurements of chlorophyll fluorescence. A reduced quantum yield may result from a salt sensitivity of PSII (Everad et al., 1994), although some authors (Lu et al., 2002) found out PSII to be highly resistant to salinity stress. It has been suggested that high external salt concentrations could affect thylakoid membranes by disrupting lipid bilayer or lipid-protein associations and thus impair electron transport activity (Ashraf and Khanum, 1997). Effect of salinity on electron transport rate could be species-specific (Lutts et al., 1996).

Thus, the obtained results may be useful for breeding salt-tolerant plants.

REFERENCES

Ali Y., Aslam Z., Ashraf M.Y., Tahir G.R. (2004) Effect of salinity on chlorophyll concentration, leaf area, yield and yield components of rice genotypes grown under saline environment. Inter. J. Environ. Sci. Tech. **1(3):** 221-225.

Aliyev J.A., Azizov I.V., Gazibekova E.G. (1998) Photosynthetic capacity and development of chloroplasts in ontogenesis of wheat. Elm, Baku: 115 p. (in Russian).

Arnon D.J. (1949) Copper enzyme in isolated chloroplasts. 1. Poliphenoloxidaze in *Beta vulgaris.* Plant. Physiol. **24:** 1-15.

Ashraf M., Khanum A. (1997) Relationship between ion accumulation and growth in two-spring wheat line differing in salt tolerance of different grow stages. J. Agron. Crop Sci. **178:** 39-51.

Azizov G.Z., Guliyev A. (1999) The salted soils of Azerbaijan, their melioration and fertility increasing. Baku: 99 p. (in Azeri).

Azizov I.V., Rasulova S.M. (2000) Features of inheritance of the photochemical activity and productivity parental and hybrid wheat form in drought conditions. Proceedings of Azerbaijan National Academy of Sciences (biological sciences) **1-3:** 17-20 (in Russian).

Everard J.D., Gucci R., Khan S.C., Flure I.M., Wayne H.L. (1994) Gas exchange and carbon partitioning in the leaves of celery at various levels of root zone salinity. Plant Physiol. **106:** 281-292.

Khan A.H., Ashraf M., Naqvi S.M., Khavzada B., Ali M. (1995) Growth ion and solute contents of sorghum grown under NaCl and Na_2SO_4 salinity stress. Acta Physiol. Plant. **17:** 261-268.

Lu C.M., Qin N.W., Wang B.S., Kuang T.Y. (2002) Does salt stress lead to increased susceptibility of photosystem II, to photoinhibition and changes in photosynthetic pigment composition in halophyte *Suaeda salsa* grown out doors. Plant Sci. **114:** 1063-1068.

Lutts S., Kinet J.M., Bouharmont J. (1996) NaCl-induced senescence in leaves of rice cultivars differing in salinity resistance. Ann. Bot. **78:** 389-398.

Discovery of Novel Phosphoenolpyruvate Carboxylase (PEPC) Genes and Their Active Polypeptides in the Green Microalga *Chlamydomonas reinhardtii*

Tarlan G. Mamedov*, Raymond Chollet

Department of Biochemistry, University of Nebraska-Lincoln, George W. Beadle Center, Lincoln, NE 68588-0664, USA

This work describes the discovery of novel phosphoenolpyruvate carboxylase (PEPC) genes and their active catalitic polypeptides in the green microalga *Chlamydomonas reinhardtii*. Green-algal PEPC has been unexplored before in molecular terms. Our recent studies have reported the molecular cloning of the two PEPC genes, *Ppc* genes in *C.reinhardtii* (*CrPpc1*, *CrPpc2*), each of which is transcribed *in vivo* and encodes a fully active, recombinant PEPC that lacks the regulatory, N-terminal seryl-phosphorylation domain typifying the vascular-plant enzyme. These distinct catalytic subunit-types differ with respect to their (a) predicted molecular mass ($\sim$108.9 (*CrPpc1*) versus $\sim$131.2 kDa (*CrPpc2*)) and critical C-terminal tetrapeptide; and (b) immuno-reactivity with antisera against the p102 and p130 polypeptides of *S.minutum* PEPC1/PEPC2 and PEPC2, respectively. Only the *Ppc1* transcript encodes the p102 catalytic subunits common to both Class-1 and Class-2 enzyme-forms in *C.reinhardtii*. We studied the distribution of these two encoded catalytic subunits in the minor Class-1 and predominant Class-2 PEPC enzyme-forms, the latter of which is a novel high-molecular-mass, hetero-oligomeric complex containing both *CrPpc1* (p109) and *CrPpc2* (p131) polypeptides. The Class-1 enzyme, however, is a typical PEPC homotetramer comprised solely of p109. The steady-state transcript levels of both *CrPpc1/2* are coordinately up-/down-regulated by changes in [CO_2] or [NH_4^+] during growth, and generally mirror the response of cytoplasmic glutamine synthetase (*Gs1*) transcript abundance to changes in inorganic [N] at 5% CO_2. We also documented that the amount of both *CrPpc1/2* catalytic subunits is up-/down-regulated by varying levels of NH_4^+ supplied to the culture medium. To our knowledge, these collective findings provide the first molecular insight into the *Ppc* genes and corresponding PEPC catalytic subunits in any eukaryotic alga.

Keywords: PEP carboxylase, Chlamydomonas reinhardtii, green microalgae

INTRODUCTION

Phosphoenolpyruvate carboxylase (PEPC [Ppc]; E.C. 4.1.1.31) is a ubiquitous cytoplasmic enzyme in vascular plants, and is also widely distributed among archaeal, bacterial, cyanobacterial and unicellular green-algal species (Chollet et al., 1996; Sánchez and Cejudo, 2003; Izui et al., 2004). It catalyzes the irreversible β-carboxylation of phosphoenolpyruvate (PEP) in the presence of HCO_3^- and Me^{2+} to yield inorganic phosphate and oxaloacetate (OAA), and thus is involved intimately in C_4-dicarboxylic acid metabolism in these organisms. While the enzyme is clearly best known for its cardinal roles in C_4-photosynthesis and *Crassulacean* acid metabolism (CAM), green-plant PEPC has also been widely studied in a diverse array of non-photosynthetic contexts. During the past 10 to 15 years an impressive list of advances in vascular-plant and prokaryotic PEPC research has been generated (Chollet et al., 1996; Izui et al., 2004). In marked contrast to this wealth of infor-

mation on vascular-plant and prokaryotic PEPC, until recently there was little or no biochemical or molecular insight into the green-microalgal enzyme. However, starting in 1996 a series of detailed biochemical studies of the PEPC enzyme-forms purified from two unicellular green algae, *Selenastrum minutum* and *Chlamydomonas reinhardtii*, were published (Rivoal et al., 1996, 1998, 2002). These collective findings revealed that the lesser abundant Class-1 PEPCs are homotetramers of $\sim$102-kDa catalytic subunits (p102). However, in neither of these cases have the various component subunits of the Class-1 and Class-2 enzymes been identified in rigorous molecular terms. Given this complete lack of molecular insight into the various component subunits of the novel Class-1 and Class-2 PEPC enzyme-forms in the green microalgae, we first set out to identify the *Ppc* gene(s) encoding the catalytic polypeptides of these two enzyme-classes in *C.reinhardtii*. As a result of these initial efforts we have cloned and characterized *two novel* and distinct *Ppc* genes in this unicellular green alga. The

*E-mail: tmammedov@gmail.com

respective sequences of *CrPpc1* and *CrPpc2* genes were deposited in GenBank under accession numbers of <u>AY517644</u> and <u>AY517643</u>. We also presented biochemical insight into the effects of a varying supply of inorganic-N to *C.reinhardtii* cultures on the CrPpc1/2 and Class-1/-2 protein levels.

MATERIALS AND METHODS

Cells and growth conditions. *C.reinhardtii* cells (strains CC-125, CC-1883, and CC-1021/2137 were cultured at 25°C in continuous light (~100 μmol m^{-2} s^{-1}, 400–700 nm) in HS medium.

Cloning of the CrPpc1 and CrPpc2 genes. cDNAs of the *C.reinhardtii Ppc* genes, were isolated as described by Mamedov et al. (2005). Both *Ppc* cDNA ORFs were cloned into pBluescript II(-) phagemid vector (Stratagene) designated as *CrPpc1* (<u>AY517644</u>) and *CrPpc2* (<u>AY517643</u>).

Sequence-alignment, phylogenetic and gene-structure analyses. Deduced amino-acid-sequence alignments of *C.reinhardtii* Ppc1 and Ppc2, together with representative plant and prokaryotic PEPCs, were performed using VECTOR NTI 7.0 software. Likewise, a phylogenetic tree was constructed with predicted, full-length PEPC amino-acid sequences aligned using the ClustalX program (version 1.81) with manual adjustments. A distance matrix for the alignment was calculated, and an unrooted tree was constructed using the Protdist (with JTT model) and Neighbor programs of the PHYLIP package (version 3.62), respectively (Felsenstein, 1996). Bootstrap analysis was performed with 1000 replications and the tree was visualized using TreeView 32 software.

Construction and purification of recombinant, His$_6$-tagged C.reinhardtii Ppc1 (rCrQNTG) and Ppc2 (rCrRNTG) proteins. PCR, plasmid construction, bacterial transformation, recombinant PEPCs expression and purification of recombinant proteins were performed as described by Mamedov et al. (2005).

Production and affinity-purification of iso-form-specific, CrPpc1 and CrPpc2 peptide antibodies. Antisera against both *Chlamydomonas* PEPC catalytic subunits (CrPpc1 [p109], CrPpc2 [p131]), hereafter designated CrPpc1/2 N-pAbs, were generated using as described elsewhere (Mamedov et al., 2005).

Native-, SDS-PAGE, in-gel PEPC assay, and immunoblotting. Native-, SDS-PAGE, in-gel PEPC assay and immunoblotting were performed as described previously (Mamedov et al., 2005). PEPC activity in the crude supernatant fractions was assayed spectrophotometrically at pH 8.4.

RNA and DNA hybridizations. Northern and Southern blot analyses were performed as described elsewhere (Mamedov et al., 2005).

RESULTS AND DISCUSSION

Cloning and sequence analyses of two novel and distinct Ppc genes in C.reinhardtii

The corresponding *CrPpc1/2* cDNAs were isolated, sequenced and cloned, and their sequences deposited in GenBank under nucleotide accession nos. AY517644/AY517643, respectively. The nucleotide sequences of these two distinct *C.reinhardtii Ppc* transcripts share 46% identity within both the open reading frame (ORF) and the 3'-UTR. A selected alignment of the deduced, full-length amino-acid sequences of these two polypeptides, along with representative plant and prokaryotic PEPCs, is depicted in Figure 1. Of special note is that both CrPpc1 and CrPpc2 (i) lack the N-terminal seryl-phosphorylation domain that typifies the green-plant enzyme; (ii) harbor all the conserved subdomains that contribute essential residues to the active site (e.g. see boxes I–III in Figure 1); and (iii) contain the conserved, hydrophobic C-terminal domain that participates in both negative allosteric regulation and maximal catalysis by PEPC. In contrast, the deduced CrPpc1 and CrPpc2 polypeptides also differ significantly in a number of important respects: they share only a 30% overall amino-acid sequence; deduced amino-acid sequence of CrPpc1 has a green-plant-like QNTG motif at its extreme C-terminus, whereas CrPpc2 has a non-archaeal, prokaryotic-like motif (RNTG) at its carboxy-terminus; near the N-terminus only the deduced sequence of CrPpc1 agrees favorably (87% identity between Gln16–Arg30 (Figure 1)) with the 15 aminoacid-residue sequence of the 102 kDa catalytic polypeptide of *C.reinhardtii*, Class-2 PEPC determined directly by N-terminal microsequencing (Rivoal et al., 1998). This notable finding indicates that only this specific *Ppc* transcript encodes the p102 catalytic subunits common to both the Class-1 and Class-2 enzyme-forms in *C.reinhardtii*. Finally, the predicted molecular mass of the 974-residue CrPpc1 (CrQNTG) polypeptide is 108 887 Da, whereas that of CrPpc2 (CrRNTG) is 131 218 Da. Notably, the deduced molecular size of CrRNTG, encompassing 1221 amino acids, is the largest PEPC catalytic subunit reported to date (Figure 1). Phylogenetic analysis of CrPpc1/2 and a number of other PEPCs revealed a clustering into three general groups (Mamedov et al., 2005): (i) the typical vascular-plant enzymes, of which CrPpc1, with its 109 kDa *Mr* and C-terminal QNTG tetrapeptide, is a distant member; (ii) the recently
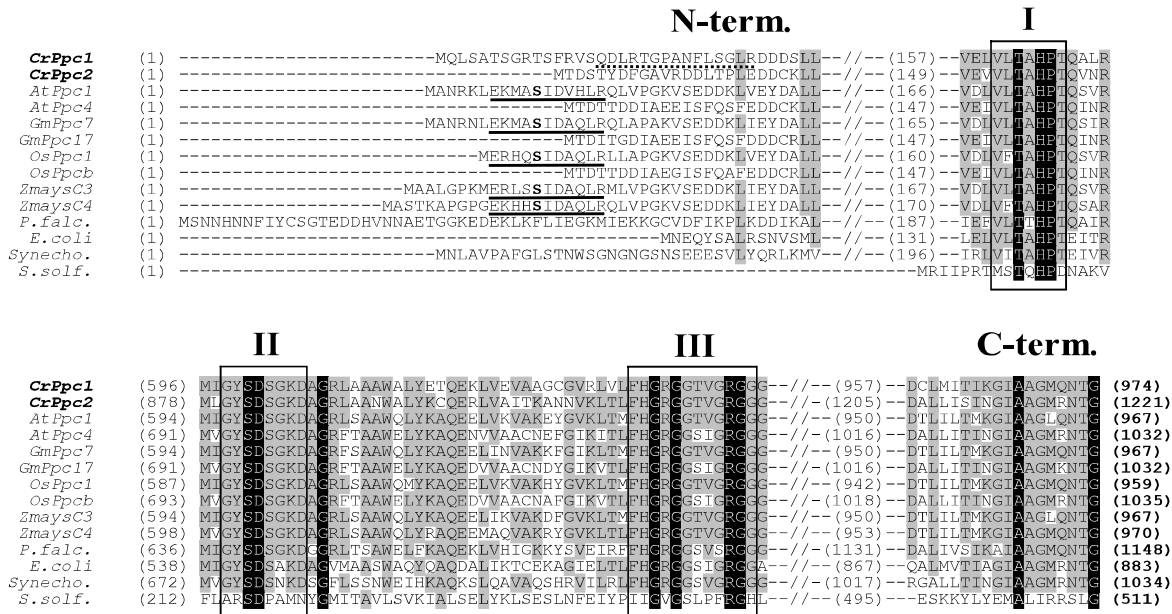
Figure 1. Selected amino-acid-sequence alignments of deduced regulatory and catalytic subdomains in PEPC from *C.reinhardtii* and representative vascular-plant and prokaryotic species. The abbreviated name of each aligned sequence is as follows: CrPpc1, *C.reinhardtii* Ppc1 (CrQNTG); CrPpc2, *C.reinhardtii* Ppc2 (CrRNTG); AtPpc1, *Arabidopsis thaliana* Ppc1; AtPpc4, *A.thaliana* Ppc4 (C-terminal RNTG ['bacterial-type']); GmPpc7, *Glycine max* Ppc7; GmPpc17, *G.max* Ppc17 (C-terminal KNTG ['bacterial-type']); OsPpc1, *Oryza sativa* Ppc1; OsPpcb, *O.sativa* Ppc-b (C-terminal RNTG ['bacterial-type']); ZmaysC3, *Zea mays* C3-form Ppc; ZmaysC4, *Z.mays* C4-form Ppc; P.falc., *Plasmodium falciparum* Ppc; E.coli, *E.coli* Ppc; Synecho., *Synechocystis sp.* PCC6803 Ppc; S.solf., *Sulfolobus solfataricus* Ppc (archaeal). Boxes I–III indicate conserved subdomains essential for catalysis by PEPC (Izui et al., 2004).

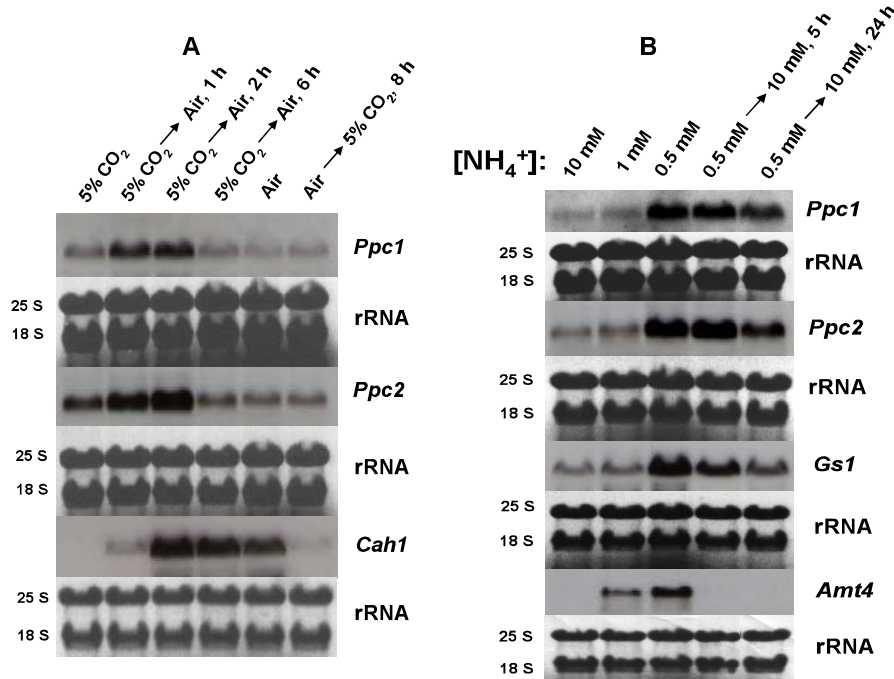**Figure 2.** **A:** Northern blot analysis of *Ppc1, Ppc2*, and a Ci-responsive control transcript (*Cah1*) in *C.reinhardtii* cells grown in high/low levels of CO_2. **B:** Northern blot analysis of *Ppc1, Ppc2*, and N-responsive control transcripts (*Gs1* and *Amt4*) in *C.reinhardtii* cells grown in high/low levels of NH_4^+, regulated within 5 h of growth under these N-sufficient conditions.

described, 'bacterial-type' plant PEPCs reported, to date, in *Arabidopsis* (AtPpc4), rice (OsPpc-b) and soybean (GmPpc17), of which *C.reinhardtii* Ppc2, with its C-terminal RNTG tetrapeptide, is a distant member; and (iii) the archaeal and (cyano)bacterial PEPCs, which consistent with PEPC's multi-faceted functional diversity in green plants, similarly small multigenic Ppc families have been reported previously (Chollet et al., 1996). At the level of overall gene structure, almost all vascular plant *Ppc* genes have a highly conserved genomic structure composed of approximately 10 exons interrupted by introns, regardless of whether they are from C_3 (e.g. AtPpc1 (Mamedov et al., 2005)), C_4 or CAM plants (Chollet et al., 1996). The deduced gene structure of *C.reinhardtii Ppc2*, with its 21 exons, is thus most similar to these 'bacterial-type' plant *Ppc* genes (Mamedov et al., 2005). The longer introns found in *CrPpc2* make it the largest *Ppc* gene (12.7 kb) identified to date.

Steady-state transcript analysis of *CrPpc1*, *CrPpc2*, and a known inorganic C-responsive gene *(Cah1)* in *C.reinhardtii* cells grown in high/low levels of CO_2 and 10 mM NH_4^+

As shown in Figure 2A, when *C.reinhardtii* cells grown at 5% CO_2 were transferred to a low-CO_2 condition (ambient air), the transcript levels of both *Ppc* genes increased transiently within 1 h, reached a maximum after 2 h, and then declined following 6 total hours of acclimation to these limiting-CO_2 conditions. In addition, the levels of both *Ppc* transcripts were down-regulated in cells grown in air relative to high CO_2-grown cells. However, when the air-grown cells were transferred to high-CO_2, the transcript levels of both *Ppc* genes remained largely unchanged after 8 h of accumulation (Figure 2A). These collective results indicate that both *CrPpc1* and *CrPpc2* are CO_2-responsive genes (Chen et al., 1997; Asamizu et al., 2000; Mamedov et al., 2001), and their steady-state transcript levels are up-/down-regulated by varying levels of CO_2 supplied to the growth medium. The similar expression responses observed for *CrPpc1* and *CrPpc2* under these various perturbations in [Ci] suggest the possibility of a similar mechanism regulation at the transcriptional level. *Cah1* which encodes a periplasmic α-carbonic anhydrase (α-CA (Fukuzawa et al., 2001)) was used as a Ci-responsive reference transcript whose expression is related directly to the induction of the CCM in *C.reinhardtii* cells. As shown in Figure 2A, little or no accumulation of the *Cah1* transcript was detected under high-CO_2 conditions, in contrast to *Ppc1* and *Ppc2*. However, the level of *Cah1* mRNA increased within 1 h of low-CO_2 acclimation and

attained its maximum after 2 h. Notably, during this transient period *Ppc1* and *Ppc2* responded in a similar manner. In contrast, there was a striking down-regulation of *Cah1* expression when air-grown cells were transferred to 5% CO_2 for 8 h, whereas *Ppc1* and *Ppc2* levels were essentially unchanged after this relatively brief period of acclimation to high CO_2.

Steady-state transcript analysis of *CrPpc1*, *CrPpc2*, and known inorganic N-responsive genes *(Gs1 and Amt4)* in *C.reinhardtii* cells grown in high/low levels of NH_4^+ at 5% CO_2

PEPC is a major anaplerotic enzyme in the green microalgae, especially in the context of replenishing citric-acid-cycle intermediates, such as 2-oxogluta- rate, consumed during the assimilation of ammonia by the GS/GOGAT cycle (Huppe and Turpin, 1994). It was thus of considerable relevance to assess the effects of varying levels of inorganic N, initially supplied as NH_4Cl, on the expression of the *Ppc1* and *Ppc2* genes in *C.reinhardtii*, and any concomitant changes in total cellular PEPC activity. As a complement to these *Ppc* northern analyses, the expression of two distinct, inorganic-N responsive reference transcripts was also monitored, namely *Amt4* and *Gs1*. Notably, the steady-state transcript levels of *Amt4* are increased specifically and dramatically under N-limiting conditions. *Gs1* represents the sole gene in *C.reinhardtii* that encodes the cytoplasmic isoform of GS, an obvious component of the N-assimilating GS/GOGAT cycle. The transcript levels of *Gs1* are significantly down-regulated under conditions of excess NH_4^+ (Chen and Silflow, 1996). As shown in Figure 2B, the transcripts for *Ppc1*, *Ppc2*, and *Gs1* were all readily detected in cells grown in 10 mM NH_4^+ and air enriched with 5% CO_2 (also see the related *Ppc* data in Figure 2A). In contrast, the exquisitely N-sensitive *Amt4* gene was not expressed under these conditions of N-sufficiency. With growth in decreasing levels of NH_4^+, all four genes were progressively up-regulated, with the maximal increase in steady-state transcript abundance occurring at 0.5 mM. Clearly, *Ppc1* and *Ppc2* are N-responsive genes in *C.reinhardtii*, and their expression profiles in response to decreasing NH_4^+ levels from 10 to 0.5 mM at 5% CO_2 mirrored that of *Gs1*. When the low-N grown cells were re-supplied directly with 10 mM NH_4^+, there was a modest but detectable down-regulation of *Ppc1*, *Ppc2* and *Gs1* expression within 24 h (Figure 2B). In contrast, the exquisitely N-sensitive *Amt4* gene was once again specifically and completely down-regulated. It is noteworthy that while concomitant changes in total *in vitro* PEPC specific activity (on a soluble protein basis) general-
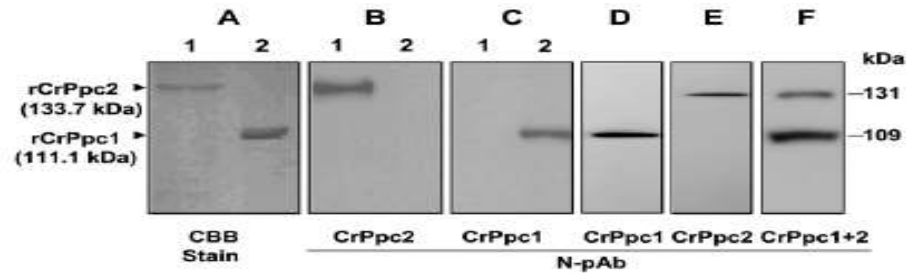
Figure 3. Immunospecificity of affinity-purified, N-terminal CrPpc1/2 peptide antibodies against the recombinant CrPpc1/2 fusion proteins and *C.reinhardtii* crude cell extracts following SDS–PAGE. (A) Coomassie Blue Staining of His6-tagged recombinant CrPpc2 (lane 1) and CrPpc1 (lane 2) marker proteins; (B, C) Immunoblot analysis of recombinant CrPpc2 (lanes 1) and CrPpc1 (lanes 2) proteins with CrPpc2 and CrPpc1 N-pAbs, respectively; (D-F) Immunoblots of *C.reinhardtii* (TAP-grown) crude soluble extracts with CrPpc1/2, and 1 + 2 N-pAbs, respectively.

ly paralleled those for *Ppc1* and *Ppc2* transcript abundance with decreasing [NH_4^+] from 10 to 0.5 mM.

Heterologous expression, and activity- and immunoblot-analysis of the C.reinhardtii recombinant CrQNTG (Ppc1) and CrRNTG (Ppc2) proteins

The expressed recombinant proteins were found to be highly soluble and effectively purified from clarified cell extracts by Ni^{2+}-immobilized metal affinity-chromatography (IMAC) as evidenced by SDS-PAGE analysis (Figure 3A). As depicted in Figures 3A and B, the *Chlamydomonas* recombinant Ppc1 and Ppc2 polypeptides were produced as 994-residue/~111 kDa and 1244-residue/~134 kDa fusion proteins, respectively, harbored a His$_6$-tag in their N-terminal extension in order to effect their separation from the resident *E.coli* PEPC. The specific activities of recombinant CrQNTG and CrRNTG were ~25 and ~22 mol min^{-1}mg^{-1}protein, respectively. These values are similar to the 18 to 22 U mg^{-1} specific activities reported for the Class-1 and Class-2 PEPCs purified from *C.reinhardtii* cell extracts (Rivoal et al., 1998). In marked contrast, affinity-purified polyclonal antibodies raised against the p102 catalytic subunit common to both green-algal PEPC1 and PEPC2, and the interacting p130 polypeptide of PEPC2 from *S.minutum* (Rivoal et al., 1996, 2002) reacted immuno-specifically with rCrQNTG or rCrRNTG, respectively (data not shown). The finding that the fully active ~134-kDa recombinant CrRNTG protein reacts immuno-specifically with anti-*S.minutum* p130 antibodies indivate that p130 is a *novel*, active PEP-carboxylase polypeptide in the green microalgae. As a result of these collective data, we conclude that there are likely two distinct PEPC catalytic subunit-types in the unusual but dominant Class-2 enzyme-complexes in the unicellular

green algae, contributed by both p102 (e.g., CrPpc2) and the interacting p130 polypeptide (e.g., CrPpc1). The affinity-purified CrPpc1/2 N-pAbs were found to immunoreact specifically with the purified, recombinant parent protein (Figure 3, panel B-F) for which they were raised. Likewise, soluble extracts with these affinity-purified N-pAbs resulted in the detection of a single p109 or p131 polypeptide which essentially co-migrated with the immunosignal from the corresponding react specifically with their divergent polypeptide targets upon denaturing immunoblot analysis, both in purified recombinant form and in soluble protein extracts from *C.reinhardtii* cells.

Denaturing immunoblot analysis of extracts from C.reinhardtii cells grown in various concentrations of NH_4^+ at 5% CO_2 or in TAP medium

As we discussed above the *CrPpc1/2* transcript levels to be coordinately up-/down-regulated under varying levels of NH_4^+ supplied to a photoautotrophic culture medium. As shown in Figure 4A, the corresponding CrPpc1/2 polypeptide levels are also up-regulated as the initial supply of NH_4Cl decreased from 10 to 0.5 mM. However, within 5 h after re-supply of 10 mM NH_4Cl to the N-deficient cells, the CrPpc1/2 levels reverted back nearly to those observed in high-N grown cells. This is in striking contrast with the corresponding transcript levels that are up-regulated in low-N cells, and remain largely elevated even after 24 h of ammonium re-supply. *In vitro* total cellular PEPC activity measurements showed an increase from ~0.035 to ~0.090 U mg^{-1} protein when the supplied [NH_4^+] was decreased from 10 to 0.5 mM, which returned to ~0.035 U mg^{-1} within 5 h of re-supplying 10 mM NH_4Cl (data not shown).
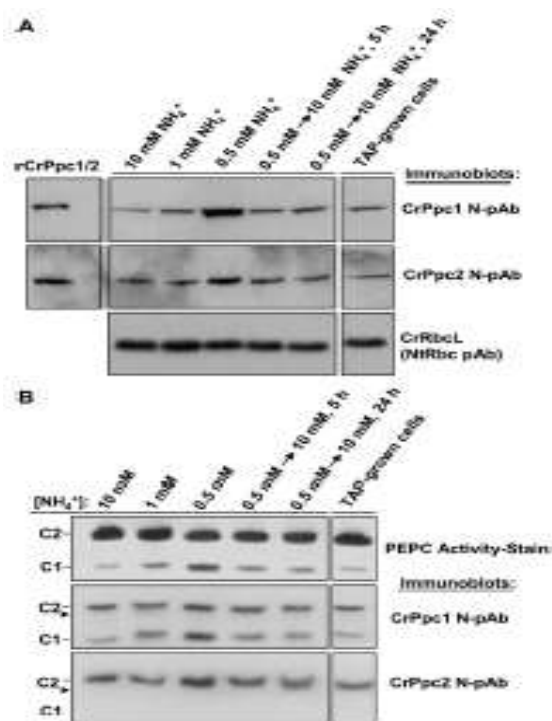
Figure 4. Immunoblot analysis and in-gel PEPC activity-staining of soluble extracts from *C.reinhardtii* cells grown at varying levels of NH_4Cl in air enriched to 5% CO_2 or in TAP medium in air. (A) Soluble proteins (22 µg) from *C.reinhardtii* cell extracts were separated by SDS-PAGE and immunoblotted with CrPpc1/2 N-pAbs or tobacco Rubisco pAb (used to detect the large subunit of *Chlamydomonas* Rubisco (CrRbcL)). (B) 1.25 mU of total PEPC activity from soluble cell extracts was separated by native-PAGE and either stained for in-gel PEPC activity in the presence of PEP as in Figure 1B, or immunodecorated with CrPpc1/2 N-pAbs.

C.*reinhardtii* cultures grown mixotrophically in acetate-containing TAP medium with 7.5 mM NH_4Cl exhibited CrPpc1/2 polypeptide levels (Figure 4A) and total cellular PEPC activity (~0.029 U mg^{-1}) approximating those in 5% CO_2-aerated cells grown at 10 mM NH_4^+ in HS medium. These complementary results show that the levels of the divergent CrPpc1/2 polypeptides generally mirror the corresponding changes in total cellular PEPC activity under the high-/low-N growth conditions examined.

1D native-PAGE and SDS-PAGE, combined with immunoblotting, establish the novel presence of the divergent CrPpc1/2 catalytic subunits in the hetero-oligomeric Class-2 PEPC complex

Non-denaturing electrophoretic analysis of *C.reinhardtii* soluble cell extracts, exploiting the Rubisco holoenzyme as an endogenous, ~550-kDa marker, revealed that both the single CrPpc2 N-pAb immunosignal and uppermost CrPpc1 N-pAb

signal co-migrated with the predominant, Class-2 PEPC activity-band, irrespective of the growth conditions examined (Figure 4B). In contrast, the lower CrPpc1 N-pAb immunosignal co-migrated with the Class-1 PEPC activity-band. These provocative results, together suggest that the divergent CrPpc1/2 catalytic subunits co-exist in the *C.reinhardtii* Class-2 PEPC complex. Interestingly, the relative proportion of Class-1 to Class-2 PEPC in *C.reinhardtii* was highest in 0.5 mM NH_4Cl-grown cells (Figure 4B). Thus, the obtained data collectively document the first definitive example of a eukaryotic PEPC holoenzyme-complex containing two, structurally distinct catalytic subunit-types, p109 and p131. Equally surprising is the realization that the former, CrPpc1 polypeptide is most closely related phylogenetically to the ~110-kDa PEPC-subunit of vascular plants, whereas the latter, CrPpc2 catalytic subunit is most homologous to the enigmatic "bacterial-type" plant PEPCs.

CONCLUDING REMARKS

To our knowledge, the above collective findings provide the first molecular insight into the two novel and distinct *Ppc* genes, and corresponding PEPC catalytic subunits, in *C.reinhardtii* or any other eukaryotic algae. It is now evident that *CrPpc1*, which encodes a fully functional, ~109-kDa PEPC polypeptide lacking the vascular-plant N-terminal phosphorylation domain, is the specific gene whose protein-product (CrQNTG) corresponds to the p102 catalytic subunit common to both the homotetrameric Class-1 and heteromeric Class-2 PEPC-forms in *C.reinhardtii*. Similarly, the divergent but highly active, ~131-kDa CrRNTG catalytic subunit, encoded by the unusual, ~12.7-kb *CrPpc2* gene, is also void of the "typical" N-terminal phosphorylation domain, and likely is equivalent to the interacting p130 polypeptide that is unique to the green-algal Class-2 PEPC complex. Thus our biochemical findings implicate the novel presence of two distinct PEPC catalytic subunit-types in the unusual but dominant Class-2 enzyme-complexes in the unicellular green algae. Class-2 PEPC enzyme-forms is a novel high-molecular-mass, hetero-oligomeric complex which containing both CrPpc1 (p109) and CrPpc2 (p131) polypeptides. The Class-1 enzyme, however, is a typical PEPC homotetramer comprised solely of p109.

At the level of expression, both of these "anaplerotic" *Ppc* genes in *C.reinhardtii* are coordinately responsive to changes in inorganic-C and -N levels during growth and they generally mirror the response of *Gs1* transcript abundance to changes in $[NH^{4+}]$ at high CO_2. This correlation between *Ppc1/Ppc2* and *Gs1* expression in *Chlamydomonas*

provides the first direct molecular evidence in support of previous physiological and biochemical studies that highlighted a key anaplerotic, non-photosynthetic role for PEPC in overall N-assimilation by the GS/GOGAT cycle in green microalgae.

REFERENCES

Asamizu E., Miura K., Kucho K., Inoue Y., Fukuzawa H., Ohyama K., Nakamura Y., Tabata S. (2000) Generation of expressed sequence tags from low-CO_2 and high-CO_2 adapted cells of *Chlamydomonas reinhardtii*. DNA Res. **7:** 305-307.

Chen Q., Silflow C.D. (1996) Isolation and characterization of glutamine synthetase genes in *Chlamydomonas reinhardtii*. Plant Physiol. **112:** 987-996.

Chen Z.-Y., Lavigne L.L., Mason C.B., Moroney J.V. (1997) Cloning and overexpression of two cDNAs encoding the low-CO_2-inducible chloroplast envelope protein LIP-36 from *Chlamydomonas reinhardtii*. Plant Physiol. **114:** 265-273.

Chollet R., Vidal J., O'Leary M.H. (1996) Phosphoenolpyruvate carboxylase: a ubiquitous, highly regulated enzyme in plants. Annu. Rev. Plant Physiol. Plant Mol. Biol. **47:** 273-298.

Felsenstein J. (1996) Inferring phylogenies form protein sequences by parsimony, distance, and likelihood methods. Meth. Enzymol. **266:** 418-427.

Fukuzawa H., Miura K., Ishizaki K., Kucho K., Saito T., Kohinata T., Ohyama K. (2001) *Ccm1*, a regulatory gene controlling the induction of a carbon-concentrating mechanism in *Chlamydomonas reinhardtii* by sensing CO_2 availability. Proc. Natl. Acad. Sci. USA **98:** 5347–5352.

Huppe H.C., Turpin D.H. (1994) Integration of carbon and nitrogen metabolism in plant and algal cells. Annu. Rev. Plant Physiol. Plant Mol. Biol. **45:** 577-607.

Izui K., Matsumura H., Furumoto T., Kai Y. (2004) Phosphoenolpyruvate carboxylase: a new era of structural biology. Annu. Rev. Plant Biol. **55:** 69-84.

Mamedov T.G., Suzuki K., Miura K., Kucho K., Fukuzawa H. (2001) Characteristics and sequence of phosphoglycolate phosphatase from a eukaryotic green alga *Chlamydomonas reinhard-*

tii. J. Biol. Chem. **276:** 45573-45579.

Mamedov T., Moellering E., Chollet R. (2005) Identification and expression analysis of two inorganic C- and N-responsive genes encoding novel and distinct molecular forms of eukaryotic phosphoenolpyruvate carboxylase in the green microalga *Chlamydomonas reinhardtii*. Plant J. **42:** 832–843.

Mamedov T.G., Moellering E.R., Chollet R. (2006) Two divergent, inorganic C- and N-responsive genes encoding novel and distinct molecular forms of eukaryotic phosphoenolpyruvate carboxylase (PEPC [Ppc]) in the green microalga *Chlamydomonas reinhardtii*: identification and expression analysis of the *CrPpc1/2* genes and PEPC catalytic subunits. 12th International Conference on the Cell and Molecular Biology of *Chlamydomonas*, Portland, USA: 81p.

Moellering E., Yexin O., Mamedov T., Chollet R. (2007). The two divergent PEP-carboxylase catalytic subunits in the green microalga *Chlamydomonas reinhardtii* respond reversibly to inorganic-N supply and co-exist in the high-molecular-mass, hetero-oligomeric Class-2 PEPC complex. FEBS Lett. **581:** 4871-4876.

Rivoal J., Dunford R., Plaxton W.C., Turpin D.H. (1996) Purification and properties of four phosphoenolpyruvate carboxylase isoforms from the green alga *Selenastrum minutum:* Evidence that association of the 102 kDa catalytic subunit with unrelated polypeptides may modify the physical and kinetic properties of the enzyme. Arch. Biochem. Biophys. **332:** 47-57.

Rivoal J., Plaxton W.C., Turpin D.H. (1998) Purification and characterization of high- and low-molecular-mass isoforms of phosphoenolpyruvate carboxylase from *Chlamydomonas reinhardtii*. Kinetic, structural and immunological evidence that the green algal enzyme is distinct from the prokaryotic and higher plant enzyme. Biochemistry **331:** 201-209.

Rivoal J., Turpin D.H., Plaxton W.C. (2002) *In vitro* phosphorylation of phosphoenolpyruvate carboxylase from the green alga *Selenastrum minutum*. Plant Cell Physiol. **43,** 785-792.

Sbnchez R., Cejudo F.J. (2003) Identification and expression analysis of a gene encoding a bacterial-type phosphoenolpyruvate carboxylase from *Arabidopsis* and rice. Plant Physiol. **132:** 949-957.

Effect of Water Stress on Protein Content of Some Calvin Cycle Enzymes in Different Wheat Genotypes

Shahniyar M. Bayramov[1,2]*, **Hesen G. Babayev**[1], **Minakhanim N. Khaligzade**[1], **Novruz M. Guliyev**[1], **Christine A. Raines**[2]

[1]*Institute of Botany, Azerbaijan National Academy of Sciences, 40 Badamdar Shosse, Baku AZ 1073, Azerbaijan*
[2]*Department of Biological Sciences, University of Essex, Colchester CO43SQ, UK*

The dynamics of protein content changes of some photosynthetic enzymes under water stress has been studied by immunoblotting method in bread (*Triticum aestivum*) and durum (*Triticum durum*) wheat genotypes differing in their drought tolerance. In all tested genotypes protein content of studied enzymes under weak and mild drought stress was similar to their content in normal watered variants. While protein content of phosphoribulokinase (PRK) and fructose-1,6-bisphosphatase (FBP) remained unchanged, sedoheptulose-1,7-bisphosphatase (SBP), transketolase (TK), NADP-glyceraldehyde-3-P-dehydrogenase (NADP-GAPDH) and Rubisco activase decreased under severe water stress. This decrease was more apparent for TK, SBP and Rubisco activase. However in drought tolerant genotypes Azamatli-95 and Barakatli-95 this decrease was less pronounced compared to genotypes Garagylchyg-2 and Giymatli-2/17, which are sensitive to drought. At the early stage of heading of the genotype Garagylchyg-2, during 2-3 days of water stress protein content of PRK, FBP and NADP-GAPDH was unchanged in flag leaves, while in ear elements protein content of these enzymes decreased significantly.

Keywords: Calvin cycle, drought, wheat genotypes

INTRODUCTION

At present in consequence of global climate changes a progressive increase of the average annual temperature of the earth results in the development of some stress factors. This leads to the significant decrease of the productivity of agricultural plants in regions having water deficit. Modern biotechnological methods have been used now to investigate molecular-genetic bases of drought resistance to create cultures tolerant to drought and high temperature (Raines, 2006). Modern investigations of genotypes differing in their drought tolerance within the same species and among the ancestors of crops may serve as a marker in obtaining more productive genotypes. Photosynthetic CO_2 assimilation in C_3-plants is affected by environmental variables including temperature, CO_2 concentration and water availability. Of these variables, water is the main biotic factor limiting plant productivity in many regions of the world (Chaves et al., 2002). Water stress can affect photosynthesis directly by causing changes in plant metabolism or indirectly by limiting the amount of CO_2 available for fixation (Lawlor and Cornic, 2002). Drought resistance of a plant is related to its ability to maintain higher relative water content in the leaves under water stress. Many changes in gene expression occur in plants growing under limited water conditions (Bray, 2002).

The data on water stress induced regulation of the activity of photosynthetic enzymes other than Rubisco are scarce. Thimmanaik et al. (2002) studied the activity of several photosynthetic enzymes under progressive water stress in two different cultivars of *Morus alba*. Unlike Rubisco, which is highly stable and resistant to water stress, the activity of some enzymes involved in the regeneration of ribulose-1,5-bisphosphate (RuBP) are progressively impaired from very early stages of water stress. Thus, these results present the possibility that some enzymes involved in the regeneration of RuBP could play a key regulatory role in photosynthesis under water stress. During water stress induced by polyethilenglycole, Rubisco activity significantly increased in young potato leaves, while decreased in mature leaves (Bussis et al., 1998). But NADP-GAPDH and PRK activities have been decreased and this change became faster in the course of drought. While decreased Rubisco activity may not be the cause of photosynthetic

---

reduction during water stress, its down-regulation may still be important because it could preclude a rapid recovery upon rewatering (Ennahli and Earl, 2005). Similarly, some reports have shown strong drought-induced reductions of Rubisco activity per unit leaf area (Maroco et al., 2002) and per mg showed that the decrease of Rubisco activity *in vivo* was not connected with the protein content. It occurs because of CO_2 concentration decrease in the carboxylation center in consequence of the partly closing of stomata (Flexas et al., 2006). But it is known, that enzyme regulation occurs not only in transcription, but also in posttranscriptional level. Activities of the tested enzymes are regulated by light as well as by the concentration of photosynthetic metabolites (Raines, 2006). Reductions of more than 50% in the levels of NADP-GAPDH, FBP, PRK, and plastid aldolase were also needed before photosynthetic capacity was affected (Stitt and Schulze, 1994). Although the level of control exerted by any single enzyme in the cycle varied with environmental conditions and developmental status, the data from the transgenic plants strongly indicated that a number of enzymes in the Calvin cycle are present in excess. The implication from this is that the levels of Rubsico, NADP-GAPDH, FBP, and PRK are not close to limiting carbon fixation through this cycle and therefore would not be useful targets for overexpression to increase photosynthetic capacity.

In contrast, photosynthesis has been shown to be sensitive to small reductions in the levels of the enzymes TK and SBP (Harrison et al., 2001). TK catalyzes three reactions in the regenerative phase of the Calvin cycle. A small decrease (20-30%) in TK resulted in a reduction of photosynthetic carbon fixation, and flux to phenylpropanoid metabolism was also decreased, making this enzyme a potential target for overexpression.

The study of gene expression and polypeptide content changes of some Calvin cycle enzymes under water stress will probably promote to evaluate the decrease of CO_2 photosynthetic assimilation.

MATERIALS AND METHODS

Plant material and growth conditions. The seeds of two bread wheat (*Triticum aestivum* L.) genotypes (Giymatli-2/17, Azamatli-95) and two durum wheat genotypes (Garagylchyg-2, Barakatli-95) were supplied by Research Institute of Crop Husbandry (Baku, Azerbaijan). The germinated seeds were planted in 12.5 cm pots filled with peat- and loam-based compost and grown in a temperature-controlled greenhouse at day/night temperature of 24/18°C. The plants were watered regularly with Hoagland's solution. Recently fully expanded 4th or 5th leaf and flag leaf and ear elements were used in experiments.

Leaf Relative Water Content (RWC) determination. RWC was measured simultaneously on two leaves from both stressed and well-watered plants. After weighing (fresh weight, FW), leaves were cut into parts and placed in water in a closed Petri dish. After 24 h at 4°C, leaf pieces were weighed (turgid weight, TW). Dry weight (DW) was measured after 48 h at 60°C. RWC was calculated as (100 x (FW-DW)/(TW-DW)).

Protein Extraction and Western-Blot Analysis. Leaf discs (two leaf discs 0.75 cm^2) were isolated from the leaves and frozen in liquid nitrogen. The frozen leaf discs were ground to a fine powder in liquid nitrogen using a mortar and pestle in extraction buffer (50 mM Hepes, pH 8.2; 5 mM $MgCl_2$; 1 mM EDTA; 1 mM TGTA; 10% glycerol; 0.1 % Triton X-100; 2 mM benzamidine; 2 mM amino capronic acid; 0.5 mM phenylmethylsulfonylfluoride (PMFS); 10 mM dithiothreitol (DTT)), transferred to a prechilled tube and spun in a microcentrifuge for 1 min at 4°C. The supernatant was removed for protein estimation and Western blotting. Protein was determined by the method of Bradford (1976) with bovine serum albumin as a standard. An equal volume of SDS-loading buffer (150 mM Tris-HCl, pH 6.8, 4% (w/v) SDS, and 10% (v/v) 2-mercaptoethanol) was added to the supernatant for Western blot. The homogenates were boiled for 5 min and centrifuged at 10 000 g for 10 min. Samples were loaded on an equal protein basis (5 mg), separated using 12% (w/v) SDS-PAGE gel according to the method of Laemmli (1970). Then blotted onto nitrocellulose in transfer buffer (50 mol m^{-3} Tris base, 380 mol m^{-3} Gly, 0.1% [w/v] SDS, and 20% [v/v] methanol) at approximately 4°C overnight at 50 V. Prior to incubation with antibody the membranes were washed in phosphate-buffered saline (PBS) containing 0.05 (v/v) Tween 20 (PBS-T) and then blocked in PBS-T containing 6% milk powder (w/v). The nitrocellulose membranes were incubated with the appropriate primary polyclonal antibodies for 1.5 h after blocking for 2 h at room temperature with 6% (w/v) skimmed milk in phosphate-buffered saline (PBS) containing 0.0005% (v/v) Tween 20. After six washes with PBS-T, blots were incubated for 2 h at room temperature with a 1:5.000 dilution in PBS-T of sheep anti-rabbit secondary antibody conjugated to horseradish peroxidase. After six PBS-T washes, the secondary antibodies were detected using enhanced chemiluminescences according to the manufacturer's directions. Prior to re-probing of the membranes, antibodies were removed following ECL detection by immersing in buffer containing 100 mM 2-

mercaptoethanol, 2% SDS, 62.5 mM Tris-HCL, pH 6.7, for 30 min at 50°C.

RESULTS AND DISCUSSION

Wheat is one of the most important food crops and its productivity is markedly influenced by soil water availability. Two durum (Barakatli-95, Garagylchyg-2) and two bread (Azamatli-95, Giymatli-2/17) wheat genotypes were used as the investigation objects. Results showed that depending on the duration and severity of drought protein content of some Calvin cycle enzymes changed differently. Effect of drought on protein content of some Calvin cycle enzymes (NADP-GAPDH, Rubisco activase, TK, PRK, SBP and FBP) was tested by immuniblotting method. When RWC reached 85-80%, protein content of tested enzymes remained unchanged. Protein content of almost all the tested enzymes under progressive stress was similar to their content in normal watered variants (Figure 1).

But at 70% of RWC, protein content of TK, FBP, NADP-GAPDH, and SBP began to decrease. This decrease was more pronounced in genotypes sensitive to drought. Protein content of SBP, TK, NADP-GAPDH, Rubisco activase decreased significantly in contrast with PRK (Figure 2) which content remained unchanged under severe water stress. This decrease was also different for each tested genotype. Thus in a drought-tolerant sort Barakatli-95 protein content of the tested enzymes was close to their content in normal watered variants.

In drought-tolerant Azamatli-95 (durum) and Barakatli-95 (bread) varieties this decrease was less apparent, though in drought sensitive Garagylchyg-2 and Giymatli-2/17 protein content of TK and SBP enzymes significantly decreased under severe water stress (Figure 3).

Protein content of PRK was unchanged independently of the severity of drought. But protein content of Rubisco activase was unchanged in drought-tolerant variety Barakatli-95 (Figure 4).

In contrast to flag leaves, in initial ear elements protein content of some photosynthetic enzymes showed different changes from the beginning of
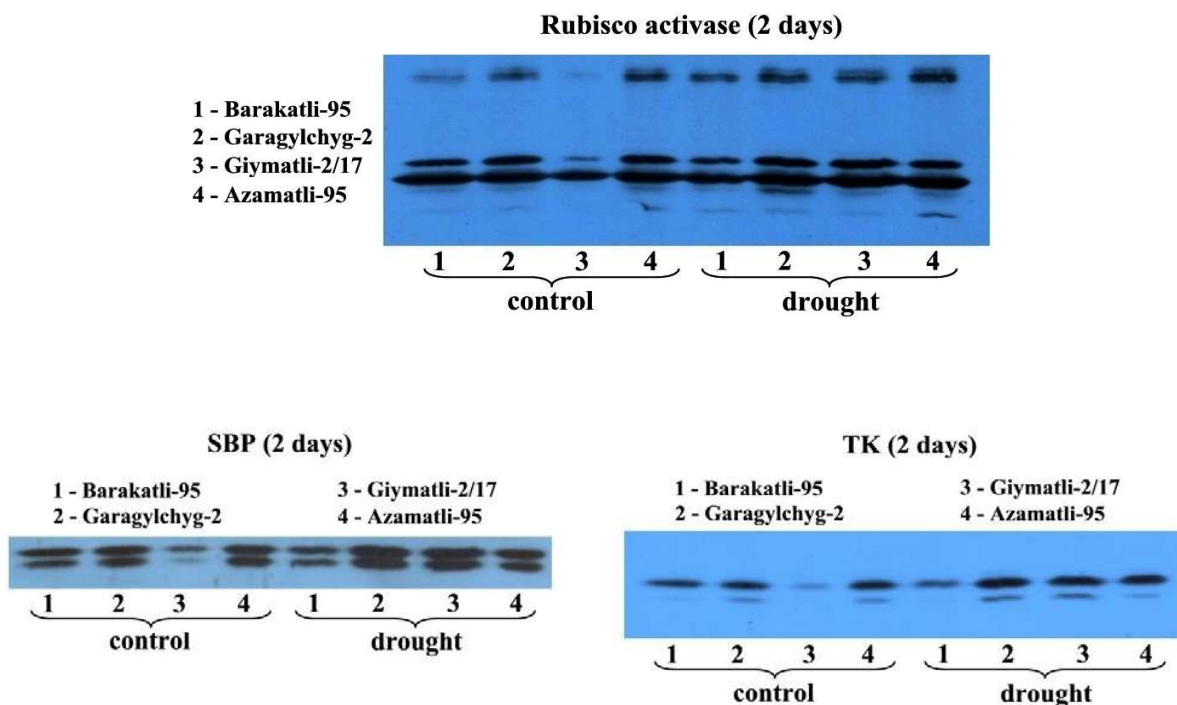

Figure 1. Effects of progressive drought stress on the protein content of Rubisco activase, SBP and TK in different wheat genotypes.
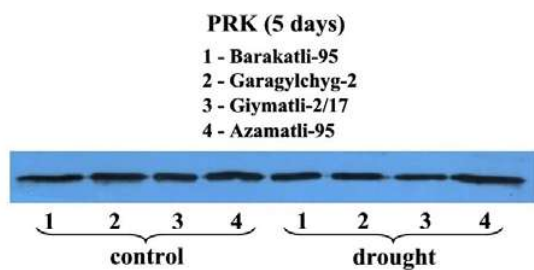
PRK (5 days)

1 - Barakatli-95
2 - Garagylchyg-2
3 - Giymatli-2/17
4 - Azamatli-95

Figure 2. Effects of severe drought stress on the protein content of PRK in different wheat genotypes.

TK (5 days)

1 - Barakatli-95   3 - Giymatli-2/17
2 - Garagylchyg-2   4 - Azamatli-95

SBP (5 days)

1 - Barakatli-95   3 - Giymatli-2/17
2 - Garagylchyg-2   4 - Azamatli-95
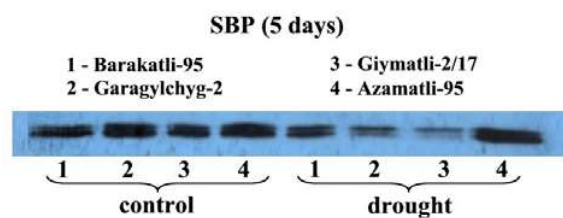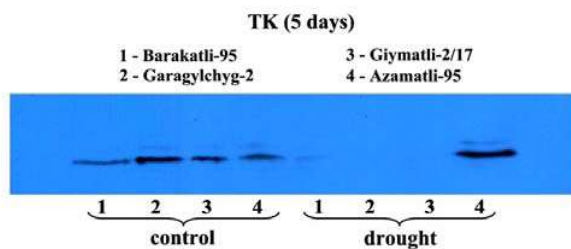
Figure 3. Effects of severe drought stress on the protein content of TK and SBP in different wheat genotypes.

Rubisco activase (5 days)

1 - Barakatli-95
2 - Garagylchyg-2
3 - Giymatli-2/17
4 - Azamatli-95
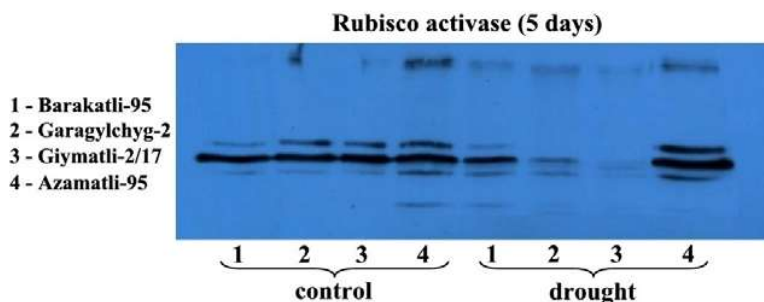
Figure 4. Effects of severe drought stress on the protein content of Rubisco activase in different wheat genotypes.

PRK (Garagylchyg-2)

1, 3 - control
2 - drought (2 days);
4 - drought (3 days)

flag leaf   ear elements

GAPDH (Garagylchyg-2)
1, 3 - control
2 - drought (2 days);
4 - drought (3 days)

flag leaf   ear elements

FBP (Garagylchyg-2)
1, 3 - control
2 - drought (2 days);
4 - drought (3 days)

flag leaf   ear elements

Figure 5. Effects of progressive drought stress on the protein content of some Calvin cycle enzymes in flag leaf and ear elements.

drought stress. During 2-3 days of drought stress protein content of NADP-GAPDH, PRK, FBP was unchanged in flag leaves, while their content sharply decreased in ear elements (Figure 5).

Previous investigations (Guliyev et al., 2008) showed that Rubisco activity was almost unchanged in drought-tolerant genotypes under weak drought stress. But when RWC was less than 80%, the activity decreased faster and this tendency was more pronounced in genotypes sensitive to drought.

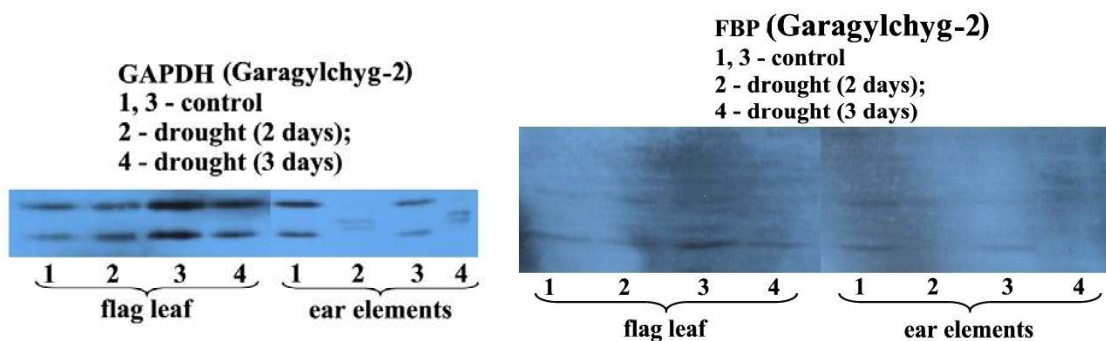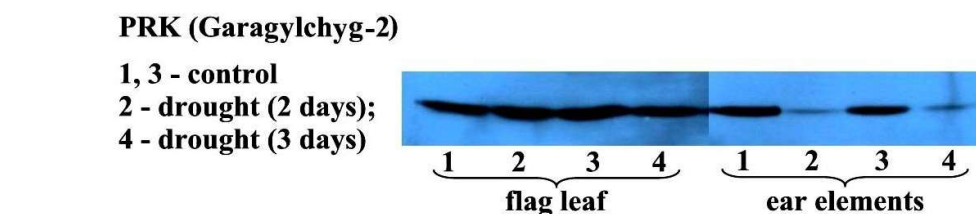In field-grown maize (*Zea mays*), losses in grain yield are maximal when drought occurs during the flowering stage (Andersen et al., 2002). In barley plants depending on the duration and severity of drought stress protein content of some Calvin cycle and photorespiration enzymes changed differently (Wingler et al., 1999). While Rubisco and plastidic FBP remained unchanged the content of SBP and NADP-GPDH decreased. The photorespiratory enzyme - chloroplastic glutamine synthetase remained unchanged as stress developed but the content of NADH-dependent hydroxypyruvate reductase increased.

In vitro assays of the content of key Calvin cycle enzymes involved in the regeneration of RuBP, by Western blot analyses, indicated that UV-B irradiation of mature leaves of oilseed rape induced a reduction in the content of SBP, but not FBP or PRK on a leaf area basis (Allen et al., 1998).

Rubisco activase has been reported to be particularly sensitive to inactivation by high temperature stress, and most of the Rubisco activase is sequestered to the thylakoid membrane from the soluble stromal fraction during high temperature stress (Rokka et al., 2001). Recently in SBP overexpression rice plant showed that the content of RuBP and Rubisco activase in the soluble stroma fractions decreased significantly under salt stress, and such a decrease was more pronounced in wild-type plants than in transgenic plants (Feng et al., 2007). Analyses of Western blotting also showed that there were no changes in the content of Rubisco and PRK in wild-type and transgenic plants during salt stress. In contrast, initial Rubisco and PRK activities clearly decreased with increasing salt concentration in rice leaves (Feng et al., 2007). Recently Xue et al. (2008) have reported that expression levels of most genes encoding chloroplast enzymes involved in carbon fixation (Calvin cycle) were reduced in the bread wheat leaves during prolonged drought stress.

The change of protein content of Calvin cycle enzymes under drought observed in our experiments were similar to that under influence of salt, heat and UV-B radiation. Therefore, we conclude that this change is independent of the stress sources.

The sharp decrease of tested enzymes in an early stage of development in the ear elements in contrast with a flag leaf verified its more sensitiveness to water deficit. Obtained results suggest that water stress effects on protein content of Calvin cycle enzymes differently depending on the development stage of the plant and also its separate organs. These results would promote to choose the right irrigation time.

REFERENCES

Allen D.J., Nogues S., Baker N.R. (1998) Ozone depletion and increased UV-B radiation: is there a real threat to photosynthesis? J. Exp. Bot. **49:** 1775-1788.

Andersen M.N., Asch F., Wu Y., Jensen C.R., Naested H., Mogensen V.O., Koch K.E. (2002) Soluble invertase expression is an early target of drought stress during the critical, abortion-sensitive phase of young ovary development in maize. Plant Physiol. **130:** 591-604.

Bradford M.M. (1976) A rapid and sensitive method for the quantification of microgram quantities of protein utilizing the principle of protein-dye binding. Anal. Biochem. **72:** 248-254.

Bray E.A. (2002) Classification of genes differentially expressed during water-deficit stress in *Arabidopsis thaliana*: an analysis using microarray and differential expression data. Ann. Bot. **89:** 803-811.

Bussis D., Kauder F., Heineke D. (1998) Acclimation of potato plants to polyethylene glycol-induced water deficit. J. Exp. Bot. **49:** 1349-1360.

Chaves M.M., Pereira J.S., Maroco J., Rodrigues M.L., Ricardo C.P., Osorio M.L., Carvalho I., Faria T., Pinheiro C. (2002) How plants cope with water stress in the field: photosynthesis and growth. Ann. Bot. **89:** 907-916.

Ennahli S., Earl H.J. (2005) Physiological limitations to photosynthetic carbon assimilation in cotton under water stress. Crop Sci. **45:** 2374-2382.

Feng L., Hari Y., Liu G., An B., Yang G., Li Y., Zhu Y. (2007) Overexpession of sedoheptulose-1,7-bisphosphatase enhances photosynthesis and growth under salt stress in transgenic rice plants. Func. Plant Biol. **34:** 822-834.

Flexas J., Ribas-Carbo M.T., Bota J., Galmes J., Henkle M., Martinez-Canellas S.F., Medrano H. (2006) Decreased Rubisco activity during water stress is not induced by decreased relative water content but related to conditions of low stromal conductance and chloroplast CO_2 concentration. New Phytol. **172:** 73-82.

Guliyev N., Bayramov Sh., Babayev H. (2008) Effect of water deficit on RUBISCO and carbonic anhydrase activities in different wheat genotypes. In: Photosynthesis, Energy from the Sun. 14th International Congress on Photosynthesis (Allen J.F., Grantt E., Golbeck J.H., Osmond R., eds.), Springer, Glasgow: 1465-1468.

Harrison E.P., Olcer H., Lloyd J.C., Long S.P., Raines C.A. (2001) Small decreases in SBPase cause a linear decline in the apparent RuBP regeneration rate, but do not affect Rubsico carboxylation capacity. J. Exp. Bot. **52**: 1779-1784.

Laemmli U.K. (1970) Cleavage of structural proteins during the assembly of the head of bacteriophage T_4. Nature **227**: 680-685.

Lawlor D.W., Cornic G. (2002) Photosynthetic carbon assimilation and associated metabolism in relation to water deficits in higher plants. Plant Cell Environ. **25**: 275-294.

Maroco J.P., Rodrigues M.L., Lopes C., Chaves M.M. (2002) Limitations to leaf photosynthesis in field-grown grapevine under drought-metabolic and modeling approaches. Func. Plant Biol. **29**: 451-459.

Parry M.A.J., Andraloje P.J., Khan S., Lea P.J., Keys A.J. (2002) Rubisco activity: effects of drought stress. Ann. Bot. **89**: 833-839.

Raines C.A. (2006) Transgenic approaches to manipulate the environmental responses of the C_3 carbon fixation cycle. Plant Cell Environ. **29**: 381-389.

Rokka A., Zhang L., Aro E.N. (2001) Rubisco activase: an enzyme with a temperature-dependent dual function. Plant J. **25**: 463-471.

Stitt M., Schulze E.-D. (1994) Does Rubisco controls the rate of photosynthesis and plant growth? An exercise in molecular ecophysiology. Plant Cell Environ. **17**: 465-487.

Thimmanaik S., Giridara K.S., Jyothsna K.G., Surnyanarayana N., Sudhakar C. (2002) Photosynthesis and the enzymes of photosynthetic carbon reduction cycle in mulberry during water stress and recovery. Photosynth. **40**: 233-236.

Wingler A., Quick W.P., Bungard R.A., Bailey K.J., Lea P.J., Leegood R.C. (1999) The role of photorespiration during drought stress: an analysis utilizing barley mutants with reduced activities of photorespiratory enzymes. Plant Cell Environ. **22**: 361-373.

Xue G.-P., McIntyre C.L., Glassop D., Shorter R. (2008) Use of expression analysis to dissect alterations in carbohydrate metabolism in wheat leaves during drought stress. Plant Mol. Biol. **67**: 197-214.

Physiological Regulation of G Protein-Linked Signal Transduction in Plants

Kerim G. Gasimov*

Institute of Botany, Azerbaijan National Academy of Sciences, 40 Badamdar Shosse, Baku AZ 1073, Azerbaijan

G-proteins represent a class of molecules that can bind guanine nucleotides (GDP or GTP) and are involved in signal transduction. The G-protein-linked signal transduction is well established in animals where it is involved in biochemical events such as vision and hormone action. Plants, like animals, use signal transduction pathways based on heterotrimeric guanine nucleotide-binding proteins (G-proteins) to regulate many aspects of developmental processes and cell signaling. Some components of G-protein signaling are highly conserved between plants and animals and some are not. By contrast, despite great complexity in their signal-transduction attributes, plants have a simpler repertoire of G-signaling components. Nonetheless, recent studies have shown the importance of plant G-protein signaling in such fundamental processes as cell proliferation, hormone perception and ion-channel regulation.

Keywords: G-proteins, signal transduction, cAMP, G-protein coupled receptors, plant hormones, phytochrome

INTRODUCTION

All cells, whether belonging to unicellular or multicellular organisms, have the capacity to communicate with their surroundings by detecting and responding to a wide range of stimuli. Extracellular signals such as hormones, neurotransmitters, growth factors and even light are detected by interaction with specific receptors present on the plasma membrane of the target cell, triggering biochemical processes that produce intracellular events.

Signal transduction is vital to the coordination and growth particularly of complex multicellular eukaryotes, since organisms must be able to respond to external stimuli. In biology signal transduction refers to any process by which a cell converts one kind of signal or stimulus into another, most often involving ordered sequences of biochemical reactions inside the cell that are carried out by enzymes, activated by second messengers resulting in what is thought of as a "signal transduction pathway".

The G-protein model of signal transduction

GPCRs and the G-protein heterotrimer. The G-protein family is involved in a wide variety of signal-transducing events controlling important processes like sensory transduction and cell division and differentiation (Gibbs et al., 1985; Barbacid, 1987; Kleuss et al., 1994). The guanine nucleotide-binding protein (G-protein) superfamily shares

a similar biological function and a common structural core. G-proteins are present in both prokaryotes and eukaryotes. They are involved in signal transduction, where external stimulation of a G-protein coupled receptor generates a signal that is transduced to the cytosolic side of the membrane.

G-protein signaling begins with the alteration of the conformation of a GPCR by agonist binding (Pierce et al., 2002). The largest gene family in animals encodes heptahelical transmembrane proteins that physically interact with a heterotrimeric G-protein. These polytopic membrane proteins are termed G-protein-coupled receptors (GPCRs) and their ligands are as diverse as is the GPCR family itself.

GPCRs have seven transmembrane (7TM)-spanning domains with an extracellular amino-terminus and cytosolic domains that are coupled to the $G\alpha$-subunit of the G-protein heterotrimer in a way that influences the activation state of the α-subunit (Figure 1). In essence, the GPCR is a guaninenucleotide-exchange factor (GEF) that promotes the exchange of GDP for GTP in the associated $G\alpha$-subunit.

Rhodopsin is a familiar example of a prototypical GPCR. It is the gateway of vision operated by a light-assisted change in the geometry of the retinal chromophore buried deep within the bundle of seven transmembrane (TM) helices. It is known that light induces a photoisomerization of a *cis* retinal moiety, which is covalently bound (within its heli-
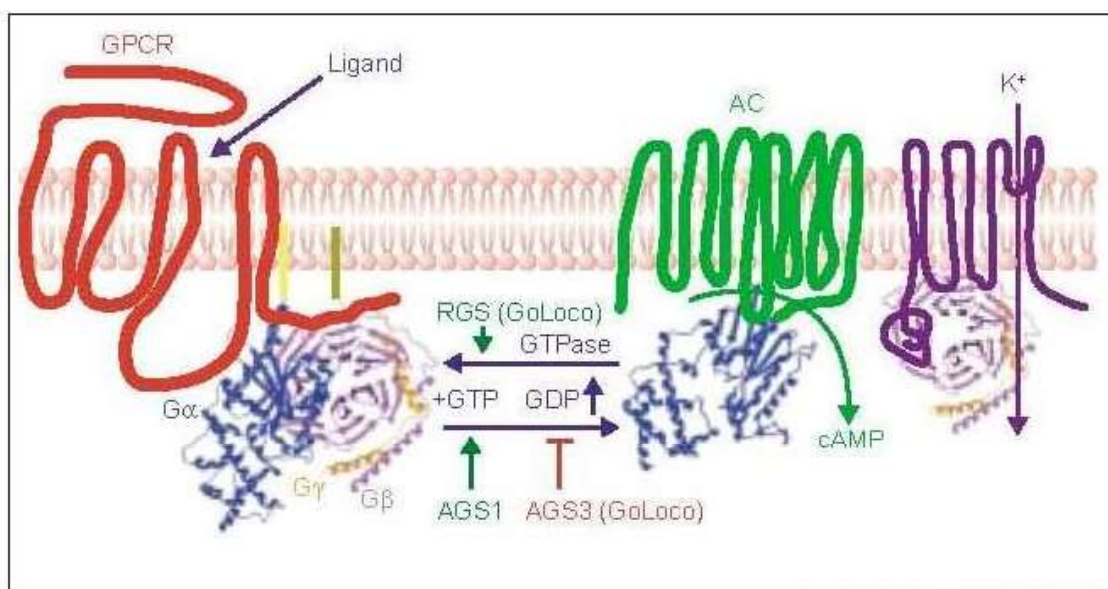
*E-mail: gasimov-k@botany.az.org

Figure 1. Classical model for G-protein-coupled signaling in animal cells. The binding of a ligand to its cognate receptor induces a conformational change that is perceived cytoplasmically. The ribbon structure of the three subunits of a heterotrimeric G-protein complex is shown to be associated with the receptor. The G-protein is tethered to the bilayer and kept proximal to the receptor by lipid modification of its α and γ subunits (green and yellow bars). The activated receptor promotes GDP for GTP exchange, which dissociates the Gα from the Gβγ subunit. Both Gα and Gβγ can then activate downstream targets, such as adenyl cyclase (AC) and ion channels, to cause changes in the levels of secondary messengers. The effect of the G-protein subunits on their targets can be either positive or negative, although only stimulation is shown. The intrinsic GTPase of the Gα subunit hydrolyses GTP to GDP and thus returns the G-protein complex to its resting state. Regulators of G-protein signaling (RGS) can facilitate the Gα GTPase (GAP) activity by interactions at their GoLoco domains. Some effectors exert GAP activity. Activities that alter the activated state of the G-protein complex independently of receptor activation are provided by AGS proteins. AGS1 facilitates GTP exchange whereas AGS3 acts as an inhibitor of GDP dissociation. AGS3 stimulates G-coupled pathways in which Gβγ is involved because AGS3 can displace the Gβγ subunit from the complex, enabling it to interact with its effectors.

cal core) to rhodopsin, to the all *trans* retinal form. The light-induced *cis-3-trans* isomerization of retinal is thought to induce rigid body movements of the TM helices forcing a transition of rhodopsin to the active metarhodopsin II (MII) state. Formation of the latter is accompanied by small but significant tertiary structural changes inthe solvent-exposed cytoplasmic interhelical loops thereby opening high affinity sites for the binding and activation of several signaling proteins. Similarly, small molecules such as serotonin, peptides such as somatostatin, and even large proteins such as thrombin bind to their cognate GPCRs and induce certain cytoplasmic conformations through shifts in helix positions that translate into specific loop conformations. These changes of loop conformation appeared in three cytoplasmic loops C2, C3 and C4 which certain conserved amino-acids are involved in G-protein of visual cascade transducin activation (Natochin et al., 2003).

The Gα-subunit contains a Ras-like domain that has a GDP/GTP-nucleotide-binding site and GTP-hydrolase activity. In the GDP-bound form of Ga, the N-terminal helix and three switch regions of

Gα interact with a seven-bladed propeller structure in the β-subunit (Gβ). On activation by a GPCR, the Gα-protein changes conformation to a structure that allows GTP binding (Morris and Malbon, 1999). Consequent reorientation of the switch regions in the Ras-domain disrupts the tight interaction between Gα and Gβ, which results in the separation of Gα from the tightly associated Gβ/Gγ-subunit dimer. When Gα is released, the interaction between Gα and its cognate effector occurs along the same interface between Gα and Gβ, Gα and/or Gβγ then interact with downstream-effector molecules. The intrinsic GTP-ase activity of Gα eventually results in GTP hydrolysis, during which a reorientation of the switch regions promotes the reassociation of Gα with Gβγ and readying Gα for another cycle of activation by its cognate GPCR. Therefore, Gβγ activity is indirectly controlled by Gα activation. Similar interaction cycles are repeated over and over for each of the thousands of signals using the GPCR pathway.

Diversity

The multiplicity of signals and their intracellular transduction raises the central question: how can so many signals, each recognized independently by a separate GPCR, specifically couple to only a dozen or fewer effectors via G-proteins? Specificity in signal coupling in metazoans is accomplished by two mechanisms. First, some G-proteins are able to recognize a specific GPCR and a specific effector. Second, promiscuous G-proteins are sequestered in signaling rafts that contain a specific GPCR, the cognate effector and all of the other components that operate on a particular pathway.

Animals have 23 different Gα, 6 Gβ, and 12 Gγ subunits, potentially assembling more than a thousand different G-proteins (Vanderbeld and Kelly, 2000). Given differences in the expression of G-proteins among different cell types and the known exclusion of some subunit pairs, we can more conservatively estimate that more than a hundred heterotrimeric complexes exist in a cell. Gα forms four subfamilies, Gs, Gi, Gq, and G12, on the basis of their sequence. In contrast to animals, *Arabidopsis* and rice have single canonical Gα - GPA1, RGA1, respectively, and single Gβ subunits AGB1 or RGB1, respectively, and possibly just two Gγ subunits AGG1 or RGG1 (Mason and Botella, 2000; Kato et al., 2004) and AGG2 or RGG2 (Ma et al., 1990; Weiss et al., 1994). The *Arabidopsis* Gα-subunit is roughly 30% identical to mammalian Gα-subunits of the Gi subfamily, and essentially all of this conservation lies in the few critical domains (Figure 2). GPA1 is most similar to the member of Gi subfamily called Gz. Like Gz, GPA1 lacks the carboxy-terminal cysteine that is targeted for ribosy-

lation by pertusis toxin. GPA1 shares slightly more identity with Gz than with other members of the Gi subtype, and contains a Gz-specific myristolization motif. Gz plays a role in cell proliferation and death via its control of potassium channeling, thus it is possible that GPA1 operates in an analogous way.

The theoretical models (Figure 2B) of the *Arabidopsis* G-protein heterotrimer monomers based on the mammalian templates (Figure 2A) are "valid" structures overall. The final theoretical structures for *Arabidopsis* Gα and Gβ are nearly as compatible with the *Arabidopsis* sequences as the experimentally determined mammalian structures of Gα and Gβ are with the mammalian sequences. Although the overall structures are valid, there are some minor differences between the *Arabidopsis* structures and the mammalian structures caused by insertions in the *Arabidopsis* proteins. The insertions generally are small, with an average size of 5.0 residues for 5 inserts in the *Arabidopsis* Gα-subunit and an average size of 2.3 residues for 10 inserts in the *Arabidopsis* Gβ-subunit. The unpredicted conformations are colored green in Figure 2B.

Are there G-protein coupled receptors in plants?

In animal most of G-protein coupled receptors (GPCRs) are proteins composed of a single chain, which possesses seven hydrophobic regions of sufficient length to span the plasma membrane. It was previously shown that plant G-proteins may interact with plant receptors such as phytochrome, and auxin binding proteins. In fact, these receptors clearly do not belong to the family of GPCRs. To date no GPCR has been isolated from plant tissues to be
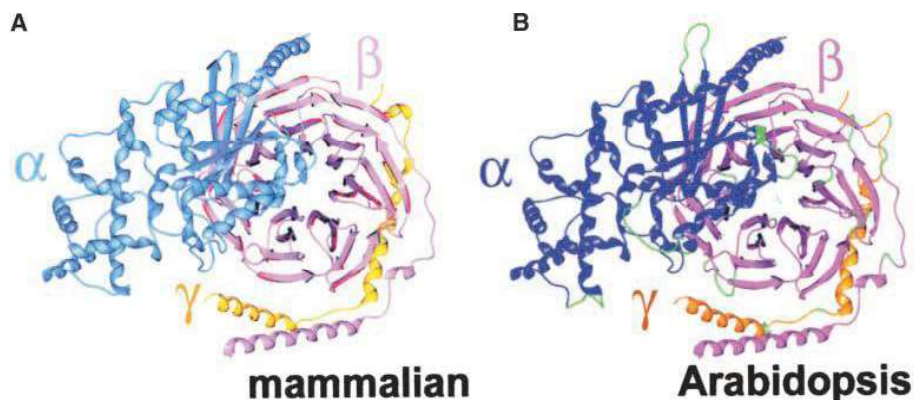
Figure 2. Modeling the *Arabidopsis* Heterotrimeric G-Protein Complex.
(A) and **(B)** Homology models were built for the GPA1, AGB1, and AGG1 deduced protein sequences from *Arabidopsis* using the Insight II molecular modeling system from Accelrys, Inc. The macromolecular structures were built using an experimentally determined structure of a mammalian G-protein heterotrimer (PDB access code 1GOT.pdb) as the template. The structure of the mammalian heterotrimer used as the template is shown in **(A)**, and the predicted structure of the *Arabidopsis* G-protein heterotrimer is shown in **(B)**. The α-monomers are shown in cyan, the β-monomers are shown in magenta, and the γ-monomers are shown in gold.

directly coupled by G-proteins. Furthermore, in contrast to the thousand or more heptahelical transmembrane proteins in animals, plants have only a few candidates confirmed to be heptahelical to date.

In a last decade there were few cases of cloning proteins which possess hydrophobic heptahelical transmembrane spanning regions.

These proteins share some sequence identity to animal GPCRs. The cloned from *Arabidopsis* seven transmembrane protein was similar to cAMP receptor from *Dictyostelium discoideurn* and author philogenetically include it to rhodopsin family (Josefsson and Rask, 1997). Cloned another 7-transmembrane plant receptor (Plakidou-Dymock et al., 1998) was identified in root and leaves of *Arabidopsis* and it was encoded with single copy of gene. Expressed by this gene protein has effect on sensitivity of plant to cytokinins.

One of these proteins, called MLO1, confers resistance to powdery mildew when present in its recessive form, but the mechanism of resistance is unknown. Recent evidence indicates that disease resistance conferred by *mlo* is not dependent on a G-protein (Devoto et al., 1999; Kim et al., 2002). However, the possibility remains that MLO is coupled by a G-protein in another signaling pathway because the function of this putative orphan receptor is unknown.

The gene cloned by Josefsson (Josefsson and Rask, 1997) from *Arabidopsis* called G-coupled receptor1 (GCR1) shares some sequence identity to animal GPCRs of the rhodopsin/serotonin family. GCR1 has a predicted heptahelical structure but this has not yet been confirmed by direct analyses. Overexpression of GCR1 modifies the cell cycle in a manner that is difficult to interpret (Colucci et al., 2002; Zhao and Wang, 2004). Specifically, M phase appears to be uncoupled from S. On the other hand, *gcr1* loss-of-function mutants do not share any of the G-protein mutant phenotypes, suggesting either that GCR1 is not coupled by GPA1 or that the GCR1 function is redundant (Chen et al., 2004).

Receptor-independent, G-protein signaling occurs in animals. Using a functional screen in yeast, Lanier's group (Cismowski et al., 2001) found three proteins (activator of G-protein signaling-1–3 [AGS1–3]) that are capable of activating G-protein signaling in the absence of a cognate receptor. Perhaps the most interesting of these is AGS3, which has subsequently been shown to be a guanine dissociation inhibitor (GDI) (Natochin et al., 2000, 2001). AGS3 binds the GDP-bound form of $G\alpha$ to release $G\beta\gamma$ via a protein interaction involving a GoLoco motif. In yeast, this interaction directly activates a mitogen-activated protein (MAP) kinase pathway (Elion, 2000). However, there are not evidence AGS3 homologs or GoLoco containing proteins exist in plants.

Thus, we are left with only three possible conclusions: in contrast to animals, plants couple only one or a few heptahelical receptors by a G-protein to downstream effectors; and/or receptor-independent G-protein signaling is the primary mechanism in plants; and/or plants couple nonheptahelical receptors. Although the jury is still out, some interesting facts shed light on this problem. First, the carboxy-terminal domain of all plant G-protein orthologs is nearly 100% conserved, whereas in animals this region is poorly conserved due to the diversity of $G\alpha$–receptor interactions. Complete conservation in sequence among plant $G\alpha$ carboxy-terminal domains suggests that there is a single or only a few receptors with which plant $G\alpha$ can interact. Second candidate as potential receptors for $G\alpha$ activation can be non membrane spanning protein like plant photoreceptors phytochromes. Previous observation indicate that special analogue of GTP - Gpp(NH)p activate that fractions of cAMP related enzymes which isolated from irradiated by red light seedlings, while enzyme isolated from etiolated seedlings wasn't sensitive to Gpp(NH)p (Gasimov and Fedenko, 1992; Fedenko and Gasimov, 1993). Third, indirect observations are consistent with G-coupling to nontraditional receptors like brassinosteroid (BR) (Ullah et al., 2002) and BR receptor-like kinase. These recent observations raise the exciting possibility that G-protein couples one or more of the more than 400 receptor-like kinases in plants (Mason and Botella, 2001).

G-proteins and plant hormones

The action of plant hormones at the cellular level is still poorly understood. However, some hormone receptors have been characterized and there is evidence that G-proteins could be involved in plant hormone mediated signalling.

Arabidopsis gpa1 mutants, which lack GPA1, have reduced cell division during hypocotyl and leaf formation (Ullah et al., 2001). The overexpression of GPA1 causes ectopic cell divisions, including massive overproliferation of meristem formation at high GPA1 expression levels. Overexpression of pea $G\alpha$ stimulates cell division in yeast (Kim et al., 2002). These observations suggest that GPA1 couples a signal that controls cell division. A likely candidate is auxin. Auxin increased $GTP\gamma S$ binding to microsomal membranes of *Daucus carota* (Zbell et al., 1990) and to rice aerobic coleoptiles (Zaina et al., 1990). Auxin was also shown to increase GTPase activity in rice coleoptile membranes (Zaina et al., 1991). However, auxin-induced cell division occurs in mutants that lack

either Gα or Gβ, indicating that auxin cannot be coupled directly by a G-protein (Ullah et al., 2003). However, although G-protein mutants respond to auxin, they have dramatically altered auxin sensitivity. It is therefore possible that some other, as yet unknown, G-protein-coupled pathway interacts with auxin signaling in a way that controls auxin sensitivity.

Ca^{2+}-dependent swelling of mesophyll protoplasts from dark-grown wheat was shown to be induced by auxin, gibberelic and abscisic acid. The swelling could be inhibited by GDPβS, indicating the involvement of G-proteins in the process (Bossen et al., 1991). Unlike auxin signaling, an abscisic acid (ABA) signaling pathway appears to be directly coupled by a G-protein. Wang et al. (2001) demonstrated that ABA inhibition of light-induced stomatal opening is completely lacking in *gpa1* mutants. Consistent with this loss of ABA responsiveness, ABA does not inhibit inward K^+-channels or activate pH-independent anion channels in *gpa1* mutants (Figure 3). Interestingly, ABA-induced stomatal closure that is mediated by a pH change remains unaffected by the loss of GPA1 function, indicating that there are ABA pathways that are independent of G-protein in guard cells (Wang et al., 2001; Assmann, 2002).

The putative GPCR GCR1 is known to modulate signaling in guard cells in an unexpected manner: *gcr1*-knockout plants are hypersensitive to both ABA and S1P in stomatal aperture responses, and also show hypersensitivity to ABA in root-growth assays and foliar gene expression (Pandey and Assman, 2004). These results indicate that GCR1 functions as a negative regulator of these responses.

Not only a specific cell type contain multiple signaling mechanisms for one hormone, such as ABA, but different cell types can also have different mechanisms for the same hormone (Ullah et al., 2002). For example, although the guard cells of *gpa1* mutants are ABA insensitive, *gpa1* seeds have wild-type sensitivity to ABA but are 100-fold less sensitive to gibberellic acid (GA) and completely insensitive to brassinosteroid (BR). Seeds that overexpress GPA1 are a million-fold more sensitive to GA than wild-type seeds but still require GA for germination. One interpretation of these loss- and gain-of-function results is that GA signaling in seed germination is not directly coupled by G, but rather that some other G-coupled pathway crosstalks in a way that controls GA sensitivity. This indirect effect on a pathway via control of sensitivity is a reoccurring theme. Because it is known that BR regulates GA sensitivity, and that seeds that have reduced GA levels will fully germinate when treated with BR, it is possible that a BR pathway coupled

by a G-protein is the sought after pathway that controls GA sensitivity (Figure 3A). Consistent with this, Ullah et al. (2002) have shown that BR synthesis and response mutants have the same reduced GA sensitivity as *gpa1* mutants, and that BR was completely ineffective at rescuing the germination of *gpa1* seeds when GA levels were reduced.

G-proteins and photosignal transduction

The classic example of the molecular mechanism of photosignal transduction by heterotrimeric G-protein to a downstream effector is vision in animals where the alpha subunit of the cognate heterotrimeric complex, transducin, couples the activated heptahelical membrane receptor rhodopsin to its cGMP phosphodiesterase effector in rod photoreceptor cells (Baylor, 1996). Plant cells are also light sensitive, especially in the red (R)/far-red (FR) light spectral region due to its highly light-sensitive family of photoreceptors called phytochrome. Therefore, an obvious question has been whether phytochrome light perception is similarly coupled by a heterotrimeric G-protein to an unidentified downstream effector.

In early 1990s it was shown the involvement of G-proteins in the phytochrome response. It was shown both red and far red light inhibits GTPγS binding in *L.paucicostata* (Hasunuma et al., 1987). In contrast, in *A.sativa* microsomal membranes (Romero et al., 1991) and in *Medicago sativa* plasma membranes (Muschietti et al., 1993), red light stimulated GTPγS binding while far red light reversed the effect of red light. Some phenotypes of a tomato (*Lycopersicon esculentum*) phytochrome mutant could be rescued to wild type by pertussis and cholera toxins, agents that stabilize the activated form of the G-protein subunit by different means (Neuhaus et al., 1993; Bowler et al., 1994). Microinjection of phytochrome A into aurea cells restored phytochrome-mediated effects. Injection of *Pertussis* toxin or GDPβS (which keep the G-proteins in their trimeric inactive form) with phytochrome A blocked the response. Injection of high GTPγS concentrations (30-100 mM) or coinjection of cholera toxin and low GTPγS concentrations (1 mM) produced an intracellular response indistinguishable from that mediated by phytochrome A.

Our observations have shown red light dependent response of cAMP phosphodiesterase to the action of GTP analog – Gpp(NH)p (Fedenko and Gasimov, 1993; Gasimov and Fedenko, 1992). Addition of Gpp(NH)p to reaction mixture resulted in increasing of phosphodiesterase activity from irradiated by relight maize seedlings, while enzyme from etiolated seedlings was insensitive to the action Gpp(NH)p. And recent our studies indicated that red light induces sensitivity of adenilylcyclase isolated from etiolated sorghum seedlings to the

action of Gpp(NH)p while far red light did not effect sensitivity of adenilylcyclase to Gpp(NH)p (Gasimov, 2008). These observations led to conclude that a heterotrimeric G-protein was positioned downstream of phytochrome (very likely phytochrome-B) in the light signal transduction pathway and upstream of a cNMP mediated step, in analogy to light perception in visual cascade.
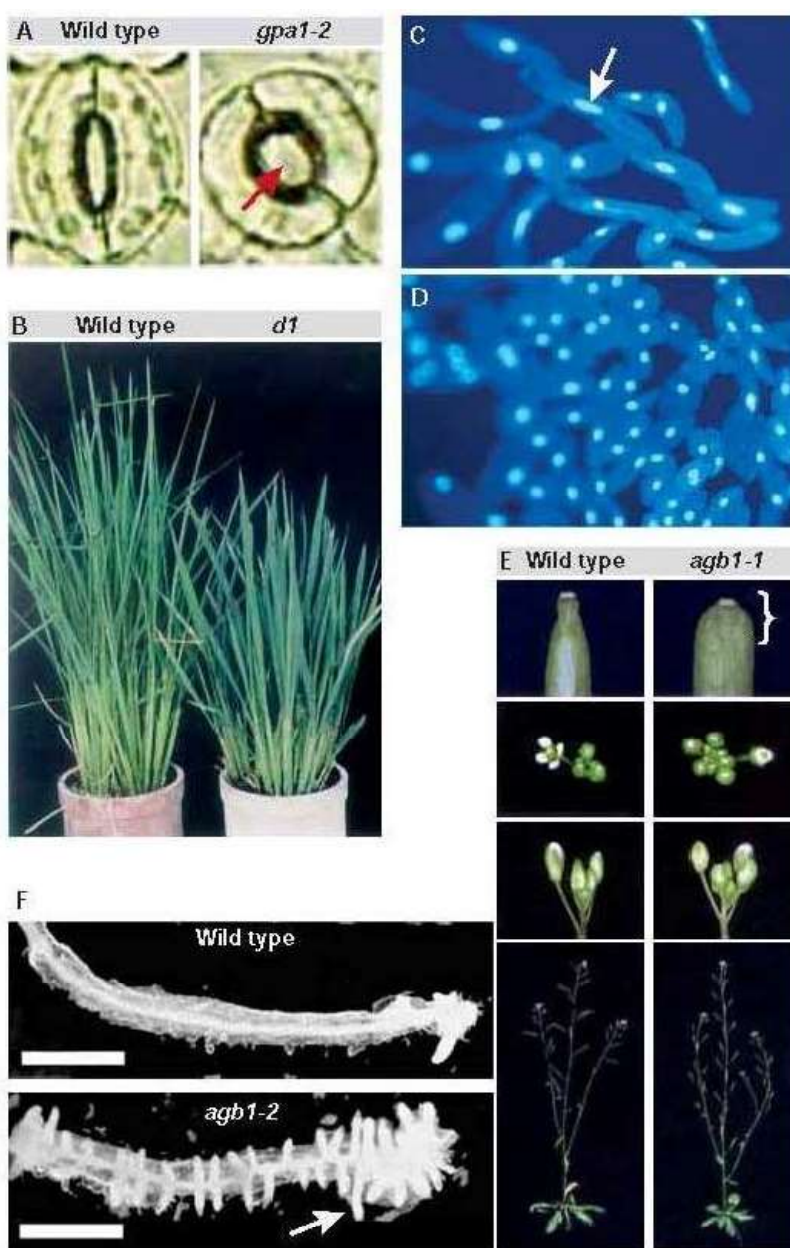
Figure 3. Selected phenotypes of plant G-protein mutants. (**A**) Guard-cell pairs on the surface of wild-type or *gpa1-2* Gα-null mutant leaves. *gpa1-2* guard cells fail to respond to the stress hormone abscisic acid (ABA) and consequently the pore of the stomate is open (red arrow). (**B**) The dwarf rice variety *d1* has a mutation in the Gα gene *RGA1*. (**C**) Ectopic *GPA1* expression in cultured tobacco cells causes a premature advance in the nuclear cycle. Note the larger nuclei (white arrow) in cells overexpressing Gα (**C**) versus control cells (**D**). (**E**) *agb1* (Gβ) mutants show phenotypes in the fruit (top two panels), flower morphology (middle four panels) and flowering stems (bottom two panels), which indicates that Gβ operates throughout development. (**F**) Gβ mutants have increased cell division in lateral root meristems, which leads to excessive root formation (white arrow) after treatment with the phytohormone auxin. AGB1 acts as a repressor of cell division in lateral root primordial.

Several other labs used pharmacological approaches in different systems and came to the same conclusion. Microinjection of GDPβS blocked R-induced protoplast swelling, whereas GTPγS induced swelling in darkness (Bossen et al., 1991). Cholera toxin was shown to increase the steady-state mRNA levels of the light-regulated gene, CAB (Romero and Lam, 1993).

More recently, Okamota and colleagues took a gain-of-function approach to test this hypothesis and concluded with all previous authors that a heterotrimeric G-protein is involved in phytochrome-mediated signal transduction (Okamota et al., 2001). The authors reported that *Arabidopsis* ectopically overexpressing the α-subunit of the heterotrimeric G-protein, regardless of the G-activation state, was hypersensitive to R and FR. And recent studies in the lab Jones (Jones et al., 2003) indicated the role of the single canonical heterotrimeric G-protein in R and FR control of hypocotyl growth using a loss-of-function approach. Single- and double-null mutants for the GPA1, AGB1 genes encoding the α- and β-subunit of the heterotrimeric G-protein, respectively, have wild-type sensitivity to R and FR. Ectopic overexpression of wild type and a constitutive active form of the α-subunit and of the wild-type β-subunit had no effect that can be unequivocally attributed to altered R and FR responsiveness. These results preclude a direct role for the heterotrimeric G complex in R and FR transduction in *Arabidopsis* leading to growth control in the hypocotyls (Jones et al., 2003).

Although heterotrimeric G-proteins appear to be involved in the phytochrome signal transduction pathway, the mechanism of interaction between the molecules is not clear. Phytochrome is a cytosolic protein and it is not structurally related to G-protein coupled receptors which are integral membrane proteins. However upon red light activation the phytochrome B precipitate in membrane fraction which can explain the way of signal transmission from photoreceptor to G-protein. On the other hand it is possible that an intermediate may transduce the signal from Pfr to G-proteins.

G-proteins and cell division

Congruent with their role in mammalian cells, G-proteins also regulate cell proliferation in plants (Ullah et al., 2001). During seed germination, massive cell proliferation occurs and the evidence supports a role for G-proteins in this process. For example, the plant hormones GA and brassinosteroid (BR) promote seed germination, whereas ABA inhibits seed germination and seedling development, and promotes seed dormancy. Seeds with ectopic overexpression of GPA1 are hypersensitive to GA (Colucci et al., 2002; Ullah et al., 2002), and overexpression of GCR1 reduces seed dormancy and promotes cell division (Apone et al., 2003). Conversely, *gpa1-* and *gcr1*-null lines show reduced seed germination in response to exogenous GA and BR (Chen et al., 2004). However, *gcr1/gpa1* double-mutants have an additively or synergistically attenuated response to GA and BR, which indicates that GCR1 has a role in seed germination that is independent of the heterotrimeric G-protein (Chen et al., 2004). Similarly to *Arabidopsis*, seeds of rice RGA1 antisense lines show reduced physiological and transcriptional responses to GA (Figure 3B) (Ueguchi-Tanaka et al., 2000).

Seeds that are mutant for *gpa1* show moderately enhanced sensitivity to ABA inhibition of germination, and seeds that lack the GPA1 interactor PIRIN1 are also hypersensitive to ABA, which indicates that PIRIN1 might be an effector in this response (Lapik and Kaufman, 2003). This is in contrast to the reduced ABA sensitivity of *gpa1* guard cells, which indicates that specific cell types might use GPA1 in different ways in response to an identical signalling molecule; a phenomenon that is also observed in mammalian G-protein pathways (Albert and Robillard, 2002). GPA1 and AGB1 are strongly expressed in meristems, in which the maintenance of a stem-cell population allows indeterminate growth (Huang et al., 1994; Kaydamov et al., 2000). Seedlings of *gpa1*-knockout lines have short hypocotyls that result from a decreased number of cells. *gpa1* mutants also show a reduced number of epidermal cells in leaves and reduced expression of a mitotic reporter, whereas GPA1-overexpressing plants show ectopic cell division in the epidermis (Ullah et al., 2003; Jones et al., 2004). Ectopic GPA1 expression in cells mimics an auxin-induced advance in the nuclear cycle (Figure 3C and D). The rice mutant *d1* has reduced GA sensitivity in internode elongation, which accounts for its dwarf phenotype, but shows wild-type growth responses in other vegetative organs (Ashikari et al., 1999; Ueguchi-Tanaka, 2000). Considering the central importance of G-proteins in many hormone-mediated cell-division pathways, it is not surprising that these mutants have pleiotropic phenotypes (Figure 3E). In mammalian cells, Gα-subunits have been identified as oncogenic determinants (Morris and Malbon, 1999), whereas Gβγ subunits have not. By contrast, in some plant organs, Gβγ seems to be the active form in controlling cell proliferation, albeit in the opposite direction. *Arabidopsis* lines that lack *AGB1* develop excessive lateral roots, whereas overexpression of *AGB1* results in the suppression of cell division stimulated by the plant hormone auxin (Ullah et al., 2003). These results indicate that free Gβγ is a negative regulator of auxin-induced cell division in the lateral root meristem. Consistent with this hypothesis, the overexpression of wild-type GPA1, which is

expected to sequester Gβγ-subunits, promotes lateral-root formation in response to auxin, whereas in *gpa1*-knockout lines this activity is reduced (Ullah et al., 2003). By contrast, in the primary root meristem, increasing the levels of active GPA1 either through the ectopic expression of a GTPase-deficient GPA1 (GPA1QL mutant) or loss-of-function of RGS1 promotes cell proliferation. Clearly, plant heterotrimeric G-proteins function in a cell-type-dependent manner. Specifically, primary root stem cells are positively regulated by the activated Gα-subunit, whereas lateral root stem cells are negatively regulated by the Gβγ-subunits (Figure 3F). The simplest model for this specificity follows the classic model of differential coupling mediated through one type of effector/receptor pair in one cell type and a different pair in another.

However, it remains plausible that there is only one set of receptor–effector coupling involving both the Gα- and Gβγ-subunits, perhaps antagonistically, and that the specificity is manifest through the balance of these subunits in different cells.

CONCLUSIONS AND FUTURE PROSPECTS

Although many details remain to be studied, the researches described above confirm that the plant heterotrimeric G-proteins are essential in at least three processes that are fundamental for the existence of all multicellular organisms: ion homeostasis, cell proliferation and photomorphogenesis. Plants probably have only two heterotrimer combinations G-proteins and analogues of the mammalian receptors and effectors. Therefore it could provide a simpler system in which to understand how these effectors are modulated in multicellular organisms. However there is not evidence confirming coupling of plant GCR and plant Gα-proteins similar in animal mechanism, but it is evident in this review that, numerous processes at all stages of plant development are modulated by heterotrimeric G-proteins.

Some of the many signals proposed to be coupled directly by G-proteins in plants may actually lie on pathways that are only indirectly regulated by G-proteins. The final integration of G-protein signalling emerges as physiological regulation. Once molecular biology completes the identification of the member(s) of the GPCR (GCR), G-protein subunits, effectors, and interacting proteins, the task at the cellular level will be to explore how regulation cell proliferation and plant morphogenesis goes on. The pace and intensity of the effort suggest that much will be gained well before decade has passed.

REFERENCES

Gasimov K.G. (2008) Reaction of photoinduced nucleotide cyclase of etiolated seedlings of sorghum under the effect of Gpp(NH)p. Transactions of Botanical Institute of Azerbaijan National Academy of Sciences. **XXVIII:** 266-270.

Fedenko Y.P., Gasimov K.G. (1993) The effect of Gpp(NH)p on basal and photoinduced activities of cyclic AMP phosphodiesterase in maize sprouts. Izvestia Rossiyskoy AN (biological sciences) **1:** 133-136.

Gasimov K.G., Fedenko Y.P. (1992) The effect of Gpp(NH)p on cyclic AMP phosphodiesterase isolated from etiolated and irradiated with red light maize sprouts. Dokladi Rossiyskoy AN **324(2):** 492-494.

Aharon G.S., Snedden W.A., Blumwald E. (1998) Activation of a plant plasma membrane Ca^{2+} channel by TGα1, a heterotrimeric G-protein α-subunit homologue. FEBS Lett. **1424:** 17-21.

Albert P.R., Robillard L. (2002) G-protein specificity: traffic direction required. Cell Signal. **14:** 407-418.

Apone F., Alyeshmerni N., Wiens K., Chalmers D., Chrispeels M.J., Colucci G. (2003) The G-protein-coupled receptor GCR1 regulates DNA synthesis through activation of phosphatidylinositol-specific phospholipase C. Plant Physiol. **133:** 571-579.

Ashikari M., Wu J., Yano M., Sasaki T., Yoshimura A. (1999) Rice gibberellininsensitive Dwarf gene *dwarf1* encodes the α subunit of GTP-binding protein. Proc. Natl. Acad. Sci. USA **96:** 10284-10289.

Assmann S.M. (2002) Heterotrimeric and unconventional GTP binding proteins in plant signalling. Plant Cell **14(Suppl.):** 355-373.

Baylor D. (1996) How photons start vision. Proc. Natl. Acad. Sci. USA **93:** 560-565.

Barbacid M. (1987) Ras Genes. Annu. Rev. Biochem. **56:** 779-827.

Bossen M.E., Tretyn A., Kendrick R.E., Vredenberg W.J. (1991) Comparison between swelling of etiolated wheat *(Triticum aestivum* L.) protoplasts induced by phytochrome and α-naftaleneacetic acid, benzylaminopurine, gibberelic acid, abscisic acid and acetylcholine. Plant Physiol. **137:** 706-710.

Bowler C., Neuhaus G., Yamagata H., Chua N.H. (1994) Cyclic GMP and calcium mediated phytochrome phototransduction. Cell **77:** 73-81.

Chen J.-G., Pandey S., Huang J., Alonso J.M., Ecker J.R., Assmann S.M., Jones A.M. (2004) GCR1 acts independently of heterotrimeric G-protein in response to brassinosteroids and gibberellins in *Arabidopsis* seed germination. Plant Physiol. **135(2):** 907-915.

Chen J.-G., Pandey S., Huang J., Alonso J.M., Ecker J.R., Assmann S.M., Jones A.M. (2004) GCR1 can act independently of heterotrimeric G-protein in response to brassinosteroids and gibberellins in *Arabidopsis* seed germination. Plant Physiol. **135**: 907-915.

Cismowski M.J., Takesona A., Bernard M., Duzic E., Lanier S.M. (2001) Receptor-independent activators of heterotrimeric G-proteins. Life Sci. **68**: 2301-2308.

Colucci G., Apone F., Alyeshmerni N., Chalmers D., Chrispeels M.J. (2002) GCR1, the putative *Arabidopsis* G protein-coupled receptor gene is cell cycle-regulated, and its overexpression abolishes seed dormancy and shortens time to flowering. Proc. Natl. Acad. Sci. USA **99**: 4736-4741.

Devoto A., Piffanelli P., Nilsson I., Wallin E., Pansruga R., von Heijne G., Schulze-Lefert P. (1999) Topology, subcellular localization, and sequence diversity of the Mlo family in plants. Biol. Chem. **274**: 34993-35004.

Elion E. (2000) Pheromone response, mating and cell biology. Curr. Opin. Microbiol. **3**: 573-581.

Gibbs J.B., Sigal I.S., Scolnick E.M. (1985) Biochemical properties of normal and oncogenic ras p21. Trends Biochem. Sci. **10**: 350-353.

Hasunuma K., Furukawa K.T., Funadera K., Kubita N., Watanabe M. (1987) Partial characterization and light-induced regulation of GTP-binding proteins in *Lemna paucicostata*. Photochem. Photobiol. **46**: 531-535.

Huang H., Weiss C., Ma H. (1994) Regulated expression of the *Arabidopsis* G protein α-subunit gene GPA1. Int. J. Plant Sci. **155**: 3-14.

Jones A.M., Ullah H., Chen J.-G. (2004) In: Tobacco BY-2 Cells, Biotechnology in Agriculture and Forestry Series (Nagata T., Lörz H., Widholm J.M., eds.), Springer, Tokyo, Japan **53**: 181-191.

Jones A.M., Ecker J.R., Chen J.G. (2003) A reevaluation of the role of the heterotrimeric G-protein in coupling light responses in *Arabidopsis*. Plant Physiol. **131**: 1623-1627.

Josefsson L.G., Rask L. (1997) Cloning of a putative G-protein-coupled receptor from *Arabidopsis thaliana*. Eur. J. Biochem. **249**: 415-420.

Kato C., Mizutani T., Tamaki H., Kumagai H., Kamiya T., Hirobe A., Fujisawa Y., Kato H., Iwasaki Y. (2004) Characterization of heterotrimeric G-protein complexes in rice plasma membrane. Plant J. **38**: 320-331.

Kaydamov C., Tewes A., Adler K., Manteuffel R. (2000) Molecular characterization of cDNAs encoding G-protein α and β subunits and study of their temporal and spatial expression patterns in *Nicotiana plumbaginifolia*. Biochim. Biophys. Acta **1491**: 143-160.

Kleuss C., Raw A.S., Lee E., Sprang S.R., Gilman A.G. (1994) Mechanism of GTP hydrolysis by G-protein alpha subunits. Proc. Natl. Acad. Sci. USA **91**: 828-831.

Kim M.C., Panstruga R., Elliott C., Muller J., Devoto A., Yoon H.W., Park H.C., Cho M.J., Schutze-Lefert P. (2002) Calmodulin interacts with MLO protein to regulate defence against mildew in barley. Nature **416**: 447-450.

Lapik V.R., Kaufman L.S. (2003) The *Arabidopsis* cupin domain protein AtPirin1 interacts with the G-protein α subunit GPA1 and regulates seed germination and early seedling development. Plant Cell **15**: 1578-1590.

Lein W., Saalbach G. (2001) Cloning and direct G-protein regulation of phospholipase D from tobacco. Biochim. Biophys. Acta **153**: 172-183.

Ma H., Yanofsky M., Meyerowitz E.M. (1990) Molecular cloning and characterization of GPA1, a G-protein alpha subunit gene from *Arabidopsis thaliana*. Proc. Natl. Acad. Sci. USA **87**: 3821-3825.

Mason M.G., Botella J.R. (2000) Completing the heterodimer: isolation and characterization of an *Arabidopsis thaliana* G-protein γ-subunit cDNA. Proc. Natl. Acad. Sci. USA **97**: 14784-14788.

Mason M.G., Botella J.R. (2001) Isolation of a novel G-protein γ-subunit from *Arabidopsis thaliana* and its interaction with Gβ. Biochim. Biophys. Acta **1520**: 147-153.

Morris A.J., Malbon C.C. (1999) Physiological regulation of G protein-linked signaling. Physiol. Rev. **79(4)**: 1373-1430.

Muschietti J.P., Martinetto H.E., Coso O.A., Farber M.D., Torres H.N., Flawia M.M. (1993) G-protein from *Medicago sativa*: functional association to photoreceptors. Biochem. **291**: 383-388.

Natochin M., Gasimov K.G., Artemyev N.O. (2001) Inhibition of GDP/GTP exchange on G alpha subunits by proteins containing G-protein regulatory motifs. Biochem. **40(17)**: 5322-5328.

Natochin M., Lester B., Peterson Y.K., Bernard M.L., Lanier S.M., Artemyev N.O. (2000) AGS3 inhibits GDP dissociation from galpha subunits of the Gi family and rhodopsin-dependent activation of transducin. J. Biol. Chem. **275(52)**: 40981-40985.

Natochin M., Gasimov K.G., Moussaif M., Artemyev N.O. (2003) Rhodopsin determinants for transducin activation a gain-of-function approach. J. Biol. Chem. **278(39)**: 37574–37581.

Neuhaus G., Bowler C., Kern R., Chua N.H. (1993) Calcium/calmodulin-dependent and independent phytochrome signal transduction pathways. Cell **73**: 937-952.

Okamota H., Matsui M., Deng X.W. (2001) Overexpression of the heterotrimeric G-protein alpha subunit enhances phytochrome-mediated inhibition

of hypocotyl elongation. Plant Cell **13**: 1639-1652.

Pandey S., Assmann S.M. (2004) The *Arabidopsis* putative G-protein-coupled receptor, GCR1, interacts with the G protein α-subunit, GPA1 and regulates abscisic acid signalling. Plant Cell **16(6)**: 1616-1632.

Pierce K.L., Premont R.T., Lefkowitz R.J. (2002) Seven-transmembrane receptors. Nat. Rev. Mol. Cell Biol. **3**: 639-650.

Plakidou-Dymock S., Dymock D., Hooley R. (1998) A higher plant seven-transmembrane receptor that influences sensitivity to cytokinins. Curr. Biol. **8(6)**: 315-324.

Romero L.C., Lam E. (1993) Guanine nucleotide binding protein involvement in early steps of phytochrome-regulated gene expression. Proc. Natl. Acad. Sci. USA **90**: 1465-1469.

Romero L.C., Sommer D., Gotor C., Song P. (1991) G-proteins in etiolated Avena seedlings. Possible phytochrome regulation. FEBS Lett. **282**: 341-346.

Ueguchi-Tanaka M., Fujisawa Y., Kobayashi M., Ashikari M., Iwasaki Y., Kitano H., Matsuoka M. (2000) Rice dwarf mutant d1, which is defective in the α-subunit of the heterotrimeric G-protein, affects gibberellin signal transduction. Proc. Natl. Acad. Sci. USA **97**: 11638-11643.

Ullah H., Chen J.G., Young J.C., Im K.H., Sussman M.R., Jones A.M. (2001) Modulation of cell proliferation by heterotrimeric G-protein in *Arabidopsis*. Science **292**: 2066-2069.

Ullah H., Chen J.-G., Wang S., Jones A.M. (2002) Role of G-protein in regulation of *Arabidopsis* seed germination. Plant Physiol. **129**: 897–907.

Ullah H., Chen J.G., Temple B., Boyes D.C., Alonso J.M., Davis K.R., Ecker J.R., Jones A.M. (2003) The beta subunit of the *Arabidopsis*

G-protein negatively regulates auxin-induced cell division and affects multiple developmental processes. Plant Cell **15**: 393-409.

Vanderbeld B., Kelly G.M. (2000) New thoughts on the role of beta-gamma subunit in G-protein signal transduction. Biochem. Cell Biol. **78**: 537-550.

Wang X.Q., Ullah H., Jones A.M., Assmann S.M. (2001) G-protein regulation of ion channels and abscisic acid signaling in *Arabidopsis* guard cells. Science **292**: 2070-2072.

Weiss C.A., Garnaat C.W., Mukai Y., Hu Y., Ma H. (1994) Isolation of cDNAs encoding guanine nucleotide-binding protein β-subunit homologues from maize (ZGB1) and *Arabidopsis* (AGB1). Proc. Natl. Acad. Sci. USA **91**: 9554-9558.

Zaina S., Reggiani R., Bertani A. (1990) Preliminary evidence for involvement of GTP-binding protein(s) in auxin signal transduction in rice (*Oryza sativa* L.) coleoptile. J. Plant Physiol. **136**: 653-658.

Zaina S., Mapelli S., Reggiani R., Bertani A. (1991) Auxin and GTPase activity in membranes from aerobic and anaerobic rice coleoptile. Plant Physiol. **138**: 760-762.

Zbell B., Hohenadel I., Schwendemann I., Walter-Back C. (1990) Is a GTP binding protein involved in the auxin-mediated phosphoinositide response on plant cell membranes? NATO ASA Series H 44. (Konijn, T.M., Houslay M.D., van Haarstert P.J.M., eds.), Springer-Verlag, Heidelberg: 255-266.

Zhao J., Wang X. (2004) *Arabidopsis* phospholipase D1 interacts with the heterotrimeric G-protein α-subunit through a motif analogous to the DRY motif in G-protein-coupled receptors. J. Biol. Chem. **279**: 1794-1800.

Development of STS and CAPS Markers Specific to Genomes in the Tribe *Triticeae*

Alamdar Ch. Mammadov[1,2]*, Xiao-Mey Li[2,3], Richard R.-C. Wang[2]

[1]*Institute of Botany, Azerbaijan National Academy of Sciences, 40 Badamdar Shosse, Baku AZ 1073, Azerbaijan*
[2]*United States Department of Agriculture, Agricultural Research Service, Forage & Range Research Laboratory, Utah State University, Logan, UT 84322-6300, USA*
[3]*Institute of Botany, Chinese Academy of Sciences, Beijing 100093, China*

Wild *Triticeae* grasses serve as important gene pools for forages and cereal crops. Knowledge on their genome compositions is pivotal for efficient utilization of this vast gene pool in germplasm enhancement programs. Using DNA sequences of genome-specific RAPD markers, selected primers have been designed to develop sequence tagged site (STS) markers. Genome specificity was lost for a majority of RAPD-to-STS conversions due to the inward extension of primer sequences. However, successful conversion has been achieved for genomes E^b, E^e, St, H, Ns, W, V and Y (an unknown genome in many polyploid *Elymus* species). Several cleaved amplified polymorphic sequence (CAPS) markers were also developed to distinguish the E^b, E^e and R genomes. The identified STS and CAPS markers are useful in suggesting the presence of certain genome(s) in *Triticeae* species and in identifying the alien chromosome or chromosomal segment in wheat addition, substitution, or translocation lines. Use of STS markers has helped to identify wheat addition lines with W- and Y-genome chromosomes derived from hybrids of hexaploid wheat *Triticum aestivum* (AABBDD) and hexaploid *Elymus rectisetus* (StStWWYY). Seven disomic wheat addition lines having different E^b-genome chromosomes are confirmed by the CAPS markers for this genome. This study also provides evidence that barley yellow dwarf virus (BYDV) resistant germplasm lines from Purdue and China are different from those developed in Australia.

Keywords: Triticeae, genome, RAPD, genome-specific markers, evolution, homology

INTRODUCTION

Perennial *Triticeae* grasses serve as important gene pools for forages and cereal crops (Dewey, 1984). Knowledge on their genome compositions is pivotal for efficient utilization of this vast gene pool in germplasm enhancement programs. Despite the vast amount of genome research on *Triticeae* species, many of the approximate 350 species have not been scientifically confirmed for their genome compositions (http://herbarium.usu.edu/Triticeae /genmsymb.htm).

A number of genome-specific random amplified polymorphic DNA (RAPD) markers have been identified and sequenced in perennial *Triticeae* species (Wei and Wang, 1995; Zhang et al., 1998; Wang, unpublished). Many species- or genome-specific repetitive sequences have also been reported (Bedbrook et al., 1980; Rayburn and Gill, 1986; Zhang and Dvorak, 1990; Tsujimoto and Gill, 1991; Anamthawat-Jonsson and Heslop-Harrison, 1993; Li et al., 1995). Genome-specific molecular markers are useful in identifying the genome constitution of species in question (Svitashev et al., 1998).

Because RAPD marker is one of many amplified DNA fragments from the polymerase chain reaction (PCR) based on a one single primer 10 bases in length, inexperienced persons may have difficulty using the RAPD technique. Sequence-tagged-site (STS) markers (Tragoonrung et al., 1992) are PCR-based markers generated by a pair of primers (~20 bases long) that are designed according to known DNA sequences. Ideally, only one DNA fragment of a specific length (STS marker) will be amplified from the template DNA containing the target sequence. The STS markers will be more reproducible and specific than the original RAPD marker. On the other hand, the restriction fragment length polymorphism (RFLP) technique requires more genomic DNA and longer time to run an assay. Therefore, PCR-based markers such as STS and cleaved-amplified polymorphic sequence (CAPS; Konieczny and Ausubel, 1993) markers are preferred by most researchers. STS and/or CAPS markers have been developed for identification of species (Li et al., 2002) and chromosomes (Talbert et al., 1994; Blake et al., 1996;

Erpelding et al., 1996).

In this study, thirty-five sequenced markers presumably specific for various genomes in *Triticeae* were tested for conversion into STS or CAPS markers. The genome symbols are those designated by Wang et al. (1995). The genome specificity and utility of successfully-converted markers were demonstrated using some polyploid *Triticeae* species and wheat-alien addition, substitution, or translocation lines having chromosomes or chromosomal segments of perennial *Triticeae* species.

MATERIALS AND METHODS

Plant materials (Table 1) are raised from seeds and grown in a greenhouse at the USDA-ARS Forage & Range Research Laboratory (FRRL), Logan, Utah. All diploid and several polyploid species having known genomes were used in developing and screening of converted STS markers. Ten BYDV-resistant and -susceptible lines were provided by Dr. Herbert Ohm, Purdue University, Indiana; whereas three lines were provided by Prof. Z.-Y. Xin, Chinese Academy of Agricultural Sciences, Beijing, China. Wheat - *Elymus rectisetus* backcross derivatives were developed at FRRL. These lines and two polyploid *Thinopyrum* species were used for testing the utility of STS and CAPS markers.

RAPD marker sequences published in Li et al. (1995), Wei and Wang (1995), Zhang et al. (1998), and those unpublished by Wang were used for development of STS markers. STS primer pairs (Table 2) were designed for each sequenced genome-specific RAPD marker using program Primers3 (Rozen and Skaletsky, 1997) available online: (http://www.genome.wi.mit.edu/cgi-bin/primer/primer3.cgi). The selected new primer sites may or may not partially overlap with the original RAPD primer sites. Procedures for DNA extraction, PCR amplification, and visualization of amplification products follow those described by Li et al. (2002) with some modifications. Amount of template DNA in the 25 μl PCR reaction mix was 40 ng for diploid, 80 ng for tetraploid, 120 ng for hexaploid and 200 ng for decaploid species. PCR conditions, mainly the annealing temperature and number of amplification cycles, were tested and optimized for each assay.

If an STS assay failed to produce a target marker for the target genome but produced seemly new genome-specific PCR products, the specific STS products were excised from agarose gel, cloned into pCR2.1 of the TA cloning kit (Invitrogen, USA), and sequenced for a second round of STS development. When necessary, STS products from different genomes were converted to CAPS markers with several restriction endonuclease enzymes. The enzyme-digested PCR product was then separated in a 2% agarose gel containing ethidium bromide in 1ÇTBE.

RESULTS

Based on known sequences of 32 RAPD markers, 33 primer pairs were designed (Table 2). Out of the 33 assays, only eight assays (3, 7, 12, 14, 17, 28, 29, and 30; Table 2) successfully amplified the targeted genome-specific sequences. Five of these are shown in Figures 1 and 2. Both assays 32 (Figure 3) and 33 produced a single band of the target length from genomes P, E^b, and V (Table 2). From the first round of STS development, some potentially genome-specific markers were identified, cloned and sequenced. Second round STS development successfully produced new STS markers for genomes E^b, V (Figure 4), and H (Table 2, assays 33 to 36). E^b-specific STS marker was also developed in assay 3 (Figure 5a). However, assay 1 amplified one product of the expected length not only from the target genome E^b but also from non-target genomes E^e and R (Figure 5b). To differentiate these three genomes, the F03-1277bp products from E^b, E^e, and R genomes have been converted to CAPS markers using two restriction enzymes (Table 3, Figure 5c).

Triticum aestivum Ç *Elymus rectisetus* backcross derivatives were tested for the presence of **St-**, **W-**, or **Y**-genome chromosomes using the STS markers. The **St**-genome marker OPD15-**St**498 was not detected in any of the lines tested (Table 4). Lines 0291, 0297, 4319, and 4348 had been tested positive for the **W**-genome marker OPB03-**W**306. The presence of **Y**-genome marker OPB14-**Y**269 was detected in lines 0293, 0294, and 4687. Line 4431 had both OPB03-**W**306 and OPB14-**Y**269 (Table 4). Line 0290 possessed the OPB03-**W**306 marker in a much lower intensity than that in 0291 (Figure 6).

Using the OPF03-1277 marker, Purdue lines P1 to P10 were tested for the presence of E^b or E^e chromosomes (Figure 7), whereas the three Chinese lines T1 to T3 were tested along with seven wheat addition lines having different E^b chromosomes (Figure 8). Those lines with or without BYD resistance yielded the CAPS markers for the **R** genome instead of markers for E^b or E^e. Each of seven E^b chromosomes produced the E^b-specific CAPS marker bands using the *Eco*RI restriction endonuclease (Figure 8).

Two polyploid *Thinopyrum* species, *Th.intermedium* and *Th.ponticum*, were assayed using STS and CAPS markers (Table 5). Both species had the **St**-genome STS marker OPB04-**St**341, while only *Th.intermedium* had the **R**-genome

CAPS markers. The use of STS and CAPS markers to detect E^b or E^e in the two species was inconsistent; however, *Th.intermedium* was positive for E^b and *Th.ponticum* was positive for E^e.

Table 1. Plant materials used in various studies to test STS or CAPS markers.

Symbols	Species	ID #	Source	Notes
E^b	*Thinopyrum bessarabicum*	PI 531710	FRRL	=J
E^e	*Th.elongatum*	PI 531718	FRRL	=E
St^{st}	*Pseudoroegneria stipifolia*	PI 236668	FRRL	=S
St^l	*P.libanotica*	PI 338391	FRRL	=S
R	*Secale montanum*	PI 531829	FRRL	
		PI 531835	FRRL	
H	*Hordeum bogdanii*	PI 499501	FRRL	perennial
I	*Hordeum vulgare* var. **Walker**	PI 557000	USU	annual
P^c	*Agropyron cristatum*	PJ-3817	FRRL	
P^m	*A.mongolicum*	PI 499392	FRRL	
Ns^j	*Psathyrostachys juncea*	PI 314521	FRRL	
Ns^h	*Ps.huashanica*	PI 531823	FRRL	
Ns^f	*Ps.fragilis*	PI 343190	FRRL	
W	*Australopyrum retrofractum*	PI 531553	FRRL	
V	*Dasypyrum villosum*	D-2990	FRRL	annual
StY	*Elymus longearistatus*	PI 401282	FRRL	
StWY	*Elymus rectisetus*	JC1050	FRRL	
JSt(V-J-R)	*Thinopyrum intermedium*	PI 547315	FRRL	
EEEEE	*Th.ponticum*	PI 261098	FRRL	
ABD	*Triticum aestivum* var. **CS**	CI*tr* 14108	Missouri	annual
P1	*T.aestivum* lines with	P107	Purdue	R to BYDV
P2	*Th.intermedium* chromosome	961341A3-2-2		R to BYDV
P3	or segment	961341A3-1-2-3		R to BYDV
P4		98131A1-1-4-9		S to BYDV
P5		98134G4-1		R to BYDV
P6		P29 = GP-541		R to BYDV
P7		169-1		R to BYDV
P8		632-21		R to BYDV
P9		177-1		S to BYDV
P10		69-1		S to BYDV
T1	*T.aestivum* lines with	Y920592	China	R to BYDV
T2	*Th.intermedium* chromosome	Y920592		R to BYDV
T3	segment	D957-3		R to BYDV
0275, 0290, 0292, 0293, 0294, 0296, 4162, 4431, 4687.	*T.aestivum* lines with *Elymus rectisetus* chromosomes		FRRL	2n = 44
0291, 4319 4348, 4419 4660, 0297 4183	*T.aestivum* lines with *Elymus rectisetus* chromosomes		FRRL	2n = 42
$1E^b$ to $7E^b$	*T.aestivum* lines with a pair of *Th.bessarabicum* chromosome		CIMMYT	2n = 44

Table 2. Primers, GenBank identification numbers of template or marker sequences, target genomes, sequence tagged sites (STS) marker length in bp, polymerase chain reaction (PCR) conditions, and results of PCR with genomes in *Triticeae* (Li et al., 1995; Zhang et al., 1998).

| Assay	Primer name	5' ——————— 3'	GenBank ID	Genome	Expected length	Tm	Cycles	Results
1	OPF03F1 OPF03R1	TGATCACCTGGTTGATAAGTCA AAAGTATTATTCACTCAACCGGATCT	U43516[1]	E^b	1277	58 60	20 20	E^b, E^e, St, R E^b, E^e, R
2	OPN01F1 OPN01R1	GGAATTAAATCACATATGCTGTATGAC CTCACGTTGGTAAGGGAAGA	BV679216	E^b	261	60	25	E^b (strong), E^e (weak)
3	OPN03F1 OPN03R1	TGGTACTCCCCTACCTAAGCA CCCTAGATGTATGCAGGGTCA	BV679215	E^e	886	62	30	E^e (900 + 1400 bp) E^b (1400 bp)
4	OPD15F OPD15R	GTGCTGGTGCGGTCATAGA ATCCGTGCTTAGAAAGGTAGCA	BV679217	St	498	60	30	St, StY, StWY
5	OPB04F OPB04R	GGACTGGAGTTCAGAGCAATC GGACTGGAGTAGCTTTTCAAACA	BV679238	St	341	60	30	St, StY, StWY
6	OPM07F OPM07R	CGTGACTCAAAGAAATATTGTCAAA CCGTGACTCATGGAAAAGGA	BV679235	Ns	440	58	30	Ns
7	OPB03F2 OPB03R2	CCCCTGCCCGATAGATTTTA CATCCCCCTGGATAAATAAGTG	BV679211	W	306	60	30	W, StWY
8	OPF15F OPF15R	ACTCCCTGATAAGTGCTTGGA CAGTACTCCCAACCAGCACA	BV679212	W	575	60	40	W, StWY
9	OPB14F1 OPB14R1	TCCGGCTCTGGGATGTGAC TCCTGAAGGTAAAACTTTCTGTTTTT	BV679236	Y	269	55	30	StY, StWY
10	C08F2 OPC08R	GGCCACGTGTAGGAATGTG TGGACCGGGTGAGATGACAG	BV679210	E^b	400	55	30	E^b
11	C08F3 C08R	CAGTCCCCTTCATGTATATCCC TGGACCGGGTGAGATGACAG	BV679208	V	755	53	40	V
12	F15F3 F15R2	TCCCTGATAAGTGCTTGGAG GCACAACCCTCATAAGGAGGTA	BV679209	H	235	55	30	H
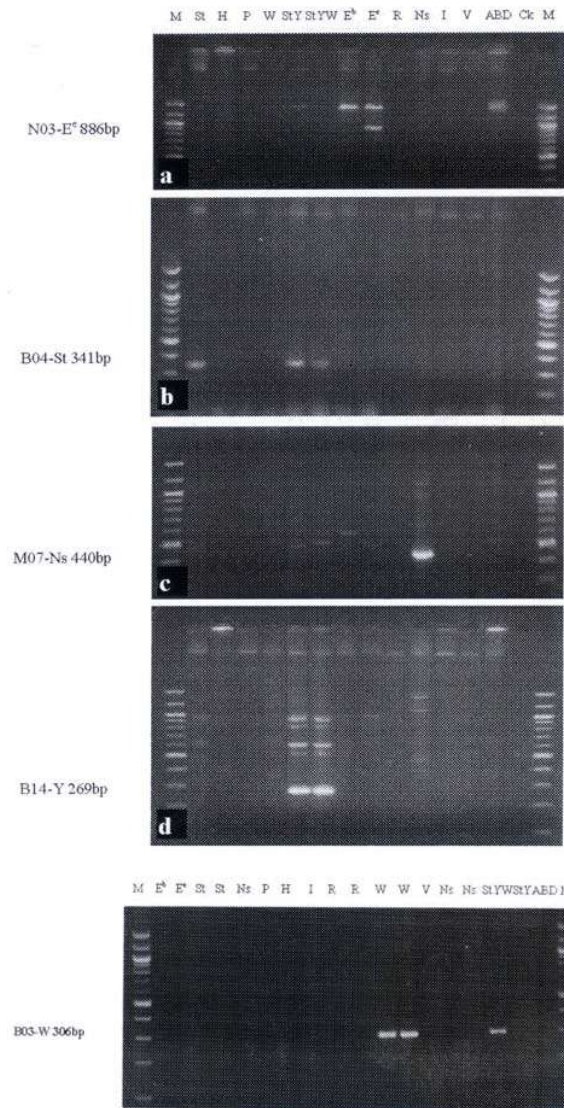
Figure 1. Four sequence-tagged-site (STS) markers for different genomes in the tribe *Triticeae*: (a) N03-E^{e}886 amplified at 62°C for 30 cycles using primers 5'-TGGT ACTCCCCTACCTAAGCA-3' and 5'-CCCTAGATGTA TGCAGGGTCA-3'; (b) B04-St341 amplified at 60°C for 30 cycles using primers 5'-GGACTGGAGTTCAGAG CAATC-3' and 5'-GGACTGGAGTAGCTTTTC AAA-CA-3'; (c) M07-Ns440 amplified at 58°C for 30 cycles using primers 5'-CGTGACTCAAAGAAATATT GTCAAA-3' and 5'-CCGTGACTCATGGAAAAGGA-3'; and (d) B14-Y269 amplified at 55°C for 30 cycles using primers 5'-TCCGCTCTGGGATGTGAC-3' and 5'-TCCTGAAGGTAAAACTTTCTGTTTTT-3'. Bands in lane M are size markers (top to bottom) 1500, 1200, 1000, 900, 800, 700, 600, 500, 400, 300, 200, and 100 bp. The control (Ck) has all reaction components except the template DNA.

Figure 2. Sequence-tagged-site (STS) marker B03-W306 for the W genome in the tribe *Triticeae*, amplified at 60°C for 30 cycles with primers 5'-CCCCTGCCCGATAGATTTTA-3' and 5'-CATCCCCCTGGATAAA TAAGTG-3'. Bands in lane M are size markers (top to bottom) 1500, 1200, 1000, 900, 800, 700, 600, 500, 400, 300, 200, and 100 bp.
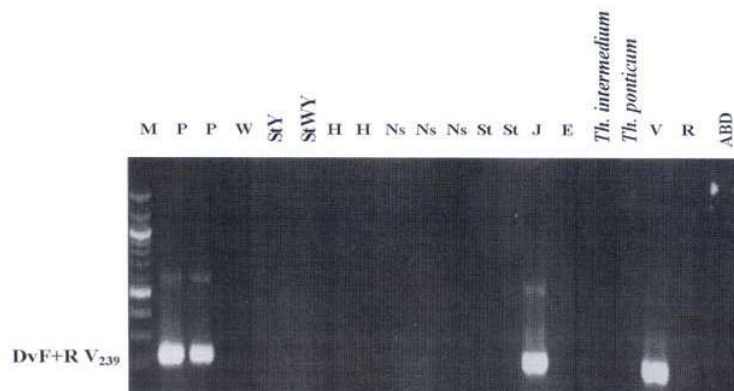

Figure 3. Sequence-tagged-site (STS) marker Dv-V239 using primers 5'-GGAACAATTTCGCA CTTACAGCTC-3' and 5'-CCTCGATACCTTTCCAACACCTAC-3' based on the sequence of AF472572 for the V genome in the tribe *Triticeae* is also amplified, at 57°C for 20 cycles, from the P genome of *Agropyron cristatum* and *A.mongolicum* as well as the E^b (=J) genome of *Thinopyrum bessarabicum*. It is amplified neither from other genomes nor from diploid *Th.elongatum*, hexaploid *Th.intermedium*, and decaploid *Th.ponticum*. Bands in lane M are size markers (top to bottom) 1500, 1200, 1000, 900, 800, 700, 600, 500, 400, 300, 200, and 100 bp.
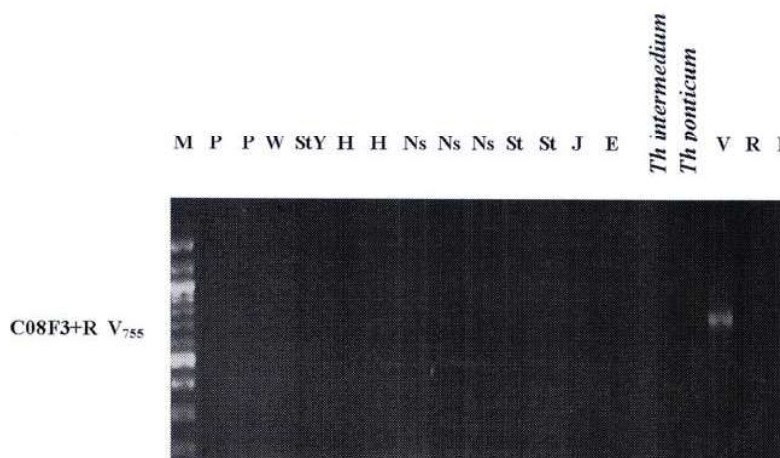
Figure 4. Second-round sequence-tagged-site (STS) marker C08-**V**755 amplified, with primers 5'-CAGTCCCCTTCATGTATATCCC-3' and 5'-TGGACCGGTGAGAT GA-CAG-3' at 53°C for 40 cycles, only from the **V** genome of *Dasypyrum villosum*. Bands in lane M are size markers (top to bottom) 1500, 1200, 1000, 900, 800, 700, 600, 500, 400, 300, 200, and 100 bp.
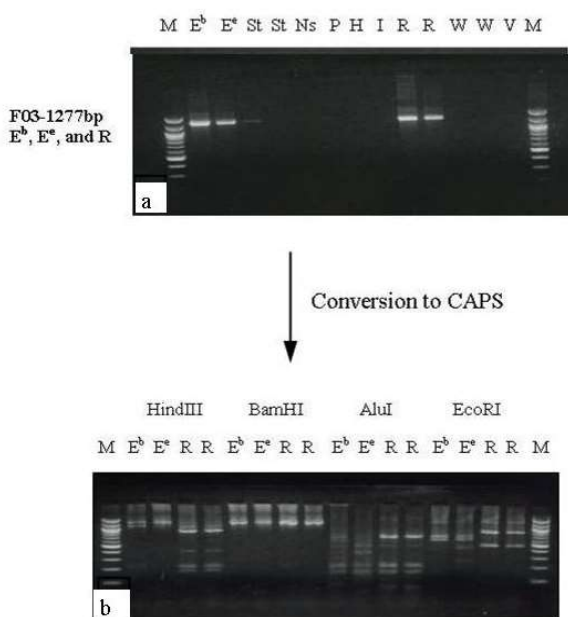

Figure 5. (a) Sequence-tagged-site (STS) marker N01-E^{b}261 amplified with primers 5'-GGAATTAA ATCACATATGCTGTATGAC-3' and 5'-CTCACG TTGGTAAGGGAAGA-3' at 60°C for 25 cycles for the E^b genome. (b) Primers 5'-TGATCACCTGGTT GATAAGTCA-3' and 5'-AAAGTATTTATTCACT CAACCGGATCT-3' amplified a 1277 bp fragment from E^b, E^e and R genomes. A faint band could be produced from the St genome. (c) The F03-1277 marker was converted to cleaved amplified polymorphic sequence (CAPS) markers using restriction endonucleases. Bands in lane M are size markers (top to bottom) 1500, 1200, 1000, 900, 800, 700, 600, 500, 400, 300, 200, and 100 bp.

Table 3. Cleaved amplified polymorphic sequence (CAPS) markers for E^b, E^e, and R genomes after restriction digestion by *Eco*RI or *Hin*dIII of the polymerase chain reaction (58° C, 20 cycles) product using primers F03F1 (5'- TGATCACCTGGTTGATAAGTCA-3') and F03R1 (5'-AAAGTATTTATTCACTCAACCGG ATCT-3'). Intense bands are highlighted in bold-face.

Genome	Restriction enzyme	Approximate length of CAPS markers
R	*Eco*RI	**500**, and **800**
	*Hin*dIII	190, 220, 400, **900**, and 1050
E^b	*Eco*RI	**600**, and **700**
	*Hin*dIII	220, **1050**, and **1250**
E^e	*Eco*RI	250, **450**, **600**, and **700**
	*Hin*dIII	**1250**

M 4687------4687 0275----------0275 0290----------0290 0291------0291 M

B03-W306
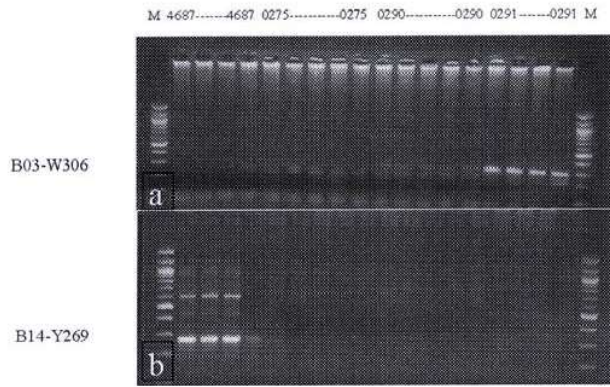
a

B14-Y269

b

Figure 6. Sequence-tagged-site (STS) markers B03-**W**306 for the **W** genome (a) and B14-**Y**269 for the **Y** genome (b) were used to detect the presence of alien-genome chromosomes in the backcross derivatives of *Triticum aestivum* Ç *Elymus rectisetus* hybrids: 4687 (2n=44, 4 plants), 0275 (2n=44, 5 plants), 0290 (2n=44, 5 plants), and 0291 (2n=42, 4 plants). 0290 and 0291 probably had different **W**-genome chromosomes, whereas 4687 had **Y**-genome chromosomes. Bands in lane M are size markers (top to bottom) 1500, 1200, 1000, 900, 800, 700, 600, 500, 400, 300, 200, and 100 bp.

Table 4. Results of STS assays on *Triticum aestivum* Ç *Elymus rectisetus* backcross derivatives to detect **St-**, **W-**, or **Y**-genome chromosomes.

Line ID	Origin	2n	OPB03-W306	OPB14-Y269	OPD15-St498
0275	1026-1-4-1	44	--	--	--
0290	1040-1-3-3	44	+	--	--
0291	1024-4-1-1	42	++	--	--
0292	1034-3-4-2	44	--	--	--
0293	1057-1-2-1	44	--	+	--
0294	1057-3-3-2	44	--	+	--
0296	1045-4-2-1	44	--	--	--
0297	1036-2-2-1	42	++	--	--
4162	1026	44	--	--	--
4183	1026	42	--	--	--
4319	1048	42	++	--	--
4348	1048	42	++	--	--
4419	1048	42	--	--	--
4431	1048	44	++	+	--
4660	1057	42	--	--	--
4687	1057	44	--	+	--

DISCUSSION

Conversion of molecular markers to STS markers is not an easy task. It requires a large number of markers from which suitable primer pairs can be designed. Then PCR conditions need to be optimized to yield discernible results for the target - a specific genome in our case. Even if the designed primer pairs encompass the 5' and 3' end sequences of the original marker, the STS assay may still fail to produce the specific marker from the target genome. We now have STS and CAPS markers for genomes E^b, E^e, **St**, **H**, **Ns**, **W**, **V**, **Y** and **R** (Tables 2 and 3). By using a combination of assays listed in Table 2, additional genomes may be identified. For example, positive assay 32 or 33 coupled with negative assays 3, 34, and 35 would help identify the **P** genome; and positive assay 26 and negative assay 17 might identify the **I** genome. In view of the low number of available genome-specific STS/CAPS markers, we might have to use

both RAPD and STS/CAPS markers in addition to other methods for genome analysis of *Triticeae* species, especially the polyploid species. However, positive results from STS/CAPS assays would first suggest the presence of specific genome(s) in polyploid *Triticeae* species; thus, reducing the number of crosses or procedures in subsequent methods of genome analysis, such as chromosome pairing in hybrids or genomic *in situ* hybridization (GISH).

Triticum aestivum Ç *Elymus rectisetus* hybrids were synthesized and backcrossed to wheat (Liu et al., 1994). Some backcross derivatives have been characterized using RAPD and GISH (Xue and Wang, 1999). Three types of addition lines were identified by RAPD markers: (1) 1048, (2) 1057, and (3) 1026 and 1034. In this study, we further verified that 1048 derivatives had **W**-genome chromosomes and 1057 derivatives had **Y**-genome chromosomes. Derivatives from 1026 and 1034 probably had **St**-genome chromosomes that were

M St Eᵇ Eᵉ R ABD P1 P2 P3 P4 P5 P6 P7 P8 P9 P10 Ck M

F03-1277bp

a

M Eᵇ Eᵉ R P2 P3 P4 P5 P8 P10 M

F03-1277bp
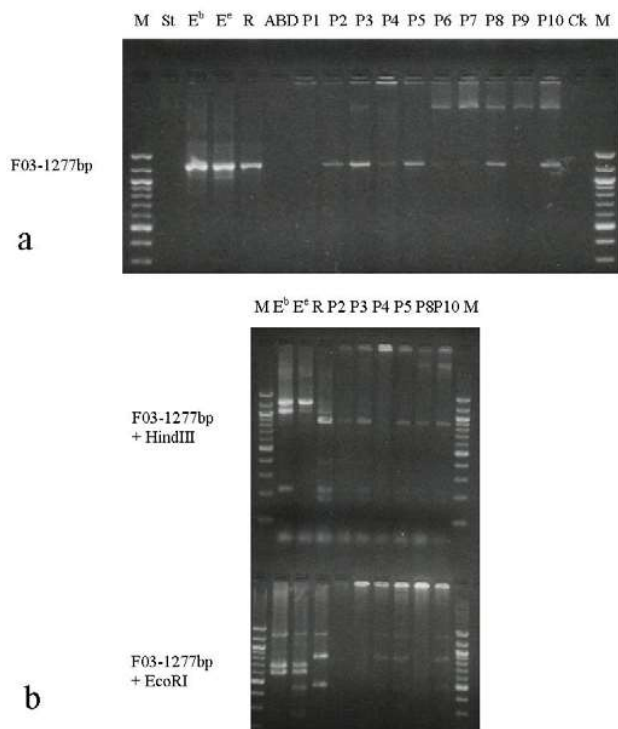+ HindIII

F03-1277bp
+ EcoRI

b

Figure 7. Purdue lines P1 to P10, developed for barley yellow dwarf virus resistance, were assayed for the sequence-tagged-site (STS) F03-1277 fragment (a) and those with the amplified product were assayed for the cleaved amplified polymorphic sequence (CAPS) markers using restriction enzymes *Hin*dIII and *Eco*RI (b). Bands in lane M are size markers (top to bottom) 1500, 1200, 1000, 900, 800, 700, 600, 500, 400, 300, 200, and 100 bp. The alien chromosomes in P2, P3, P4, P5, P8, and P10 contained the **R** genome-specific sequence instead of **E**- or **St**-specific sequence.

M Eᵇ Eᵉ R T1 T2 T3 1Eᵇ2Eᵇ3Eᵇ4Eᵇ5Eᵇ6Eᵇ7Eᵇ M
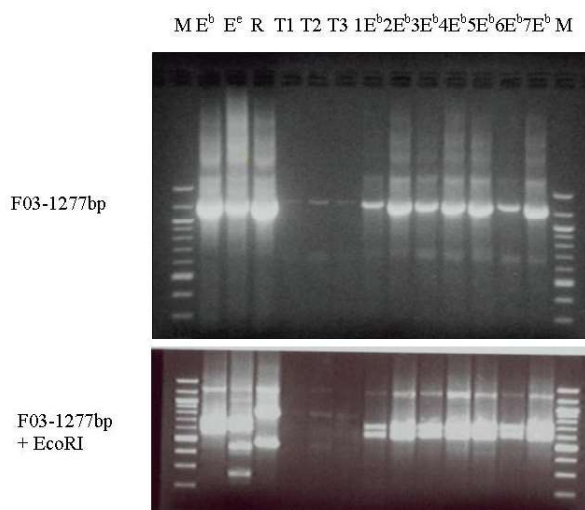

F03-1277bp

F03-1277bp
+ EcoRI

Figure 8. Chinese lines T1 to T3, developed for barley yellow dwarf virus resistance, and seven disomic wheat - *Thinopyrum bessarabicum* addition lines having different **Eᵇ** chromosomes, 1Eᵇ to 7Eᵇ, were assayed for the sequence-tagged-site (STS) F03-1277 fragment (top) and for the cleaved amplified polymorphic sequence (CAPS) markers using restriction enzyme *Eco*RI (bottom). Bands in lane M are size markers (top to bottom) 1500, 1200, 1000, 900, 800, 700, 600, 500, 400, 300, 200, and 100 bp. The alien chromosomes in T1, T2, and T3 contained the **R** genome-specific sequence instead of **E**- or **St**-specific sequence. All seven **Eᵇ** chromosomes contain the dispersed sequence U43516 from which the F03-1277 fragment was amplified.

not carrying the OPD15-**St**498 sequence. The fact that this **St**-genome STS marker worked with the whole **St** genome but not with individual **St** chromosomes, suggesting it is a repeated sequence occurring in few of the seven chromosomes, limits its usefulness. Nevertheless, we have identified: (1) 0291 as a wheat substitution lines having a pair of **W**-genome chromosomes, (2) 0290 as a wheat addition line having a different pair of **W**-genome chromosomes, (3) 0293, 0294, and 4687 as wheat

addition lines having a pair of **Y**-genome chromosomes, (4) 4431 as a wheat substitution-addition line with a pair of **W**-genome chromosomes and a pair of **Y**-genome chromosomes, and (5) 0297, 4319 and 4348 as wheat substitution lines having **W**-genome chromosomes in addition to probable **St** chromosomes. Lines 1036 and 1048 had been observed to possess 4 to 6 alien chromosomes in GISH studies (Xue and Wang, 1999 and unpublished).

Using F03-1277bp CAPS markers, we confirmed the presence of E^b-specific fragment in all seven chromosomes of the E^b genome (Figure 8). It has been shown by FISH that this sequence is a dispersed repetitive sequence occurring on all seven E^b genome chromosomes (Zhang et al., 1998). In contrast, the V-genome markers Dv-V239 or Dv-V205 (assays 32 or 33) developed from AF472572 should be present in six of the seven chromosomes of V-genome (Li et al., 1995). In the present study, these markers were also amplified from E^b and P genomes (Table 2), making them less genome-specific than the E^b CAPS markers.

The most surprising results in this study are the CAPS markers for the R genome observed in the Purdue and Chinese lines (Figures 7 and 8). All these lines were also developed from hybrids of wheat and *Th.intermedium* (Sharma et al., 1997, 1999; Crasta et al., 2000; Xin et al., 2001) but believed to be different from those developed in Australia (Banks and Larkin, 1995). The Australian derivatives were developed from the addition line L1 of Cauderon (1966), which has a pair of group-7 St chromosome (Hohmann et al., 1996; Wang and Zhang, 1996). *Thinopyrum intermedium* was given the E^bE^eSt and the JJ^sSt genome symbol by Liu and Wang (1993) and Chen et al. (1998), respectively. Therefore, the R-genome CAPS markers in the Purdue and Chinese lines were speculated as markers for the 1R/1B translocation until Kishii et al. (2005) found that *Th.intermedium* has one J, one St, and one variant V genome. The J genome has 11 chromosomes showing fluorescent St probe signals at telomeric or subtelomeric sites. The variant V genome has nine chromosomes whose centromeric regions were strongly hybridized by St-genome probe; thus it is equivalent to the J^s genome designated by Chen et al. (1998). Because *Th.intermedium* is lacking the two V-genome STS markers (Figures 3 and 4) but having the R-genome CAPS markers and the variant V genome could be weakly hybridized by the R genome probe, Kishii et al. (2005) designated the third genome as $(V-J-R)^S$ to suggest that it is a progenitor genome prior to the divergence of these three genomes. The Purdue and Chinese lines appeared to have chromosome or chromosomal segment from this $(V-J-R)^S$ genome rather than from one St-genome chromosome as the Australian materials. Because the J^s genome is also present in *Th.ponticum* (Chen et al., 1998), the $(V-J-R)^S$ genome should be present in this decaploid species. However, *Th.ponticum* did not show the R-genome CAPS markers but had only the E^e-specific CAPS marker following the *Hind*III digestion (data not shown). Before a GISH study is carried out to show that the J^s genome in *Th.ponticum* can be hybridized by the V genome

probe, the genome symbol for this decaploid species remains EEEEE (Table 1).

The present study demonstrated both the usefulness and limitations of STS and CAPS markers for genomes of *Triticeae*. Positive results would always suggest the presence of genome-specific sequences; whereas negative results are not necessarily an indication of their absence due to the very nature of PCR. Furthermore, it is now well known that polyploidization or alloploidy would result in rapid changes in genome organization (Liu et al., 1998a, 1998b; Han et al., 2003). Therefore, use of these genome-specific STS or CAPS markers requires cautions. It is hereby advised that these genome-specific STS or CAPS markers are used as the first-step of genome analysis, followed by GISH and chromosome pairing of appropriate hybrids.

REFERENCES

Banks P.M., Larkin P.J. (1995) Registration of three BYDV-resistant wheat germplasms: TC5, TC6, and TC9. Crop Sci. **35**: 600-601.

Blake T.K., Kadyrzhanova D., Shepard K.W., Islam A.K.M.R., Langridge P.L., McDonald C.L., Erpelding J., Larson S., Blake N.K., Talbert L.E. (1996) STS-PCR markers appropriate for wheat-barley introgression. Theor. Appl. Genet. **93**: 826-832.

Cauderon Y. (1966) Etude cytogenetique de l'evolution du materiel issu de croisement entre *Triticum aestivum* et *Agropyron intermedium*. I. Creation de types d'addition stables. Ann. Amelior Plant (Paris) **16**: 43-70.

Chen Q., Conner R.L., Laroche A., Thomas J.B. (1998) Genome analysis of *Thinopyrum intermedium* and *Th.ponticum* using genomic *in situ* hybridization. Genome **41**: 580-586.

Crasta O.R., Francki M.G., Bucholtz D.B., Sharma H.C., Zhang J., Wang R.-C., Ohm H.W., Anderson J.M. (2000) Identification and characterization of wheat-wheatgrass translocation lines and localization of barley yellow dwarf virus resistance. Genome **43**: 698-706.

Erpelding J.E., Blake N.K., Blake T.K., Talbert L.E. (1996) Transfer of sequence tagged site PCR markers between wheat and barley. Genome **39**: 802-810.

Han F.P., Fedak G., Ouellet T., Liu B. (2003) Rapid genomic changes in interspecific and intergeneric hybrids and allopolyploids of *Triticeae*. Genome **46**: 716-723.

Hohmann U., Badaeva K., Busch W., Friebe B., Gill B.S. (1996) Molecular cytogenetic analysis of *Agropyron* chromatin specifying resistance to barley yellow dwarf virus in wheat. Genome **39**:

336-347.

Kishii M., Wang R.R.C., Tsujimoto H. (2005) GISH analysis revealed new aspect of genomic constitution of *Thinopyrum intermedium*. In: 5th Int. *Triticeae* Symp. Prague, Czech Republic, Book of Abstracts: 21.

Konieczny A., Ausubei F.M. (1993) A procedure for mapping *Arabidopsis* mutations using codominant ecotype-specific PCR-based markers. Plant J. **4:** 403-410.

Li W.L., Chen P.D., Qi L.L., Liu D.J. (1995) Isolation, characterization and application of a species-specific repeated sequence from *Haynaldia villosa*. Theor. Appl. Genet. **90:** 526-533.

Li X.M., Gardner D.R., Ralphs M.H., Wang R.R.C. (2002) Development of STS and CAPS markers for identification of three tall larkspur (*Delphinium*) species. Genome **45:** 229-235.

Liu B., Vega J.M., Segal G., Abbo S., Rodova M., Feldman M. (1998a) Rapid genomic changes in newly synthesized amphiploids of *Triticum* and *Aegilops*. I. Changes in low-copy noncoding DNA sequences. Genome **41:** 272-277.

Liu B., Vega J.M., Feldman M. (1998b) Rapid genomic changes in newly synthesized amphiploids of *Triticum* and *Aegilops*. II. Changes in low-copy coding DNA sequences. Genome **41:** 535-542.

Liu Z.-W., Wang R.R.C. (1993) Genome analysis of *Elytrigia caespitosa, Lophopyrum nodosum, Pseudoroegneria geniculata* ssp. *scythica*, and *Thinopyrum intermedium*. Genome **36:** 102-111.

Liu Z.-W., Wang R.R.C., Carman J.G. (1994) Hybrids and backcross progenies between wheat (*Triticum aestivum* L.) and apomictic Australian wheatgrass (*Elymus rectisetus* (Nees in Lehm.) A. Lüve and Connor): karyotypic and genomic analyses. Theor. Appl. Genet. **89:** 599-605.

Ozkan H., Levy A.A., Feldman M. (2002) Rapid differentiation of homoeologous chromosomes in newly-formed allopolyploid wheat. Israel J. Plant Sci. **50:** 65-76.

Sharma H.C., Ohm H.W., Perry K.L. (1997) Registration of barley yellow dwarf virus resistant wheat germplasm line P29. Crop Sci. **37:** 1032-1033.

Sharma H.C., Franki M., Crasta O., Gyulai G., Bucholtz D., Ohm H.W., Anderson J., Perry K.L., Patterson P. (1999) Cytological and molecular characterization of wheat lines with *Thinopyrum intermedium* chromosome additions, substitutions and translocations resistant to barley yellow dwarf virus. Cytologia (Tokyo) **64:** 93-100.

Svitashev S., Bryngelssonl T., Li X.-M., Wang R.R.C. (1998) Genome specific repetitive DNA and RAPD markers for genome identification in *Elymus* and *Hordelymus*. Genome **41:** 120-128.

Talbert L.E., Blake N.K., Chee P.W., Blake T.K., Magyar G.M. (1994) Evaluation of "sequence-tagged-site" PCR products as molecular markers in wheat. Theor. Appl. Genet. **87:** 789-794.

Tragoonrung S., Kanazin V., Hayes P.M., Blake T.K. (1992) Sequence-tagged-site-facilitated PCR for barley genome mapping. Theor. Appl. Genet. **84:** 1002-1008.

Wang R.R.C., Zhang X.-Y. (1996) Characterization of the translocated chromosome using fluorescence *in situ* hybridization and random amplified polymorphic DNA on two *Triticum aestivum-Thinopyrum intermedium* translocation lines resistant to wheat streak mosaic or barley yellow dwarf virus. Chrom. Res. **4:** 583-587.

Wang R.R.C., von Bothmer R., Dvorak J., Fedak G., Linde-Laursen I., Muramatsu M. (1995) Genome symbols in the *Triticeae*. In: Proc. of 2nd Int. Triticeae Symp. (Wang R.R.C., Jensen K.B., Jaussi C., eds.), Logan, Utah: 29-34.

Wei J.-Z., Wang R.R.C. (1995) Genome- and species-specific markers and genome relationships of diploid perennial species in *Triticeae* based on RAPD analyses. Genome **38:** 1230-1236.

Xin Z.Y., Zhang Z.Y., Chen X., Lin Z.S., Ma Y.Z., Xu H.J., Banks P.M., Larkin P.J. (2001) Development and characterization of common wheat - *Thinopyrum intermedium* translocation lines with resistance to barley yellow dwarf virus. Euphytica **119:** 161-165.

Xue X., Wang R.R.C. (1999) Detection of *Elymus rectisetus* chromosome segments added to wheat by RAPD and genomic in situ hybridization. Acta Genetica Sinica **5:** 539-545.

Zhang X.-Y., Dong Y.-S., Li P., Wang R.R.C. (1998) Distribution of E- and St-specific RAPD fragments in few genomes of *Triticeae*. Acta Genetica Sinica **25:** 131-141.

Screening for Drought Stress Tolerance in Wheat Genotypes Using Molecular Markers

Irada M. Huseynova*, Samira M. Rustamova
Institute of Botany, Azerbaijan National Academy of Sciences, 40 Badamdar Shosse, Baku AZ 1073, Azerbaijan

Wheat that is one of the most important staple food crops in the world is adversely affected by drought. Understanding its genetics and genome organization using molecular markers is of great value for plant breeding purposes. Several screening tests were evaluated in the present research for ability to estimate drought resistance in total 12 wheat genotypes including tolerant, semi-tolerant and non-tolerant. Randomly Amplified Polymorphic DNA primers (RAPDs) associated with drought tolerance were used initially to search genetic diversity in wheat plants. It was found out that primer P6 (TCGGCGGTTC) produced respectively a 920-bp band present mainly in drought tolerant and semi-tolerant (absent in sensitive) genotypes. Primer P7 (TCGGCGGTTC) produced a 750-bp band that is not absolutely universal for our genotypes. Genome-wide investigation was also conducted using *Dreb 1* genes as an example. Five pairs of genome-specific primers designed for the wheat *Dreb 1* genes were used for DNA amplification. Two primers, P21F/P21R and P25F/PR, amplified 596- and 1113-bp fragments, respectively, from the A genome. The P18F/P18R primer amplified a 717-bp fragment from the B genome. It was found out that *Dreb 1* gene was located on chromosome 3A in all genotypes, including drought-tolerant and drought-sensitive ones, excepting semi-tolerant genotype Tale-38. Contrary to other genotypes, a 717-bp PCR product of *Dreb-B1* gene was located on B genome from drought-tolerant variety Barakatli-95. Primers P22F/PR and P20F/P20R that amplify 596- and 1193-bp fragments, respectively, from D genome, that is common for hexaploid *Triticum aestivum* L. genotypes, did not reveal positive results.

Keywords: *wheat genotypes, RAPD primers, functional markers, Dreb genes, PCR analysis*

INTRODUCTION

Plant growth and productivity are greatly affected by environmental stresses such as drought, high salinity, and low temperature (Zheng et al., 2010). Upon exposure to abiotic stress conditions, plants undergo a variety of changes from physiological adaptation to gene expression (Shinozaki and Yamaguchi-Shinozaki, 2007). Drought is a major abiotic stress that adversely affects wheat production and quality in many regions of the world, the loss of which is the total for other natural disasters, with increasing global climate change making the situation more serious (Shao et el., 2005; Kirigwi et al., 2007). Currently, drought study has been one of the main directions in global plant biology and biological breeding. Many advances in relation to this hot topic, including molecular mechanism of anti-drought and corresponding molecular breeding have taken place (Patnaikt and Khurana, 2001; Rellegrineschi et al., 2002; Chen and Gallie, 2004; Rampino et al., 2006;

Zhao et al., 2008; Wei et al., 2009; Ashraf, 2010).

The expression of many genes is induced by drought, and their gene products function directly in stress tolerance and regulation of gene expression and signal transduction in stress responses (Zhou et al., 2010). Among the products of many stress-inducible genes are those that directly protect against environmental stress: osmoprotectants, chaperones, and detoxification enzymes. Others include transcription factors and protein kinases that regulate gene expression and signal transduction during the stress responses (Seki et al., 2003). Thus, the timely expression of stress-responsive genes is crucial for the plants' ability to survive under different environmental stress conditions (Chinnusamy et al., 2007; Shinozaki and Yamaguchi-Shinozaki, 2007).

The identification of downstream target genes of stress-relating transcription factors (TFs) is desirable in understanding the cellular responses to various environmental stimuli (Agarwal et al., 2006; Wang et al., 2008). Genes regulated by a given TFs is partially

---

determined by the DNA binding domain (DBD) of a protein (Pabo and Sauer, 1992).

The DBD in TFs binds to a specific DNA motif at the regulatory region of the target genes. Availability of genome sequences made it possible to discover the target genes of a specific TFs by looking for the locations of the specific recognition motifs in genome (Wang et al., 2009).

Dehydration responsive element binding proteins (DREBs) constitute a large family of TFs that induce the expression of a large number of functional genes and impart stress endurance to plants (Riechmann et al., 2000; Agarwal et al., 2006). The dehydration-responsive element (DRE) as a cis-acting element was found in the promoter regions of many drought- and low-temperature-inducible genes (Thomashow, 1999; Shinozaki and Yamaguchi-Shinozaki, 2007). All DREB genes feature three conserved regions, a EREBP/AP2 DNA binding domain, an N-terminal nuclear localization signal, and conserved Ser/Thr-rich region adjacent to the EREBP/AP2 domain. DREB TFs play key roles in plant stress signaling transduction pathway, they can specifically bind to DRE/CRT element (G/ACCGAC) and activate the expression of many stress inducible genes.

Although the obtained transgenic crops, mainly wheat, by different types of gene transfer technology all exhibit drought resistance to some extent, they have many shortfalls related to agronomical performance and/or development (Wang et al., 2003; Kern, 2002). These results imply that systemic, deeper and comprehensive understanding of physiological mechanism in crops under drought stress is not enough to manipulate the physiological regulatory mechanism and take advantage of all this potential for productivity, study of which is the bridge between molecular machinery of drought and anti-drought agriculture because the performance of genetic potential of crops is expressed by physiological realization in fields (Shao et al., 2005).

Wheat is a staple food crop for more than 35% of the world population and also one of the widely cultivated crops in Azerbaijan, where drought is the main abiotic stress limiting its grain yields. So wheat anti-drought mechanism study is of great importance to wheat production and biological breeding for the sake of coping with abiotic and biotic conditions. Much research is involved in this hot topic, but the pace of progress is not so large because of drought resistance being a multiple-gene-control quantitative character and wheat genome being larger (16,000 Mb). However, despite all the recent technological breakthroughs, the overall contribution of genomics-assisted breeding to the release of drought-resilient wheat cultivars has so far been marginal (Zhao et al., 2008). The elucidation of genomic regions associated with the expression of traits involved in drought adaptation, the novel genes discovery or the determination of their expression patterns in response to drought stress will provide the basis of effective engineering strategies leading to enhanced wheat germplast for specific agroecological niches. For any molecular assessment to be performed, it is paramount to firstly establish the plant adaptation strategy to overcome drought (Zhao, 2008).

Marker-assisted selection (MAS) provides a strategy for accelerating the process of wheat breeding (Wei et al., 2009). Through marker-assisted breeding (MAB) it is now possible to examine the usefulness of thousands of genomic regions of a crop germplasm under water limited regimes, which was, in fact, previously not possible (Ashraf, 2010). However, conventional markers, such as restriction fragment length polymorphism (RFLPs), random amplified polymorphic DNA (RAPDs), amplified fragment length polymorphism (AFLPs) and simple sequence repeats (SSRs), used in common wheat, are usually not developed from the genes themselves because the cloning of genes in wheat is complicated by its allohexaploid nature and large genome size. In contrast, functional markers (FMs) are usually designed from polymorphisms within transcribed regions of functional genes. Such markers are completely correlated with gene function (Anderson and Lübberstedt, 2003). Therefore, FMs can dramatically facilitate accurate selection of target genes (Wei et al., 2009).

In the present research screening for drought stress tolerance was conducted in 12 wheat (*Triticum* L.) genotypes using RAPD primers and functional markers based on genome-specific primers for each of the ortologous *Dreb 1* loci on chromosomes 3A, 3B and 3D.

MATERIALS AND METHODS

Plant Materials. A total of 12 wheat genotypes including drought tolerant, semi-tolerant and non-tolerant were used (Table 1). Six of them are known as drought tolerant and extensively are planted by local farmers under drought conditions. Three genotypes were tetraploid (*Triticum durum* L., AABB, 2n = 4x = 28) and nine - hexaploid (*Triticum aestivum* L., AABBDD, 2n = 6x = 42). Different sensitivities of these genotypes to drought have been determined during few years in different regions of Azerbaijan based on grain yield (Aliev, 1998; Aliev, 2001). The plants were provided by Experimental Station of the Research Institute of Crop Husbandry. Leaf samples of all plant materials were harvested from 7 day-old seedlings.

Table 1. Wheat genotypes and their drought tolerance status

No	Genotype name	Ploidity level and genomes	Reaction to drought
		Triticum durum L.	
1	Barakatli-95	Tetraploid (AABB)	Tolerant
2	Garagylchyg-2		Sensitive
3	Gyrmyzy bugda		Tolerant
		Triticum aestivum L.	
4	Azamatli-95	Hexaploid (AABBDD)	Tolerant
5	Giymatli-2/17		Sensitive
6	Gobustan		Tolerant
7	Gyrmyzy gul		Semi-tolerant
8	Tale-38		Semi-tolerant
9	Ruzi-84		Tolerant
10	12nd FAWWON No 97 (130/21)		Sensitive
11	4th FEFWSN No 50 (130/32)		Semi-tolerant
12	Saratovskaya		Tolerant

DNA extraction. Total genomic DNA was extracted from leaves using CTAB method (Murray and Thompson, 1980) with some modifications. In the growth room 5-7 cm long piece of fresh leaf material was cut from the plants and the leaf tissues were ground in a preheated 2×CTAB extraction buffer (100 mM Tris, pH 8, 1.4 M sodium chloride, and 20 mM EDTA, pH 8.0). Liquid nitrogen ground samples were also processed with CTAB buffer. The samples were incubated for 60 minutes in 60°C water bath with occasional vigorous shaking. The samples were mixed gently after adding 400 μl of chloroform and placed on an orbit shaker for 20 minutes at room temperature. After centrifugation at 5000 rpm, an equal volume of cold absolute isopropanol was added to the supernatant. The solution was well mixed and incubated for 60 minutes at 20°C. The sample was centrifuged for 5 minutes at 5000 rpm to pellet the DNA was followed by washing with 70% alcohol and then dried at 56°C for 5 minutes. DNA was resuspended by adding 300 μl TE buffer (10 mM Tris, 1 mM EDTA, pH 8.0).

DNA Quantification. After diluting the DNA was quantified by taking the optical density (OD) at λ = 260 with a spectrophotometer ULTROSPEC 3300 PRO ("AMERSHAM", USA). The purity of genomic DNA was determined by the A260/A280 absorbance ratio. The quality was also examined by running the extracted DNA samples on 0.8% agarose gel stained with 10 mg/ml ethidium bromide in 1×TBE (Tris base, Boric acid, EDTA) buffer. The gel was visualized and photographed under UV light.

Polymerase chain reaction conditions. RAPD-PCR was carried out essentially as described by Williams et al. (1990). Two 10-mer oligonucleotide primers (Eurogentec S.A., Belgique) were used for

DNA amplification (Table 2). Amplifications were performed in "Applied Biosystems 2720 Thermal Cycler" first 4 min at 94°C followed by 10 cycles of: 1 min at 94°C, 1 min at 36°C and 1 min at 72°C. After that, for next 35 cycles, 0.2°C was added to annealing temperature. After the final cycle, samples were incubated at 72°C for 15 min and then hold at 4°C prior to analysis.

Table 2. Primer nucleotide sequence used to amplify DNA

Primer designation	Sequence 5′→ 3′
P6	TCGGCGGTTC
P7	CTGCATCGTG

The RAPD fragments were analyzed by electrophoresis on 1.2% agarose gels and detected using ethidium bromide (10 ng/100 mL of agarose solution in Tris-Borate-EDTA buffer). The bands were counted by starting from the top of the lanes to the bottom. All visible and unambiguously scorable fragments amplified by the primers were scored under the heading of total scorable fragments. Amplification profiles of the twelve genotypes were compared with each other, and bands of DNA fragments were scored as present or absent.

To identify polymorphisms in DNA sequences of the *Dreb* gene in each genome, five pairs of genome-specific primers were used for DNA amplification (Wei et al., 2009; http://www.premierbiosoft.com) (Table 3). Genome-specific PCR was performed in a total volume of 20 μl containing 80 ng of genomic DNA, 1 × PCR reaction buffer, 0.25μM of each primer, 0.45 mM of each deoxyribonucleotide, 4.0 mM MgCl$_2$ and 1.6 U of *Taq* DNA polymerase (Sigma, USA).

Table 3. Genome-specific primers used for chromosome assignment of the wheat *Dreb 1* genes

Primers	Sequences (5′→3′)	Chromosome location	Expected size (bp)	Ann. temp. (°C)
P18F	CCCAACCCAAGTGATAATAATCT	3B	717	50
P18R	TTGTGCTCCTCATGGGTACTT			
P20F	TCGTCCCTCTTCTCGCTCCAT	3D	1193	63
P20R	GCGGTTGCCCCATTAGACATAG			
P21F	CGGAACCACTCCCTCCATCTC	3A	1113	63
P21R	CGGTTGCCCCATTAGACGTAA			
P22F	CTGGCACCTCCATTGCCGCT	3D	596	63
P25F	CTGGCACCTCCATTGCTGCC	3A	596	57
PRa	AGTACATGAACTCAACGCACAGGACAAC			

a PR is a public primer matched with P22F and P25F, respectively

The PCR was carried out as follows: initial denaturation at 94°C for 3 min; 34 cycles of 94°C for 1 min, an annealing step at variable annealing temperatures depending on the primer pairs for 1 min, 72°C for 1.5 min; and a final extension at 72°C for 10 min and then held at 4°C prior to analysis. The PCR products were electrophoresized on 2.5% agarose gels, stained with ethidium bromide and visualized under UV light by "Gel Documentation System *UVITEK*".

RESULTS AND DISCUSSION

RAPD-PCR analysis was performed with a subset (12 genotypes) of wheat (*Triticum* L.) genotypes with different levels of drought tolerance (Table 1). P6 and P7 primers associated with drought tolerance were used (Pakniyat and Tavakol, 2007). According to the literature data in tolerant genotypes these primers should produce appropriate fragments.

Figure 1 shows the electrophoretic pattern generated by RAPD primer P6 (TCGGCGGTTC). This primer produced a 920-bp band present in drought tolerant and semi-tolerant genotypes and absent in sensitive durum wheat genotype Garagylchyg-2 and bread wheat genotypes Giymatli-2/17 and Gyrmyzy gul.

This band may be associated with drought stress tolerance in wheat (*Triticum* L.) and may be used in selection of tolerant genotypes in breeding programs.
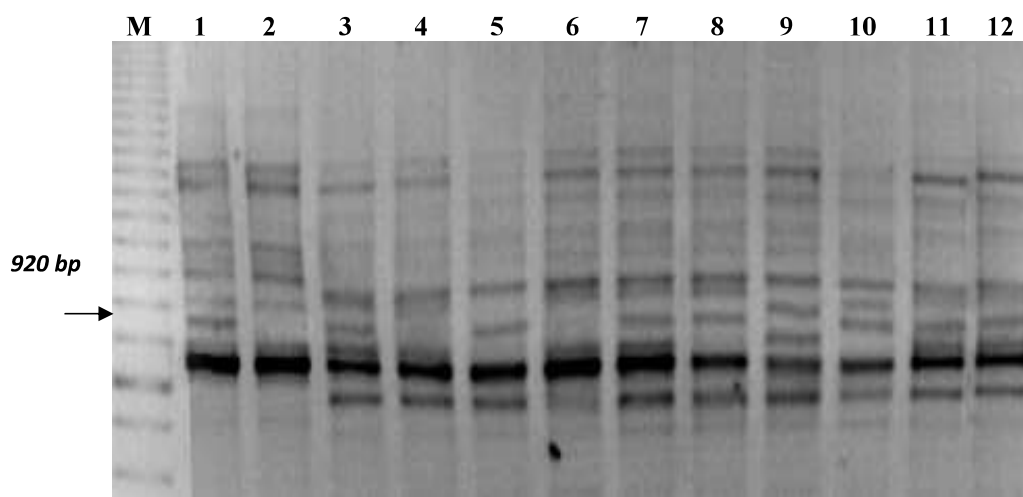

Figure 1. PCR amplification profiles of *Triticum* L. wheat genotypes using P6 primer (5′ TCGGCGGTTC 3′). Arrow shows 920-bp DNA fragment, present in drought tolerant and semi-tolerant wheat genotypes and absent in sensitive ones. M - DNA ladder 100-bp. 1 - Barakatli-95; 2 - Garagylchyg-2; 3 - Azamatli-95; 4 - Giymatli-2/17; 5 - Gyrmyzy bugda; 6 - Gyrmyzy gul; 7 - Tale-38; 8 - Ruzi-84; 9 - 12 [nd] FAWWON No 97 (130/21); 10 - 4 [tn] FEFWSN No 50 (130/32); 11 - Nurlu-99; 12 - Gobustan.

It is important to note that 12nd FAWWON No 97 (130/21) is considered to be non-tolerant genotype. However, a 920-bp band is also present in 12nd FAWWON No 97 (130/21) genotype. Probably, it may have a potential for tolerance, but for some reasons expression of these genes are not realized.

It should be noted that P7 primer (TCGGCGGTTC) produces a 750-bp band. Electrophoretic pattern generated by RAPD primer P7 (Figure 2) demonstrates that this band has occurred neither in tolerant genotype Barakatli-95, nor in non-tolerant genotypes Garagylchyg-2 and Giymatli-2/17. Meanwhile, in drought-sensitive genotype Gyrmyzy gul this band is present. Therefore, it was conclude that P7 primer is not absolutely universal for drought tolerance.

Thus, RAPD technology is a powerful tool in quick identifying markers related to drought tolerance in wheat. Results obtained from RAPD-PCR analysis are promising beginning for further research of plant tolerance to water stress on molecular-genetic basis. Marker-assisted selection based on genotype will greatly increase breeding efficiency (Manavalan et al., 2009). Recent advances in wheat researches, ranging from breeding programs to genome sequencing and genomics technologies, provide unprecedented opportunities to understand global patterns of gene expression and their association with the development of specific phenotypes, as well as promising tools for the genetic improvement of plants cultivated in adverse environments by molecular breeding or transgenic approaches.

DREB proteins are also important in determining tolerance or resistance to water deficit. Therefore, we then conducted genome-wide investigation using *Dreb 1* genes as an example. Five pairs of genome-specific primer sets will be useful as FMs to trace each locus during MAS in search of more drought-tolerant wheat genotypes. Primer P25F/PR was designed to amplify a 596-bp DNA fragment downstream of *Dreb-A1* in the A genome. P21F/P21R was selected to amplify an upstream region (a 1113-bp DNA fragment) of the same gene. Primers P22F/PR and P20F/P20R were designed to amplify sequences from the D genome, with the amplifications resulting in 596 and 1193-bp DNA fragments, respectively. The P18F/P18R primer which amplify a 717-bp DNA fragment, were designed as a B genome-specific primer pair (Table 3). To confirm these genome-specific primers, the genomic DNAs of various wheat genotypes were amplified using the primer pairs.

PCR amplification profiles of DNA from *Triticum* L. genotypes with primer pair P21F/P21R are shown in Figure 3. Fragment amplified with this primer in 1113-bp band revealed in all genotypes, excepting semi-tolerant bread wheat genotype Tale-38. However, this band is seemingly indicated in drought-tolerant durum wheat genotypes Barakatli-95. These results indicate that *Dreb 1* gene responsive for the tolerance to drought located in the third chromosome of A genome in these genotypes. 596-bp fragments that amplify by P25F/PR primer were not observed in these samples. Absence of these fragments can be explained by some mutations that, probably, took place in *Dreb 1* gene region, complementary to this primer.
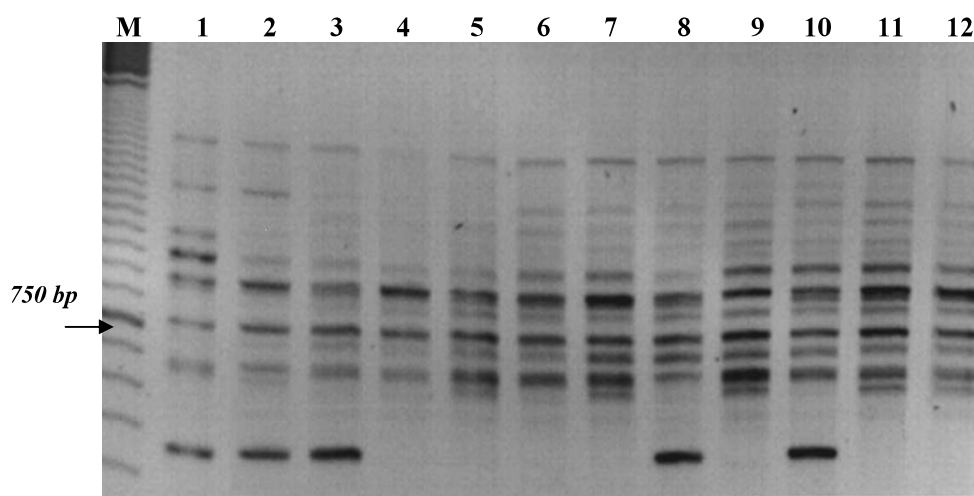

Figure 2. PCR amplification profiles of wheat genotypes *Triticum* L. using a primer P7 (5' TCGGCGGTTC 3'). Arrow shows a 750-bp band. M - DNA ladder 100-bp. 1-Barakatli-95, 2 - Garagylchyg-2, 3 - Azamatli-95, 4 - Giymatli-2/17, 5 - Gyrmyzy bugda, 6 - Gyrmyzy gul, 7 - Tale-38, 8 − Ruzi-84, 9 - 12 [nd] FAWWON No 97 (130/21), 10 - 4 [tn] FEFWSN No 50 (130/32), 11 - Nurlu-99, 12 - Gobustan.
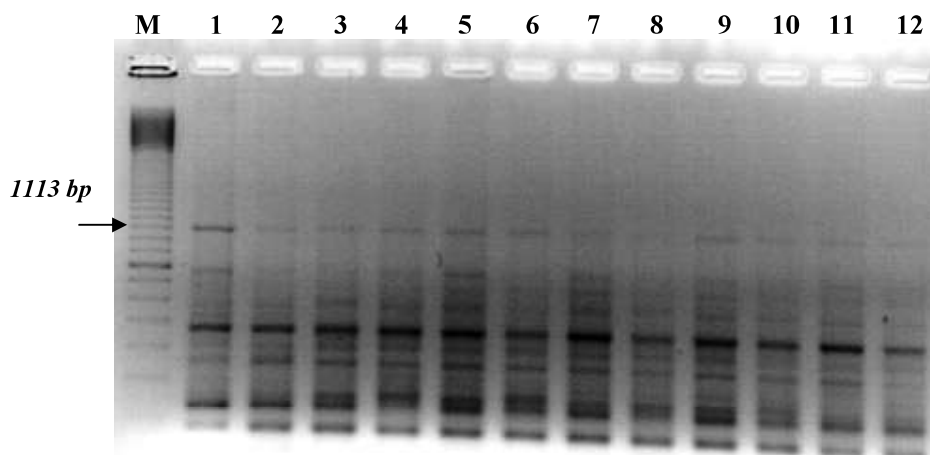
Figure 3. PCR-based chromosome assignments of the *Dreb 1* genes in wheat *Triticum* L. genotypes using an A genome-specific primer pair P21F/P21R. Arrow shows a 1113-bp DNA fragment. M – DNA ladder 100-bp. 1 - Barakatli-95, 2 - Garagylchyg-2, 3 - Gyrmyzy bugda, 4 - Azamatli-95, 5 - Giymatli-2/17, 6 - Gobustan, 7 - Gyrmyzy gul, 8 - Tale-38, 9 - Ruzi-84, 10 - 12nd FAWWON No 97 (130/21), 11- 4th FEFWSN No 50 (130/32), 12 - Saratovskaya.
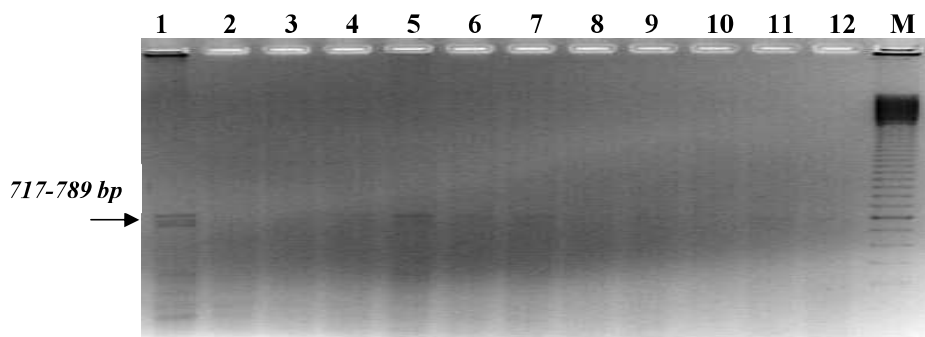

Figure 5. PCR amplification profiles of wheat genotypes *Triticum* L. using a B genom-specific primer pair P18F/P18R. Arrow shows a 717-789-bp DNA fragment. M – DNA ladder 100-bp. 1 - Barakatli-95, 2 - Garagylchyg-2, 3 - Gyrmyzy bugda, 4 - Azamatli-95, 5 - Giymatli-2/17, 6 - Gobustan, 7 - Gyrmyzy gul, 8 - Tale-38, 9 - Ruzi-84, 10 - 12nd FAWWON No 97 (130/21), 11 - 4th FEFWSN No 50 (130/32), 12 - Saratovskaya.

Results obtained from primer pair P18F/P18R, specific for *Dreb 1* gene in B genome, are shown in Figure 5. A 717-789-bp fragment present only in tolerant genotype Barakatli-95. It is interesting to note that this genotype also demonstrates high drought tolerance in other parameters (Aliev, 1998; Aliev, 2001). The absence of 717-789-bp fragments in other wheat genotypes can be explained by the fact that the DREB1 proteins showed the most specific variations in the B genome, including three single amino acid mutations (amino acids 46, 140 and 200) and a deletion of 24 amino acids in a region rich in *Ser* and *Thr* in the orthologous A and D genomes (Wei et al., 2009).

PCR analysis was also performed with P22F/PR and P20F/P20R primers specific for D genome. It is known that hexaploid wheat (*Triticum aestivum* L.) genotypes have D genome. However, in our experiments there were not any appropriate fragments amplified by these primers. This data indicates that hexaploid wheat genotypes, possibly, were nulliosomics, i.e. chromosome pair which has a *Dreb 1* gene is absent in their D genomes.

Hence, using functional markers was identified the presence of *Dreb 1* gene located in A genome for 3 tetraploid and 8 hexaploid wheat genotypes. Unlike other genotypes *Dreb 1* gene was also revealed in B genome in tetraploid genotype

Barakatli-95.

Thus, understanding the functions of these stress-inducible genes helps to unravel the possible mechanisms of stress tolerance. Marker-assisted selection was also employed to improve the staygreen trait involved in drought tolerance of wheat. The obtained results open an excellent opportunity to develop stress tolerant crops in future. These results may be helpful in wheat breeding programs aimed at improving drought tolerance.

REFERENCES

Agarwal M., Hao Y., Kapoor A., Dong C.H., Fujii H., Zheng X., Zhu J.K. (2006) A R2R3 type MYB transcription factor is involved in the cold regulation of CBF genes and in acquired freezing tolerance. J. Biol. Chem. **281(49):** 37636-37645.

Aliev J.A. (1998) Importance of photosynthesis of various organs in protein synthesis in grain of wheat genotypes under water stress. In: "Photosynthesis: Mechanisms and Effects" (Garab G., ed.). Kluwer Academic Publishers, Dordrecht, Boston, London **5:** 3829-3832.

Aliev J.A. (2001) Physiological bases of wheat breeding tolerant to water stress. In: "Wheat in a Global Environment" (Bedo Z., Lang L., eds.). Kluwer Academic Publishers, Dordrecht, Boston, London **9:** 693-698.

Andersen J.R., Lübberstedt T. (2003) Functional markers in plants. Trends Plant Sci. **8:** 554-560.

Ashraf M. (2010) Inducing drought tolerance in plants: recent advances. Biotech. Adv. **28:** 169-183.

Chen Z., Gallie D.R. (2004) The ascorbic acid redox state controls guard cell signaling and stomatal movement. Plant Cell **16:** 1143-1162.

Chinnusamy V., Zhu J., Zhu J.K. (2007) Cold stress regulation of gene expression in plants. Trends Plant Sci. **12:** 444-451.

Kern M.J. (2002) Food, feed, fibre, fuel and industrial products of the future: challenges and opportunities. Understanding the strategic potential of plant genetic engineering. Agric. Crop Sci. **188:** 291-302.

Kirigwi F.M., Van Ginkel M., Brown-Guedira G., Gill B.S., Paulsen G.M., Fritz A.K. (2007) Markers associated with a QTL for grain yield in wheat under drought. Mol. Breed. **20:** 401-413.

Manavalan L.P., Gutticonda S.K., Tran L.P., Nguyen T.H. (2009) Physiological and molecular approaches to improve drought resistance in soybean. Plant Cell Physiol. **50:** 1260-1276.

Murray M.G., Thompson W.F. (1980) Rapid isolation of high molecular weight plant DNA. Nucleic Acids Res. **8:** 4321-4325.

Pabo C.O., Sauer R.T. (1992) Transcription factors: structural families and principles of DNA recognition. Annu. Rev. Biochem. **61:** 1053-1095.

Pakniyat H., Tavakol E. (2007) RAPD markers associated with drought tolerance in bread wheat (*Triticum aestivum* L.). Pakistan J. Biol. Sci. **10:** 3237-3239.

Patnaitk D., Khurana P. (2001) Wheat biotechnology: a mini-review. Elec. J. Biotech. **4:** 74-102.

Rampino P., Pataleo S., Gerardi C., Perotta C. (2006) Drought Stress Responses in Wheat: Physiological and Molecular Analysis of Resistant and Sensitive Genotypes. Plant Cell Envir. **29:** 2143-2152.

Rellegrineschi A., Ribaut J.M., Trethowan R. (2002) Looking beyond the details: a rise in system-oriented approaches in genetics and molecular biology. Curr. Genet. **41:** 1-10.

Riechmann J.L., Heard J., Martin G., Reuber L., Jiang C., Keddie J., Adam L., Pineda O., Ratcliffe O.J., Samaha R.R., Creelman R., Pilgrim M., Broun P., Zhang J.Z., Ghandehari D., Sherman B.K., Yu G. (2000) Arabidopsis transcription factors: genome-wide comparative analysis among eukaryotes. Science **290:** 2105-2110.

Seki M., Kamei A., Yamaguchi-Shinozaki K., Shinozaki K. (2003) Molecular responses to drought, salinity and frost: common and different paths for plant protection. Curr. Opin. Biotech. **14:** 194-199.

Shao H.B., Liang Z.S., Shao M.A., Sun Q. (2005) Dynamic changes of anti-oxidative enzymes of 10 wheat genotypes at soil water deficits. Colloids and Surfaces B: Biointerfaces **42:** 187-195.

Shinozaki K., Yamaguchi-Shinozaki K. (2007) Gene networks involved in drought stress response and tolerance. J. Exp. Bot. **58:** 221-227.

Thomashow M.F. (1999) Plant cold acclimation: freezing tolerance genes and regulatory mechanisms. Annu. Rev. Plant Physiol. Plant Mol. Biol. **50:** 571-599.

Wang S., Assman S.M., Fedoroff N.V. (2008) Characterization of the Arabidopsis heterotrimeric G protein. J. Biol. Chem. **283:** 13913-13922.

Wang S., Yang S., Yin Y., Guo X., Wang S., Hao D. (2009) An *in silico* strategy identified the target gene candidates regulated by dehydration responsive element binding proteins (DREBs) in Arabidopsis genome. Plant Mol. Biol. **69(1-2):** 167-178.

Wang W.X., Vinocur B., Altman A. (2003) Plant Responses to Drought, Salinity and Extreme Temperature: Towards Genetic Engineering for Stress Tolerance. Planta **218:** 1-14.

Wei B., Jing R., Wang Ch., Chen J., Mao X., Chang X., Jia J. (2009) Dreb1 genes in wheat (*Triticum aestivum* L.): development of functional markers and gene mapping based on SNPs. Mol. Breeding **23:** 13-22.

Williams J.G., Kubelik K.J., Livak J.A., Tingey S.V. (1990) DNA polymorphisms amplified by arbitrary primers are useful genetic markers. Nucleic Acids Res. **18:** 6531-6535.

Zhou G.-A., Chang R.-Z. Qiu L.-J. (2010) Overexpression of soybean ubiquitin-conjugating enzyme gene GmUBC2 confers enhanced drought and salt tolerance through modulating abiotic stress-responsive gene expression in Arabidopsis. Plant Mol. Biol., **72:** 357-369.

Zhao C.-X., Guo L.-Y., Cheruth A.J., Shao H.-B., Yang H.-B. (2008) Prospective for applying molecular and genetic methodology to improve wheat cultivars in drought environments. C. R. Biologies **331:** 579-586.

Zheng J., Fu J., Gou M., Huai J., Liu Y., Jian M., Huang Q., Guo X., Dong Z., Wang H., Wang G. (2010) Genome-wide transcriptome analysis of two maize inbred lines under drought stress. Plant Mol. Biol. **72:** 407-423.

Gene Discovery and Advances in Biotechnology

Shakhira M. Zakhrabekova[1]*, Leif Lundh[2], Mats Hansson[1]
[1]Department of Biochemistry, Lund University, Box 124, SE-22100 Lund, Sweden
[2]Department of Cell and Molecular Biology, Gothenburg University, Box 462, 405 30 Gothenburg, Sweden

History of biotechnology is very old and covers such well known and important applications as brewing beer, fermenting vine, baking bread, producing of monoclonal antibodies and many others. Discovery of recombinant DNA techniques culminated with the birth of genetic engineering and became a scientific beginning in the epoch of modern biotehnology. Today's advances in biotechnology could not be achieved without the major sources for gene discovery: availablity of complete genomic sequence information for the organism, access to high-throughput genotyping technologies, success in developing computational biology tools and developing of different molecular markers techniques. There are four major industrial applications in modern biotechnology: crop production and agriculture; non-food uses of crops and other products; medicine (health care) and environmental uses. In this article, we will in more details describe advantages and disadvantages of several molecular marker techniques and make a short review of the different applications in modern biotechnology.

Keywords: biotechnology, genetic variation, genetic markers, crop production, environment, medicine

Genomic resources and tools for gene discovery

DNA markers, quantitative trait loci (QTL), and marker-assisted selection (MAS)

All organisms are subjected to mutations, leading to a natural genetic variation (polymorphism). For these variations to be valuable to researchers, it is necessary that they are heritable and sensible. Natural variations must be recognizable by phenotype or have a genetic mutation distinguishable through molecular techniques.

Different types of genetic variation at the DNA level can be classified in four classes: SNPs - single nucleotide polymorphism, indels - insertions or deletions of nucleotide sequences, inversion and rearrangements (Table 1).

DNA marker technology can be used to detect these mutations, discover the natural genetic variations and facilitate the construction of high-resolution genetic linkage maps for different species. More recent and popular types of genetic markers include: restriction fragment length polymorphism (RFLP), amplified fragment length polymorphism (AFLP), randomly amplified polymorphic DNA (RAPD), single nucleotide polymorphism (SNP), microsatellite, allozymes, mitochondrial DNA and expressed sequence tag (EST) markers. There are two types of molecular markers: type I represent markers, which were identified during analysis of known genes and class II are associated with genes of unknown functions (O'Brien, 1991; Table 2). The power of the various marker types can be defined by their PIC (polymorphic information content) value (Botstein et al., 1980). PIC value of a marker detects polymorphism in a population and can give an idea of the power of the usefulness of molecular marker.

Characteristics of molecular markers and their potential applications

RFLP-markers

The traditionall technique for detecting RFLPs involves four steps: restriction of genomic DNA with restriction endonucleases; separation of the resulting DNA fragments by length in agarose gel electrophoresis, transfer of procedure; hybridization of the membrane to a labeled DNA probe and determination if the size of detected fragments varies between individuals (Botstein et al., 1980). Most recent analyses exchange the laborious Southern blot method with techniques based on the PCR. If flanking sequences are known for a locus, the piece of DNA, containing the RFLP region is amplified via PCR. If the length polymorphism is caused by a relatively large indels, gel electrophoresis of the PCR products should directly detect the size difference. However, if the length polymorphism is caused by SNP mutation at a restriction site, PCR products must be digested with a restriction enzyme to reveal the RFLP.

The PIC value of RFLP markers in revealing

Table 1. Different types of genetic variation and their characteristics

Genetic variation	Characteristics
SNPs	Nucleotide base substitutions
Indels	Insertions or deletions of nucleotide sequences within a locus
Inversion	Inversion of a segment of DNA within a locus
Rearrangement	Rearrangement of DNA segments around a locus of interest

Table 2. Major types of DNA markers and their applications

Marker name	Type	The usefulness of molecular markers can be measured based on their PIC value	Applications
RFLP	I	relatively low	Linkage mapping
RAPD	II	intermediate	Fingerprinting for population studies
AFLP	II	high	Linkage mapping, population studies
Microsatellite (SSR)	Normally Type II	high	Linkage mapping, population studies
EST	I	low	Linkage mapping, physical mapping, comparative mapping
SNP	I or II	high	Linkage mapping

genetic variation is relatively low compared to more recently developed markers and techniques discussed below. Insertions or deletions of nucleotide sequences and rearrangements of regions containing restriction sites are possibly widespread in the genomes of most species, but the chances of such occasion within the locus of interest should be rare. The main power of RFLP markers is that they are codominant markers, i.e., both alleles in an individual are detected in the analysis.

RAPD-markers

RAPD procedures (Welsh and McClelland, 1990; Williams et al., 1990) use PCR to randomly amplify unknown fragments of nuclear DNA with an identical pair of primers 8-10 bp in length. Because of the low annealing temperatures and the short length of the primers, the probability of amplifying multiple products is very high, with each product likely representing a different locus. RAPD polymorphisms can occur due to the SNP at the primer binding sites and due to insertion or deletion in the regions between the sites. The PIC values of RAPD markers are relatively high, but RAPDs may not be as informative as AFLPs, because fewer loci are generated simultaneously.

AFLP - markers

AFLP is a PCR-based fingerprinting method (Vos et al., 1995) that combines the power of both RFLP and RAPD methods. While RFLP allows analysis of one locus at a time, AFLP has the potential to analyze number of loci simultaneously. The strength and reproducibility of AFLP analysis is ex-

tremely high. One major weakness of AFLP method is the need for special equipment such as automated gene sequencers for electrophoretic analysis of fluorescent labels.

Microsatellites

Microsatellites are composed of multiple copies of tandemly arranged simple sequence repeats (SSRs), which are more or less evenly spread in the genome on all chromosomes. They have been detected inside gene coding regions (Liu et al., 2001), introns, and in the non-gene sequences.

Most microsatellite loci are relatively small and can be amplified using PCR. The abundant amount of alleles per locus results in very high PIC values for microsatellite markers. Even genomic distribution and high PIC number makes microsatellite markers very popular and useful in population studies, although application of microsatellite markers requires a large amount of effort. Each microsatellite locus has to be determined and PCR primers designed in its flanking region.

Single nucleotide polymorphism

Single nucleotide polymorphism is caused by point mutations. SNPs are the most abundant in any organism and usually restricted to one of two alleles, although in theory, a SNP within a locus can produce up to four alleles, each carrying one of four bases at the SNP site: A, T, C, and G. SNPs are evolutionarily conserved and have been advised as markers for quantitative trait loci analysis instead of microsatellites. There are many different methods available for SNP genotyping, among which microarray (gene

chip) technology and quantitative PCR are very useful in medical and clinical studies (Hacia et al., 1999).

Crop production and agriculture

Improving grain yield, resistance of crops to environmental stresses, improving taste, texture and appearance of food, increasing nutritional qualities of food crops, production of novel substances in crop plants are very important applications of modern agricultural biotechnology (Figure 1).

The limitations on the commercial use of genetically modified plants, has led to a rise of interest in investigating natural biodiversity to increase the productivity, quality and nutritional value of crops. The exploration of such natural variations is very actual both in crop species and in the model species *Arabidopsis thaliana*.

Number of studies, concerning the genetics of crop yield, has been carried out in recent years, including a broad class of species like rice, barley, soybean and tomato (Xiao et al., 1996; Concibido et al., 2003; Huang et al., 2003; Septiningsih et al., 2003; Gur and Zamir, 2004). A recent study in rice discovered the QTL Gn1a, which improve crop yield
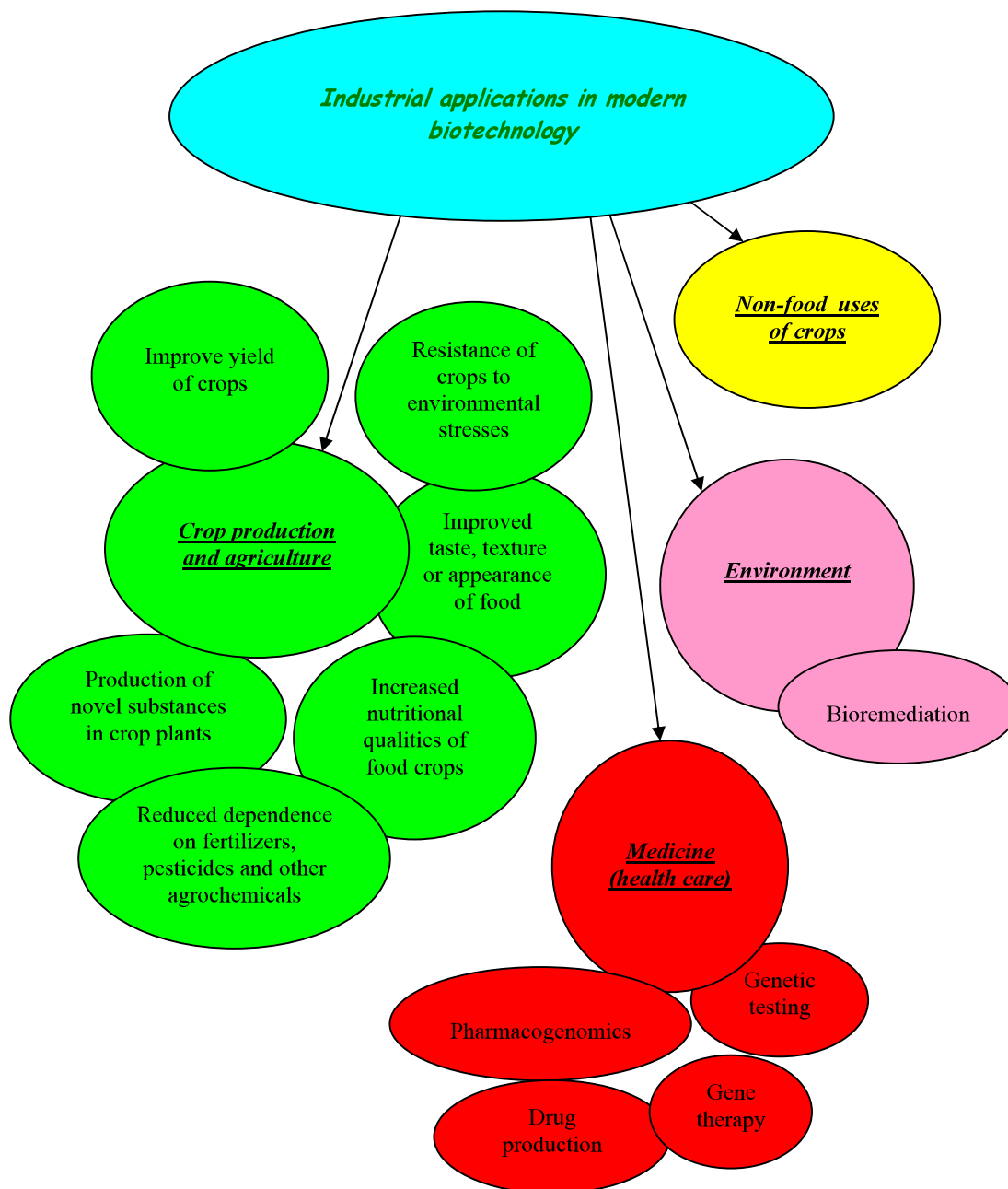

Figure 1. Industrial applications in modern biotechnology.

and encodes a cytokinin oxidase/dehydrogenase (OsCKX2), an enzyme that break down the phytohormone cytokinin. Down regulation of OsCKX2 lead to the accumulation of cytokinin in inflorescence meristems, resulting in an elevated number of reproductive organs and improved grain yield (Ashikari, 2005). Improving of crop yield can be as well achieved by so called QTL pyramiding. Studies, performed on rice showed that combined loci for grain number and plant height in the same genetic background generated lines that exhibited both beneficial traits (Ashikari, 2005).

Increasing nutritional qualities, such as protein, starch and oil content of food crops are very much in the focus of modern biotechnology. It was shown that, introgression of a high-grain-protein quality trait from *Triticum dicoccoides* into in the Canadian durum wheat (*Triticum turgidum* L.) resulted in elevated protein quality lines of durum wheat and markedly improved the quality of pasta made from flour of wheat carrying the QTL (Kovacs et al., 1998).

Vitamins, pigments and antioxidants have been studied extensively in the last ten years (Ye et al., 2000; Giuliano et al., 2003; Lewinsohn et al., 2005). The production of rice, containing relatively high levels (2 mg/g) of provitamin A have been considered of great importance. Golden rice was created by transforming rice with two beta-carotene biosynthesis genes: *psy* (phytoene synthase) from daffodil (*Narcissus pseudonarcissus*) and *crt1* from the soil bacterium *Erwinia uredovora* (Ye et al., 2000). Due to various concerns about using genetically engineered crops, researcher now are trying the conventional breeding approaches for breeding varieties with increased beta-carotene in the aleurone.

Medicine

The promising applications of modern biotechnology in medicine cover such topics as pharmacogenomics; drug production; genetic testing; and gene therapy. *Pharmacogenomics* is the study of how variations in the human genome affect body's response to drugs. Such studies help to produce drugs, associated with specific genes and diseases.

Genetic testing includes the diagnosis of genetic disease and the detection of future disease risks.

Gene therapy

A "normal" gene is transferred into the genome to replace an "abnormal," disease-causing gene by using different types of viruses, such as retroviruses, adenoviruses, adeno-associated viruses and herpes simplex viruses. There are several non-viral techniques for gene delivery available now: direct introduction of therapeutic DNA into target cells; the use of liposome carrying the therapeutic DNA; chemical linking of the DNA to a molecule that will bind to special cell receptors.

Despite of developments in gene therapy research, there are many factors that create problems in effectively using gene therapy. Immune responses reduce possibility of gene therapy and the use of viral vectors causes toxicity and inflammatory responses. The main limitation of gene therapy is the fact that the most commonly occurring disorders are caused by combination of different genes and is difficult to treat using gene therapy.

Many reports and review articles demonstrate the latest developments in gene therapy for cancer and ther human diseases. It was reported that gene therapy is a promising approach for treatment of stroke and other cerebrovascular diseases (Chu et al., 2007).

Environment

The role of new biotechnology in solving environmental problems is very important. Bioremediation is one of the main branches of environmental biotechnology. Bioremediation can be characterised as any approach that apply microorganisms, fungi and green plants to restore the contaminated environment to its native condition. Various issues associated with water, air and soil pollution can be solved with new biotechnology. Nature evolved mechanisms for self-regeneration. The role of biotechnology is to efficiently apply these existing platforms to clean up environmental contamination. Different microorganisms are being examined for the ability to remediate various chemicals often present at polluted industrial sites. Researchers make the attempts to genetically modify certain microorganisms to increase their effectiveness to metabolize particular chemicals, such as hydrocarbons, in contaminated locations.

The future of biotechnology

Progress in biotechnology is aimed to achieve healthier planet, find solutions against deadly diseases. Stem cell research may find effective treatments for Parkinson's disease, multiple sclerosis, and muscular dystrophy. The future of biotechnology is directed to the improvement of the quality of life, finding solutions to cure different diseases and stop the hunger.

REFERENCES

Ashikari M., Sakakibara H., Lin S.Y., Yamamoto T., Takashi T., Nishimura A., Angeles E.R., Quian Q., Kitano H., Matsuoka M. (2005) Cytokinin oxidase regulates rice grain production. Science **309**: 741-745.

Botstein D., White R.L., Skolnick M., Davis

R.W. (1980) Construction of a genetic linkage map in man using restriction fragment length polymorphisms. Am. J. Hum. Genet. **32:** 314-331.

Chu Y., Miller J.D., Heistad D.D. (2007) Gene therapy for stroke: 2006 overview. Curr. Hypertens Rep. **1:** 19-24.

Concibido V.C., La Valee B., McLaird P., Pineda N., Meyer J., Hummel L., Yang J., Wu K., Delannay X. (2003) Introgression of a quantitative trait locus for yield from *Glycine soja* into commercial varieties. Theor. Appl. Genet. **106:** 575-582.

Giuliano G., Al-Babili S., Von Linting J. (2003) Carotenoid oxygenases: cleave it or leave it. Trends Plant Sci. **8:** 145-149.

Gur A., Zamir D. (2004) Unused natural variation can lift yield barriers in plant breeding. PLoS Biol. **2:** e245.

Hacia J.G., Fan J.B., Ryder O., Jin L., Edgemon K., Ghandour G., Mayer R.A., Sun B., Hsie L., Robbins C.M., Brody L.C., Wang D., Lander E.S., Lipshutz R., Fodor S.P., Collins F.S. (1999) Determination of ancestral alleles for human single-nucleotide polymorphisms using high-density oligonucleotide arrays. Nat. Genet. **22:** 164-167.

Huang X.Q., Coster H., Ganal M.W., Roder M.S. (2003) Advanced backcross QTL analysis for the identification of quantitative trait loci alleles from wild relatives of wheat (*Triticum aestivum* L.). Theor. Appl. Genet. **106:** 1379-1389.

Kovacs M., Howes N.K., Clarke J.M., Leisle D. (1998) Quality characteristics of durum wheat lines deriving high protein from *Triticum dicoccoides* (6b) substitution. J. Cereal Sci. **27:** 47-51.

Lewinsohn E., Sitrit Y., Bar E., Azulay Y., Meir A., Zamir D., Tadmor Y. (2005) Carotenoid pigmentation affects the volatile composition of tomato and watermelon fruits, as revealed by comparative genetic analysis. J. Agric. Food Chem. **53:** 3142-3148.

Liu Z.J., Li P., Kocabas A., Ju Z., Karsi A., Cao D., Patterson A. (2001) Microsatellite-containing genes from the channel catfish brain: evidence of trinucleotide repeat expansion in the coding region of nucleotide excision repair gene RAD23B. Biochem. Biophys. Res. Commun. **289:** 317-324.

O'Brien S.J. (1991) Molecular genome mapping: lessons and prospects. Curr. Opin. Genet. Dev. **1:** 105-111.

Septiningsih E.M., Prasetiyono J., Lubis E., Tai T.H., Tjubaryat T., Moeljopawiro S., McCouch S.R. (2003) Identification of quantitative trait loci for yield and yield components in an advanced backcross derived from the *Oryza sativa* variety IR64 and the wild relative *O.rufipogon.* Theor. Appl. Genet. **95:** 418-423.

Welsh J., McClelland M. (1990) Fingerprinting genomes using PCR with arbitrary primers. Nucleic Acids Res. **18:** 7213–7218.

Williams J.G.K., Kubelik A.R., Livak K.J., Rafalski J.A., Tingey S.V. (1990) DNA polymorphisms amplified by arbitrary primers are useful as genetic markers. Nucleic Acids Res. **18:** 6531–6535.

Vos P., Hogers R., Bleeker M., Reijans M., van de Lee T., Hornes M., Frijters A., Pot J., Peleman J., Kuiper M., Zabeau M. (1995) AFLP: a new technique for DNA fingerprinting. Nucleic Acids Res. **23:** 4407-4414.

Xiao J.H., Grandillo S., Ahn S.N., McCouch S.R., Tanksley S.D., Liu J.M., Yuan L.P. (1996) Genes from wild rice improve yield. Nature **384:** 223-224.

Ye X., Al-Babli S., Kloti A., Zhang J., Lucca P., Beyer P., Potrykus I. (2000) Engineering the provitamin A (beta-carotene) biosynthetic pathway into (carotenoid-free) rice endosperm. Science **287:** 303-305.

Hexenyl Acetate Mediates Indirect Plant Defense Responses

Wassim E. Chehab, Roy Kaspi, Tatyana A. Savchenko, Katayoon Dehesh*
Department of Plant Biology, University of California Davis, Davis, California 95616, USA

Oxylipins, lipid-derived signaling molecules have important functions in plant development, reproduction and responses to external stimuli. Jasmonates (JAs), C_6-aldehydes, and their corresponding derivatives, produced by the two main competing branches of the oxylipin pathway, the allene oxide synthase (AOS) and hydroperoxide lyase (HPL) branches, respectively. These two branches share a substantial overlap in their regulatory functions. Majority of experiments to define the role of C_6-aldehydes in plant defense responses were restricted to external application of aldehydes or the use of genetic manipulation of *HPL* expression levels in plant genotypes with intact ability to produce the competing AOS-derived metabolites. To uncouple the roles of the C_6-aldehydes and jasmonates in mediating direct and indirect plant-defense responses, we generated *Arabidopsis* genotypes lacking either one or both of these metabolites. These genotypes were subsequently challenged with a phloem-feeding insect (aphids: *Myzus persicae*) and the volatiles emitted by these plants upon aphid infestation or mechanical wounding were characterized. These experiments led to identification of hexenyl acetate as the predominant compound in these volatile blends. Subsequently, we examined the signaling role of this compound in attracting the parasitoid wasp (*Aphidius colemani*), a natural enemy of aphids.

Keywords: jasmonates, C_6-aldehydes, hexenyl acetate, volatiles, aphids, plant defense responses

INTRODUCTION

Plants employ a complex array of physical and chemical defense mechanisms to resist or evade biotic attacks. In addition to the constitutive defense mechanisms such as trichomes, thick secondary wall or toxic compounds, plants are also equipped with inducible defense mechanisms (Paiva, 2000; Walling, 2000). The inducible defenses function either directly via mechanisms such as production of amino acid catabolizing enzymes, antidigestive proteins, and toxic or repelling chemicals (Schoonhoven et al., 1998; Weber et al., 1999; Chen et al., 2005), or indirectly through production and release of volatile organic compounds (VOC) as a signal to the natural enemies of invaders that their prey is in the vicinity (Pare and Tumlinson, 1999; Kessler and Baldwin, 2001; Engelberth et al., 2004; Kessler et al., 2004; van Poecke and Dicke, 2004). Many inducible defense responses are activated by oxylipins, the oxygenated derivatives of fatty acids generated via the oxylipin branch pathways (Creelman and Mullet, 1997; Blee, 2002).

Allene oxide synthase (AOS) and hydroperoxide lyase (HPL) are the two main competing oxylipin-pathway branches producing stress-inducible compounds (Feussner and Wasternack, 2002). The metabolites of the AOS branch are jasmonates (jasmonic acid (JA), methyl jasmonate (MeJA) and their biosyn-

thetic intermediate, 12-oxophytodienoic acid (12-OPDA)). Jasmonates were shown to be involved in many defense responses, including microbial pathogens, herbivores, mechanical and high UV light damages, as well as regulation of carbon partitioning (Devoto and Turner, 2003). The best characterized metabolites of the HPL branch are the green leafy volatiles (GLVs) that predominantly consist of C_6-aldehydes ((Z)-3-hexenal, n-hexanal) and their respective derivatives such as (Z)-3-hexenol, (Z)-3-hexen-1-yl acetate, and the corresponding E-isomers (Matsui, 2006). The functional role of JAs in mediating plant defense responses has received far more attention than the HPL-derived metabolites (Devoto and Turner, 2003). To examine the defensive function of C_6-aldehydes and their respective derivatives, investigators have altered the levels of GLVs either by the exogenous application of synthetic metabolites (Hildebrand et al., 1993; Bate and Rothstein, 1998; Hamilton-Kemp et al., 1998; Farag et al., 2005; Kishimoto et al., 2005), or by genetic manipulation of the *HPL* expression levels in plant genotypes that are intact in their ability to produce the competing AOS-derived metabolites (Vancanneyt et al., 2001; Halitschke et al., 2004; Kessler et al., 2004; Shiojiri et al., 2006). Collectively, these studies provide strong support for the important role of the HPL-derived metabolites in mediating plant defense responses. However, given the well documented substrate competition between the two branch pathways

*E-mail: kdehesh@ucdavis.edu

(Feussner and Wasternack, 2002; Matsui, 2006), and the considerable overlap in regulation of gene expression by HPL- and AOS-derived oxylipins (Halitschke et al., 2004), it has not been possible to conclusively determine whether or not each of these metabolites plays a distinct role in mediating direct and/or indirect plant defense responses. To uncouple the signaling roles of the C_6-aldehydes from those of the jasmonates in defense responses, we have generated an ensemble of plant genotypes lacking either one or both metabolites, and subsequently challenged them with various invaders as well as an insect parasitoid. The outcome of the analysis clearly establishes that hexenyl acetate, an acetylated C_6-aldehyde is the predominant wound-inducible volatile that mediates indirect defense responses by attracting the natural enemies of plant invaders to their prey.

MATERIALS AND METHODS

Plant lines and growth conditions

All transgenic and mutant *Arabidopsis thaliana* plants employed in this report were in Columbia-0 background (Col-0) and grown as previously described (Chelab et al., 2006). All the described experiments were performed with 5 week-old plants unless otherwise noted. The *gl-1* seeds (Herman and Marks, 1989) were kindly provided by Dr. Tom Jack (Dartmouth College, Hanover, NH). Seeds for the *aos* plants (CS6149), which were generated in *gl-1* background as a result of a T-DNA insertion in the *AtAOS* (*aos-ko*), were purchased from the *Arabidopsis* Biological Resource Center (Columbus, OH). We performed PCR analyses and further confirmed the presence of T-DNA insertion within *AtAOS* as previously described (Park et al., 2002). In order to generate *Col-GFP* plants, here designated as Col, the open reading frame of GFP from pEZS-NLGFP vector was cut with *Not*I restriction enzyme and the generated DNA fragment was subsequently subcloned into the binary vector pMLBart, kindly provided by Dr. John Bowman (Monash University, Australia). Upon verification of the DNA insert by sequencing, the construct was used to transform Col-0. In addition, the *Os*HPL3-GFP construct in pMLBart previously described in (Chelab et al., 2006) was used to transform Col-0 and to generate *HPL-OE* plants. Transformation was performed by the floral-dip method (Clough and Bent, 1998), and the *Agrobacterium* strain used was EHA101. T_1 plants were germinated on soil. Selection of transgenics was by treating 10- to 12-d-old seedlings with 1:1.000 Finale (the commercial product that is 5.78% glufosinate ammonium) twice a week. Surviving plants were further screened to select for transgenics containing single inserts which were fur-

ther propagated to get the homozygous lines used in this report.

To obtain *aos-hpl-GFP*, also designated as *aos-hpl*, and *aos-HPL-OE* plants, pollen from homozygous Col and *HPL-OE* were used to fertilize the male sterile *aos-ko* flowers. Homozygous lines of *aos-hpl* and *aos-HPL-OE* were generated from the segregating F_1 population using kanamycin as well as glufosinate ammonium as selection markers. All transgenes were verified by a number of approaches including PCR analyses using gene-specific primers as described below, in concert with the examination of male sterile phenotype and metabolic profiling of jasmonates and aldehydes, the products of the AOS and HPL branches respectively. All *Arabidopsis* lines containing a T-DNA insertion within the *AtAOS* were confirmed by PCR as previously described (Park et al., 2002). The following primers were further used to verify the presence of the *HPL-OE* transgene (5'-ATGGTGCC GTCGTTCCCGCA-3' and 5'-TTAGCTGGGAGT GAGCTC-3') and the *GFP* transgene (5'-ATGGTG AGCAAGGGCGAGGA-3' and 5'-TACTTGTA CAGCTCGTCCATGCCGAGAGT-3').

Upon flowering, plants containing the *aos* genotype were sprayed every other day with 2 mM MeJA (Sigma) dissolved in 0.03% Silwett in order to maintain homozygous *aos-ko* and permit an otherwise male sterile plant to produce seeds.

Quantification of AOS- and HPL-derived metabolites

Extraction of JAs (MeJA and JA) as well as 12-OPDA were carried out as previously described (Engelberth et al., 2003; Schmelz et al., 2003) with minor adjustments. In brief, leaf material (~300 mg fresh weight) was collected from intact plants, quickly weighed, and immediately frozen in liquid nitrogen to minimize wound-induced accumulation of oxylipins. Samples were finely ground in mortar while frozen and transferred to a 4 ml screw top Supelco vial containing 1200 μl of 2-propanol/H_2O/HCl (2:1:0.002) and sonicated in a water bath for 10 min. Dichloromethane (2 ml) was added to each sample and re-sonicated for 10 min. The bottom dichloromethane/2-propanol layer was then transferred to a 4 ml glass vial, evaporated under a constant air stream and the resultant pellet was subsequently dissolved in 300 μl of diethyl ether/methanol (9:1, vol/vol) followed by the addition of 9 μl of a 2.0 M solution of trimethylsilyldiazomethane in hexane in order to convert the carboxylic acids into the methyl esters. During this step JA is converted to MeJA. The vials were then capped, vortexed, and incubated at room temperature for 25 min. Then 9 μl of 12% acetic acid in hexane were added to each sample and left at room temperature for another 25 min in order to destroy all excess trime-

thylsilyldiazomethane. The above-mentioned procedure was also used to derivatize carefully calculated amounts of JA (Sigma Inc.) as well as 12-OPDA (Larodan Fine Chemicals Inc., Sweden) in triplicates to generate calibration curves. Methyl ester volatiles were captured on Super-Q (Alltech Inc., State College, PA) columns by vapor-phase extraction as described (Engelberth et al., 2003). The trapped metabolites were then eluted with 150 μl of dichloromethane and analyzed by GC-MS using a Hewlett and Packard 6890 series gas chromatograph coupled to an Agilent Technologies 5973 network mass selective detector operated in electronic ionization (EI) mode. One μl of the sample was injected in splitless mode at 250°C and separated using an HP-5MS column (30 m × 0.25 mm, 0.25 μm film thickness) held at 40°C for 1 min after injection, and then at increasing temperatures programmed to ramp at 15°C/min to 250°C (10 min), with helium as the carrier gas (constant flow rate 0.7 ml/min). Measurements were carried out in selected ion monitoring (SIM) mode with retention times and M^+ m/z ions as follows: JA-ME (*trans* 12.66 min, *cis* 12.91 min, 224) and 12-OPDA-ME (*trans* 18.31 min, *cis* 18.75 min, 306).

C_6-aldehydes were measured as previously described (Chelab et al., 2006).

Adsorptive headspace collection and analyses of volatiles emitted from wounded or aphid infested plants

GLVs collections were performed on ~2.2 g of either non wounded or mechanically wounded 5 week-old *Arabidopsis* plants in ~4 L glass desiccators-style containers (Duran Inc., Germany). GLVs were also collected from plants that were either intact or infested with ~500 aphid/plant. These plants were maintained, for the duration of sample collection (72 h), in ~4 L glass desiccators-style containers.

The dynamic headspace collection was performed using an air pump, circulating charcoal purified air in a closed loop at a rate of ~2 L min^{-1}. Emitted volatiles were trapped in a filter containing 50 mg of Porapak Q® (Waters Inc., Milford, MA) at the indicated times and the metabolites were subsequently eluted by applying 200 μl of dichloromethane to the filter. GLVs were analyzed on the same GC-MS instrument described above. One μl of the eluted sample was injected at 250°C in splitless mode and separated on a DB1MS (m×0.25mm×0.25μm). The GC oven temperature was programmed as follows: 5 min at 40°C, ramp to 200°C at 6°C/min with no hold time, but with a post run of 5 min at 250°C. Helium was the carrier gas at 53 ml/min. The mass spectrometer was run in the scan mode. Triplicate measurements from three independent biological samples were carried out for each time point. The identity of (Z)-3-hexen-1-yl acetate was determined by

comparing the retention time (12.68 min) and mass spectra with that of an authentic standard. The amount of the volatile was computed subsequent to careful preparation of a calibration curve using (Z)-3-hexen-1-yl acetate as a standard.

Sources of insects and their maintenance

Green peach aphid (*M. persicae*) colonies were maintained on cabbage seedlings (*Brassica oleracea* var. *capitata*) at laboratory conditions (25±5°C, 50±20% relative humidity, 16 h light). *A. colemani* pupae were obtained from Koppert Inc. (Netherlands). The parasitoids emerged in closed containers at the above described laboratory conditions employed for the development of aphids.

Y-tube olfactometer bioassay using parasitoid wasp

The following bioassay was performed as previously described (Pareja et al., 2007) but with minor adjustments. Briefly, a glass Y-tube (diameter: 2.5 cm; trunk: 26 cm; arm: 12 cm) was used as the bioassay arena. The gas carrying the volatiles was clean in-house air which was filtered through activated charcoal before being split in two. Each stream was passed at 400 ml/min through ~4 L glass container having 2.2 g of mechanically wounded *Arabidopsis* leaves. All connections between the parts described were with Teflon tubing. After every fourth run, the Y-tube and glass vessels washed and rinsed with acetone and placed in an oven at 60°C. All bioassays were carried out at room temperature under artificial lighting in a white cardboard box with the Y-tube vertically placed.

In order to test the response of *A.colemani* to HPL-derived metabolites, volatiles from wounded *aos-hpl* leaves were tested against those of *aos-HPL-OE*. In addition, the parasitoid's response to synthetic hexenyl acetate was tested by allowing it to choose between volatiles from wounded *aos-hpl* leaves placed next to filters spotted with either 100 ng of synthetically pure hexenyl acetate (10 ng μl^{-1} in hexane) or 10 μl of hexane as the control. One-tailed binomial tests were performed to test the significance of the predators' choices for nymph deposition (Zar, 1999).

RESULTS AND DISCUSSION

Hexenyl acetate is the predominant plant volatile synthesized de novo in a transient fashion in response to wounding

We generated an ensemble of plant genotypes lacking either one or both sets of AOS- and HPL-derived metabolites using natural genetic variation and transgenic technologies. The *Arabidopsis* accession Columbia-0, is a natural loss-of-function

mutant in *hpl* and thereby lacks C$_6$-aldehydes (Duan et al., 2005). The double mutant lacking both C$_6$-aldehydes and jasmonates (*aos-hpl*) is an engineered T-DNA insertion line in *AOS* resulting in generation of *aos* loss-of-function plants in the trichomeless background (*gl-1*, accession Col-0) (Park et al., 2002). Hence this plant genotype is impaired in its ability to accumulate both JAs and C$_6$-aldehydes. In addition, this plant is male sterile and can only be maintained as homozygous for the *aos* mutation by spraying the developing flowers with MeJA (Park et al., 2002). We genetically modified these existing single and double mutant lines

to produce C$_6$-aldehydes. To restore the aldehyde-producing capabilities of the wild type Col (WT) background, we had previously generated transgenic plants overexpressing a rice *Os*HPL3-GFP fusion construct (*HPL-OE*), as well as lines expressing GFP alone as the control (for simplicity designated here as Col) (Chehab et al., 2006). The basal and wound induced levels of C$_6$-aldehydes (hexenals and hexanals) in *HPL-OE* plants were at least 50-fold higher than the negligible levels produced via non enzymatic cleavage of the substrate in the control lines (Figure 1A). Wounding induces
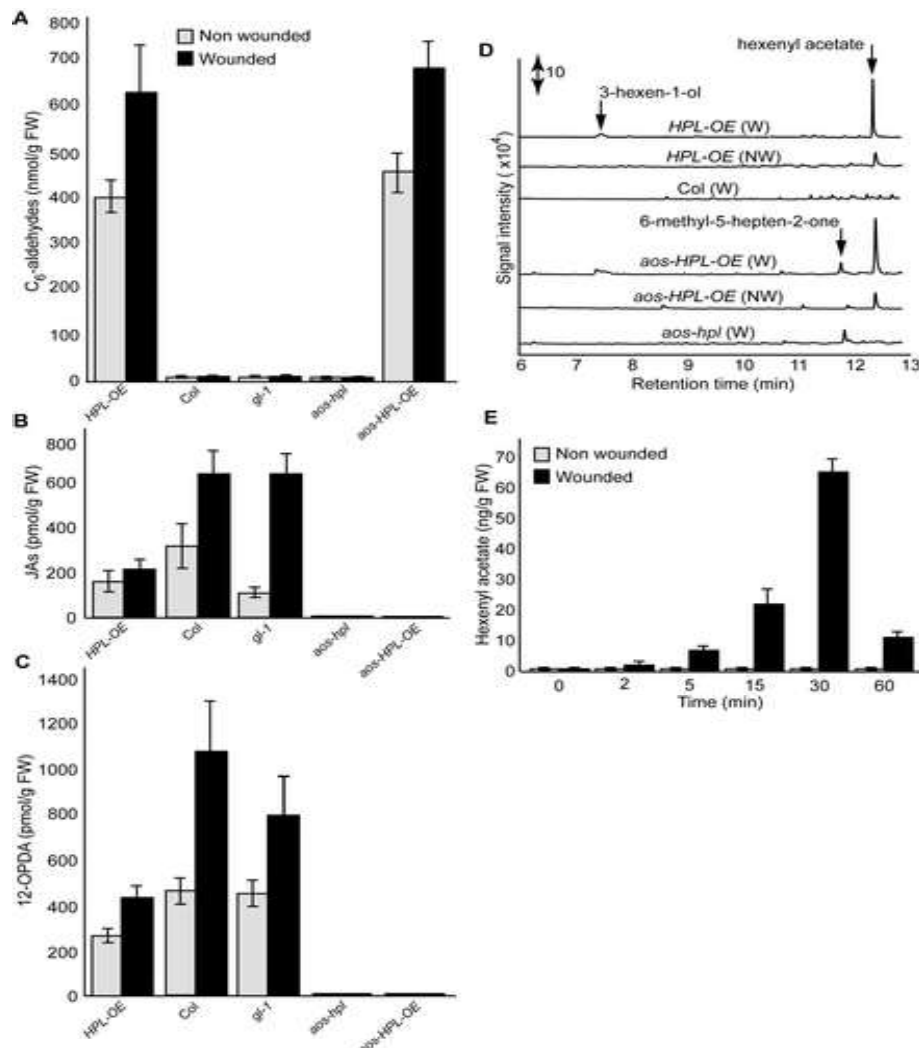

Figure 1. Profiling of the HPL- and AOS-branch pathways metabolites. (A) Levels of C$_6$-aldehydes, (B) JAs (JA+MeJA), and (C) 12-OPDA determined in non-wounded (grey bar), or wounded leaves 2 hours after mechanical damage (black bar). Each measurement is derived from the mean±standard deviation (SD) of three independent biological replicates. (D) Characterization and quantification of GLVs by adsorptive headspace collection and GC-MS analyses performed on three repeats of three independent biological replicates from wounded and non-wounded *Arabidopsis* genotypes show that hexenyl acetate is the predominant volatile produced in wounded leaves of plants with a functional *HPL*. Double-headed arrow represents a scale for signal intensity. (E) Analyses of the emission rate of hexenyl acetate in non-wounded (grey bar) or mechanically wounded (black bar) *aos-HPL-OE* plants, performed three times on three independent biological replicates show that emission of hexenyl acetate is wound-inducible and transient.

a 33% increase of these C_6-aldehydes in the *HPL-OE* line (Figure 1A). This is in spite of the constitutive expression of *HPL* under the 35S promoter, which may indicate the limited availability of the basal levels of substrates. Concomitant with these increases in the levels of C_6-aldehydes there is a ~60% reduction in the basal and wound-induced levels of JAs (JA and MeJA) and 12-OPDA in the *HPL-OE* as compared to the levels in the control Col, the naturally *hpl* mutant background (Figure 1B and C). These data, consistent with the previous reports (Halitschke et al., 2004), confirm the controlling role of substrate flux in biosynthesis of oxylipins and demonstrate that overexpression of the HPL branch reduces the pool of substrate available for the biosynthesis of jasmonates.

To restore C_6-aldehyde metabolism in the double mutant background (*aos-hpl*), while circumventing any potential influence of the transgene's insertion site or accumulation of second site mutations as the result of the transformation process, we out-crossed the *HPL-OE* to the *aos-hpl* and generated F_1 lines. To select a homozygous *aos-HPL-OE* plant in the subsequent segregating populations, we exploited the male sterile phenotype observed in plants lacking jasmonates (Park, 2002), in combination with the use of the selectable marker employed in generation of *HPL-OE* lines. Profiling of AOS- and HPL-derived metabolites of wounded and non-wounded *aos-HPL-OE* homozygous plants determined that while their jasmonates are below detection levels, their C_6-aldehydes are at levels comparable to those present in the *HPL-OE* line (Figure 1A, B and C). As a control we also out-crossed *aos-hpl* to Col, and generated a homozygous *aos-hpl-GFP* line for simplicity now designated also as *aos-hpl*. These plants, similar to the parental *aos* loss-of-function line in the *gl-1* background, are impaired in the production of both jasmonates and C_6-aldehydes in contrast to the *gl-1* background that is deficient only in C_6-aldehydes (Figure 1A, B and C).

To simultaneously characterize and quantify the wound induced VOCs, we conducted adsorptive headspace collection from all the above described genotypes. This analysis identified 3-hexen-1-yl acetate (hexenyl acetate), the acetylated derivative of (Z)-3-hexenol, as the predominant volatile which was released only from the aldehyde-producing plants namely, the *aos-HPL-OE* and *HPL-OE* lines (Figure 1D). Wounding of *aos-HPL-OE* or *HPL-OE* lines led to emission of ~20-fold higher levels of hexenyl acetate than the corresponding non-wounded plants. Additional analyses designed to measure the emission rate of hexenyl acetate established that this plant volatile is synthesized *de novo* and is released rapidly and transiently in response to wounding. Specifically, these data show that a

negligible basal level of hexenyl acetate is emitted from the non-wounded plants (Figure 1E). However, 2 minutes after wounding these levels are increased by ~2-fold (3 ng/g FW), reaching the maximum levels (68 ng/g FW) at 30 minutes, and declining by ~6.5-fold (12 ng/g FW) by 60 minutes.

Figure 2. The dynamic headspace collection set.

To specifically examine the role of hexenyl acetate, the predominant wound-induced volatile among the complex blend emitted by the plants, we also performed volatile bioassays with wounded *aos-hpl* in the presence or absence of chemically synthesized hexenyl acetate. These data clearly show that 60% of wasps were attracted to the jar containing *aos-hpl* plants along with the filters spotted with synthetic hexenyl acetate ($P = 0.034$) (Figure 3C).

Hexenyl acetate is the volatile signal from plants to natural enemies of aphids

To characterize VOCs produced by aphid infested plants we conducted adsorptive headspace collection from intact and infested *aos-hpl* and *aos-HPL-OE* plants (Figure 2). Similar to the data obtained from mechanically wounded leaves (Figure 1D), these analyses also identified hexenyl acetate as the prevalent volatile that is predominantly released from the *aos-HPL-OE* plants infested with aphids (Figure 3A). To further examine the role of aldehydes in general and hexenyl acetate in particular in mediating plant indirect responses, we performed volatile bioassays using a glass Y-tube olfactometer
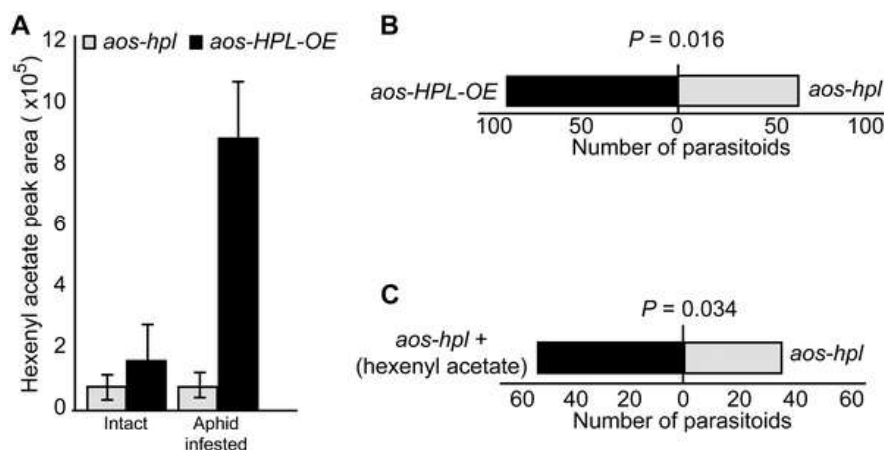
Figure 3. Attraction of parasitoid wasp, *Aphidius colemani,* to the *in vivo* wound-induced or chemically synthesized hexenyl acetate. (A) Characterization and quantification of GLVs by adsorptive headspace collection and GC-MS analyses performed on three repeats of five independent biological replicates from intact and aphid infested *aos-hpl* and *aos-HPL-OE* genotypes show that hexenyl acetate is the predominant volatile produced in aphid infested plants with a functional *HPL*. (B) Volatile bioassays using glass Y-tube olfactometer was employed to determine the response of *A.colemani* to the volatile blend produced from mechanically wounded *aos-hpl* and *aos-HPL-OE* plant genotypes. The bar graph represents the number of parasitoids examined and shows that they are significantly attracted more to the wounded *aos-HPL-OE* than to the *aos-hpl* plants (P = 0.016). (C) Volatile bioassays using glass Y-tube olfactometer was employed to determine the response of *A.colemani* to the presence or absence of synthetic hexenyl acetate in chambers containing wounded *aos-hpl* plant genotype. The bar graph represents the number of parasitoids examined and shows that they are significantly attracted towards the chamber of wounded *aos-hpl* plants with hexenyl acetate-spotted filters as compared to the plant chamber containing the same plant genotype but with hexane-spotted filters as the control (P = 0.034). One-tailed binomial tests were used to determine significance.

and examined attraction of *Aphidius colemani* to wounded *aos-hpl* versus *aos-HPL-OE*. This wasp is parasitic to a range of aphids including green peach aphid. The female wasp finds aphid colonies from a long distance by "alarm signals" produced by an infected plant and lays its egg directly inside the aphid, where the larva feeds and develops into a fully formed wasp killing the aphid in the process. Preference tests using 160 *A.colemani* females released individually show that a statistically significant number of these female parasitoid wasps are attracted to *aos-HPL-OE*, as compared to *aos-hpl* plants (P = 0.016) (Figure 3B).

SUMMARY

This study conclusively establishes the role of C_6-aldehydes in plant defense responses. We exploited the genotypes generated in our laboratory lacking either one or both sets of AOS- and HPL-derived metabolites to demonstrate role of hexenyl acetate, an acetylated C_6-aldehyde, as the predominant wound-inducible volatile signal that mediates indirect defense responses by directing tritrophic (plant-herbivore-natural enemy) interactions.

REFERENCES

Bate N.J., Rothstein S.J. (1998) C_6-volatiles derived from the lipoxygenase pathway induce a subset of defense-related genes. Plant J. **16:** 561-569.

Blee E. (2002) Impact of phyto-oxylipins in plant defense. Trends Plant Sci. **7:** 315-322.

Chehab E.W., Raman G., Walley J.W., Perea J.V., Banu G. et al. (2006) Rice hydroperoxide lyases with unique expression patterns generates distinct aldehyde signatures in *Arabidopsis*. Plant Physiol. **141:** 121-134.

Chen H., Wilkerson C.G., Kuchar J.A., Phinney B.S., Howe G.A. (2005) Jasmonate-inducible plant enzymes degrade essential amino acids in the herbivore midgut. Proc. Natl. Acad. Sci. USA **102:** 19237-19242.

Clough S.J., Bent A.F. (1998) Floral dip: a simplified method for Agrobacterium-mediated transformation of *Arabidopsis thaliana*. Plant J. **16:** 735-743.

Creelman R.A., Mullet J.E. (1997) Biosynthesis and action of jasmonates in plants. Annu. Rev. Plant Physiol. Plant Mol. Biol. **48:** 355-381.

Devoto A., Turner J.G. (2003) Regulation of jasmonate-mediated plant responses in *Arabidopsis*. Ann. Bot. **92:** 329-337.

Duan H., Huang M.Y., Palacio K., Schuler M.A. (2005) Variations in CYP74B2 (hydroperoxide lyase) gene expression differentially affect hexenal signaling in the Columbia and Landsberg erecta ecotypes of *Arabidopsis*. Plant Physiol. **139:** 1529-1544.

Engelberth J., Schmelz E.A., Alborn H.T., Cardoza Y.J., Huang J. et al. (2003) Simultaneous quantification of jasmonic acid and salicylic acid in plants by vapor-phase extraction and gas chromatography-chemical ionization-mass spectrometry. Anal. Biochem. **312:** 242-250.

Engelberth J., Alborn H.T., Schmelz E.A., Tumlinson J.H. (2004) Airborne signals prime plants against insect herbivore attack. Proc. Natl. Acad. Sci. USA **101:** 1781-1785.

Farag M.A., Fokar M., Abd H., Zhang H., Allen R.D. et al. (2005) (Z)-3-Hexenol induces defense genes and downstream metabolites in maize. Planta **220:** 900-909.

Feussner I., Wasternack C. (2002) The lipoxygenase pathway. Annu. Rev. Plant Biol. **53:** 275-297.

Halitschke R., Ziegler J., Keinanen M., Baldwin I.T. (2004) Silencing of hydroperoxide lyase and allene oxide synthase reveals substrate and defense signaling crosstalk in *Nicotiana attenuata*. Plant J. **40:** 35-46.

Hamilton-Kemp T.R., Archbold D.D., Langlois B.E., Collins R.W. (1998) Antifungal activity of E-2-hexenal on strawberries and grapes. Abstr. Pap. Am. Chem. Soc. **216:** U34.

Herman P.L., Marks M.D. (1989) Trichome Development in *Arabidopsis thaliana*. II. Isolation and Complementation of the GLABROUS1 Gene. Plant Cell **1:** 1051-1055.

Hildebrand D.F., Brown G.C., Jackson D.M., Hamilton-Kemp T.R. (1993) Effects of some leaf-emitted volatile compounds on aphid population increase. J. Chem. Ecol. **19:** 1875-1887.

Kessler A., Baldwin I.T. (2001) Defensive function of herbivore-induced plant volatile emissions in nature. Science **291:** 2141-2144.

Kessler A., Halitschke R., Baldwin I.T. (2004) Silencing the jasmonate cascade: induced plant defenses and insect populations. Science **305:** 665-668.

Kishimoto K., Matsui K., Ozawa R., Takabayashi J. (2005) Volatile C$_6$-aldehydes and Alloocimene activate defense genes and induce resistance against *Botrytis cinerea* in *Arabidopsis thaliana*. Plant Cell Physiol. **46:** 1093-1102.

Matsui K. (2006) Green leaf volatiles: hydroperoxide lyase pathway of oxylipin metabolism. Curr. Opin. Plant Biol. **9:** 274-280.

Paiva N.L. (2000) An introduction to the biosynthesis of chemicals used in plant-microbe communication. J. Plant Growth Regul. **19:** 131-143.

Pare P.W., Tumlinson J.H. (1999) Plant volatiles as a defense against insect herbivores. Plant Physiol. **121:** 325-332.

Pareja M., Moraes M.C., Clark S.J., Birkett M.A., Powell W. (2007) Response of the aphid parasitoid *Aphidius funebris* to volatiles from undamaged and aphid-infested *Centaurea nigra*. J. Chem. Ecol. **33:** 695-710.

Park J.H., Halitschke R., Kim H.B., Baldwin I.T., Feldmann K.A. et al. (2002) A knock-out mutation in allene oxide synthase results in male sterility and defective wound signal transduction in *Arabidopsis* due to a block in jasmonic acid biosynthesis. Plant J. **31:** 1-12.

Schmelz E.A., Alborn H.T., Engelberth J., Tumlinson J.H. (2003) Nitrogen deficiency increases volicitin-induced volatile emission, jasmonic acid accumulation, and ethylene sensitivity in maize. Plant Physiol. **133:** 295-306.

Schoonhoven L.M., Jermy T., Van Loon J.J.A. (1998) Insect-plant biology – from physiology to evolution. Plant Growth Regul. **28:** 217-218.

Shiojiri K., Kishimoto K., Ozawa R., Kugimiya S., Urashimo S. et al. (2006) Changing green leaf volatile biosynthesis in plants: an approach for improving plant resistance against both herbivores and pathogens. Proc. Natl. Acad. Sci. USA **103:** 16672-16676.

van Poecke R.M., Dicke M. (2004) Indirect defence of plants against herbivores: using *Arabidopsis thaliana* as a model plant. Plant Biol. (Stuttg.) **6:** 387-401.

Vancanneyt G., Sanz C., Farmaki T., Paneque M., Ortego F. et al. (2001) Hydroperoxide lyase depletion in transgenic potato plants leads to an increase in aphid performance. Proc. Natl. Acad. Sci. USA **98:** 8139-8144.

Walling L.L. (2000) The myriad plant responses to herbivores. J. Plant Growth Regul. **19:** 195-216.

Weber H., Chetelat A., Caldelari D., Farmer E.E. (1999) Divinyl ether fatty acid synthesis in late blight-diseased potato leaves. Plant Cell **11:** 485-494.

Zar J.H. (1999) Biostatistical analysis. 4th edition, Prentice Hall, Upper Saddle River, New Jersey: 929 p.

Single-Stranded DNA Plant Viruses in Azerbaijan, the State of the Art

**Ioana Grigoras[1], Heinrich-Josef Vetten[2], Nargiz F. Sultanova[3], Stephan Winter[4],
Irada M. Huseynova[3], Alamdar Ch. Mamedov[3], Ahmed Kheyr-Pour[5], Bruno Gronenborn[1]***

[1]*Institut des Sciences du Végetal, CNRS, 91198 Gif sur Yvette, France*
[2]*Julius Kühn Institute, Bundesforschungsinstitut für Kulturpflanzen, Institut für Epidemiologie und
Pathogendiagnostik, D-38104 Braunschweig, Germany*
[3]*Institute of Botany, Azerbaijan National Academy of Sciences, 40 Badamdar Shosse, Baku AZ 1073,
Azerbaijan*
[4]*DSMZ Plant Virus Department, Inhoffenstrasse 7B, 38124, Braunschweig, Germany*
[5]*31 Allée des Joncherettes, 91190 Gif sur Yvette, France*

**We describe an initial assessment of plant viruses with a single-stranded DNA genome in Azerbaijan.
In the years 2009 and 2010, a limited survey of cultivated and wild legumes as well as of tomato has
uncovered the presence of three different nanoviruses, two distinct faba bean necrotic yellows viruses
and one faba bean necrotic stunt virus. In addition, tomato plants showing symptoms typical of tomato
yellow leaf curl virus, a geminivirus, were encountered. The results presented provide proof for the
efficiency of combining serological diagnosis with the power of DNA rolling circle amplification (RCA)
to rapidly obtain genetic information on viral plant pathogens with a circular DNA genome.**

Keywords: single-stranded DNA virus, geminivirus, nanovirus, rolling circle amplification, legumes

INTRODUCTION

The remarkable floral biodiversity of
Azerbaijan has triggered some recent interest in the
biodiversity of endemic plant viruses as well, in
particular plant viruses with a single-stranded (ss)
DNA genome. Plant viruses with an ssDNA
genome have been assigned to two families,
Geminiviridae and *Nanoviridae* (Stanley et al.,
2005; Vetten et al., 2005).

Geminiviruses are distributed worldwide and
some of them cause very severe and economically
important diseases. Examples include viruses
responsible for maize streak disease (the maize
streak virus group), cassava mosaic virus disease
(the African and Indian cassava mosaic viruses),
and viruses causing tomato (yellow) leaf curl
disease, the tomato-infecting geminiviruses.
Whereas the former two groups are restricted to
Africa and the Indian Subcontinent, members of the
latter are found worldwide in tropical, subtropical,
semi-arid and Mediterranean climate zones. For a
comprehensive recent assessment of the disease
caused by tomato yellow leaf curl virus, the
molecular biology of the virus and its worldwide
agronomical impact on tomato cultivation see
contributions in (Czosnek, 2007). Geminiviruses
are transmitted by different leafhopper species or
the whitefly *Bemisia tabaci* and are assigned, based
upon their transmission vector in combination with
their respective genome organization, to four
genera in the family *Geminiviridae*. All tomato-
infecting geminiviruses belong to the genus
Begomovirus with an ever-increasing number of
tomato (yellow) leaf curl viruses transmitted by
B.tabaci.

Compared to the geminiviruses, members of
the family *Nanoviridae* are by far less numerous
and also much less studied and understood.
Nanoviruses are transmitted by various aphid
species in a persistent and non-propagative manner.
An economically very important nanovirus causes
bunchy top disease in banana and is indigenous in
Southeast Asia and the Pacific region including
Australia (Nelson, 2006). Banana bunchy top virus,
the causal agent of the disease, currently invades
Africa and the Indian subcontinent (Khalid and
Smooro, 1993; Karan et al., 1994). The other very
important nanovirus is faba bean necrotic yellows
virus (FBNYV), indigenous in regions of West
Asia and North Africa. In some years yield losses
of faba bean production due to FBNYV were con-
siderable and have had serious impacts on food
supply in Egypt during the 1990ies (Makkouk and
Kumari, 2009). In recent years, diseases caused by
nanoviruses emerged in numerous countries of the

Mediterranean Basin and the Near East. First reports of nanoviruses from European countries date from 2005 for Spain (Ortiz et al., 2006), 2008 for Azerbaijan (Kumari et al., 2009) and 2009 for Germany (Grigoras et al., 2010). Contrary to the well studied geminiviruses, knowledge on the biology and molecular genetics (Grigoras et al., 2010). Contrary to the well studied geminiviruses, knowledge on the biology and molecular genetics of nanoviruses is still less advanced (Gronenborn, 2004), yet recent progress in diagnosis and reverse genetics of faba bean necrotic stunt virus (FBNSV) is expected to allow for rapid compensation for the deficit (Grigoras et al., 2009).

The advent of the multiple displacement amplification or rolling circle amplification (RCA) technique has considerably facilitated diagnosis and molecular identification of viruses with ssDNA genomes (Haible et al., 2006). RCA and subsequent cloning and sequencing have allowed us to identify three distinct nanoviruses from Azerbaijan. In the following a short summary of the progress in the molecular characterization of nanoviruses from Azerbaijan is provided.

MATERIAL AND METHODS

Field prospecting

In June 2009 and in June 2010 several tomato (*Solanum lycopersicum*) fields as well as fields and gardens with chickpea (*Cicer arietinum*), lentil (*Lens culinaris*) and faba bean (*Vicia faba*) were surveyed for plants showing symptoms of a potential infection by a geminivirus and/or a nanovirus. Surveys of tomato plantings were near Khachmaz, Goychay, Masalli (Onjagala) and Lenkoran; legumes were surveyed in Lahij-Arakit (faba bean, wild legumes), Farzili near Jalilabad (chickpea), Peshtatuk (chickpea, lentil), and Jangamiran near Lerik (chickpea). The locations in Lahij-Arakit and Onjagala were visited in both 2009 and 2010 as samples of the 2009 survey had yielded interesting results. Samples were collected as fresh leaf material until they were frozen at -80°C. In 2009, sample tissue was also blotted onto Whatman FTA® classic cards for later DNA analyses.

Serological analyses were done as described in Grigoras et al. (2009).

Molecular analyses and sequencing

Frozen plant samples were ground in liquid nitrogen, and DNA was prepared using the method of Edwards et al. (1991), modified as described by Grigoras et al. (2009). We used 5-μL aliquots of the amplified DNA for diagnostic digests by restriction endonucleases, see examples shown in Figure 4. Preparative restriction endonuclease digests for

cloning of the respective nanovirus genome components were carried out using between 10 and 50 μL of RCA product and subsequent resolution by preparative 0.7% agarose gel electrophoresis. One kb fragments were cut from the gel, purified, cloned and sequenced as described by Grigoras et al. (2009).

RESULTS

Tomato

The tomato fields visited appeared generally healthy and productive. In particular, no widespread symptoms of tomato yellow leaf curl virus (TYLCV), a very devastating virus in neighbouring Iran, were noticed. However, a particular case of damage of tomato crops was encountered in the Goychay region in 2009, where tomato was grown in plastic greenhouses. Here, the plants suffered from severe infestation with probably several pathogens (Figure 1A), and the fruits were of non-marketable quality (Figure 1B). Analyses carried out at the DSMZ, Braunschweig, Germany, identified tomato bushy stunt virus, a soil- and waterborne pathogen, as the major cause of the detrimental disease.

Other tomato samples collected in 2009 and 2010 were analyzed in part at the Institute of Botany, Azerbaijan National Academy of Sciences, Baku, and at the ISV, Gif sur Yvette, France. Contrary to earlier surveys of tomato and cucurbits in 2003 and 2005, when no TYLCV or watermelon chlorotic stunt virus were detected (A. Kheyr-Pour), a few tomato plants showing symptoms typical of TYLCV infections were found in a small tomato plot at Onjagala, south of Masalli, both in 2009 and 2010 (Figure 2). In 2009, one single plant with an apparently late infection was encountered. In 2010, several plants with serious infections were scored, which means that the virus and its vector are established in the area.

First molecular analyses of the extracted DNA after RCA at Baku hinted at a geminivirus as the causative agent. However, the final confirmation of the specific TYLCV species or strain by polymerase chain reaction (PCR), RCA-based RFLP analysis or molecular cloning is still pending.

An epidemiological follow-up of these findings is of major importance, as in southern Azerbaijan the climatic conditions for the viral vector *B.tabaci* are ideal and the as yet only sporadic occurrence of the virus may turn into a serious threat for tomato cultivation in that region.

Legumes

Since in late June there were not too many

Figure 1. Damaged and non-marketable tomatoes from plastic greenhouses in the region of Goychay (2009).

Figure 2. Typical symptoms of tomato yellow leaf curl virus. Left: Example from 2009; right: example from 2010, same field.

legume crops in the field anymore, only two larger chickpea fields were inspected, one near Jalilabad (Farzili) in 2009, and one near Lerik (Jangamiran) in 2010.

No obvious symptoms of a viral infection were observed in both cases. This assessment was later confirmed by the serological analyses carried out at the Julius Kğhn Institute (JKI), Braunschweig, Germany, where a panel of antisera specific for various legume-infecting viruses was used for diagnosis. Only one chickpea sample from Farzili near Jalilabad was diagnosed as infected by a (non-specified) luteovirus.

Therefore, we specifically looked in more remote areas and in private gardens to find and identify potential reservoir plants containing legume-infecting gemini- or nanoviruses. All samples collected originated from small gardens with only a few faba bean plants intercropped with potato (Lahij-Arakit). The lentil and chickpea samples from Peshtatuk were also from garden-sized plots with about 50 to 100 plants each. In addition, a number of wild legume species were sampled both around Lahij as well as in the Lerik area, but none of them proved to be infected with a nanovirus or a geminivirus.

A selected number of samples were analyzed at the Institute des Sciences du Vygytal, CNRS, Gif sur Yvette, France, by molecular DNA analyses, and in parallel at the JKI, Braunschweig, Germany, by ELISA-based serology. For instance, out of 32 wild- and cultivated legume samples collected in 2010 two were found infected by alfalfa mosaic virus (AMV), two by bean yellow mosaic virus (BYMV), one by bean leaf roll virus (BLRV), one with both AMV and BLRV, and two with a nanovirus.

Whereas one garden in Lahij-Arakit (family Muslim) in 2009 was infested by a nanovirus and luteoviruses (not specified) at about 50% incidence, no nanovirus infection was detected in the same two gardens in Arakit (family Muslim and Gilexanim) when visited in 2010. This contrasts the increased incidence of TYLCV in Onjagala (Masalli) in 2010 compared to that of 2009.

Figure 3 shows two examples of nanovirus-infected legumes, faba bean infected by (as we now know from the molecular analyses) faba bean necrotic yellows virus (FBNYV) and lentil infected with (as we now know from the molecular analyses) faba bean necrotic stunt virus (FBNSV). The faba bean sample was collected at Arakit in

Figure 3. Faba bean necrotic yellows virus-infected faba bean from Lahij-Arakit (left) and faba bean necrotic stunt virus-infected lentil from Peshtatuk (right).

2009, and the lentil sample is from Peshtatuk collected in 2010. The identity of the two aforementioned nanoviruses has been confirmed by both serology and molecular analyses (see below).

Molecular characterization

Only a fraction of all samples has been analyzed to date. Legume samples, in which a nanovirus was serologically detected, were given priority and analyzed at greater details. DNA of selected samples was prepared, subjected to RCA and analyzed by restriction endonuclease treatment. Resulting DNA fragments were resolved by agarose gel electrophoresis, and eventually cloned and sequenced (ISV, Gif).

An example of the molecular analyses of four legume samples from Peshtatuk collected in 2010 is shown in Figure 4.
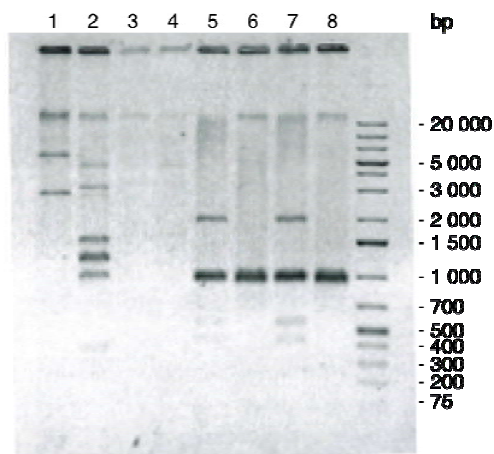

Figure 4. Restriction analysis of RCA-amplified DNAs of chickpea and lentil from Peshtatuk.

DNA of two chickpea (Figure 4, lanes 1-4) and two lentil (lanes 5-8) samples was amplified by RCA, restricted by endonuclease *Aat*II (lanes 1, 3, 5, 7) or *Hind*III (lanes 2, 4, 6, 8), and resolved by agarose gel electrophoresis. The DNA in lanes 5-8 was restricted into a major fragment of 1 kb; in case of the *Aat*II digests (lanes 5 and 7) also a minor product of 2 kb was produced. Our experience with nanovirus DNA segments shows that without exception so far, at least some genomic DNAs of a nanovirus have an *Aat*II site. Hence, the predominant 1-kb fragment produced by *Aat*II was a strong indication of the presence of a nanovirus in the two samples from lentil. No nanovirus-specific DNA pattern after restriction with *Aat*II or *Hind*III was obtained for the two chickpea samples shown. The same two lentil samples also reacted not only with broad-spectrum nanovirus antibodies but also with FBNSV-specific antibodies.

Consequently, DNA of the sample shown in lanes 7 and 8 (Peshtatuk #12b) was amplified at a preparative scale, restricted by *Aat*II or various other restriction endonucleases, and the purified 1kb fragments were cloned and sequenced. In a similar way, DNA of faba bean samples collected in Lahij-Arakit in 2009 was analyzed, and from two distinct locations about 0.5 km apart, garden of family Muslim (example shown in Figure 3, left), and garden of Gilexanim, several nanovirus positive samples were identified by serology and DNA analyses.

As of October 2010, all eight DNAs of a typical faba bean necrotic yellows virus were identified in a faba bean sample from Lahij-Arakit (collected in 2009 from family Muslim's garden), and were cloned and sequenced. From a sample collected in the garden of Gilexanim, Lahij-Arakit, in 2009 six DNAs of a typical, yet different faba bean necrotic
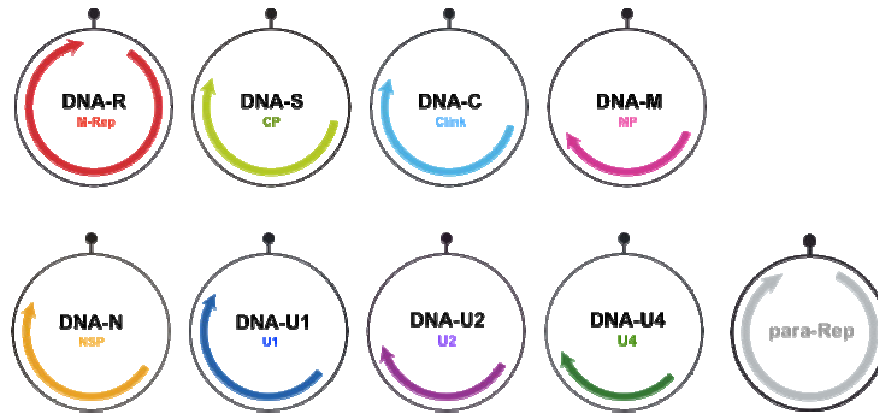
Figure 5. Genome organization of a typical nanovirus. The eight single-stranded virus DNAs are shown as circles with the common short inverted repeat sequences displayed as a stem loop. All are about 1 kb in size, coding regions for the eight different proteins are symbolized by proportionally sized arrows. Genome component names are shown along with the names of the encoded proteins. M-Rep, master replication initiator protein (Timchenko et al., 2000); CP, capsid protein; Clink, cell cycle link protein (Aronson et al., 2000); MP, movement protein; NSP, nuclear shuttle protein (Wanitchakorn et al., 2000); U1, U2, U4, proteins of as yet unknown function. A non-essential alphasatellite DNA encoding a para-Rep is also shown.

yellows virus, were also cloned and sequenced. DNA-U2 and -U4 have not yet been identified from the latter isolate, however, an additional para-Rep encoding DNA (alphasatellite) of the para-Rep1-type (Timchenko et al., 1999) was found here.

From the lentil sample #12b (Figure 3, right) collected in Peshtatuk in 2010 (garden of Nabiyev family), seven DNAs of a typical FBNSV isolate were cloned and sequenced, with identification of a DNA-U2 still pending. Interestingly, the partial FBNYV capsid protein gene sequences of a lentil and a vetch isolate of FBNYV determined by Kumari and colleagues (Kumari et al., 2009) are similar to DNA-S of FBNYV isolate #13-5 (faba bean) from family Muslim's garden, Lahij-Arakit, and to that of a faba bean isolate from Kermanshah, Iran (GenBank acc. AM493900), whereas the DNA-S of the FBNYV isolate AZ.12 from faba bean collected in Gilexanim's garden, only about 0.5 km away from the previous one in Lahij-Arakit, is more closely related to a FBNYV isolate from Alashtar, Iran, originating from chickpea (GenBank acc. AM493899). The sequences of the Iran isolates had been determined some years ago in our laboratory (Bananej K., Timchenko T., Gronenborn B.). The relationships between the Azerbaijani nanoviruses with the rest of the virus family were established by phylogenetic analysis. We aligned all available genome sequences using ClustalW and calculated the respective genetic distances based upon their pairwise sequence similarity. The phylogeny revealed that the FBNSV isolate from Peshtatuk is more closely related to a FBNSV isolate from Morocco (Abraham et al., 2010) than

to FBNSV from Ethiopia, where the virus was found first. This finding raises some intriguing questions about the natural evolution of that virus or its eventual human distribution. Further surveys may shed more light on the phylogeography of these emerging pathogens.

CONCLUSION

In summary, the still limited analyses of tomato and legume samples collected in our surveys of 2009 and 2010 have already led to the identification of three distinct nanoviruses from Azerbaijan. The symptoms of a TYLCV-like infection in tomato make it almost certain that this geminivirus is present also in southern Azerbaijan, notwithstanding the fact that final molecular proof is pending. A thorough epidemiological follow-up of these findings will be important, as the climatic conditions in the Jalilabad, Masalli, Lenkoran region are ideal for *B.tabaci*, the viral vector of TYLCV and other begomoviruses. Therefore, the as yet only sporadic occurrence of TYLCV may turn into a serious threat for tomato cultivation in that region.

The floral biodiversity of Azerbaijan may well harbour also quite diverse ssDNA plant viruses, and that our initial analyses may have only touched the tip of the iceberg. We are convinced that further extended surveys and in-depth characterization of the material collected might reveal more ssDNA viruses and maybe even ones that were never before described.

ACKNOWLEDGEMENTS

REFERENCES

Abraham A.D., Bencharki B., Torok V., Katul L., Varrelmann M., Vetten H.J. (2010) Two distinct nanovirus species infecting faba bean in Morocco. Arch. Virol. **155:** 37-46.

Aronson M.N., Meyer A.D., Gyürgyey J., Katul L., Vetten H.J., Gronenborn B., Timchenko T. (2000) Clink, a nanovirus-encoded protein, binds both pRB and SKP1. J. Virol. **74:** 2967-2972.

Czosnek H. (2007) Tomato Yellow Leaf Curl Virus Disease: Management, Molecular Biology, Breeding for Resistance. Springer, Dordrecht, The Netherlands: 350 p.

Edwards K., Johnstone C., Thompson C. (1991) A simple and rapid method for the preparation of plant genomic DNA for PCR analysis. Nucleic Acids Res. **19:** 1349.

Grigoras I., Gronenborn B., Vetten H.J. (2010) First Report of a Nanovirus Disease of Pea in Germany. Plant Dis. **94:** 642.

Grigoras I., Timchenko T., Katul L., Grande-Pyrez A., Vetten H.J., Gronenborn B. (2009) Reconstitution of authentic nanovirus from multiple cloned DNAs. J. Virol. **83:** 10778-10787.

Gronenborn B. (2004) Nanoviruses: genome organisation and protein function. Vet. Microbiol. **98:** 103-109.

Haible D., Kober S., Jeske H. (2006) Rolling circle amplification revolutionizes diagnosis and genomics of geminiviruses. J. Virol. Methods **135:** 9-16.

Karan M., Harding R.M., Dale J.L. (1994) Evidence for two groups of banana bunchy top virus isolates. J. Gen. Virol. **75:** 3541-3546.

Khalid S., Smooro M.H. (1993) Banana bunchy top disease in Pakistan. Plant Pathol. **42:** 923-926.

Kumari S.G., Attar N., Mustafayev E., Akparov Z. (2009) First Report of Faba bean necrotic yellows virus Affecting Legume Crops in Azerbaijan. Plant Dis. **93:** 1220.

Makkouk K.M., Kumari S.G. (2009) Epidemiology and integrated management of persistently transmitted aphid-borne viruses of legume and cereal crops in West Asia and North Africa. Virus Res. **141:** 209-218.

Nelson S. (2006) Banana Bunchy Top Virus. *http://wwwctahrhawaiiedu/banana/*.

Ortiz V., Navarro E., Castro S., Carazo G., Romero J. (2006) Incidence and transmission of *Faba bean necrotic yellows virus* (FBNYV) in Spain. Span. J. Agric. Res. **4:** 255-260.

Stanley J., Bisaro D.M., Briddon R.W., Brown J.K., Fauquet C.M., Harrison B.D., Rybicki E.P., Stenger D.C. (2005) *Geminviridae*. In: Virus Taxonomy: Eighth Report of the International Committee on Taxonomy of Viruses (Fauquet C.M., Mayo M.A., Maniloff J., Desselberger U. and Ball L.A., eds.), Elsevier, Academic Press, London: 301-326.

Timchenko T., de Kouchkovsky F., Katul L., David C., Vetten H.J., Gronenborn B. (1999) A single rep protein initiates replication of multiple genome components of faba bean necrotic yellows virus, a single-stranded DNA virus of plants. J. Virol. **73:** 10173-10182.

Timchenko T., Katul L., Sano Y., de Kouchkovsky F., Vetten H.J., Gronenborn B. (2000) The master rep concept in nanovirus replication: identification of missing genome components and potential for natural genetic reassortment. Virology **274:** 189-195.

Vetten H.J., Chu P.W.G., Dale J.L., Harding R., Hu J., Katul L., Kojima M., Randles J.W., Sano Y., Thomas J.E. (2005) *Nanoviridae*. In: Virus Taxonomy: Eighth Report of the International Committee on Taxonomy of Viruses. (Fauquet C.M., Mayo M.A., Maniloff J., Desselberger U. and Ball L.A., eds.), Elsevier, Academic Press, London: 343-352.

Wanitchakorn R., Hafner G.J., Harding R.M., Dale J.L. (2000) Functional analysis of proteins encoded by banana bunchy top virus DNA-4 to -6. J. Gen. Virol. **81:** 299-306.

First Detection and Characterization of *Ca. P. brasiliense* From Yellowing Peach Tree in Guba Region of Azerbaijan

Gulnara Sh. Balakishiyeva[1,2]*, Jean-Luc Danet[2], Pascal Salar[2], Alamdar Ch. Mammadov[1], Xavier Foissac[2]

[1]*Institute of Botany, Azerbaijan National Academy of Sciences, 40 Badamdar Shosse, Baku AZ 1073, Azerbaijan*
[2]*UMR-1090 Génomique Diversité Pouvoir Pathogène, INRA and Université de Bordeaux 2, BP 81, 33883 Villenave d'Ornon, France*

"Candidatus Phytoplasma brasiliense", a new phytoplasma taxon associated with hibiscus witches broom disease was firstly described in 2001 in Brazil. The disease was characterized by symptoms of witches' broom, i.e. leaf yellowing and malformation.Yellowing peach tree (*Prunus persica*) samples reminiscent of phytoplasma infection were collected in September 2007 in Guba region, which is an important fruit and vegetable growing area in Azerbaijan. A phytoplasma was detected in the diseased peach tree by amplification of its 16 S rDNA by nested PCR with universal primers for phytoplasmas. It was furthermore characterized by RFLP and nucleotide sequence analyses of 16S rDNA. It was shown that a phytoplasma infected peach tree is *Candidatus Phytoplasma brasiliense*. This report constitutes the first detection of this phytoplasma in a plant other than hibiscus and elsewhere than in Brazil. To set up a specific detection test, cloning of a '*Ca. P. brasiliense*' DNA fragment was undertaken by comparative RAPD. The amplified *dna*K-*dna*J genetic locus was used to design a specific PCR test that amplify all '*Ca. P. brasiliense*' isolates of the group 16SrXV-A without amplifying the related members of the group 16SrII.

Keywords: "Ca. P. brasiliense", RFLP, RAPD, cloning, DNA sequencing, phylogenetic tree

INTRODUCTION

Phytoplasmas are plant pathogenic bacteria belonging to the class *Mollicutes*, a group of wall-less microorganisms phylogenetically related to low G+C content, Gram-positive bacteria (Weisburg et al., 1989). They cause hundreds of diseases worldwide and are transmitted from plant to plant by sap-feeding hemiteran insects (Lee et al., 2000; Weintraub and Beanland, 2006). As of today, the many diseases induced by phytoplasmas cannot be cured and the control of disease spread consist of implementing prophylactic measures, such as quarantine, destruction of infected plant material and pesticide treatment against the insect vectors. Implementing phytoplasma-induced diseases control requires the taxonomic characterization of the agent, the determination of its plant host range and the identification of its insect vector(s) (Lee et al., 1998). All these studies necessitate the development of methods for diagnosis which are relying on the molecular detection of phytoplasma DNA (Kirkpatrick et al., 1987; Deng and Hiruki, 1991). Phytoplasmas have been classified according to 16S-rDNA phylogeny and RFLP profiles into 30 phylogenetic groups and 28 '*Candidatus Phytoplas-*

ma' species (Zhao et al., 2010). Among these species, '*Ca. P. brasiliense*' has been described as the agent of hibiscus witches' broom in Brazil. During a survey of temperate fruit tree orchards of the North of Azerbaijan, a phytoplasma could be detected by 16SrDNA PCR in a chlorotic peach tree (*Prunus persica*). *Ca. P. prunorum*, the agent of European stone fruit yellows in the Euro-Mediterranean basin (Ahrens et al., 1993; Jarausch et al., 1998) and *Ca. P. pruni* the agent of peach western-X in North America (Purcell et al., 1981) are the two main phytoplasma damaging peach orchards in the world. We report in this paper its identification as an isolate of '*Ca. P. brasiliense*' and the development of a specific PCR detection test developed from a '*Ca. P. brasiliense*' sequence cloned after comparative RAPD.

MATERIALS AND METHODS

Plant material and DNA extraction. Yellowing peach tree (*Prunus persica*) samples reminiscent of phytoplasma infection were collected in September 2007 in Guba region. The DNAs were extracted from 1g fresh leaf midribs of diseased and healthy plants as

*E-mail: gbalakishiyeva@yahoo.com

control, following the CTAB extraction protocol (Maixner et al., 1995). In this study we also used the DNA of reference phytoplasma isolates (Table 1).

DNA amplification and RFLP analysis. Detection of phytoplasma infection was performed on 2μl of each DNA extracts tested by 16S-rDNA nested PCR with the universal primers for phytoplasmas R16mF2/R16mR1 and R16F2n/R16R2. PCR mixtures and cycling conditions were as described in the original article (Gundersen and Lee, 1996). The PCR products (7 μL) were analyzed by electrophoresis in the 1ÇTBE buffer through 1% agarose gel, stained with ethidium bromide, and DNA bands visualized using a UV transilluminator. Nested PCR products were analysed by single-restriction endonuclease digestion. 4μL PCR products were digested with 2.5 U *Alu*I (Promega) according to the manufacturer's instructions. The restriction fragments, together with the 1-kb-plus DNA size marker (Invitrogen), were separated by 2% agarose gel electrophoresis in 1ÇTBE buffer, stained with ethidium bromide and visualized under UV.

DNA sequencing. The PCR product obtained from peach tree were also sequenced by COGEN-ICS (Grenoble, France) on MegaBACE capillary sequencing instruments. The raw sequence chromatograms were assembled and edited using an assembling programs (GAP4 Staden package) and were compared with reported sequences in GenBank using BlastN program (Altschul et al., 1997). Multiple sequences alignments were performed with the edited 16S sequence of the phytoplasma detected on peach tree and the 16S reference phytoplasma sequences using Clustal W program (Thompson et al., 1994). Phylogenetic analyses were conducted using MEGA version 4 (Tamura et al., 2007) using maximum parsimony with rando-

mized bootstrapping evaluation of branching validity.

RAPD amplification. The 48 RAPD 15-mer primers ATGCATGWSSWWS (called CATG1 to CATG48) with 40% GC contents were designed and used for random PCR on 100 ng of DNA extracted from healthy periwinkle and Surinam virescence-infected periwinkle. Samples were amplified through 40 cycles of 30 s at 94°C, 30 s at 37°C, and 1 min at 72°C using a single primer at 1 mM and 2 U of *Taq* polymerase in a 50 ml reaction mixture containing PCR Buffer 1Ç, MgCl$_2$ 2 mM, and 200μM of dNTP mix. Amplification results were analyzed on ethidium bromide-stained 1% agarose gels. DNA size marker was 1kb DNA ladder plus from Invitrogen.

Cloning and sequence analysis. When a DNA band was consistently observed in RAPD profile of "Surinam viresence"-infected periwinkle but not in healthy plant control, a PCR product obtained from "Surinam virescence"-infected periwinkle were ligated into pGEMt easy vector (Promega, Madison, Wis.). Plasmids were electroporated into *Escherichia coli* DH10B cells, and inserts were sequenced. Sequences were edited with two different sequence-editing and assembling programs (Chromas and GAP4 Staden package) and were compared with reported sequences in GenBank using Blast program.

Group specific PCR test. The non ribosomal dnaK gene based PCR test was carried out with 100 ng of plant DNA using PCR primers Bra-dnaKF1(CCC TTT AAA ACA GGT GTT AG) and Bra-dnaKR1 (TCT TCA AAC TCG GCA TCA AC) followed by nested PCR primers Bra-dnaKF2 (TTG GTC GGC GGA TCA ACA AG) and Bra-dnaKR2

Table 1. List of used reference phytoplasma isolates

| Isolate	Disease	Host	Country	16Sr Group
SV	Virescence	*Catharanthus roseus*	Surinam	XV-A
Bas	Yellows	*Ocimum basilicum*	Lebanon	XV-A
Hib121	Witches' -broom	*Hibiscus rosa-sinensis*	Brazil	XV-A
Hib122	Witches' -broom	*Hibiscus rosa-sinensis*	Brazil	XV-A
HibCB2	Witches' -broom	*Hibiscus rosa-sinensis*	Brazil	XV-A
CRP	Crotolaria phyllody	*Catharanthus roseus*	Thailand	II-C
CLP	Cleome phyllody	*Catharanthus roseus*	Thailand	II-A
SEP	Sesame phyllody	*Catharanthus roseus*	Thailand	II-A
TBB	Tomato big bud	*Catharanthus roseus*	Australia	II-D
SOYP	Soybean phyllody	*Catharanthus roseus*	Thailand	II-C
SPLL	Sweet potato little leaf	*Catharanthus roseus*	Australia	II
WBDL	Lime witches' -broom	*Catharanthus roseus*	Oman	II-B
COWB	Cotton witches' -broom	*Catharanthus roseus*	Burkina Faso	II-F
ESFY	Apple proliferation	*Catharanthus roseus*	Italy	X-B
MOL	Stolbur	*Catharanthus roseus*	France	XII-A
PTL	Tomato proliferation	*Catharanthus roseus*	Lebanon	VI-A
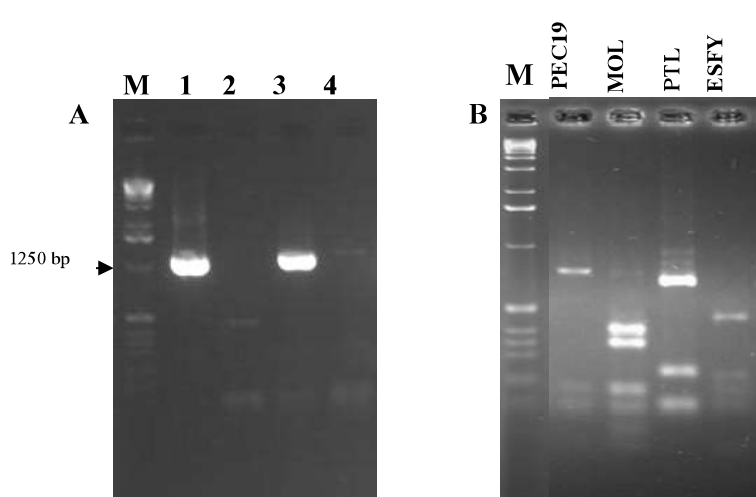
Figure 1. PCR-RFLP analysis. A - Nested PCR amplification of phytoplasma 16S rDNA fragment with the universal primers for phytoplasmas R16mF2/R16mR1 and R16F2n/ 16R2. Lane M, 1-Kb DNA ladder (Invitrogen), lane 1-the diseased peach tree *Prunus persica*, lane 2 - healthy peach tree, lane 3 - Stolbur Moliere-infected periwinkle, and lane 4 - healthy reference strain maintained in periwinkle hosts. B - RFLP analysis with restriction enzyme *Alu*I. Lane M, 1-Kb DNA ladder (Invitrogen), lane PEC19, the diseased peach tree *Prunus persica*, lanes MOL., PTL and ESFY, reference phytoplasma isolates maintained in periwinkle host.

(TGG AGA TTC TTC TGA AGT AG). PCR was performed in 50 µL containing 2µl of nucleic acid (about 100 ng), PCR Buffer 1Ç, MgCl₂ 2 mM, 0.5 mM of each primer, 200µM of dNTP mix, and 50 units/ml *Taq* polymerase. Following PCR conditions were used: initial denaturation step at 94°C for 4min, followed by 35 cycles consisting of denaturation at 94°C for 30 sec, annealing (hybridation) at 55°C during 30 sec, and primer extension (elongation) at 72°C for 1 min and 10 min in the final cycle. The PCR products (7 µL) were analyzed by electrophoresis in the 1ÇTBE buffer troughs 1% agarose gel, stained with ethidium bromide, and DNA bands visualized using a UV transilluminator.

RESULTS AND DISCUSSION

Detection and taxonomic characterization of phytoplasma. The amplicons of the expected size (1250 bp) were obtained from yellowing peach tree, and from the reference phytoplasma infected periwinkle (as positive control) by Nested PCR with the universal primers for phytoplasmas R16mF2/R16mR1 and R16F2n /R16R2. No PCR products were obtained from healthy control plants (healthy peach tree and healthy reference plant) (results illustrated in Figure 1A). For taxonomic characterization of detected phytoplasma, the PCR products obtained from peach tree and from reference phytoplasma strains were submitted to enzymatic restriction fragment polymorphism (RFLP) analysis with restriction enzyme *Alu*I. Results of RFLP analysis (Figure 1B) shown that the RFLP pattern obtained from peach tree is different from RFLP patterns of the reference phytoplasma strains used.

The PCR product from peach tree was se-

quenced. The 16S sequence of the phytoplasma detected in the peach tree shared 100% identity with the rDNA-16S sequence of '*Candidatus Phytoplasma brasiliense*' of the phylogenetic group 16SrXV (Hibiscus witches broom phytoplasma, Montano and *al.*, 2001). It is the first detection of this phytoplasma in a plant other than hibiscus and elsewhere than in Brazil.

The 16S sequence of detected peach tree phytoplasma was aligned with 16S sequences of reference phytoplasma *Candidatus* species and a phylogenetic tree constructed using the neighbor joining method. The resulting phylogenetic tree is presented on Figure 2.

Random amplification and cloning of the SVG28 fragment. RAPD patterns primed with 48 15-mer primers were obtained from Surinam virescence infected periwinkle and compared to those obtained from healthy periwinkle of the same cultivar. The G28 15-mer (ATGCATGACTCGAAC) primer allowed amplification of a 1.6 kbp DNA fragment from "Surinam virescence"-infected periwinkle (Figure 3, lane 1) but not from healthy periwinkle (Figure 3, lane 2). This amplicon, called SVG28, was cloned and sequenced. The sequence was 1651 bp long and shared 84% similarity with the Peanut witches'-broom phytoplasma genes coding for heat shock protein DnaK and heat shock protein DnaJ. Group specific primers Bra-dnaKF1/R1 for first PCR and nested internal primers Bra-dnaKF2/R2 were designed on SVG28 sequence, and a PCR test based on non-ribosomal *dna*K gene was developed with the aim of specifically detect phytoplasmas of group 16SrXV-A ('*Ca. P. brasiliense*').

According to the sequence, an 886-bp amplicon is expected. To verify the specificity of Bra-

dnaKF1/R1 and Bra-dnaKF2/R2, they were used on DNAs extracted from diseased peach tree (Figure 4, lane 6), healthy peach tree (Figure 4, lane 7), Surinam virescence infected periwinkle (Figure 4, lane

4), a'*Ca. P. brasiliense*'-infected basil (Figure 4, lane 5), three '*Ca. P. brasiliense*'-infected *Hibiscus rosa-sinensis* plants (Figure 4, lanes 1, 2, 3), and
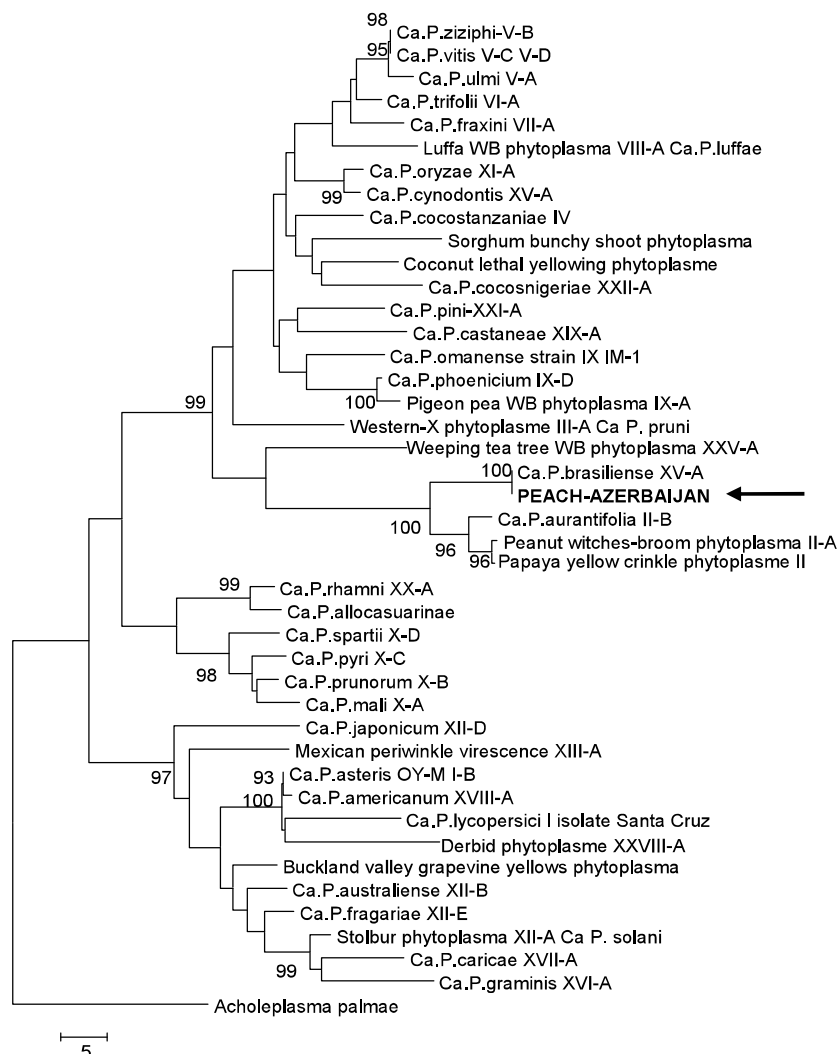

Figure 2. Phylogenetic tree of 16S rRNA gene sequences constructed by the neighbour-joining method showing relationships between the phytoplasma identified in peach tree from Azerbaijan and reference phytoplasmas from GenBank. Numbers above or below branches are bootstrap values obtained for 1000 replicates. Branch lengths are proportional to the number of inferred character-state transformations. Bar represents 5 inferred character state changes. A. palmae ATCC 49389T was used as outgroup.

ten phytoplasma strains belonging to the 16SrII group, a group phylogenetically related to group 16SrXV (Figure 4, lanes 8 to 17). An 886-bp fragment was obtained only with diseased peach tree, Surinam virescence infected periwinkle, basil and the three '*Ca. P. brasiliense*'-infected *Hibiscus* plants.

In conclusion, the detection of '*Ca. P. brasiliense*' was performed for the first time in a plant other than hibiscus and elsewhere than Brazil. This phytoplasma, new for the old world was detected in a peach tree in the Guba region of Azerbaijan. A detection test specific to '*Ca. P. brasiliense*' was developed and was based on the amplification of the non ribosomal dnaK gene.
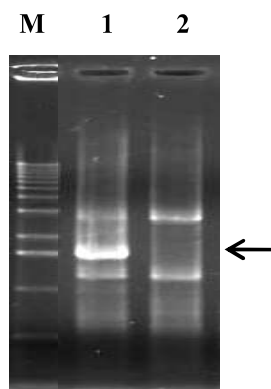
Figure 3. RAPD with 15-mer G28. Lane M, 1-Kb DNA ladder (Invitrogen), lane 1, Surinam virescense infected reference isolate maintained in periwinkle and lane 2, healthy periwinkle control.
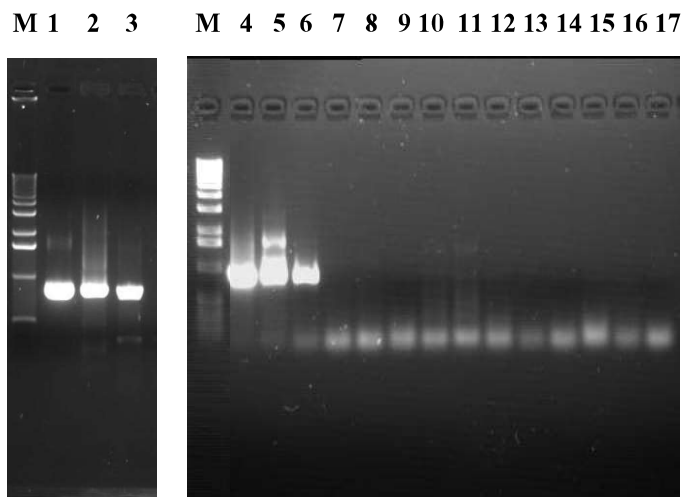

Figure 4. Nested PCR amplification with the specific primers bradnaK F1/ bradnaK R1 and bradnaK F2/bradnaK R2 for phytoplasmas of 16SrXV group based on non-ribosomal sequence *dna*K Lane M, 1-Kb DNA ladder (Invitrogen), lane 1 - Hib121, lane 2 - Hib122, lane 3 - Hib Cb02, lane 4 - Surinam virescence infected perwinkle, lane 5 - Basilic from Liban, lane 6 - diseased peach tree, lane 7 - healthy peach tree, lane 8 - Cr.Ph, lane 9 - Cl.Ph, lane 10 - J.Ph, lane 11 - Cr.W.B., lane 12 - Ce.Ph., lane 13 - TBB, lane 14 - So.Ph., lane 15 - SPLL, lane 16 - WBDL, lane 17 - Co.W.B. Abbreviations of phytoplasma names are defined in Table 1.

AKNOWLEDGEMENTS

REFERENCES

Ahrens U., Lorenz K.H., Seemuller E. (1993) Genetic diversity among mycoplasmalike organisms associated with stone fruit diseases. Mol. Plant-Micr. Interac. **6:** 686-691.

Altschul S.F., Madden T.L., Schdffer A.A., Zhang J., Zhang Z., Miller W., Lipman D.J. (1997) Gapped BLAST (Basic Local Alignment Search Tool) and PSI-BLAST: a new generation of protein database search programs. Nucleic Acids Res. **25:** 3389-3402.

Deng S.J., Hiruki C. (1991) Amplification of 16S ribosomal-RNA genes from cultivable and noncul-turable mollicutes. J. Microbiol. Meth. **14:** 53-61.

Gundersen D.E., Lee I.-M. (1996) Ultrasensitive detection of phytoplasmas by nested-PCR assays using two universal primer pairs. Phytopath. Mediter. **35:** 114-151.

Jarausch W., Lansac M., Saillard C., Broquaire J.M., Dosba F. (1998) PCR assay for specific detection of European stone fruit yellows phytoplasmas and its use for epidemiological studies in France. Europ. J. Plant Pathol. **104:** 17-27.

Kirkpatrick B.C., Stenger D.C., Morris T.J., Purcell A.H. (1987) Cloning and detection of DNA from a nonculturable plant pathogenic mycoplasmalike organism. Science **238:** 197-200.

Lee I.M., Gundersen-Rindal D.E., Bertaccini A. (1998) Phytoplasma: Ecology and Genomic Diver-

sity. Phytopathol. **88:** 1359-1366.

Lee I.M., Davis R.E., Gundersen-Rindal D.E. (2000) Phytoplasma: phytopathogenic mollicutes. Annu. Rev. Microbiol. **54:** 221-255.

Maixner M., Ahrens U., Seemuller E. (1995) Detection of the German grapevine yellows (Vergilbungskrankheit) MLO in grapevine, alternative hosts and a vector by a specific PCR procedure. Europ. J. Plant Pathol. **101:** 241-250.

Purcell A.H., Nyland G., Raju B.C., Heringor M.R. (1981) Peach yellow leaf roll epidemic in Northern California: effects of peach cultivar, tree age and proximity to pear orchards. Plant Dis. **65:** 365-368.

Tamura K., Dudley J., Nei M., Kumar S. (2007) MEGA4: Molecular Evolutionary Genetics Analysis (MEGA) software version 4.0. Mol. Biol. Evol. **24:** 1596-1599.

Thompson J.D., Higgins D.G., Gibson T.J. (1994) CLUSTAL W: improving the sensitivity of progressive multiple sequence alignment through sequence weighting, position-specific gap penalties and weight matrix choice. Nucleic Acids Res. **22:** 4673-4680.

Weintraub P.G., Beanland L. (2006) Insect vectors of phytoplasmas. Annu. Rev. Entomol. **51:** 91-111.

Weisburg W.G., Tully J.G., Rose D.L., Petzel J.P., Oyaizu H., Yang D., Mandelco L., Sechrest J., Lawrence T.G., Etten J.V., Maniloff J., Woese C.R. (1989) A phylogenetic analysis of the mycoplasmas: basis for their classification. J. Bacteriol. **171:** 6455-6467.

Zhao Y., Wei W., Davis R.E., Lee I.M. (2010) Recent advances in 16S rRNA gene-based Phytoplasma differenciation, classification and taxonomy. In: Phytoplasmas: genomes, plant hosts and vectors. (Weintraub P.G., Jones P., eds.), CAB International, Wallingford: 64-92.

Influence of Agrochemical Countermeasures on Accumulation of ^{90}Sr and ^{137}Cs in Various Agricultural Crops

Mahmud A. Abdullayev*
Research Institute of Crop Husbandry, Ministry of Agriculture of Azerbaijan Republic, Pirshagi Village, II Sovkhoz, Baku AZ 1098, Azerbaijan

It was proved by long-term field experiments that agrochemical countermeasures, i.e. use of an optimal and higher doses of complete mineral fertilizers (NPK) along with significant increase in crop yields leads to appreciable decrease in accumulation of artificial radionuclides (^{90}Sr and ^{137}Cs) in various agricultural crops grown on grayish brown soils of Absheron.

Keywords: agrochemical countermeasures, radionuclids, biosphere, mineral and organic fertilizers

INTRODUCTION

As a result of accident at Chernobyl Nuclear Power Plant (NPP), significant number of artificial radionuclides falls out into soils. Significant increase of artificial radionuclides in environment (in soils) after Chernobyl accident along with their existing contents in soils accumulated during the period of intensive nuclear tests, poses a potential threat of radioactive pollution to plant products and whole environment. Among artificial radionuclides the most significant are long-living ^{90}Sr and ^{137}Cs, which are quickly included into biological cycles of migration, accumulated in skeleton and soft tissues, and are one of the major dose-forming radionuclides in living organisms.

Use of countermeasures in agriculture holds one of the central places in system of measures on elimination of the consequences of the Chernobyl accident. One of the significant countermeasures of inflow of artificial radionuclides into the plants is incorporating into the soils various combinations and doses of organic and mineral fertilizers. From all countermeasures this protective measure refers to the most effective and practically realized. Existing literature data on this subject is contradictive (Pavlotskaya and Babicheva, 1973; Marey et al., 1974; Aleksakhin, 1982; Aliyev and Abdullayev, 1983; Prister et al., 1991; Ponikarova et al., 1992; Abdullayev and Aliyev, 1998). Thus, the aim was to study the influence of incorporation of an optimal and higher doses of complete mineral fertilizers (NPK) on accumulation of ^{90}Sr and ^{137}Cs in grain cereals (winter wheat and winter barley) and legumes (soybean and garbanzo) grown on grayish brown arable soils of Absheron.

MATERIALS AND METHODS

Field researches were carried out on the plot of Absheron Subsidiary Experimental Station of the Research Institute of Crop Husbandry. The soil was grayish brown of loamy mechanical composition. The used fertilizers were: nitrogen - in form of ammonium nitrate, phosphorus - in form of double superphosphate, and potassium - in form of sulfuric potassium. Whole norm of phosphorous and potassium fertilizers and 20% of nitrogen fertilizers were incorporated into the soil just before sowing and other part of nitrogen fertilizers - as dressing in phases of heading and blossoming. Recorded square of test allotments with wheat and barley was 10 m^2, with soybean and garbanzo - 16 m^2. Experiments were repeated 3 times. All rules of agritechnology providing high harvest were followed in experiments. Experiments were carried out with winter wheat variety Vugar, winter barley variety Garabakh-7, garbanzo variety AzNIIZ-304 and soybean variety Beyson.

Sampling for radioactive chemical analysis was made at the end of vegetation period. The plant samples were incinerated at temperature not higher than 450°C. The latter is due to the fact that when incinerated at above shown temperature the possibility of volatilization and mechanical capture with smoke of radionuclides is not excluded (Pavlotskaya and Babicheva, 1973).

^{90}Sr concentration was measured in extract 6N of hydrochloric acid by oxalate method by derived ^{90}Y, and ^{137}Cs activity concentration – by iodimeantimony method. Activity of radionuclides was measured using low background radiation device

*E-mail: mahmud.su@ mail.ru

Table 1. Influence of mineral fertilizers appilication on different crops productivity (average in 2 years)

| Variants | Yield, cwt ha^{-1} | | Increase in comparison to control | | | |
| | | | Grain | | Straw | |
	Grain	Straw	cwt ha^{-1}	%	cwt ha^{-1}	%
		Winter wheat				
Control (without fertilizers)	53.7	58.4	-	-	-	-
N160P90K60 (optimal dose)	66.2	69.1	12.5	23.3	10.7	18.3
N240P360K240	78.7	78.5	25.0	46.6	20.1	34.3
N320P720K480	84.2	88.6	30.5	56.8	30.2	51.7
		Winter barley				
Control (without fertilizers)	46.6	56.9	-	-	-	-
N90P90K60 (optimal dose)	56.2	70.2	9.6	20.6	13.3	23.3
N135P360K240	63.9	78.7	17.3	37.1	21.8	38.3
N180P720K480	72.7	86.2	26.1	56.0	29.3	51.5
		Garbanzo				
Control (without fertilizers)	19.0	25.9	-	-	-	-
N30P60K30 (optimal dose)	21.6	30.3	2.6	13.3	4.4	17.0
N45P240K120	24.8	33.9	5.8	30.5	8.0	30.9
N60P480K240	27.2	38.8	8.2	43.2	12.9	49.8
		Soybean				
Control (without fertilizers)	20.2	29.8	-	-	-	-
N90P60K30 (optimal dose)	25.9	41.9	5.7	28.2	12.1	40.6
N135P240K120	30.8	44.4	10.6	52.5	14.6	49.0
N180P480K240	32.9	47.2	12.7	62.9	17.4	58.4

UMF-1500M with SBT-13 scintillation counter and scaler device PP-16.

RESULTS AND DISCUSSION

The obtained results showed that the use of optimal and higher doses of complete mineral fertilizers significantly raises crop productivity of grain cereals and legumes. Thus, the average increase in grain yield due to addition of optimal and higher doses of mineral fertilizers for wheat grain in comparison to non-fertilized variant was 12.5-30.5 cwt ha^{-1} (23.3-56.8%), barley – 9.6-26.1 cwt ha^{-1} (20.6-56.0%), garbanzo – 2.6-8.2 cwt ha^{-1} (13.3-43.2%), soybean – 5.7-12.7 cwt ha^{-1} (28.2-62.9%) and for straw – 10.7-30.2 cwt ha^{-1} (18.3%-51.7%); 13.3-29.3 cwt ha^{-1} (23.3-51.5%); 4.4-12.9 cwt ha^{-1} (17.0-49.8%); 12.1-17.4 cwt ha^{-1} (40.6-58.4%), respectively (Table 1).

As known, due to use of mineral fertilizers it is possible to limit accumulation of artificial radionuclides in crops (Gulyakin and Yudintseva, 1973). The addition of potassium fertilizers is the most important for decreasing the ^{137}Cs accumulation in plants (Moiseyev et al., 1986). Thus, in area of Chernobyl accident it was possible to decrease the ^{137}Cs content 1.5-2.5-times in plants by limiting the acid soils and incorporation into soils of potassium fertilizers in increased quantities (Korneyev et al., 1988).

In present research use of mineral fertilizers resulted in decreased concentration of ^{90}Sr and ^{137}Cs in vegetative and generative parts of winter wheat,

winter barley, garbanzo and soybean plants, and maximum decrease of radionuclides concentration in all crops was observed in samples, where high doses of mineral fertilizers were used (especially phosphorus and potassium). Incorporation into the soil of optimal and higher doses of mineral fertilizers decreased ^{90}Sr concentration in the grain of wheat by 24.0-41.1% (10.5-18.0 cBq/kg), barley - 18.4-52.2% (23.8-67.7 cBq/kg), garbanzo - 36.0-53.8% (65.9-98.4 cBq/kg) and soybean - 30.6-59.7% (57.5-112.0 cBq/kg) on average in two years. Concentration of ^{90}Sr in comparison to non-fertilized samples decreased in straw by 22.2-54.3% (94.2-230.7 cBq/kg), 21.1-45.2% (102.7-220.0 cBq/kg), 25.4-37.7% (176.7-262.1 cBq/kg) and 14.7-39.0 % (132.2-352.0 cBq/kg), correspondingly (Figure 1A).

^{137}Cs accumulation decreased in grain of wheat by 40.1-62.5% (6.1-9.5 cBq/kg), barley - 33.2-56.8% (8.3-14.2 cBq/kg), garbanzo - 32.4-53.8% (7.3-12.1 cBq/kg) and soybean - 20.3-54.1% (6.2-16.5 cBq/kg), and in straw by 25.8-45.4% (12.0-21.1 cBq/kg), 18.7-45.8% (10.4-25.4 cBq/kg), 24.1-47.3% (19.1-37.4 cBq/kg) and 26.6-48.8%, respectively (28.0-51.4 cBq/kg) (Figure 1B).

Thus, incorporation into the soils of mineral fertilizers in optimal and higher doses along with increase of grain yield, also leads to significant decreasing in accumulation of artificial radionuclides in yields (grain and straw) of various crops.

Decrease in ^{90}Sr and ^{137}Cs concentration in plants under influence of mineral fertilizers (especially in high doses) may be as the result of "diluti-
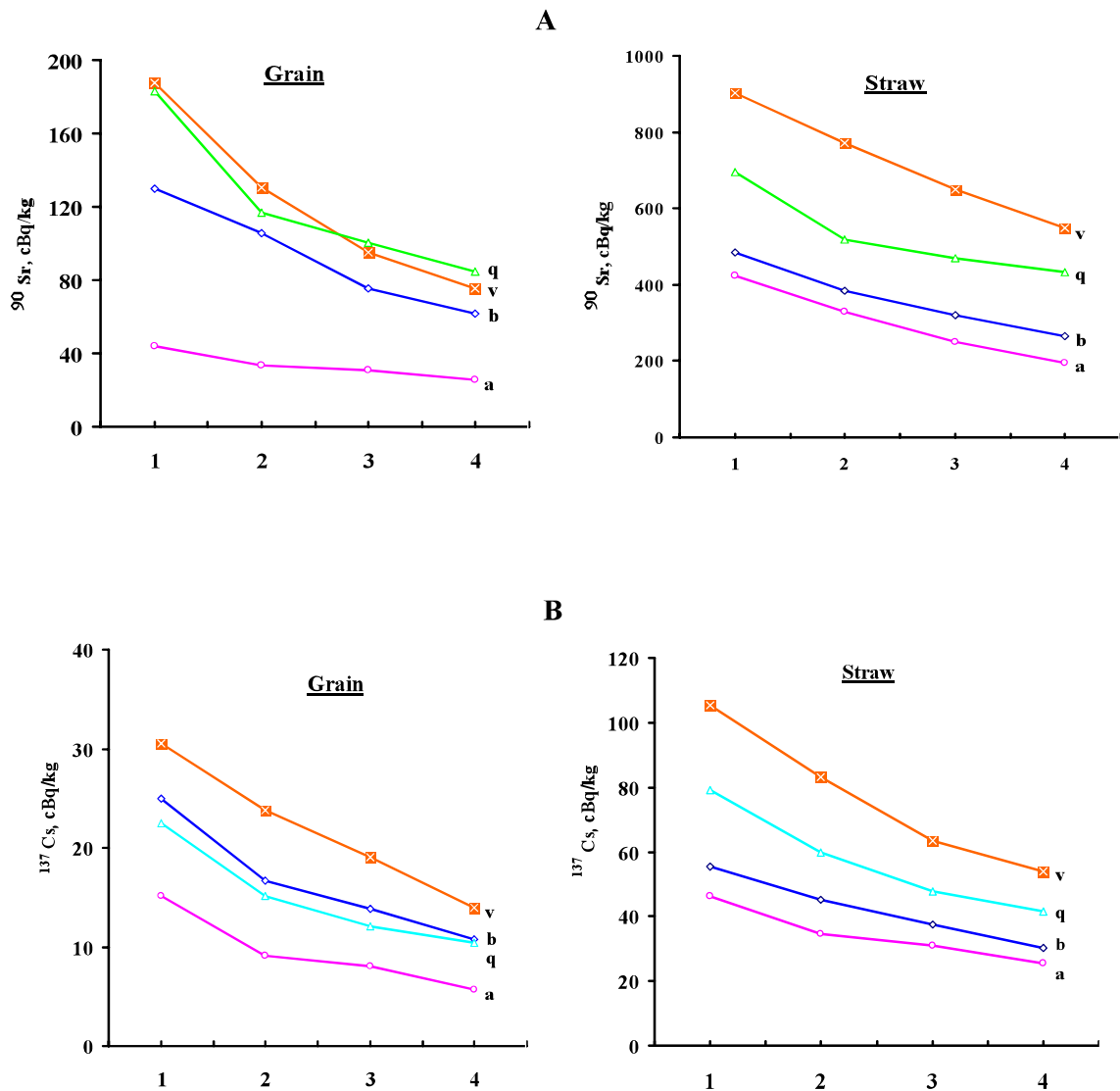
A

B

Fiqure 1. Influence of mineral fertilizers on accumulation of strontium-90 (**A**) and caesium-137 (**B**) in grain and straw of various agricultural crops (average data in 2 years).
(a) Wheat: 1 - Control (without fertilizers), 2 - N160P90K60 (optimal dose), 3 - N240P360K240, 4 - N320P720K480;
(b) Barley: 1 - Control (without fertilizers), 2 - N90P90K60 (optimal dose), 3 - N135P360K240, 4 - N180P720K480;
(v) Soybean: 1 - Control (without fertilizers), 2 - N90P60K30 (optimal dose), 3 - N135P240K120, 4 - N180P480K240
(q) Garbanzo: 1 - Control (without fertilizers), 2 - N30P60K30 (optimal dose), 3 - N45P240K120, 4 - N60P480K240.

on" of radionuclides in increasing phytomass, decreasing of radionuclides access for root assimilation as a result of decrease of ^{90}Sr and ^{137}Cs mobility or change in correlation of accessible macro- and microelements for plants (including radionuclides) in soils.

CONCLUSIONS

1. Use of complete mineral fertilizers in optimal and higher doses led to significant increase in

productivity of winter wheat, winter barley, garbanzo and soybean. The biggest effect was observed at highest doses of mineral fertilizers.

2. Incorporation into the soil of increasing doses of complete mineral fertilizers along with increase of crops productivity led to significant decrease in ^{90}Sr and ^{137}Cs accumulation in yields of winter wheat, winter barley, garbanzo and soybean, maximum decrease of radionuclides concentration in plants was observed in samples, where highest doses of phosphorous-potassium fertilizers were used.

REFERENCES

Aleksakhin R.M. (1982) Nuclear energy and biosphere. Energoizdat, Moscow: 215 p. (in Russian).

Aliyev J.A., Abdullayev M.A. (1983) Strontium-90 and caesium-137 in soil-plant cover of Azerbaijan. Nauka, Moscow: 104 p. (in Russian).

Abdullayev M.A., Aliyev J.A. (1998) Migration of artificial and natural radionuclides in soil-plant system. Elm, Baku: 239 p. (in Russian).

Prister B.S., Loshilov N.A., Nemets O.F., Poyarkov V.A. (1991) Fundamentals of agricultural radiology. Urozhai, Kiev: 472 p. (in Russian).

Ponikarova T.M., Strukov V.N., Panasov M.N., Drichko V.F., Semyonov Y.I. (1992) Radioactivity of chestnut soils and main agricultural crops of arid zone of Povolzhye. Agrichem. **4:** 96-100 (in Russian).

Pavlotskaya F.I., Babicheva Y.V. (1973) Long-live artificial and natural radioisotopes in grain of agricultural crops in Moscow surroundings. Atomizdat, Moscow: 31 p. (in Russian).

Marey A.N., Barkhudarov R.M., Novikova N.Y. (1974) Global precipitations of caesium-137 and human being. Atomizdat, Moscow: 166 p. (in Russian).

Gulyakin I.V., Yudintseva Y.V. (1973) Agricultural radiobilogy. Kolos, Moscow: 272 p. (in Russian).

Moiseyev I.T., Rerikh L.A., Tikhomirov F.A. (1986) To the question of influence of mineral fertilizers at access of ^{137}Cs from soil of agricultural plants. Agrochem. **2:** 89 p. (in Russian).

Korneyev N.A., Povalyayev A.P., Aleksakhin R.M. et al. (1988) Sphere of agroindustrial production-radiologic consequences at Cernobyl NPP and main protective measures. Nuclear Energy **65(2):** 129 (in Russian).